
# Transcriptional Regulation of the *mra* region in *Escherichia coli*

**Robyn Emmins**

Thesis presented for the degree of Doctor of Philosophy

The University of Edinburgh

2006

## Declaration

I declare that this is my own work and that any contribution made by other parties is clearly acknowledged.

Robyn Emmins
July 2006

## Acknowledgements

I would first like to thank my supervisor, Garry Blakely, for all his support and guidance during my time in his laboratory. I am fully aware how lucky I have been to have had a supervisor whose door was always open (even for my endless stupid questions!), but who also gave me the space to make my own mistakes. I will forever be indebted to him for helping me gain all that I have from my PhD – and for making me employable! I would like to extend special thanks to Zubin Thacker - my surrogate big brother, who has kept me in line since day one, who is a fountain of all knowledge and who always knows what to say. I would also like to thank my lab mates Fran Parry and Helen Williamson for brightening up a very lonely lab and for making every day unpredictable, but always fun! I also thank the past and present staff and students of the Darwin 8$^{th}$ floor for their encouragement and more importantly, random banter during my time in the lab. A special thanks are made to my 6$^{th}$ floor drinking buddies, in particular Laura, Manuel, John B, John E, Anna and Martin, who have made me laugh each and every day and who have helped make the last four years fly by. Finally I would like to thank my family and friends outside of work who have kept me sane and reminded me what the "real" world is like and who have all made admirable efforts to understand what on earth I've been up to for the last four years. I also thank the BBSRC for funding my PhD. This thesis is dedicated to my parents.

## Abstract

Cell division in *Escherichia coli* is a complex process requiring strict regulation to maintain both spatial and temporal control of the septation event. The *mra* region in *E. coli* is a large cluster of 16 contiguous genes, many of which are involved in peptidoglycan biosynthesis and cell division. A single promoter, designated $P_{mra}$, was previously identified in the *fru*R-*yab*B intergenic region upstream of the *mra* region. $P_{mra}$ was reported to be essential for expression of genes up to *fts*W in the centre of this gene cluster. This study investigates potential mechanisms of transcriptional regulation at $P_{mra}$, in addition to the regulation of two newly identified promoters ($P_{mra}2$ and $P_{mra}3$) also located in the *fru*R-*yab*B intergenic region. Slow growing cells are smaller than fast growing cells of the same strain and therefore require greater expression of cell division proteins to form the septal machinery. We therefore hypothesised that transcription of the *mra* region may be regulated by growth rate. Using *lac*Z reporter strains we determined that transcription from the $P_{mra}$ promoters was inversely related to growth rate. We then identified mechanisms of transcriptional regulation of the $P_{mra}$ promoters, mediated by factors such as FIS and ppGpp, which may contribute to the inverse growth rate control. Promoters $P_{mra}1$ and $P_{mra}3$ were the major contributors to the transcription of early genes in the *mra* region. Transcripts originating from these promoters were detected by RT-PCR to span at least as far as *fts*L. $P_{mra}3$ activity was repressed by many factors, in particular by the presence of the entire *fru*R-*yab*B intergenic region, this indicated that transcriptional regulators interact with the DNA upstream of the promoter. The 50S subunit ribosomal protein L3 was shown to bind to the DNA upstream of $P_{mra}3$. We hypothesise that L3 may represent a transcriptional regulator of the $P_{mra}$ promoters that is directly linked to the growth rate of the cell. Although $P_{mra}3$ was highly repressed under the experimental conditions, it was not possible to delete it from the chromosome, indicating that it makes an important contribution to transcription of the *mra* region, which may be essential for cell viability.

# Contents.


**Chapter 1: Introduction** 1

**1.1: Cell division in *Escherichia coli*** 2
1.1.1: FtsZ and Assembly of the Z-ring 4
1.1.2: Division Site Selection in *E. coli* 7
1.1.3: The Septal Ring 11
1.1.4: Peptidoglycan Biosynthesis during Cell Division 18
1.1.5: The *mra* region 21
**1.2: Transcriptional Regulation in *Escherichia coli*** 27
1.2.1: Transcriptional Regulation by CRP 33
1.2.2: Transcriptional Regulation by FIS 36
1.2.3: Transcriptional Regulation by ppGpp and the Stringent Response 40
**1.3: Project Aims** 46

**Chapter 2: Materials and Methods** 47

**2.1: Growth Media** 48
**2.2: Antibiotics and Reagents** 49
**2.3: Strains** 50
**2.4: Plasmids** 51
**2.5: Primers** 55
**2.6: Bacterial Methodology** 58
2.6.1: Preparation of Competent Cells 58
2.6.2: Heat Shock Transformation of Plasmid DNA 59
2.6.3: P1 Transduction 60
2.6.4: Preparation of a P1 Lysate 60
2.6.5: Transposon Mutagenesis 61
2.6.6: Growth Curves 61
2.6.7: β-galactosidase Assays 61
**2.7: DNA Techniques** 62
2.7.1: DNA Purification 62
2.7.2: Ethanol Precipitation of DNA 63
2.7.3: Quantification of DNA 63
2.7.4: Polymerase Chain Reaction 63
2.7.5: Agarose Gel Electrophoresis 64
2.7.6: Digestion of DNA with Restriction Endonucleases 65
2.7.7: Dephosphorylation of DNA 65
2.7.8: Recovery of DNA from an Agarose Gel 65
2.7.9: Ligation of DNA 65
2.7.10: Single Colony Gels 66
2.7.11: Single Colony PCR 66
2.7.12: DNA Sequencing 66
2.7.13: Radiolabelling of DNA 67
2.7.14: Radioactive PCR 68
2.7.15: Non-denaturing Acrylamide Gel Electrophoresis 68
2.7.16: Gel Extraction and Purification of Radioactive PCR products 69
**2.8: RNA Techniques** 69
2.8.1: RNA Purification 69
2.8.2: Quantification of RNA 70
2.8.3: DEPC Treatment of Solutions 70
2.8.4: Reverse Transcription Polymerase Chain Reaction 70
2.8.5: Phenol Extraction of RNA 71
2.8.6: *In vitro* Transcription Reactions 72
2.8.7: Primer Extension Reactions 73
2.8.8: Northern Blots 74

**2.9: Protein Techniques** 76
2.9.1: SDS-Polyacrylamide Gel Electrophoresis 76
2.9.2: Preparation of Soluble Protein Lysates 77
2.9.3: Protein Purification 78
2.9.4: Quantification of Protein Concentration 79
2.9.5: Ammonium Sulfate Precipitation 80
2.9.6: Fast Performance Liquid Chromatography (FPLC) 81
2.9.7: Dialysis of Proteins 81
2.9.8: Concentration of Protein Samples 81
2.9.9: Western blots 82
**2.10: Analysis of Protein:DNA Interactions** 83
2.10.1: Electrophoretic Mobility Shift Assays (EMSAs) 83
2.10.2: Sequencing Gels 83
2.10.3: Chain Termination Sequencing Reactions 84
2.10.4: Maxam Gilbert AG Ladder 84
2.10.5: Footprinting of Protein Bound DNA 85
2.10.6: Stable Complex Assays 85
**2.11: Microscopy** 86

**Chapter 3: Transcriptional Regulation of the *mra* region in *E. coli*** 87

**3.1: Introduction** 88
**3.2: Expression of the *mra* region in response to growth rate** 89
3.2.1: Effect of growth rate on transcription from the $P_{mra}$ promoters 89
3.2.2: Comparison of *yab*B and *fts*Z transcription 96
3.2.3: Comparison of FtsI and FtsZ expression 101
**3.3: Transcriptional Regulation of the $P_{mra}$ promoters** 104
3.3.1: Construction of $P_{mra}$-*lac*Z reporter vectors 105
**3.4: Identifying Transcriptional Regulators of the $P_{mra}$ promoters** 108
3.4.1: A Role for CRP in the regulation of the $P_{mra}$ promoters? 109
3.4.2: A Role for FIS in the regulation of the $P_{mra}$ promoters? 115
3.4.3: Effect of FIS on the expression of *fts*Z 122
3.4.4: Involvement of other DNA-binding protein in the regulation of the $P_{mra}$ promoters 132
**3.5: The Effect of Changing Growth Rate on the individual $P_{mra}$ promoters** 138
**3.6: Regulation of $P_{mra}3$ by ppGpp** 141
3.6.1: The Effect of ppGpp on $P_{mra}3$ Activity 141
3.6.2: Role of the GC-rich Discriminator Region in Regulation of $P_{mra}3$ 144
3.6.3: A Role for DksA in the Regulation of the $P_{mra}$ Promoters? 146
**3.7: Determination of Transcript Length from the $P_{mra}$ promoters** 149
3.7.1: Determination of Transcript Length by Primer Extension 149
3.7.2: Determination of Transcript Frequency by *in vitro* Transcription 150
3.7.3: Determination of Transcript Length by Northern Blot 150
3.7.4: Determination of Transcript Length by RT-PCR 151
3.7.5: Detection of Additional Promoters in the *fru*R-*yab*B intergenic region 155
**3.8: Is $P_{mra}3$ Essential for Expression of the *mra* region and for Cell Viability?** 157
**3.9: Summary** 159

**Chapter 4: Additional Factors involved in the Regulation of the *mra* region** 163

**4.1: Introduction** 164
**4.2: Identification of Transcriptional Regulators by Transposon Mutagenesis** 165
**4.3: Purification and Identification of a DNA-binding protein shown to interact with the *fru*R-*yab*B intergenic region** 166
**4.4: Identification of additional promoters of the *mra* region** 181
**4.5: Summary** 189

## Chapter 5: Discussion 192

**5.1: Regulation of the $P_{mra}$ promoters by Growth Rate** 193
**5.2: Regulation of the $P_{mra}$ promoters by FIS** 194
**5.3: Repression of $P_{mra}3$** 195
**5.4: Ribosomal Protein L3 – A Potential Mediator of Growth Rate Regulation?** 196
**5.5: Regulation of $P_{mra}3$ by ppGpp** 197
**5.6: Do the $P_{mra}$ promoters drive transcription of *ftsZ*?** 197
**5.7: Project Overview** 198

## List of Figures

**Figure 1.1:** Cell division in *E. coli*. 3
**Figure 1.1.1:** FtsZ and its localisation to the Z-ring. 6
**Figure 1.1.2.1:** Division site selection in *E. coli*. 8
**Figure 1.1.2.1:** The Min System in *E. coli*. 10
**Figure 1.1.3.1:** Order of assembly of the septal ring. 12
**Figure 1.1.4.1:** Formation of Peptidoglycan precursors involves enzymes encoded by the genes of the *mra* region. 19
**Figure 1.1.4.2:** The "Three for One" model of growth for the Peptidoglycan sacculus. 20
**Figure 1.1.5.1:** The *mra* region in *E. coli*. 22
**Figure 1.1.5.2:** Potassium permanganate footprints and primer extension products of $P_{mra}1$, $P_{mra}2$ and $P_{mra}3$. 26
**Figure 1.1.5.3:** Positions of the $P_{mra}$ promoters within the *fru*R-*yab*B intergenic region. 27
**Figure 1.2.1:** RNA Polymerase bound at a $\sigma^{70}$ promoter. 28
**Figure 1.2.2:** Examples of transcriptional regulation at prokaryotic promoters . 30
**Figure 1.2.1.1:** Structure of CRP bound to DNA. 34
**Figure 1.2.2.1:** Structure of FIS and its DNA binding site. 37
**Figure 1.2.3.1:** RelA-mediated (p)ppGpp synthesis. 41

**Figure 3.2.1.1:** Illustration of the *yab*B reporter cassette on the EDCM647 chromosome. 90
**Figure 3.2.1.2:** Optical densities and β-galactosidase activity of EDCM647 at two different growth rates. 91
**Figure 3.2.1.3:** Cell Length of MG1655 and EDCM647 at different growth rates. 94
**Figure 3.2.2.1:** Illustration of the transcriptional Φ(*ftsZ-lacZ*) reporter fusion integrated into the chromosome of VIP407. 97
**Figure 3.2.2.2:** Comparison of β-galactosidase activity in the reporter strains EDCM647 and VIP407. 98
**Figure 3.2.3:** Western blots showing levels of FtsI and FtsZ in MG1655 soluble protein lysates. 102
**Figure 3.3.1.1:** Illustration of pRS551. 105
**Figure 3.3.1.2:** Mutations introduced into $P_{mra}1$ and $P_{mra}3$ -10 regions by site-directed mutagenesis. 106
**Figure 3.3.1.3:** Construction and expression of $P_{mra}$-*lacZ* reporter plasmids. 107
**Figure 3.4.1.1:** Potential CRP binding sites in the 601 bp *fru*R-*yab*B intergenic region. 110
**Figure 3.4.1.2:** Purification of HIS-tagged CRP. 111
**Figure 3.4.1.3:** Purification of CRP fused to Maltose Binding Protein. 112
**Figure 3.4.1.4:** EMSA to determine whether CRP-MBP binds to DNA. 114
**Figure 3.4.2.1:** FIS binding sites identified in the 601 bp *fru*R-*yab*B intergenic region. 116
**Figure 3.4.2.2:** Effect of FIS on transcription from the $P_{mra}$ promoters. 117
**Figure 3.4.2.3:** Filamentation of RE201 (*fis*::Km) with continued exponential phase growth. 120
**Figure 3.4.2.4:** Growth, β-galactosidase activity and total β-galactosidase activity of EDCM647 & RE111. 121
**Figure 3.4.3.1:** Growth, β-galactosidase activity and total β-galactosidase activity of VIP407 & RE301. 123
**Figure 3.4.3.2:** Western blots of FtsZ in MG1655 and RE102 during batch culture. 125
**Figure 3.4.3.3:** Morphology of MG1655, RE102, RE104 & RE106 from exponential cultures in LB. 127
**Figure 3.4.3.4:** Morphology of MG1655, RE102, RE104 & RE106 grown in M9 Glycerol + CAA. 130
**Figure 3.4.3.5:** Mis-segregation of DNA in *fis*⁻ filaments. 131

**Figure 3.4.4.1:** Autoradiograph of binding reactions containing either purified FIS or a protein lysate from a *fis*⁻ strain with DNA from the *fru*R-*yab*B intergenic region. 133
**Figure 3.4.4.2:** Expression of β-galactosidase from the $P_{mra}$ promoters in derivatives of TP8503. 137
**Figure 3.5.1:** Expression of β-galactosidase from the $P_{mra}$ promoters at two different growth rates. 139
**Figure 3.6.1:** The effect of *rel*A and *rel*A/*spo*T mutations on β-galactosidase expression from pRS3M. 143
**Figure 3.6.2:** The effect of *rel*A and *rel*A/*spo*T mutations on transcription from $P_{mra}$3dis⁻. 145
**Figure 3.6.3:** Growth, β-galactosidase activity and total β-galactosidase activity of EDCM647 & RE302. 148
**Figure 3.7.4.1:** PCR and RT-PCR spanning $P_{mra}$1-*fts*Z. 152
**Figure 3.7.4.2:** Maximum transcript length detectable by RT-PCR from the $P_{mra}$ promoters. 153
**Figure 3.7.4.3:** Detection of transcript spanning *fts*W-*mur*G using RT-PCR. 155
**Figure 3.7.5.1:** RT-PCRs to determine which of the $P_{mra}$ promoters contribute to transcription of the *mra* region. 156
**Figure 3.8.1:** Construction of the $P_{mra}$3 knockout vector pUCko3. 158

**Figure 4.3.1:** Autoradiograph of binding reactions using TP8503, RE201 (*fis*::Km) and RE202 (*fis*::Cm) soluble protein lysates with *fru*R-*yab*B intergenic region DNA. 167
**Figure 4.3.2:** Fractionation of DNA-binding proteins from a RE201 (*fis*::Km) soluble protein lysate using FPLC. 169
**Figure 4.3.3:** Autoradigraphs of interactions between DNA-binding proteins from a RE201 (*fis*::Km) lysate and fragments of the *fru*R-*yab*B intergenic region. 170
**Figure 4.3.4:** Autoradiograph of interactions between DNA-binding proteins in the C14 fraction, with the 400-600 bp DNA of the *fru*R-*yab*B intergenic region. 172
**Figure 4.3.5:** SDS-PAGE of the protein fractions produced by Ammonium sulfate precipitation of an RE201 (*fis*::Km) soluble protein lysate. 173
**Figure 4.3.6:** Autoradiographs of binding reactions between DNA from the *fru*R-*yab*B intergenic region with DNA-binding protein from a RE201 (*fis*::Km) soluble protein lysate, fractionated by ammonium sulfate precipitation. 175
**Figure 4.3.7:** Fractionation of DNA-binding proteins from a 60% ammonium sulfate cut of a RE201 (*fis*::Km) soluble protein lysate. 177
**Figure 4.3.8:** Autoradiograph of binding reactions between concentrated protein fraction 26 and the 400-600 bp DNA of the *fru*R-*yab*B intergenic region. 178
**Figure 4.3.9:** SDS-PAGE of the proteins present in fraction 26. 179
**Figure 4.3.10:** Identification of proteins present in fraction 26 by Mass Spectrometry. 180
**Figure 4.4.1:** Autoradiographs of stable complex assays using DNA with and without promoter regions. 183
**Figure 4.4.2:** Autoradiographs of stable complex assays using DNA fragments containing potential promoter sequences in the presence of RNA Polymerase. 184
**Figure 4.4.3:** β-galactosidase activity from potential promoters within the *mra* region. 188

**Figure 5.7:** Transcriptional Regulation of the $P_{mra}$ promoters. 200

## List of Tables

**Table 1.1:** $P_{mra}$ promoter sequences. 27
**Table 2.1:** List of antibiotics and reagents. 49
**Table 2.2:** List of strains used, their genotypes and their sources 50
**Table 2.3:** List of plasmids used, their construction and their sources. 51
**Table 2.4:** List of primers used in this study. 55
**Table 2.5:** Final Concentration of Ammonium sulfate. 80
**Table 4.1:** Promoter sequences, affinities for RNAP and relative activities of potential promoters of the *mra* region. 182

# Abbreviations.

| | |
|---|---|
| Amp | Ampicillin |
| APS | Ammonium persulphate |
| ADP | Adenosine 5′-diphosphate |
| ATP | Adenosine 5′-triphosphate |
| bp | Base pair |
| β-gal | β-galactosidase |
| *B. subtilis* | *Bacillus subtilis* |
| BSA | Bovine Serum Albumin |
| °C | Degrees Centrigrade |
| CAA | Casamino Acids |
| cDNA | Complementary DNA |
| Cm | Chloramphenicol |
| CRP | cAMP Receptor Protein |
| cps | Counts per second |
| CSPD | disodium 3-(4-methoxyspiro {1, 2-dioxetane-3, 2′-(5′-chloro) trichloro [3,3,1,1$^{3,7}$] decan}-4-yl) phenyl phosphate |
| CTD | Carboxy Terminal Domain |
| CTP | Cytosine 5′-triphoshsphate |
| DAPI | 4′-6-Diamidino-2-phenylindole |
| dATP | Deoxyriboadenosine-5′-triphosphate |
| dCTP | Deoxyribocytosine-5′-triphosphate |
| dGTP | Deoxyriboguanosine-5′-triphosphate |
| dTTP | Deoxyribothymine-5′-triphosphate |
| dNTP | Deoxyribonucleotide-5′-triphosphate |
| DEPC | Diethylpyrocarbonate |
| DIG | Digoxigenin |
| $dH_2O$ | Distilled water |
| DNA | Deoxyribonucleic acid |
| DNase | Deoxyribonuclease |
| ds | Double stranded |
| DTT | Dithiothreitol |
| *E. coli* | *Escherichia coli* |
| EDTA | Ethylenediamine-tetra-acetic acid |
| EMSA | Electrophoretic Mobility Shift Assay |
| FIS | Factor for Inversion Stimulation |
| FPLC | Fast Protein Liquid Chromatography |
| *fts* | Filamenting temperature sensitive |
| g | Gram |
| *g* | Gravitational force |
| GFP | Green Fluorescent Protein |
| GlcNAc | N-acetylglucosamine |
| GDP | Guanosine 5′-diphosphate |
| GTP | Guanosine 5′-triphoshsphate |
| H-NS | Histone-like Nucleoid Structuring Protein |
| HRP | Horse Radish Peroxidase |
| IHF | Integration Host Factor |
| iNTP | Initiating nucleotide-5′-triphosphate |
| IPTG | Isopropyl-$\beta_D$-thiogalactoside |

| | |
|---|---|
| Km | Kanamycin |
| kDa | Kilo Daltons |
| kb | Kilobase pairs |
| l | Litre |
| LB | Luria Broth |
| M | Molar |
| mA | Milli Ampere |
| MBP | Maltose Binding Protein |
| MBq | Mega Becqueral |
| mg | Milligram |
| ml | Millilitre |
| mM | Millimolar |
| MOPS | [3-(*N*-morpholino)-propanesulphonic acid |
| *mra* | Murein region A |
| mRNA | Messenger RNA |
| MU | Miller Units |
| MurNAc | N-acetylmuramic acid |
| M9 | Minimal Medium |
| Nal | Nalidixic acid |
| ng | Nanogram |
| nm | Nanometre |
| nmol | Nanomole |
| nM | Nanomolar |
| NTD | Amino Terminal Domain |
| OD | Optical density |
| ONPG | *Ortho*-nitrophenyl-$\beta$-$_D$-galactopyranoside |
| PBP | Penicillin Binding Protein |
| PCR | Polymerase chain reaction |
| PG | Peptidoglycan |
| pH | Power of Hydrogen |
| pmol | Picomole |
| PMSF | Phenyl Methyl sulfonyl fluoride |
| poly dIdC | Poly-deoxyinosinedeoxycytosine |
| ppGpp | Guanosine 3′, 5′ - bispyrophosphate |
| PVDF | Polyvinylidene difluoride |
| $^R$ | Resistant |
| rATP | Riboadenosine-5′-triphosphate |
| rCTP | Ribocytosine-5′-triphosphate |
| rGTP | Riboguanosine-5′-triphosphate |
| rUTP | Ribouridine -5′-triphoshsphate |
| rNTP | Ribonucleotide -5′-triphosphate |
| rRNA | Ribosomal RNA |
| Rif | Rifampicin |
| RNA | Ribonucleic acid |
| RNAP | RNA Polymerase |
| rpm | Revolutions per minute |
| RT-PCR | Reverse Transcription PCR |
| $^S$ | Sensitive |
| SDS-PAGE | Sodium Dodecyl Sulphate – Polyacrylamide Gel Electrophoresis |
| ss | Single stranded |

| | |
|---|---|
| Tet | Tetracycline |
| TEMED | *N, N, N', N'*-tetramethylethylenediamine |
| Tris | tris (hydroxymethyl)aminomethane |
| tRNA | Transfer RNA |
| TTP | Thymine 5'-triphosphate |
| XGAL | 5-bromo-4-chloro-3-indolyl-$\beta_D$-galactopyranoside |
| U | Units |
| UAS | Upstream Activating Sequence |
| UDP | Uridine diphosphate |
| UTP | Uridine triphosphate |
| UV | Ultra violet |
| V | Volts |
| µg | Microgram |
| µl | Microlitre |
| µM | Micromolar |
| µmol | Micromole |
| ~ | Approximately |

# Chapter 1: Introduction

## 1.1 Cell division in *Escherichia coli*

Cell division is one of the most fundamental processes that all living organisms, both unicellular and multicellular. In order to generate progeny, cells must replicate their chromosomes and divide. Cell division in bacteria is a highly complex process relying on strict regulation in order to co-ordinate the spatial and temporal initiation of septation with cell growth and the termination of DNA replication. Aberrant cell division could, for example, result in progeny failing to receive a full complement of DNA (Margolin, 2000).

Much of our knowledge about the parameters within the division cycle of *Escherichia coli* is based on definitive studies performed in the 1960s by Cooper & Helmstetter using synchronous cultures of *E. coli* B/r (Cooper & Helmstetter, 1968). *E. coli* is a Gram negative bacterium which divides by binary fission (Figure 1.1). First, a new-born cell grows by lateral extension of the cell wall. Once the cell has reached the initiation mass, $2M_u$ (where $M_u$ is the minimum 'unit' cell mass; Donachie, 1991), replication of DNA is initiated from the single *ori*C site (Donachie, 1968). Replication of the single circular chromosome occurs bi-directionally and takes approximately 40 minutes to complete (Cooper & Helmstetter, 1968). Lateral wall elongation continues during DNA replication and results in the cell reaching a critical length of $2L_u$ (where $L_u$ is the minimum 'unit' cell length), which coincides with termination of DNA replication and segregation of the sister nucleoids towards the cell poles (Donachie *et al.*, 1976; Donachie, 1991). Completion of nucleoid segregation coincides with localisation of the tubulin-like protein FtsZ at the midcell and the onset of septation. (reviewed by Dewar & Dorazi, 2000). The Z-ring acts as a scaffold for the septal ring – a macromolecular complex consisting of at least 13 different proteins which are sequentially recruited to the midcell. Many of these proteins are membrane-associated and tether the cytoplasmic membrane to the contractile Z-ring (reviewed by Weiss, 2004). Inward growth of the peptidoglycan layer is associated with constriction of the Z-ring which leads to invagination of the cytoplasmic membrane and formation of the cell septum (Höltje, 1998). Elongation of the cell continues during septation, a process which lasts for approximately 20 minutes (Cooper & Helmstetter, 1968), until the septum fuses releasing two new daughter cells.

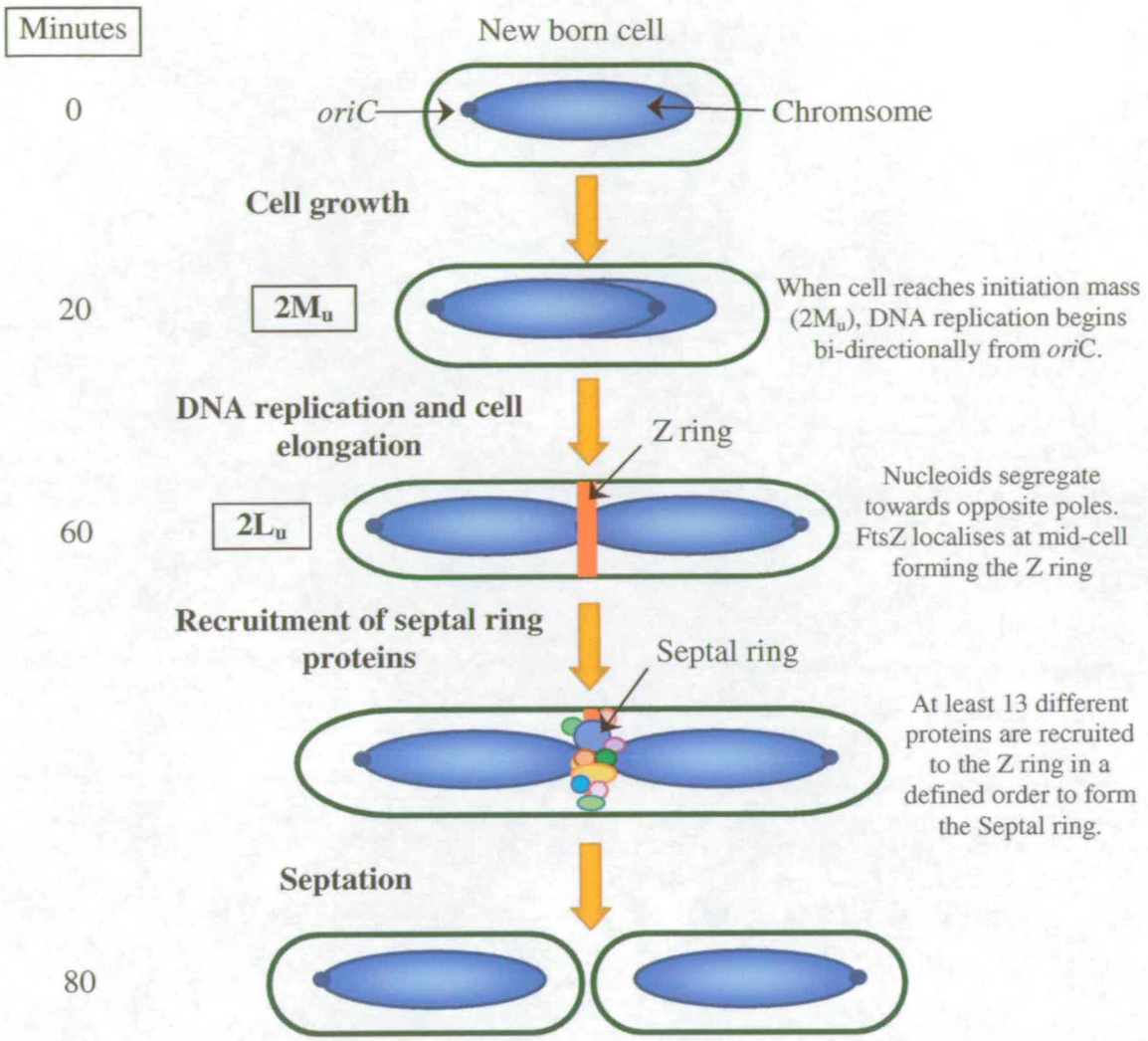


**Figure 1.1: Cell division in *E. coli*.**
Illustration of the key steps during cell division in *E. coli* with a doubling time of 80 minutes. The cell grows by lateral extension of the cell wall, until the mass of the cell has increased to the initiation mass ($2M_u$). The time taken to do this depends on the growth rate of the cell. This figure depicts a cell with a doubling time of 80 minutes, therefore it takes approximately 20 minutes for a new born cell to reach $2M_u$. At the initiation mass, replication of the single circular chromosome begins in a bi-directional fashion from *ori*C. Replication of the entire chromosome takes around 40 minutes, and terminates at the same time as the cell reaches the critical length of $2L_u$ (where $L_u$ is the minimum 'unit' cell length). As the nucleoids begin to segregate toward opposite cell poles there is an accumulation of FtsZ at the mid-cell where it forms the Z-ring. The Z-ring acts as a scaffold for interactions with at least 13 other proteins. These proteins are recruited to the mid-cell in a defined order to form the septal ring, which tethers the contractile Z-ring to the cytoplasmic membrane. Septation ensues with contraction of the Z-ring associated with inward growth of the peptidoglycan. This generates a septum and after approximately 20 minutes the septum walls fuse to release two new daughter cells.

Rapidly growing cells are larger than slow growing cells and initiate additional rounds of replication every time they double their basic mass and reach $2M_u$ (Donachie, *et al.*, 1976; Donachie, 1991), therefore cells with doubling times less than 40 minutes, initiate multiple rounds of DNA replication within a single division cycle (Cooper & Helmstetter, 1968). Only the oldest round of replication is terminated 20 minutes prior to division, therefore newly born cells already contain partially replicated chromosomes. This allows cells to divide more rapidly than if they had to initiate replication after each division event.

Since rapidly growing cells are larger than slow growing cells (Donachie *et al.*, 1976), it is predicted that they may require fewer cell division proteins per mass to form the septal machinery than a slow growing cell of the same strain. This is based on evidence that the amount of FtsZ and FtsA sets the frequency of division (Begg, *et al.*, 1998). This may indicate that the expression of many cell division proteins is regulated by changes in growth rate or cell size, as has been shown for expression of FtsZ (Aldea *et al.*, 1990).

### 1.1.1: FtsZ and assembly of the Z-ring.

FtsZ is one the most important proteins involved in septation of the cell as it is the first protein to accumulate at the mid-cell prior to division, where it forms a ring or tight spiral which acts as a scaffold for the other proteins of the septal ring (Romberg & Levin, 2003). FtsZ is the most abundant cell division protein and is essential for cell viability. *Fts* (for filamenting temperature sensitive) genes acquired their names from the screening of conditional lethal mutants that formed aseptate filaments with regularly spaced nucleoids at nonpermissive temperatures (Lutkenhaus & Mukherjee, 1997). FtsZ mutants produce smooth filamentous cells at non-permissive temperatures, in contrast to mutations in genes that encode septal ring proteins such as *ftsA* which exhibit indented filaments where septation has begun but not completed (Taschner *et al.*, 1988). FtsZ is a cytosolic protein of 40 kDa (Löwe & Amos, 1998), with approximately 3,000-5,000 molecules per cell (Rueda *et al.*, 2003). FtsZ levels remain relatively constant during the growth cycle in batch culture, with FtsZ dispersed throughout the cytosol (Rueda *et al.*, 2003; Weart & Levin, 2003). However, *ftsZ* transcription has been shown to oscillate during the division cycle due to transient

inhibition of transcription when the *mra* region is being replicated (Zhou & Helmstetter, 1994).

FtsZ is a ubiquitous protein with homologues found in almost all bacteria, many archaebacteria and even organelles such as chloroplasts and mitochondria (Wang & Lutkenhaus, 1996; Lutkenhaus & Mukherjee, 1997; Margolin, 2000). FtsZ is a tubulin-like protein with GTPase activity (Erickson, 1995; Wang & Lutkenhaus, 1996). There is only 10-18% sequence identity between FtsZ and tubulin, however structurally both proteins are remarkably similar (Figure 1.1.1.a). In addition, both FtsZ and tubulin exhibit GTP-dependent polymerisation into filamentous structures (van den Ent *et al.*, 2001). FtsZ can be divided into two domains; a large and highly conserved N-terminal domain containing the GTPase region and a highly variable C-terminal domain (Wang *et al.*, 1997). Polymerised FtsZ has been observed to assemble into protofilaments (Bramhill & Thompson, 1994) with monomers interacting end on end with GTP sandwiched in this interface (Redick *et al.*, 2005). FtsZ protofilaments are around 7nm wide and the presence of $CaCl_2$ promoted lateral interactions between the protofilaments, resulting in bundles of FtsZ of around 38nm (4-5 protofilaments) in width (Mukherjee & Lutkenhaus, 1999). FtsZ protofilaments have also been observed to form sheets, ribbons and ring like structures via lateral interactions (Wang *et al.*, 1997; Mingorance *et al.*, 2001). These interactions are dependent on the hydrophobic loop located between helix 6 and helix 7 of FtsZ monomers (Figure 1.1.1.a ; Koppelman *et al.*, 2004).

Immunolocalisation has shown that, prior to division, FtsZ migrates to midcell (Figure 1.1.1.b) where it initially forms a small focus of protein that extends bi-directionally around the circumference of the cell, a process that takes around one minute (Addinall & Lutkenhaus, 1996; Sun & Margolin, 1998). The Z-ring is thought to be composed of bundled protofilaments localised just beneath the surface of the cytoplasmic membrane (Liu *et al.*, 1999). However, the FtsZ polymer has yet to be observed by microscopy, although its width is predicted to be 6-8 protofilaments (Anderson *et al.*, 2004). This prediction is based on there being 15,000 molecules of FtsZ per cell as measured by Lu *et* al, (1998), however recent quantification of cellular FtsZ by Rueda *et al.*, (2003) indicates there may only be 3,000-5000

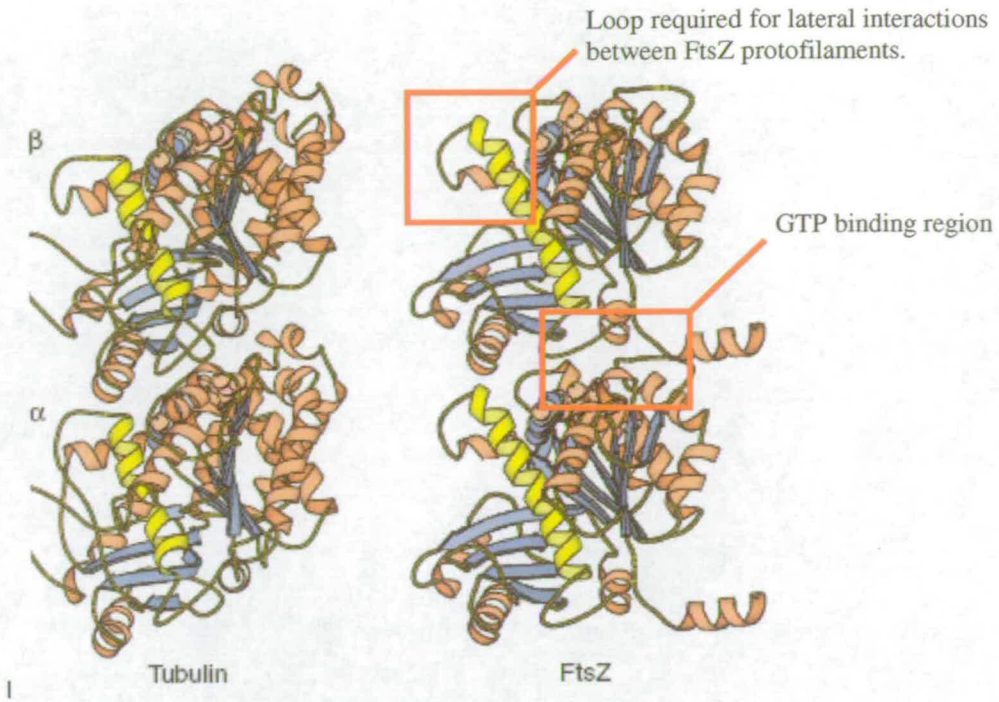


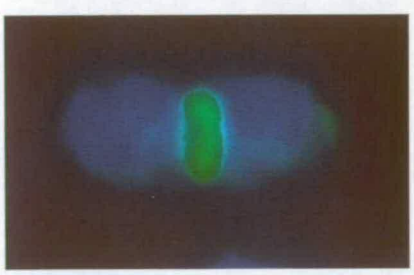


**Figure 1.1.1: FtsZ and its localisation to the Z-ring.**
**a.** Three-dimensional structures of a tubulin heterodimer and an FtsZ dimer which highlights their structural similarity despite low sequence identity. The GTP binding region between the FtsZ monomers is shown. The hydrophobic loop located between helices 6 and 7 is essential for lateral interaction between FtsZ protofilaments. Figures taken from van den Ent *et al.*, (2001).
**b.** Immunostaining of FtsZ using anti-FtsZ mAb. The Z-ring is localised to the midcell. Micrograph courtesy of G. Blakely.

molecules per cell which would reduce the width of the Z-ring to 2 protofilaments, similar to the Z-ring width predicted for *B. subtilis* (Anderson *et al.*, 2004). It is still unclear what initiates the polymerisation of FtsZ at midcell at a defined time in the division cycle. Weart & Levin (2003) report that FtsZ levels remain relatively constant during the cell cycle suggesting that assembly of the Z-ring is governed by

changes in FtsZ polymerisation dynamics. For example, at the appropriate time for Z-ring formation the cell may either express an activator of polymerisation (this may be activation of an FtsZ nucleation site, as suggested by Lutkenhaus, 1993), or relieve potential inhibition of polymerisation (Weart & Levin, 2003). The Z-ring is a highly dynamic structure, as shown by FRAP analysis (Stricker *et al.*,2002; Anderson *et al.*, 2004). These experiments showed that only 30% of cellular FtsZ forms the Z-ring, but that the FtsZ in the ring undergoes continuous and rapid exchange, potentially exchanging every 9 seconds with FtsZ polymers present in the cytosol (Anderson *et al.*, 2004). The rate of this exchange is governed by GTP hydrolysis mediated by FtsZ in the Z-ring (Stricker *et al*, 2002). It is unclear whether the Z-ring is comprised of a few very long protofilaments that could encircle the 3,000 nm circumference of the cell, or if it is an assembly of short protofilaments. It has been predicted that during the 9 second turnover time of FtsZ polymers at the Z-ring, protofilaments could grow around 45 subunits in length. A 45 subunit protofilament would be 200nm in length suggesting that the Z ring consists of numerous short FtsZ protofilaments (Anderson *et al*, 2004).

### 1.1.2: Division site selection in *E. coli*

In the past decade much work has focused on the mechanisms involved in division site placement. Two key processes have been identified; nucleoid occlusion and inhibition of polar FtsZ assembly by the Min system. These mechanisms prevent aberrant cell division and focus assembly of the Z-ring to the midcell division site in vegative cells (Figure 1.1.2.1).

Nucleoid occlusion was first postulated by Mulder and Woldringh (1989), when they observed that cell division was inhibited when DNA replication or segregation was blocked. The nucleoid occupies a large percentage of the cell, with the only nucleoid free regions occurring at the cell poles and at midcell following segregation of the replicated chromosomes (Margolin, 2001). The nucleoid occlusion model suggests that all positions along the cell are potential division sites, but that division is prevented in the vicinity of the nucleoid (Yu & Margolin, 1999). Recently, two proteins that appear to mediate nucleoid occlusion have been identified; Noc in *B. subtilis* (Wu & Errington, 2004) and SlmA in *E. coli* (Bernhardt & de Boer, 2005).

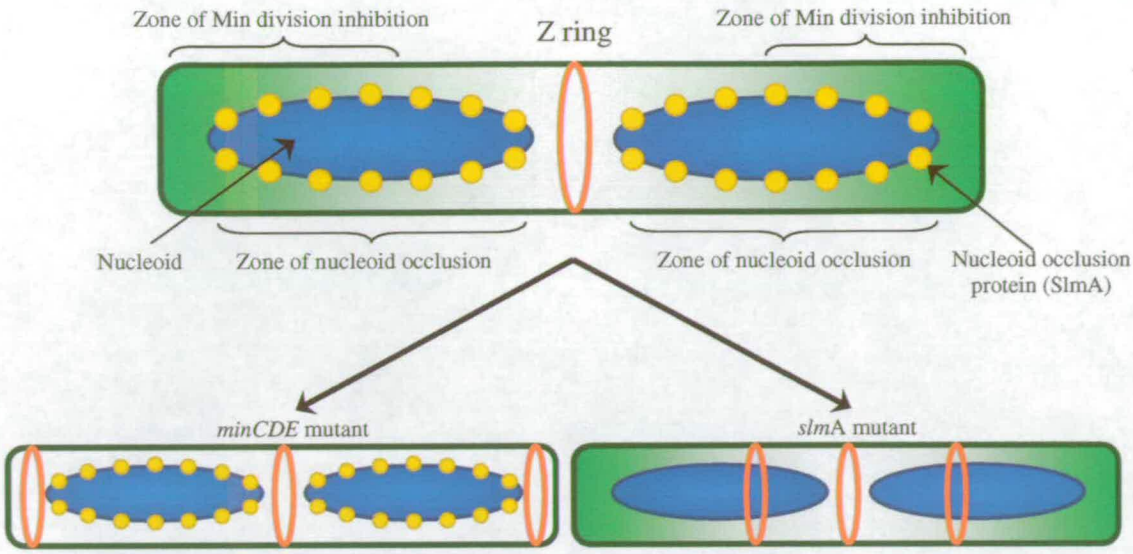


**Figure 1.1.2.1: Division site selection in *E. coli*.**
The positioning of FtsZ at the future division site at mid-cell is determined by two mechanisms; the Min system and nucleoid occlusion. When genes of the Min system are knocked out, anucleate mini cells are produced as a result of Z-ring formation and septation near the cell pole. This polar division would usually be prevented by the Z-ring inhibitor MinC, which requires MinD for association with the membrane and MinE for pole to pole oscillation. When a cell is unable to make nucleoid occlusion proteins guillotining of the chromosome can be observed. This is usually prevented by a nucleoid associated protein such as SlmA which inhibits Z-ring assembly in the vicinity of the nucleoid. The combined inhibitory mechanisms of the Min system and nucleoid occlusion allow Z-ring assembly to occur only at the midcell. Figure adapted from Goehring & Beckwith (2005) and Rothfield *et al.*, (2005).

These proteins were identified because they were essential for division in cells with non-functional Min systems. GFP-fusions of Noc and SlmA were localised to the nucleoid and SlmA was shown to interact directly with FtsZ. It is not yet clear whether SlmA destabilises FtsZ polymerisation or if it acts to sequester FtsZ at the nucleoid therefore inhibiting assembly of the Z ring (Wu & Errington, 2004; Bernhardt & de Boer, 2005). It should be noted that nucleoid occlusion is perturbed in *muk*B mutants since Z-rings can assemble on top of decondensed nucleoids, suggesting that the topology and compactness of chromosomal DNA plays an important role in preventing Z-ring formation (Sun & Margolin, 1998). Nucleoid occlusion is similar to a eukaryotic cell-cycle checkpoint; it inhibits cell division at mid-cell during much of the cell cycle and ensures that septation only occurs when the replicated chromosomes have segregated sufficiently to relieve the inhibition of Z-ring assembly (Margolin, 2001). In addition, nucleoid occlusion may represent a fail

safe mechanism for the cell to inhibit division if chromosome replication or segregation is perturbed (Wu & Errington, 2004; Rothfield *et al.*, 2005).

The second mechanism required for accurate positioning of the Z-ring is the Min system. The Min system is based on the positional oscillation of three proteins within the cell; MinC, MinD and MinE (reviewed by Margolin, 2001; Figure 1.1.2.2). In the absence of these proteins, anucleate mini cells are produced as a result of division occurring not only at midcell but also near the cell poles (Lutkenhaus & Mukherjee, 1997). MinC is a homodimer, with each monomer consisting of two domains connected by a flexible linker. The N-terminal domain interacts with FtsZ and inhibits assembly of the Z-ring, while the C-terminal domain is involved in dimerisation and interactions with the ATPase MinD which recruits MinC to the membrane (Hu *et al.*, 1999; Hu & Lutkenhaus, 2000). MinD requires ATP for dimerisation and it is thought that dimerisation affects the conformation of the C-terminal region of MinD, enabling it to bind to the membrane (Hu & Lutkenhaus, 2003). MinD rapidly oscillates from pole to pole along a helical path every 20 seconds (Raskin & de Boer, 1999a). MinC oscillates passively along the same path due to its interactions with MinD, resulting in the time averaged concentration of MinC being greatest at the cell poles. This allows formation of the Z-ring only at midcell where MinC concentrations are lowest (Raskin & de Boer, 1999b; Hu & Lutkenhaus, 1999). The topological specificity of the Min system in imparted by MinE (de Boer *et al.*, 1989). GFP fusions have shown that MinE follows MinCD to the cell pole along a concentration gradient, where it stimulates MinD-ATP hydrolysis causing the release of MinD from the membrane (Lutkenhaus, 2002). MinE was initially reported as a static ring near the midcell, but has been shown to migrate from pole to pole (Hale *et al.*, 2001; Fu *et al.*, 2001). Recently Shih *et al.*, (2003) observed that MinE also migrated along the same helical path as MinD and MinC, and it has been suggested that the proteins may interact with a permanent helical framework in the cell. This protein scaffold was initially predicted to be the helical array of MreB, an actin like protein involved in maintaining the rod shape of the cell (Shih *et al.*, 2003), however, the MreB coiled structures have a greater pitch than the MinCDE spirals (Gitai & Shapiro, 2003). It may be the case that MinD and MinE form a permanent scaffold for the movement of Min proteins, since MinD has been shown to form extended linear structures *in vitro* which are

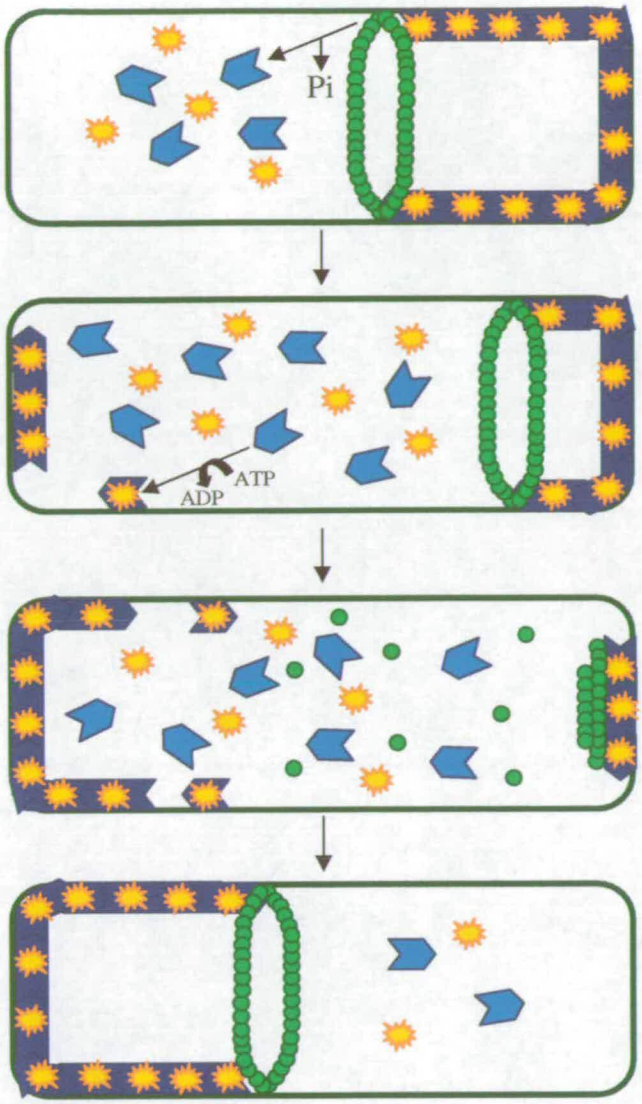


**Figure 1.1.2.2: The Min System in *E. coli*.**
Illustration of the pole to pole oscillations of the Min proteins in *E. coli*. The Min system inhibits aberrant assembly of Z-rings at locations other than midcell. MinC (yellow) is an inhibitor of Z-ring assembly and is recruited to the cell membrane in an ATP-dependent fashion by MinD (ATP) (dark blue). MinE (green) follows MinCD to the membrane along a concentration gradient. MinE causes the release of MinD from the membrane by stimulating ATP hydrolysis. MinD (ADP) (light blue) and MinC are redispersed separately through the cell as MinC only interacts with ATP bound MinD. MinD undergoes nucleotide exchange allowing it to interact with the membrane at the opposite pole, where it recruits MinC resulting in the time averaged concentration of the Z-ring inhibitor being lowest at midcell. The oscillation of Min proteins from pole to pole occurs along a helical path and has been observed to take 20 seconds. Figure adapted from Lutkenhaus, (2002).

stabilised by MinE. It has been suggested that these linear MinD filaments may interact as protofilaments to form the coiled arrays observed using YFP fusions (Shih *et al.*, 2003).

The Min system is present in many prokaryotes with homologs of MinD observed across a broad range of species and even present in *Arabidopsis* where it is required for proper positioning of the chloroplast division site, however MinC and MinE are less well conserved (Margolin, 2001; Errington *et al.*, 2003). For example, *B. subtilis* has no MinE homologue, and MinCD are recruited to the membrane by DivIVA (Edwards & Errington, 1997). DivIVA remains stably associated with MinCD at newly formed poles after division, therefore preventing future division at those sites (Marston & Errington, 1999). A number of bacterial species, in particular gram-positive cocci such as *S. aureus* lack any full Min system and it is thought that nucleoid occlusion may be the principle mechanism for accurate division site placement in such organisms (Margolin, 2001; Errington *et al.*, 2003).

### 1.1.3: The Septal Ring.

Once the Z-ring has formed at midcell it becomes the recruitment site for the 13 other proteins so far identified to form the septal ring (reviewed by Weiss, 2004). It is not yet clear how these proteins interact with each other, but a hierarchical order of localisation has been established using GFP fusions and immunolocalisation in different *fts* mutant backgrounds (Addinall & Lutkenhaus, 1996; Hale & de Boer, 1999; Weiss *et al.*, 1999; Buddelmeijer & Beckwith, 2002). A series of bacterial two-hybrid assays has also been used to determine interactions between proteins of the septal ring (Di Lallo, *et al.*, 2003). The results suggested that there are numerous interactions between the constituent parts of the septal ring, but the reported order of recruitment was in agreement with previous observations with a linear assembly sequence of FtsZ, FtsA, ZipA, FtsK, FtsQ, FtsL, FtsW, FtsI, FtsN (Di Lallo *et al.*, 2003). In recent years five additional proteins; ZapA, FtsL, AmiC, FtsE and FtsX have been localised to the septal ring (Gueiros-Filho & Losick, 2002; Buddelmeijer *et al,* 2002; Bernhardt & de Boer, 2003; Schmidt *et al*, 2004). Figure 1.1.3.1 illustrates the current understanding of the order of recruitment of proteins to the septal ring.

FtsA, ZipA and ZapA appear to localise immediately after formation of the Z-ring at the midcell, and are required for its stabilisation (Rueda *et al.*, 2003; Gueiros-Filho &

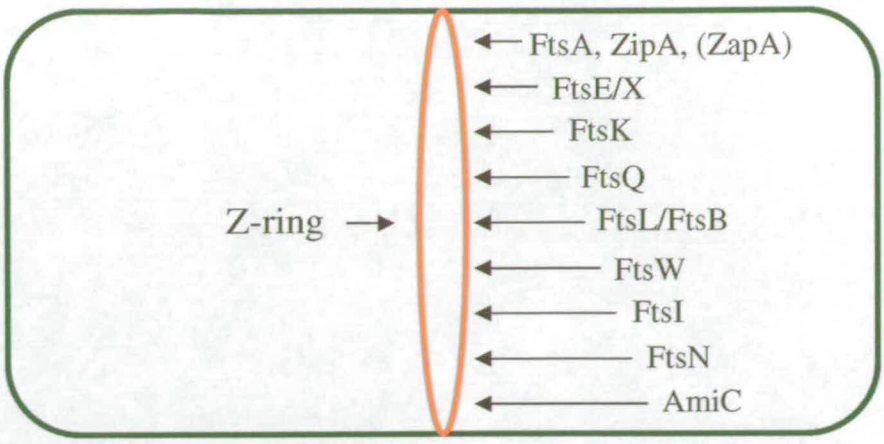


**Figure 1.1.3.1. Order of assembly of the septal ring.**
FtsZ localises to midcell and assembles into a ring structure. FtsA, ZipA and ZapA are then localised to midcell where they function to stabilise the Z-ring. Localisation of FtsE/X requires the presence of FtsA and ZipA, although ZapA is not necessary for recruitment of later proteins to the septal ring. FtsK follows FtsE/X to the septal ring and is required for the recruitment of FtsQ and the co-dependent localisation of FtsL/B. FtsW followed by FtsI and FtsN arrive at the division site, with AmiC being the last component of a fully competent septal ring. Figure copied from Schmidt *et al.* (2004).

Losick, 2002; Pichoff & Lutkenhaus, 2002). The essential cell division protein FtsA is an ATPase and a member of the actin family (Sánchez *et al.*, 1994). FtsA has been shown to interact directly with the distal end of the unconserved C-terminus of FtsZ (Wang *et al.*, 1997; Ma & Margolin, 1999). FtsA is a cytosolic protein that has been shown to be membrane-associated due to a C-terminal amphipathic helix that targets the protein to the membrane; this may indicate that a role of FtsA is to tether the Z-ring to the membrane (Sánchez *et al.*, 1994; Pichoff & Lutkenhaus, 2005). A fixed ratio of FtsZ to FtsA must be maintained for septation to occur since it has been shown that overexpression of FtsA will block cell division (Dai & Lutkenhaus, 1992; Dewar *et al.*, 1992). The ratio of FtsZ to FtsA was thought to be 100:1, but this was based on an estimated 15,000-20,000 molecules of FtsZ and 200 molecules of FtsA (Bi & Lutkenhaus, 1991; Pla *et al.*, 1990). However, recent quantification of protein concentrations by Rueda *et al.*, (2003) indicates that there are 3,000-5000 molecules of FtsZ and around 740 molecules of FtsA. This reduces the FtsZ to FtsA ratio to 5:1 which is similar to the ratio determined for *B. subtilis* (Feucht *et al.*, 2001).

Z interacting protein or ZipA, was identified by affinity purification of proteins that interacted directly with FtsZ (Hale & de Boer, 1997). *zipA* mutants exhibit filamentation with fewer Z rings than would be expected, suggesting a role for ZipA in stabilisation of the Z ring (Hale & de Boer, 1999). *In vitro* ZipA has been shown to

bind and bundle FtsZ polymers, this may be the method by which ZipA stabilises the Z ring *in vivo* (Hale *et al.*, 2000). ZipA is a cytoplasmic membrane protein with 1,000-1,500 molecules per cell (Rueda *et al.*, 2003). ZipA contains an N-terminal membrane anchor domain (Hale & de Boer, 1997; Liu *et al.*, 1999), and a C-terminal domain that binds to the final 20 C-terminal amino acid residues of FtsZ (Hale *et al.*, 2000). ZipA and FtsA appear to have overlapping roles in cell division. They both stabilise the Z-ring and potentially tether it to the cytoplasmic membrane and they both interact with the small C-terminal domain of FtsZ, although they probably do not compete for binding sites on the same FtsZ molecule (Pichoff & Lutkenhaus, 2002). A mutation of FtsA at R268 has been shown to compensate entirely for the loss of ZipA and cells can divide normally (Geissler *et al.*, 2003), which may suggest that FtsA has the potential to perform all of the FtsZ stabilisation, membrane interaction and septal ring recruitment functions of ZipA. This may also explain why FtsA is well conserved in many other bacteria while only a few Gram negative organisms contain ZipA homologues (Goerhing and Beckwith, 2005).

ZapA (YgfE) is a recently discovered *E. coli* orthologue of the *Bacillus subtilis* protein ZapA, found to co-localise with the Z ring *in vivo* (Gueiros-Filho & Losick, 2002). ZapA increases the stability of FtsZ protofilaments and is thought to function in the assembly of higher order FtsZ structures. Although ZapA is recruited to the Z-ring at the same time as FtsA and ZipA, it functions independently. In addition, ZapA is not essential for cell viability and is not required to recruit downstream proteins to the septal ring (Gueiros-Filho & Losick, 2002).

The protein complex of FtsE and FtsX are the next components of the septal ring to be recruited to midcell (Schmidt *et al.*, 2004). The *ftsE* and *ftsX* genes are located at 76 minutes on the *E. coli* chromosome and were linked to cell division in the 1960s when it was observed that *ftsEX* mutants had a division defect, although division could be restored by the addition of NaCl into the growth medium (Ricard & Hirota, 1973). FtsE and FtsX have homology to the ABC transporter family of proteins (Gill *et al.*, 1986). It has been speculated that FtsEX may be required for the insertion of a division protein into the cytoplasmic membrane, or that FtsX may act as a membrane anchor, while FtsE hydrolyses ATP to provide energy for the constriction of the septal ring (Schmidt *et al*,. 2004).

FtsK is the sixth protein to localise to the septal ring. It is a large 1330 amino acid, essential cell division protein, with three functional domains and is highly conserved throughout the eubacteria (Begg *et al.*, 1995; Bigot *et al.*, 2004, Errington *et al.*, 2003). The small N-terminal domain targets FtsK to the developing septum and has been predicted to span the membrane four times (Draper *et al.*, 1998; Dorazi & Dewar, 2000). A flexible linker connects the N-terminal domain to the large 1128 amino acid, cytoplasmic C-terminal domain (Steiner *et al.*, 1999; Geissler & Margolin, 2005). The C-terminal domain is not required for cell division, but plays two roles in chromosome dimer resolution (Bigot *et al.*, 2004). It directly activates XerCD-*dif* site-specific recombination, and it translocates DNA at ~6.7kbp/s in an ATP-dependent manner through the closing septum (Bigot *et al.*, 2004; Saleh *et al.*, 2004). It has recently been shown that division can occur in the absence of FtsK, if other cell division proteins such as FtsZ, FtsA, FtsB, FtsQ and ZipA are overexpressed. This indicates that FtsK is not directly required for the recruitment of later cell division proteins but that it may stabilise the Z-ring and formation of the septal ring, which itself may be sufficient for recruitment of downstream proteins (Geissler & Margolin, 2005).

FtsQ is recruited to the septum after FtsK. It is a low abundance 276 amino acid protein with only around 22 molecules per cell (Carson *et al.*, 1991). FtsQ has a short N-terminal cytoplasmic domain attached by a single transmembrane region to the C-terminal periplasmic domain which is essential for its role in cell division (Chen *et al.*, 2002). Although the short cytoplasmic domain linked to the transmembrane region of FtsQ is dispensable for cell division, it is thought that it may contribute to stabilisation of the Z-ring, since this region was sufficient to permit viability in the absence of FtsK (Geissler & Margolin, 2005). FtsQ can localise to the septum on its own, but it has recently been shown that FtsQ also interacts with FtsL and FtsB to increase the stability of their interactions with each other, and to localise them to the septum (Buddelmeijer & Beckwith, 2004).

FtsL and FtsB are small transmembrane proteins, each with a single cytoplasmic, transmembrane and periplasmic domain. The periplasmic domains each contain a leucine zipper-like motif used for interactions between the two proteins (Ghigo & Beckwith, 2000; Buddelmeijer & Beckwith, 2004). A bioinformatic search was used

to find potential interacting partners for FtsL that also contained a leucine zipper-like motif and that were predicted to be integral cytoplasmic membrane proteins. A match was made with a *Vibrio cholerae* protein also present in *E. coli* called YgbQ (FtsB) (Buddelmeijer *et al.*, 2002). FtsL is unstable in the absence of FtsB and it is predicted that the two proteins interact, forming a coiled coil structure within the heterodimer (Buddelmeijer *et al.*, 2002). This heterodimer requires FtsQ to stabilise the protein:protein interactions and to localise the complex to the division site (Buddelmeijer & Beckwith, 2004).

FtsW is present in almost all bacteria that have a peptidoglycan cell wall (Pastoret *et al.*, 2004). It is a large integral membrane protein of around 46kDa in mass, which contains 10 transmembrane segments (TMSs) (Boyle *et al.*, 1997; Lara & Ayala, 2002). FtsW has been shown to localise to the septum, however nothing is yet known about FtsW function or how it is recruited to the septal apparatus (Wang *et al.*, 1998). FtsW was initially thought to play a role in stabilising the Z-ring (Khattar *et al.*, 1997), however bacterial two-hybrid analysis failed to detect any FtsW-FtsZ interactions (Di Lallo, *et al.*, 2003). The periplasmic loop between TMS 9 and 10 was shown to be involved in recruiting FtsI to the septum, while the loop between TMS 7 and 8 was shown to be essential for the functioning of FtsW (Pastoret *et al.*, 2004). Since FtsW is a transmembrane protein it is possibly involved in peptidoglycan biosynthesis by directing the flow of lipid II precursors towards the periplasmic domain of Penicillin Binding Protein 3 (PBP3) (Figure 1.1.4.1)

FtsI is also known as Penicillin Binding Protein 3 (PBP3), and is recruited to the septum by FtsW (Mercer & Weiss, 2002). FtsI is a high molecular weight protein (63.7kDa) with a short cytoplasmic domain and single membrane-spanning segment required for recruitment to the septum. The membrane spanning segment is attached to a non-catalytic domain of unknown function and a large periplasmic domain which is involved in the transpeptidation of septal peptidoglycan (Weiss *et al.*, 1999, Wissel & Weiss, 2004). FtsI is involved in the cross-linking of new peptidoglycan strands which insert into the growing cell sacculus (Lutkenhaus & Mukherjee, 1997). The transpeptidase catalytic activity of FtsI is the target of β-lactam antibiotics such as Penicillin, Cephalexin and Furazlocillin (Begg *et al.*, 1986; Eberhardt *et al.*, 2003). It has been reported that the catalytic activity of FtsI is dependent on interactions with

other septal ring proteins, which would temporally and spatially regulate the activity of this enzyme (Eberhardt *et al.*, 2003). These interactions, particularly those required for recruitment of FtsN, have been located to the periplasmic non-catalytic domain of FtsI (Wissel & Weiss, 2004).

FtsN is the penultimate cell division protein recruited to the septal ring (Addinall *et al.*, 1997). It was first isolated as a suppressor of a temperature sensitive *ftsA* mutation and was also found to suppress *ftsI* and *ftsQ* mutations (Buddelmeijer & Beckwith, 2002). FtsN is a 36kDa protein, with around 1,000 molecules per cell (Ursinus *et al.*, 2004; Aarsman *et al.*, 2005). FtsN contains a short cytoplasmic domain, linked via a membrane-spanning helix to a large C-terminal periplasmic domain (Yang *et al.*, 2004). The role of FtsN in division is not well understood, however the periplasmic domain is responsible for its septal localisation and its function (Yang *et al.*, 2004). FtsN shows weak sequence similarity to cell wall amidases (for example, Cw1C and SpoIIB in *B. subtilis*) suggesting a possible role in hydrolysis and shaping of the new cell poles at the septum (Errington *et al.*, 2003). It has also been shown that FtsN binds to the glycan chains of peptidoglycan during cell division, however this function was not found to be essential for septation (Ursinus *et al.*, 2004).

The protein recruited last to the septal ring is the periplasmic protein amidase C. AmiC is a member of the *E. coli* N-acetylmuramoyl-$_L$-alanine amidases which remove murein crosslinks by cleaving peptides from N-acetylmuramic acid (MurNAc) (Bernhardt & de Boer, 2003). Amidase mutants form chains, suggesting a role in cell division (Höltje & Heidrich, 2001), and AmiC was observed to localise to the division site using a GFP fusion (Bernhardt & de Boer, 2003). AmiC has four functional domains; an N-terminal Tat signal sequence required for transport to the periplasm, a targeting domain which is necessary and sufficient for localisation to the septal ring, a linker sequence and an amidase catalytic domain (Weiss, 2004).

An additional protein has recently been shown to localise to the midcell, however its position in the hierarchy of recruitment is as yet undetermined therefore it is not included in Figure 1.1.3.1. EnvC is a periplasmic protein with two recognisable domains; a large N-terminal domain that is predicted to form two or three coiled-coil structures, and a small C-terminal domain predicted to have peptidase activity (Hara

*et al.*, 2002). It has been predicted that the coiled-coils of EnvC may interact with the coiled-coils in the periplasmic domains of FtsL and FtsB (Bernhardt & de Boer, 2004). In addition, EnvC has weak endopeptidase activity on β-casein and is structurally similar to the endopeptidase lysostaphin suggesting that it may cleave the peptide cross-links in peptidoglycan (Ichimura, *et al.*, 2002; Hara *et al.*, 2002).

Recently, a two-stage model for the formation of the septal ring was proposed (Aarsman *et al.*, 2005). In the first stage, FtsZ is polymerised into the Z-ring which is stabilised by the recruitment of ZipA, FtsA and ZapA. It is not clear whether FtsE/X and FtsK are involved in this first stage of septum formation or if they are included in the second stage. The second stage occurs 17 minutes after the first with the recruitment of the remaining septal ring proteins, which are predicted to be involved in determining the shape of the new cell poles. The recruitment of proteins during this second stage of septal ring formation is predicted to take 1-3 minutes (Aarsman *et al.*, 2005). The requirement of a two-stage recruitment process is thought to be linked to inward growth of the septal peptidoglycan. It has been suggested that FtsZ initiates cell division by switching lateral peptidoglycan synthesis to increased inward peptidoglycan growth at midcell. When sufficient new peptidoglycan has formed at the future cell poles, the second stage of recruitment can occur which brings proteins to midcell that can determine the shape of the new cell pole (Aarsman *et al.*, 2005). It is possible that the time delay in formation of the septal ring is mediated by the methylation state of FtsE/X or FtsK, since proteins recruited downstream of these are not localised to the septum in strains lacking S-adenosylmethionine synthetase (Wang *et al.*, 2005).

With the septal ring in place the cell can initiate division. Formation of the septum in *E. coli* is thought to be driven by two mechanisms; the inward growth of the cell envelope (cytoplasmic membrane, peptidoglycan wall and outer membrane), and constriction of the Z-ring (Weiss, 2004; Errington *et al.*, 2003). The occurrence of FtsZ in wall-less bacteria, archaebacteria and chloroplasts suggests that constriction of the Z-ring may be the predominant force that drives septation, and that invagination of the cytoplasmic membrane may indirectly stimulate septal peptidoglycan synthesis (Wang & Lutkenhaus, 1996; Lutkenhaus & Mukherjee, 1997). It is still unclear what drives constriction of the Z-ring, however Lu *et al.*, (2000) reported that FtsZ

protofilaments were straight in the presence of GTP but curved and formed a helical structure in the presence of GDP. They propose that FtsZ-GTP is required for assembly of the Z-ring from straight protofilaments, but that assembly induces GTP-hydrolysis resulting in curvature of the protofilaments and constriction of the Z-ring (Lu *et al.*, 2000).

### 1.1.4: Peptidoglycan biosynthesis during cell division.

*E. coli* cells are surrounded by a single, monolayered, highly dynamic macromolecule called the peptidoglycan (or murein) sacculus (de Pedro *et al.*, 1997). Peptidoglycan provides a stress-bearing, and shape maintaining protective wall between the cell and its environment. The cell wall has been shown to contain molecules which act as virulence factors and others which trigger the innate immune response in humans (de Pedro *et al.*, 2001; Varma & Young, 2004). Peptidoglycan is composed of glycan strands formed from disaccharide units of N-acetylglucosamine (GlcNAc) and N-acetylmuramic acid (MurNAc). These chains are interconnected by peptide bonds between peptide side chains on the glycan strands (Nanninga, 1998). The sacculus is able to grow due to the insertion of new peptidoglycan strands with the aid of Penicillin Binding Proteins (PBPs) (de Pedro *et al.*, 2001). The insertion of these peptidoglycan strands during lateral growth was thought to occur randomly (de Pedro *et al.*, 1997), however Daniel & Errington (2003) showed that incorporation of new peptidoglycan occurred in a helical pattern that resembled the helical pattern, of Mbl – an MreB like protein required for determining the rod shape of *B. subtilis* (Daniel & Errington, 2003; Stewart, 2005). New strands of peptidoglycan are synthesised in the cytoplasm as uridine diphosphate (UDP)-activated precursors, from where they are translocated as lipid associated compounds across the membrane, into the periplasm and inserted into the pre-existing sacculus (de Pedro *et al.*, 1997; Nanninga, 1998; Höltje, 1998).

Seven of the enzymes involved in the conversion of peptidoglycan precursors into their mature form are encoded by genes located in the *mra* region (*murE, murF, mraY, murD, murG, murC* and *ddlB*). Each protein carries out an enzymatic step in the complex production of peptidoglycan (Reviewed by Höltje, (1998); Figure 1.1.4.1).

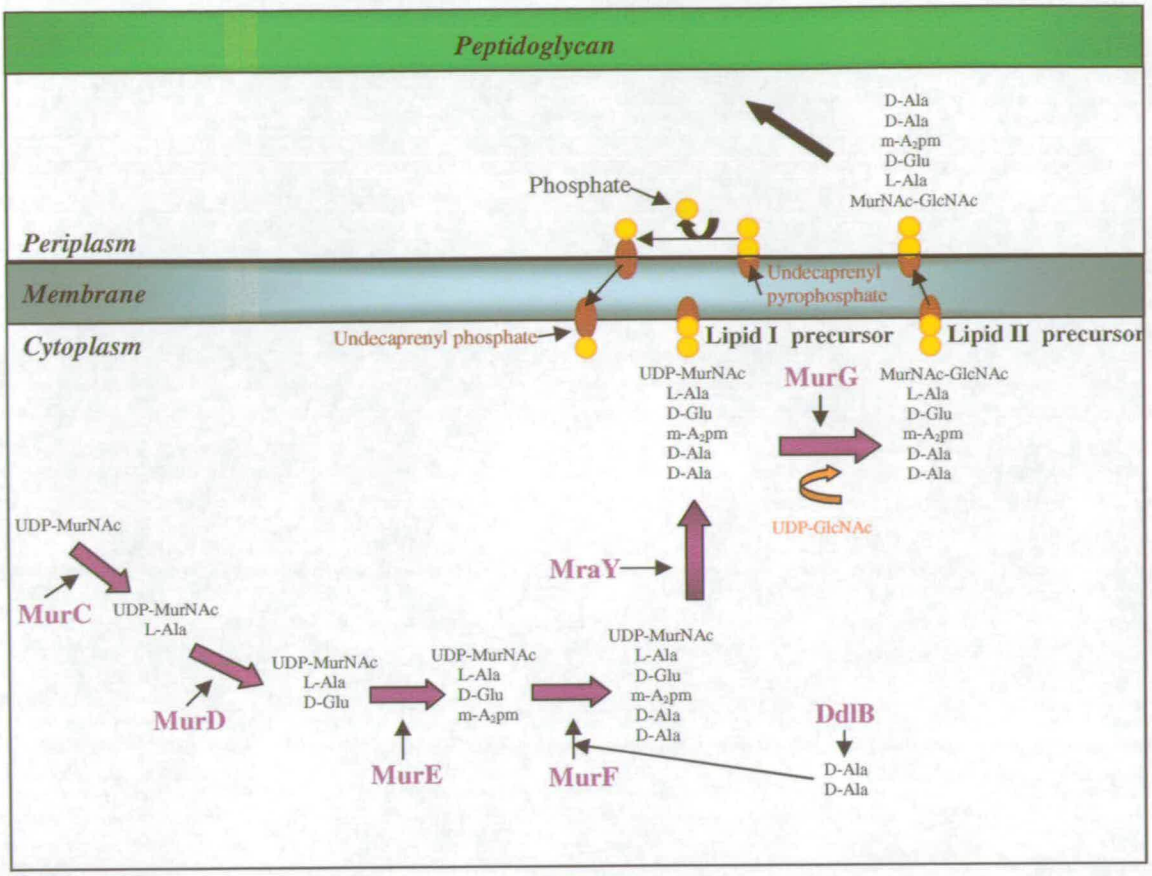


**Figure 1.1.4.1: Formation of Peptidoglycan precursors involves enzymes encoded by genes of the *mra* region.**

Formation of peptidoglycan precursors involves a number of enzyme catalysed steps using proteins produced from the mra region. MurC is an $_{L}$-Alanine adding enzyme that forms UDP-N-acetylmuramyl (MurNAc)-$_{L}$-Ala from UDP-MurNAc. MurD then adds $_{D}$-Glutamic acid to this substrate to form UDP-MurNAc-$_{L}$-Ala-$_{D}$-Glu. The formation of UDP-MurNAc tripeptides involves the action of the meso-$A_2$pm-adding enzyme MurE, the product of this reaction; UDP-MurNAc-$_{L}$-Ala-$_{\gamma}$-$_{D}$-Glu-meso-$A_2$pm is then used by the $_{D}$-Alanyl-$_{D}$-alanine adding enzyme MurF to form UDP-MurNAc pentpeptides. The $_{D}$-Alanine-$_{D}$-alanine dipeptide added by MurF is formed by the action of DdlB, the $_{D}$-Alanine:$_{D}$-alanine ligase. Finally MraY is a phospho-MurNAc pentapeptide translocase that assists MurG to generate undecaprenyl-pyrophosphoryl-MurNAc pentapeptide. This is the Lipid I precursor which is added to the GlcNAc from UDP-GlcNAc to become the lipid II precursor. The lipid II precursor is translocated across the membrane to the periplasm where it inserts into the peptidoglycan sacculus with the aid of PBPs; in particular PBP3 which is septation specific. (Figure adapted from Höltje and Heidrich, 1998).

MurNAc is converted to UDP-MurNAc-$_{L}$-Ala following the addition of $_{L}$-Alanine by MurC. MurD subsequently catalyses the addition of $_{D}$-Glutamic acid, to form UDP-MurNAc-$_{L}$-Ala-$_{D}$-Glu. The formation of UDP-MurNAc-$_{L}$-Ala-$_{D}$-Glu-*meso*-$A_2$pm involves the action of the *meso*-diaminopnelic acid (*meso*-$A_2$pm) adding enzyme MurE. This is then used as a substrate by the enzyme MurF, which adds $_{D}$-Alanine-$_{D}$-Alanine to form the UDP-MurNAc pentapeptide. The $_{D}$-Alanine-$_{D}$-Alanine is produced by DdlB which is a $_{D}$-Alanine-$_{D}$-Alanine ligase. MraY is a phospho-MurNAc pentapeptide translocase which stimulates interactions of the UDP-MurNAc

pentapeptide with the membrane, where it becomes phosphorylated to form undecaprenyl-pyrophosphoryl-MurNAc pentapeptide. This is the Lipid I precursor that is converted to a Lipid II precursor with the addition of UDP-GlcNAc by the actions of MurG. The Lipid II precursor is translocated across the membrane, possibly by FtsW or another membrane spanning protein, into the periplasm where it is incorporated into the growing sacculus by the transglycosylation and transpeptidation reactions performed by the PBPs (Höltje, 1998). Höltje (1998) also proposed a model for the growth of the stress bearing sacculus without risk of autolysis, it is known as the 'three-for-one' growth mechanism (Figure 1.1.4.2a).

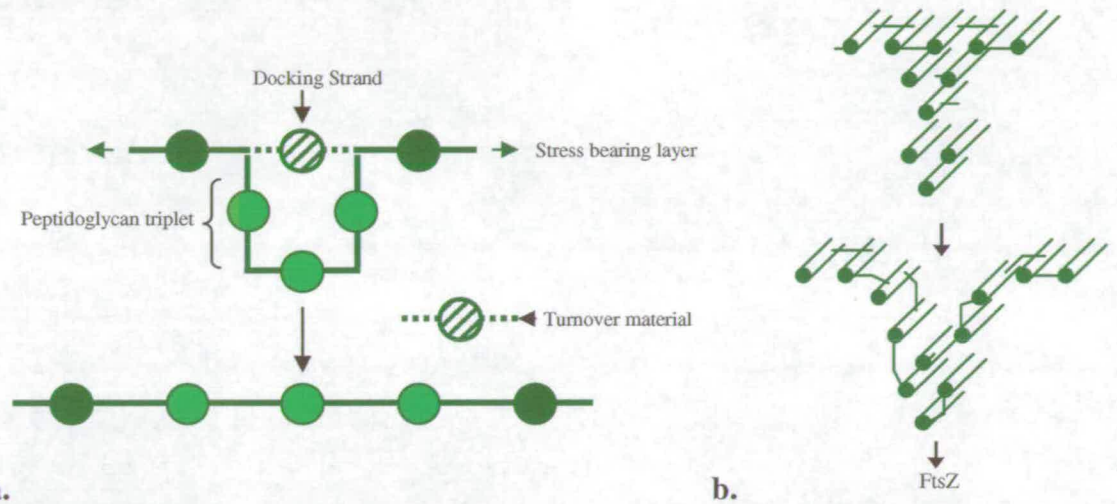


**Figure 1.1.4.2: The "Three for One" model of growth for the Peptidoglycan sacculus.**
**a.** During elongation, a peptidoglycan triplet is linked to the peptide cross bridges either side of a docking strand. The docking strand is removed allowing insertion of the peptidoglycan triplet.
**b.** During septation, constriction occurs as a result of repeated addition of peptidoglycan triplets, release of the docking strand and a subsequent inward pull of membrane anchored enzymes due to the contracting FtsZ ring. (Figure a is redrawn from Höltje, 2001), figure b is redrawn from Höltje, 1998).

Initially, three peptidoglycan strands are synthesised and cross linked to each other (Höltje & Heidrich, 2001). Transpeptidases such as PBP3 (FtsI) then link this triplet to free amino groups in the peptide cross bridges, either side of a single glycan strand in the sacculus, which is referred to as the docking strand. Removal of the docking strand allows insertion of the triplet into the sacculus in its place while the docking strand is recycled (Höltje, 1998). During septation, release of the docking strand is connected to an inward pull of membrane anchored proteins as a result of constriction by FtsZ. By this method invagination of the growing septum occurs (Figure 1.1.4.2b). The septum eventually fuses to release two daughter cells with newly formed polar

caps where the septa have terminated (de Pedro *et al.*, 1997). Polar peptidoglycan has been shown to be very stable and it is proposed that after division, septal peptidoglycan becomes metabolically inert (Lutkenhaus & Mukherjee, 1997; de Pedro *et al.*, 1997).

### 1.1.5: The *mra* region.

The *mra* (murein region A) region, also known as the *dcw* (division and cell wall) cluster is located at 2 minutes on the *E. coli* chromosome. It consists of 16 contiguous genes spanning 17.9kb, from *yab*B to *lpx*C where the only transcriptional terminator is found (Figure 1.1.5.1). The *mra* region contains six genes which encode proteins involved in the septal ring (*fts*L, *fts*I, *fts*W, *fts*Q, *fts*A and *fts*Z), and seven genes encoding proteins involved in the production of peptidoglycan precursors (*mur*E, *mur*F, *mra*Y, *mur*D, *mur*G, *mur*C and *ddl*B). The *mra* region also contains two genes of unknown function *yab*B and *yab*C. It is not known whether the proteins encoded by these genes are involved in cell growth or division, however they are non-essential (Merlin *et al.*, 2002), and it therefore seems unlikely that they would play a significant role. The final gene of the *mra* region is *lpx*C. LpxC catalyses a step in the synthesis of Lipid A. Lipid A forms an anchor for lipo-polysaccharides which are important constituents of the bacterial outer membrane. Lipid A is required for growth and inhibition of its biosynthesis is lethal to Gram negative bacteria (Clements *et al.*, 2002).

The *mra* region is highly conserved in bacteria with the gene order remaining almost unchanged in species as varied as *B. subtilis* and *N. gonorrhoeae* (Francis *et al.*, 2000). This may indicate that the regulation of the entire *mra* region is co-ordinated (Vicente *et al.*, 1998). There are eight promoters known to contribute to transcription of the *mra* region; $P_{mra}$ located upstream of the *mra* region, *fts*Q2p, *fts*Q1p, *fts*Ap, *fts*Z4p, *fts*Z3p, and *fts*Z2p located upstream of *fts*Q, A and Z and $P_{lpxC}$ located upstream of *lpx*C (Figure 1.1.5.1). The best studied of these are the six promoters for the *fts*QAZ genes, reviewed by Joseleau-Petit *et al.*, (1999). All six promoters are recognised by sigma factor $\sigma^{70}$ with *fts*Q2p, Q1p, Z2p3p and 4p showing inverse growth rate dependence (Joseleau-Petit, *et al.*, 1999). Of the six promoters proximal to *fts*Z,

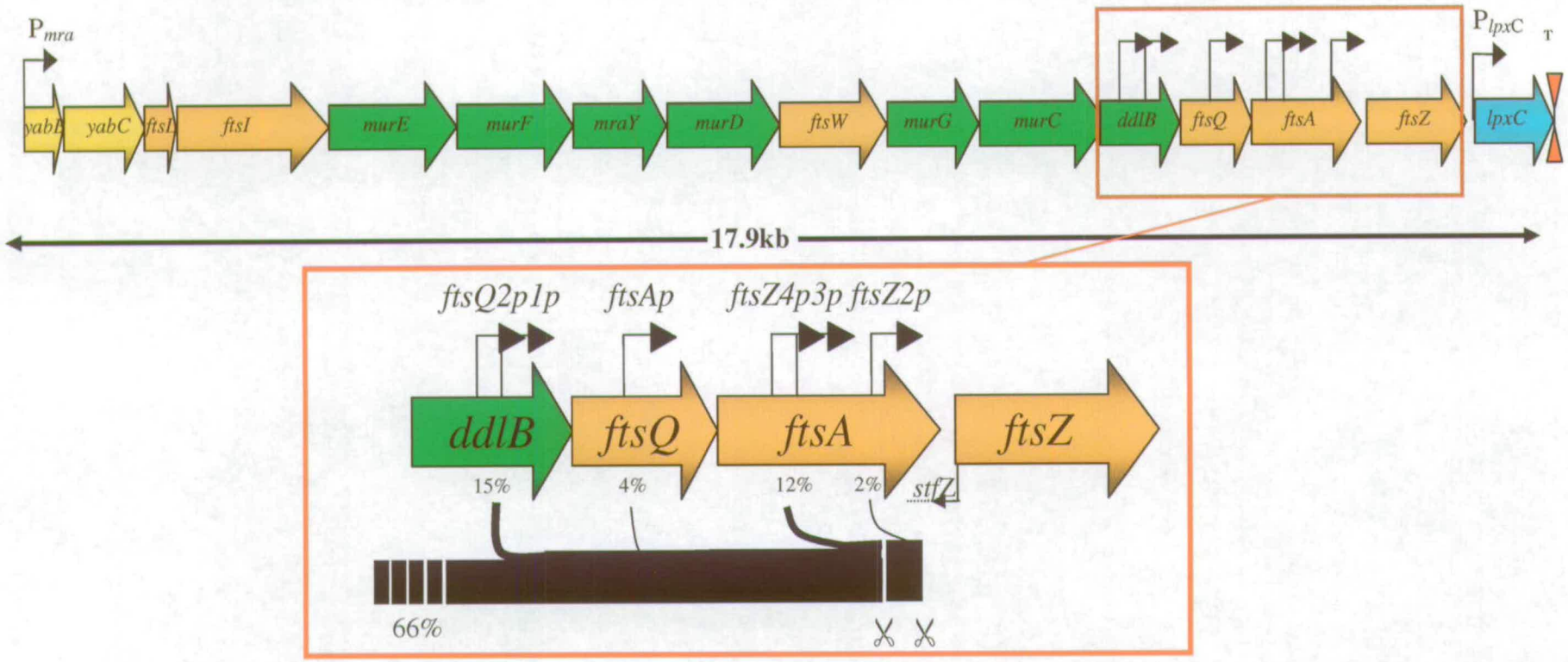


**Figure 1.1.5.1: The *mra* region in *E. coli***

Illustration of the 17.9 kb *mra* region in *E. coli*. The 16 contiguous ORFs are depicted, with the genes of unknown function coloured yellow, the genes which encode proteins involved in the septal ring are coloured orange, and genes encoding proteins involved in peptidoglycan biosynthesis are coloured green. The single transcriptional terminator is coloured red and situated downstream of *lpx*C (coloured blue). The eight reported promoters of this region are also shown. $P_{mra}$ is located upstream of *yab*B and is necessary for expression of genes at least as far as *fts*W; while the 6 promoters of the *ftsQAZ* operon are illustrated in the magnified region. $P_{lpxC}$ is also illustrated. The *ftsQAZ* promoters fine tune the transcription of *fts*Q, *fts*A and *fts*Z, however 66% of *fts*Z transcription originates upstream of these promoters. RNaseE cleavage sites are shown as scissors, cleavage results in differential translation of *fts*Z and *fts*A transcripts. The antisense RNA *stf*Z which inhibits translation of *fts*Z is also depicted. Figure redrawn with modifications from Dewar & Dorazi (2000), and Flärdh *et al*, 1998).

*fts*Q1p and Q2p contribute the most to *fts*Z transcription, however they only account for 15% of the total transcription of *fts*Z (Figure 1.1.5.1). *Fts*Q2p is activated by the transcriptional regulator SdiA, in response to a quorum sensing mechanism which is triggered by an increase in cell density (García-Lara *et al.*, 1996). As growth rate declines the gearbox promoter *fts*Q1p is induced (Aldea *et al.*, 1990), this is achieved because in addition to $\sigma^{70}$, this promoter is also recognised by the stationary phase sigma factor $\sigma^{S}$ (Ballesteros *et al.*, 1998). Gearbox promoters are defined as those that yield a constant amount of gene product per cell and per cell cycle at any growth rate (Vicente *et al.*, 1991). Therefore at any particular cell size or growth rate, the regulation of *fts*Q2p and *fts*Q1p ensures that sufficient *fts*Q, A and Z are expressed for the formation of a single septum per cell. The presence of the weak promoter *fts*Ap was inferred from genetic complementation tests and confirmed by reporter fusions to *lac*Z, however, its precise position is yet to be determined (Vicente *et al.*, 1998). Transcription from *fts*Ap was shown to be activated by RcsB, the regulator element of a two-component system RcsB-RcsC which regulates genes involved in the synthesis of capsular polysaccharide (Gervais *et al.*, 1992; Joseleau-Petit *et al.*, 1999). It is not yet clear how cell division and the RcsB-RcsC system are connected.

Differential transcription of the *fts*QAZ genes is accompanied by differential translation, with variations in the abundance of each individual protein. There are around 25 molecules of FtsQ (Lutkenhaus & Mukherjee, 1997; Dewar & Dorazi, 1996), and recent studies suggest there are around 740 molecules of FtsA and up to 3,200 molecules of FtsZ per cell (Rueda *et al.*, 2003). This variation in protein expression is achieved in part by two RNaseE processing sites present in the transcripts from the $P_{ddlB}$-$P_{fts}$ promoters (Figure 1.1.5.1; Cam *et al.*, 1996). RNaseE cleavage alters the ratio of *fts*Z to *fts*A mRNA by five-fold by decreasing the stability of the *fts*A and possibly *fts*Q mRNA. The authors, however, also suggest that the altered ratio of mRNA may occur by premature termination of transcripts originating from *fts*Z2p, Z3p and Z4p (Cam *et al.*, 1996). Transcripts for *fts*Q, A and Z are also translated with different efficiencies, FtsQ being translated at a lower level than FtsA, which is translated at a lower level than FtsZ. The transcripts for *fts*A and *fts*Q have separate low affinity ribosome binding sites (RBS) indicating that these genes are not co-translated (Mukherjee & Donachie, 1990). In addition, FtsZ translation is inhibited by antisense RNA. A 53-nucleotide mRNA transcribed from the *dic*F gene present in

the Qin prophage, is complementary to the RBS region of *fts*Z, and interactions between the two cause an inhibition of *fts*Z translation (Bouché & Bouché, 1989; Tétart & Bouché, 1992). A second antisense mRNA (*stf*Z) was identified in the *fts*A-*fts*Z junction that was complimentary to the same region as *dic*F. Overexpression of this region at elevated temperatures caused a block in cell division, possibly due to interactions with *fts*Z transcripts and inhibition of its translation, however its precise role in cell division is still unknown (Dewar & Donachie, 1993). It has also recently been reported that Hfq, a pleiotropic regulator which binds to DNA and RNA, causes inhibition of *fts*Z translation by binding to the RBS region of *fts*Z transcripts during stationary phase (Takada *et al.*, 1999; Takada *et al.*, 2005).

Studies on the regulation of the *fts*QAZ genes have shown that the six promoters located in the *ddl*B-*fts*A region only contribute 33% of total *fts*Z transcription (Flärdh *et al.*, 1998), which leads to the question of the origin for the remaining 66% of *fts*Z transcription.

Dai and Lutkenhaus (1991), described how a null allele of *fts*Z could not be complemented by the presence of a λ lysogen carrying 6 kb of DNA upstream of *fts*Z, from the middle of *fts*W to beyond *lpx*C. They proposed that 30-40% of *fts*Z expression must originate from one or more promoters upstream of *fts*W. Subsequently, Hara *et al,* (1997), constructed a null allele of *fts*I. When *fts*I was supplied *in trans* it required transcription from a promoter located 1.9kb upstream for complementation. This promoter, designated $P_{mra}$, is situated at the start of the *mra* cluster and was initially found to be necessary for expression of the first nine genes in this region. They speculated that due to the lack of transcriptional terminators within the *mra* region, transcription originating from the P*mra* promoter may proceed along the entire *mra* cluster to the only terminator, found downstream of *lpxC*. It was also predicted that $P_{mra}$ may be at least partly responsible for expression of all genes in this cluster (Hara *et al.*, 1997). Mengin-Lecreulx *et al,* (1998), showed that the $P_{mra}$-*fts*W region was under the sole control of $P_{mra}$, while uninduced $P_{mra}$::$P_{lac}$ cells showed a large depletion in protein products distal to *ftsW*. Expression of *fts*Z was also significantly reduced when $P_{lac}$ was repressed, leading to the conclusion that distal genes in the *mra* cluster are also largely dependent on the $P_{mra}$ promoter (Mengin-Lecreulx *et al.*, 1998). This evidence was supported by the work of Flärdh *et al.*,

(1997) which showed that 66 % of FtsZ expression originates from *cis*-acting signals upstream of *ddlB*. It was subsequently shown that these *cis*-acting signals represented significant levels of transcription originating from promoters upstream of *ddl*B, rather than enhancing effects of transcriptional activators binding to sequences upstream of the *ddl-fts* promoter region (de la Fuente *et al.*, 2001).

Hara *et al* (1997), and Mengin-Lecreulx *et al* (1998) disrupted the $P_{mra}$ promoter with a replacement cassette containing the *cat* gene, two transcriptional terminators, the *lacI*$^q$ gene and $P_{lac}$, inserted at the HindIII restriction site located between the -35 and -10 sequences of $P_{mra}$. They concluded that since cells carrying the $P_{mra}$::$P_{lac}$ insertion required complementation *in trans* by the region from $P_{mra}$ to *fts*W on a plasmid, that $P_{mra}$ was solely responsible for expression of these genes. However, a significant drawback of these experiments is that they did not rule out the possibility that transcription from upstream promoters contributed to expression of the *mra* region.

Upstream of the *mra* region is a 601bp intergenic region, located between *fru*R and *yab*B (chromosomal coordinates 89033-89634). Any promoters located between here and $P_{mra}$, that are in the correct orientation, may also contribute to transcription of the *mra* region. G. Blakely identified two such promoters by potassium permanganate footprinting of RNA Polymerase bound to the *fru*R-*yab*B intergenic region (unpublished data; Figure 1.1.5.2a). These newly identified promoters were named $P_{mra}2$ and $P_{mra}3$, their positions are depicted in Figure 1.1.5.3. $P_{mra}$ will now be referred to as $P_{mra}1$.

Transcripts were detected from both $P_{mra}1$ and $P_{mra}3$ by primer extension using RNA from cells during exponential growth in LB (Figure 1.1.5.2a), Two transcriptional start sites were detected for $P_{mra}1$ at the adenine and guanine positioned 45 and 44 bp upstream of *yab*B, respectively. The transcription start site from $P_{mra}2$ is a guanine, positioned 135 nucleotides upstream of *yab*B (data not shown). Transcripts from $P_{mra}2$ could only be detected when the *fru*R-*yab*B intergenic region was cloned into a multicopy plasmid, indicating that the transcripts may be of low abundance or unstable during the experimental conditions. The absence of a primer extension

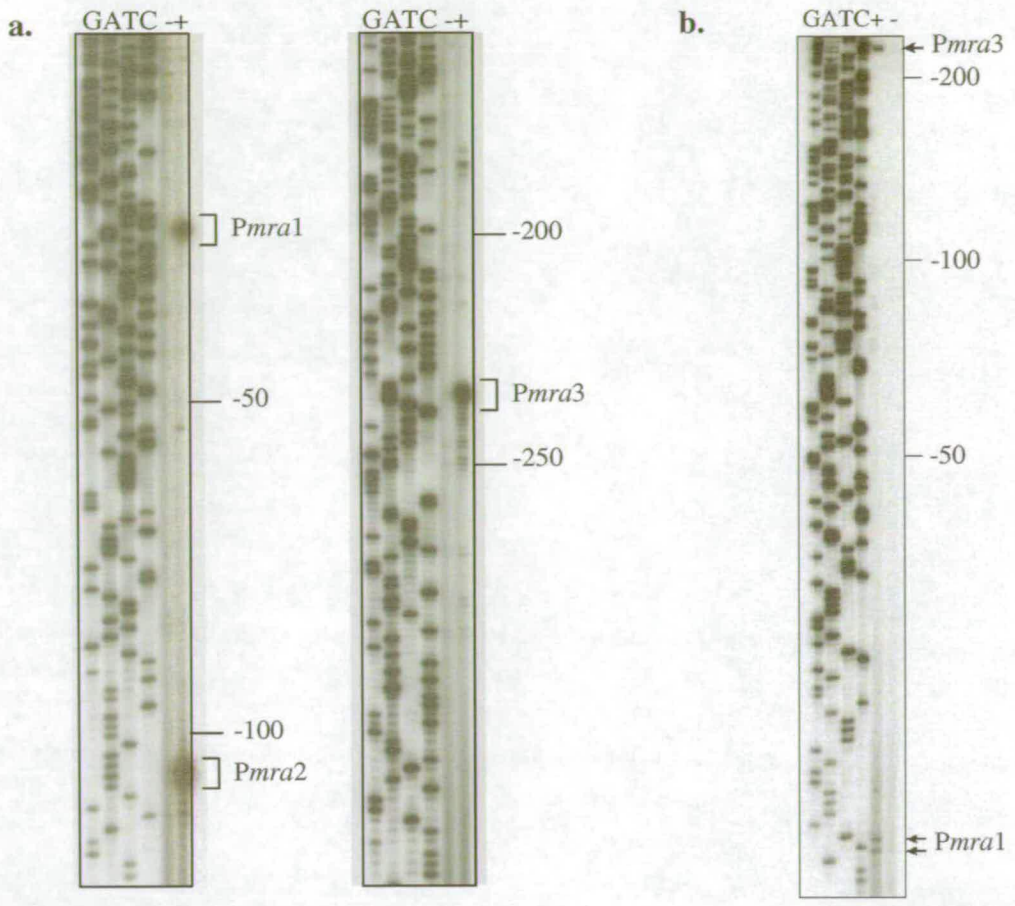


**Figure 1.1.5.2: Potassium permanganate footprints and primer extension products of $P_{mra}1$, $P_{mra}2$ and $P_{mra}3$.**

**a.** Potassium permanganate footprints showing the position of three promoter regions, recognised by $\sigma^{70}$ RNA Polymerase, relative to the start of *yab*B. GATC ladders are shown on the left of each autoradiograph, with footprints in the absence or presence of $\sigma^{70}$ RNAP on the right hand side.
**b.** Products of primer extension reactions showing transcripts originating at $P_{mra}1$ and $P_{mra}3$. $P_{mra}1$ exhibits two transcriptional start sites at an adenine, and guanine located -45 and -44 bp respectively from the start of *yab*B. Autoradiographs courtesy of G. Blakely.

product for $P_{mra}2$ in Figure 1.1.2 suggests that it is a weak promoter, despite it exhibiting a good match to the $\sigma^{70}$ consensus sequence with 18bp spacing between -10 and -35 (Table 1.1). $P_{mra}3$ does not exhibit a good match to the $\sigma^{70}$ consensus sequence at -35, and it also has a shorter spacing between -10 and -35 of 17 bp (Table 1.1). Transcription initiated from $P_{mra}3$ results in a 271 nucleotide leader sequence upstream of *yab*B, which could potentially play a role in the transcriptional regulation of this promoter.

These newly identified promoters have the potential to contribute to the expression of the *mra* region (Figure 1.1.5.3). One aim of this thesis will be to determine how

significant the transcriptional contribution is from each $P_{mra}$ promoter, in addition to investigating the potential mechanisms of transcriptional regulation at these promoters which may modulate expression of the *mra* region.

| | -35 -10 Start | Leader |
|---|---|---|
| $P_{mra}1$ | TTGACAAGCTTTTCCTCAGCTCCGTAAACTcctttcaG | 44 |
| $P_{mra}2$ | TTGCTTCGCACGTTGGACGTAAAATAAACAacG | 135 |
| $P_{mra}3$ | TGTTAACCGGGGAAGATATGTCCTAAAATgccgctcG | 271 |
| $\sigma^{70}$ Consensus | TTGACA 17-19 nucleotides TATAAT | |

**Table 1.1: $P_{mra}$ promoter sequences**
Table presenting the $P_{mra}$ promoter sequences and transcriptional start sites; as determined by $KMnO_4$ footprinting and primer extension (G.Blakely., unpublished data). The length of leader sequence produced, relative to the translational start of *yab*B is also shown. The consensus $\sigma^{70}$ promoter sequence is included as a comparison.

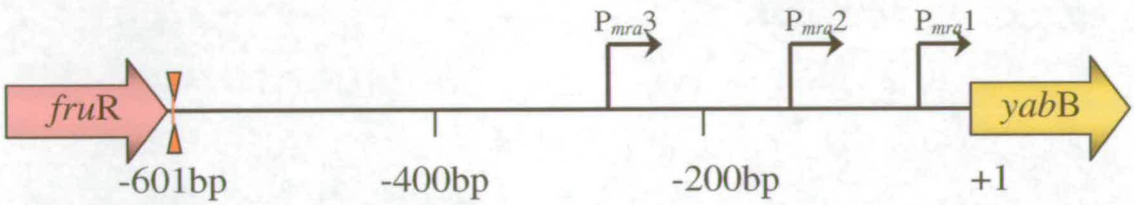


**Figure 1.1.5.3: Positions of the $P_{mra}$ promoters within the *fru*R-*yab*B intergenic region.**
Illustration of the positions of the $P_{mra}$ promoters, located within the 601bp intergenic region between *fru*R and *yab*B. The transcriptional terminator of *fru*R is indicated in red. The direction of transcription for the three promoters is based on data from primer extension experiments

## 1.2: Transcriptional Regulation in *Escherichia coli*.

Transcriptional regulation at prokaryotic promoters has been well studied (for reviews see Browning & Busby, 2004, and Busby & Ebright, 1994). Regulation can occur at any point during transcription, but the key stage for regulation is transcription initiation, including recruitment of RNA Polymerase (RNAP), open complex formation, and promoter clearance (Helmann, 1999).

The recruitment and affinity of RNAP for a promoter is dependent upon the recognition of appropriate sequences by the σ subunit of RNAP (Paget & Helmann, 2003). RNA polymerase consists of a core enzyme containing $\alpha^{I}$, $\alpha^{II}$, β, β′, and ω subunits. This core enzyme interacts with interchangeable σ factors to form the RNA polymerase holoenzyme capable of initiating transcription (Vrentas *et al.*, 2005; Helmann, 1999). σ factors are involved in the recognition of promoter regions and in the melting of DNA for open complex formation. σ factors have up to four domains connected by linkers (Browning & Busby, 2004). Domains 2-4 are involved in promoter recognition, with domain 2 (specifically region 2.4) involved in the recognition of promoter -10 elements, while domain 4 (specifically region 4.2) recognises -35 elements (Paget & Helmann, 2003; Watson *et al.*, 2004). The function of domain 1 is not known and it is absent from many σ factors (Browning & Busby, 2004). The predominant σ factor in *E. coli* is $\sigma^{70}$, which recognises the promoter consensus sequence TTGACA – (17-19 bp) – TATAAT (Figure 1.2.1), however few $\sigma^{70}$ promoters completely match this consensus sequence (Busby & Ebright, 1994).

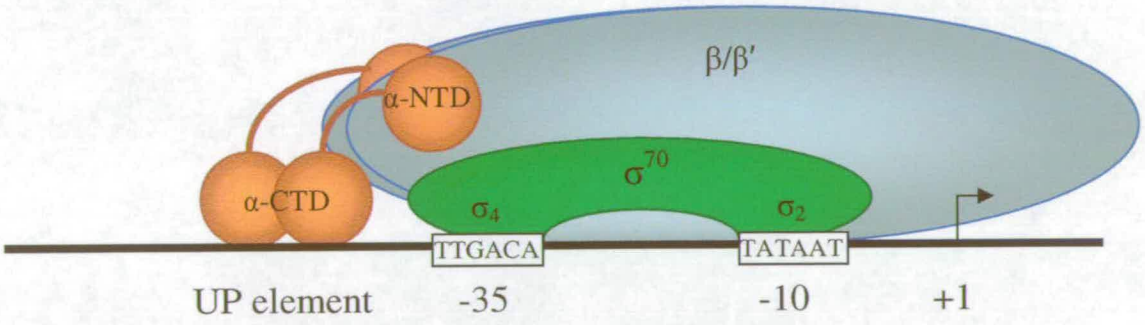


**Figure 1.2.1: RNA Polymerase bound at a $\sigma^{70}$ promoter**
Illustration of the RNA Polymerase holoenzyme with $\sigma^{70}$ binding to its consensus recognition sequence, via region 2 at the -10 sequence, and region 4 at the -35 sequence. The α subunit with its two distinct domains, joined by a flexible linker is also shown. Interactions between the α-CTD and the UP element are also indicated. (Figure redrawn with modifications, Watson et al, 2004)

Binding of RNAP to the promoter can be stabilised with interactions between the α-CTD (Carboxyl Terminal Domain) and upstream promoter elements (UP element). The α-NTD (Amino Terminal Domain) which is involved in RNAP assembly is embedded in the holoenzyme and connects to the α-CTD by a flexible linker (Lloyd *et al.*, 2002). This flexibility enables the α-CTD to interact with both proximal regions and UP-elements, and it is a common site for interactions with transcriptional regulators (Busby & Ebright, 1994).

Transcription can be regulated by combinations of protein:DNA and protein:protein interactions between RNAP and transcriptional regulators such as FIS (Factor for Inversion Stimulation) (Finkel & Johnson,1992), CRP (cAMP Receptor Protein) (Malan *et al.*, 1984) and IHF (Integration Host Factor) (Goosen & van de Putte, 1995). FIS and IHF are transcriptional regulators that are also known as nucleoid associated, or histone-like proteins as they bend DNA and assist in condensing the nucleoid. This ability to bend DNA helps such proteins to alter transcription from many promoters (Dorman & Deighan, 2003).

Transcriptional activators may bind upstream of a promoter and interact directly with the σ factor or with the α-CTD of RNAP to increase transcription levels; as is the case with CRP at the $P_{lac}$ promoter (Takami & Aiba, 1995), and cI at the phage λ $P_{RM}$ promoter (Li *et al.*, 1994; Figures 1.2.2a & b). Activation by this method requires that the protein binding site exhibit the same helical phasing as the promoter sequence, as a result most regulator binding sites are centred on -41, -51, -61 etc (Busby, 1999). Upstream promoter (UP) elements are also important with regards to transcriptional regulation. UP elements usually consist of ~20bp of AT rich DNA directly upstream of the promoter (Busby & Ebright, 1994). AT rich regions are intrinsically curved which might facilitate interactions that stabilise the binding of RNAP (Busby, 1999). At some promoters, a regulator may interact with an upstream activating sequence (UAS) which is a considerable distance from the promoter region, in such cases additional proteins often bind between the regulator and RNAP bending the DNA sufficiently for the regulator to interact with the α-CTD. This is the situation at the $P_{narG}$ promoter where FNR makes direct contact with RNAP via region 4 of the σ factor and IHF bends the upstream DNA to enable NarL to also interact with RNAP (Figure 1.2.2c; Schroder, *et al.*, 1993). Transcriptional regulators may also bind within a promoter region; this can have both positive and negative effects. At the $P_{merT}$ promoter, transcription is activated by the binding of MerR directly between the -10 and -35 regions (Frantz & O'Halloran, 1990). Binding of this regulator causes a conformational twist at the promoter region, improving the affinity of the sub-optimally spaced promoter for RNAP and thereby increasing transcription (Figure 1.2.2d; Ansari *et al.*, 1992). In contrast, at the $P_{gyrA}$ promoter, FIS interacts with an extended binding site between -16 and -68 which causes steric hindrance and

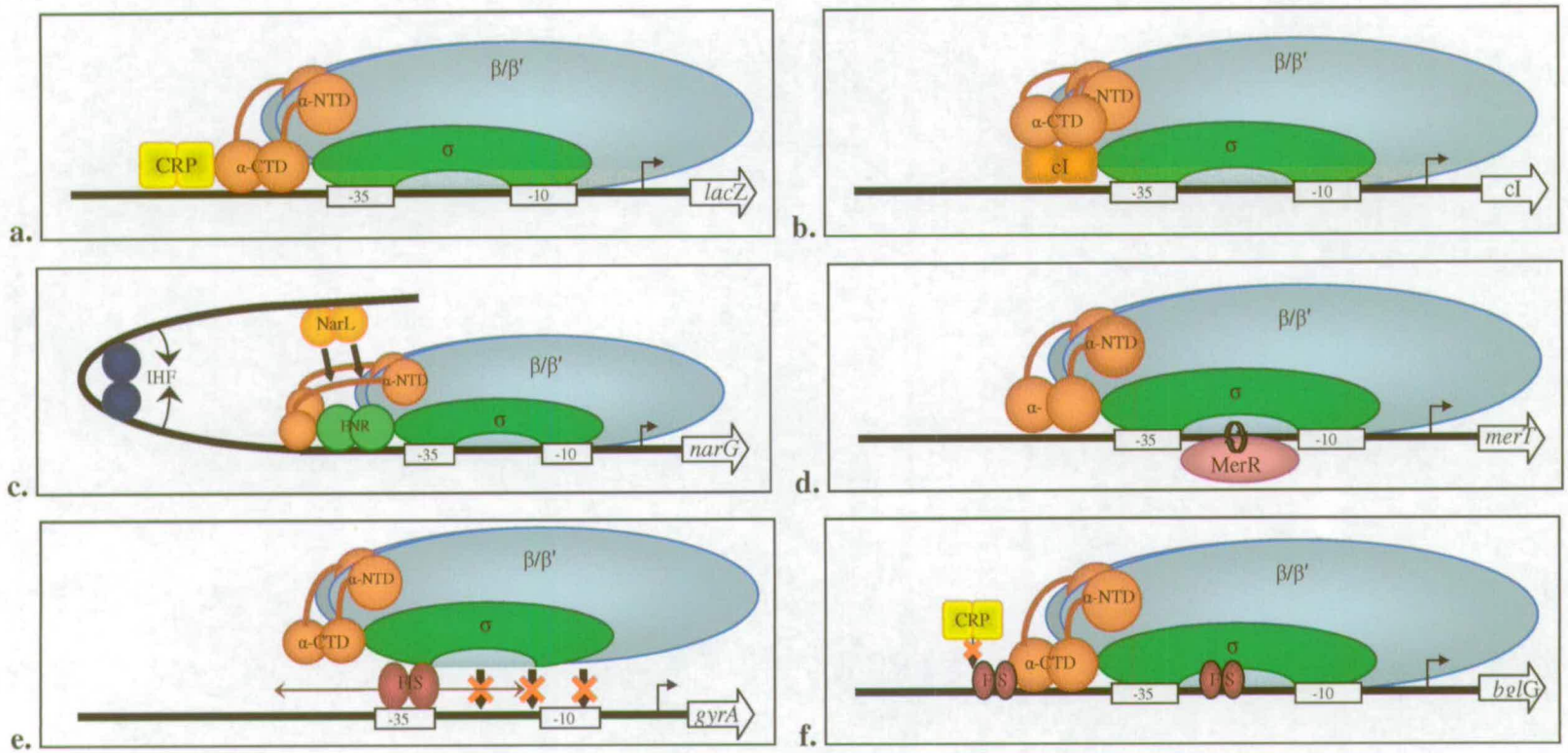


**Figure 1.2.2: Examples of transcriptional regulation at prokaryotic promoters.**

**a.** CRP-mediated activation at $P_{lac}$: CRP binds to -61.5, upstream of $P_{lac}$ in the presence of cAMP. When bound; CRP interacts with the α-CTD to activate transcription.

**b.** Autoregulation of cI: The phage λ repressor cI, can also act as an activator to autoregulate its own expression. cI binds just upstream of the $P_{RM}$ promoter at -42. It makes direct contact with RNAP via region 4 of the σ subunit causing activation of transcription.

**c.** Co-activation by distantly bound regulators: The $P_{narG}$ promoter is co-activated by FNR and NarL which bind at around -41 and -200 respectively. IHF binds to a site between these proteins, inducing a bend which enables NarL to interact with the FNR-RNAP complex.

**d.** Activation by improving promoter affinity for RNAP. The MerR regulator binds at the $P_{merT}$ promoter between the -10 and -35 regions. Binding of MerR creates a conformational change in the promoter region, improving its affinity for RNAP, and thereby increasing transcription.

**e.** Repression by steric hindrance. At the $P_{gyrA}$ promoters, FIS binds to an extended region between -16 and -68, which prevents RNAP from gaining access to the promoter region, therefore repression of transcription is observed.
**f.** Repression via anti-activation. The $P_{bgl}$ promoter is activated by CRP binding at -60.5 and interacting with the α-CTD. However, in the presence of FIS which binds to an overlapping site at -52, CRP is displaced and the promoter is repressed due to lack of activation.
(Figures a-d; redrawn with changes from Chapter 4, Prokaryotic Gene Expression, S. Baumberg, 1999, Oxford University press. Figure e & f; redrawn with changes from McLeod and Johnson, 2001).

repression of transcription by preventing RNAP from binding to the promoter (Figure 1.2.2e; Schneider *et al.*, 1999; McLeod & Johnson, 2001).

Repression of promoter activity can also occur if a binding site for a repressor protein occupies the same region as the binding site for an activator, for example at the $P_{bgl}$ promoter (Figure 1.2.2f). At this promoter FIS binds to two positions centred at -27 and -52. Binding at -27 has little effect on promoter activity, however the upstream binding site overlaps a site for CRP binding. CRP activates transcription from the $P_{bgl}$ promoter but is displaced during competition with FIS for the overlapping binding site resulting in FIS mediated repression. (Caramel & Schnetz, 2000; McLeod & Johnson, 2001).

The final stage in transcription initiation is promoter escape (reviewed by Hsu, 2002). For a promoter to be transcriptionally active it must not only recruit and bind RNAP efficiently, it must also be able to release RNAP at the correct time to enable transcription elongation to ensue (Helmann, 1999, Hsu, 2002). An example of regulation at the stage of promoter clearance is seen at the *rrnB* P1 promoter (Schroder & Wagner, 2000). The regulator H-NS binds at a site centred on -25, which overlaps the -35 promoter recognition sequence. Binding of H-NS does not interfere with the recruitment of RNAP or the formation of an open complex, however it prevents the formation of transcripts longer than 3 nucleotides in length. This repression of transcription is thought to be due to an H-NS-mediated conformational change in the open complex (Schroder & Wagner, 2000). Promoter clearance can also be affected by the downstream sequence region, as RNAP binds DNA up to 20 nucleotides or more downstream of the site of transcription initiation (Helmann, 1999).

In addition to transcriptional regulators, it is important to also consider the sigma factor with the greatest affinity for RNAP core enzyme during the experimental

conditions. σ factors are involved in the recognition of promoter regions as part of the RNAP holoenzyme, however they each bind to different consensus sequences (Gruber & Gross, 2003). *E. coli* produces 7 different sigma factors ($\sigma^{70}$, $\sigma^{S}$, $\sigma^{32/H}$, $\sigma^{54/N}$, $\sigma^{28/F}$, $\sigma^{24/E}$, $\sigma^{19}$) each of which are expressed under specific conditions to ensure that the cell transcribes the appropriate genes in response to external conditions (Gruber & Gross, 2003; Rafaelle *et al.*, 2005). For example, during balanced growth the cell mainly produces $\sigma^{70}$, which transcribes many house-keeping genes that encourage proliferation of the cell. However, as cells shift to stationary phase, $\sigma^{S}$ becomes the prominent σ factor in the cell due to high levels of $\sigma^{S}$ expression and the production of Rsd (anti $\sigma^{70}$ factor) (Travers & Muskhelishvili, 2005). In contrast to $\sigma^{70}$, $\sigma^{S}$ exhibits a high affinity for promoters which drive the transcription of maintenance and stress resistance genes, which are necessary for potentially long periods in stationary phase (Hengge-Aronis, 1999).

Switching σ factors has been identified as a very efficient mechanism of transcriptional regulation, since it enables different subsets of genes to be expressed at specific times (Hengge-Aronis, 1999; Rafaelle *et al.*, 2005). The σ factor dissociates from the holoenzyme within ~ 50 nucleotides of transcription initiation, and is rapidly recycled by binding to new core enzyme in order to start a fresh round of transcription at a new promoter (Rafaelle *et al.*, 2005; Mooney *et al.*, 2005).

Finally, DNA supercoiling plays a significant role with regards to transcriptional regulation (reviewed by Travers & Muskhelishvili, 2005). The activity of a promoter region can be altered dramatically by local changes in superhelicity, which can have significant effects on RNAP recruitment and binding (Drilca *et al.*, 1999; Schneider *et al.*, 2000). Negative supercoiling is favoured at most $\sigma^{70}$ recognised promoters as it facilitates the melting of DNA at the -10 region. Interestingly, $\sigma^{S}$ preferentially binds and initiates transcription at more topologically relaxed promoter regions (Travers & Muskhelishvili, 2005).

Negative supercoiling has been shown to be of particular importance at promoters with sub-optimal consensus recognition sequences or spacing (Travers & Muskhelishvili, 2005). For example, the rRNA and tRNA promoters are the most active promoters in the cell, however, they have quite divergent -35 recognition

sequences and sub-optimal spacing between recognition sites (Figuero-Bossi, *et al.*, 1998; Ohlsen *et al.*, 1992). These promoters are particularly sensitive to supercoiling, and it is thought that additional twists in the DNA may facilitate interactions between the promoter and RNAP. In addition the rRNA and tRNA promoters contain GC rich discriminator regions which slow the formation of an open complex. The presence of negative supercoils facilitates melting of this region of DNA, and increases the stability of the RNAP: promoter complex (Auner *et al.*, 2003; Pemberton *et al.*, 2000).

### 1.2.1: Transcriptional regulation by CRP:

CRP (cAMP Receptor Protein) regulates many genes in *E. coli* and has previously been implicated in the regulation of cell division (D'Ari *et al.*, 1988). Strains carrying *cya* and *crp* mutations show altered morphology and are resistant to the antibiotic mecillinam, which acts on PBP2 and prevents lateral cell wall growth. In addition, transcription of *ftsZ* is higher in a *cya* mutant although actual FtsZ levels were shown to remain the same as a wild type strain, leading to the conclusion that *ftsZ* is not directly regulated by CRP (D'Ari *et al.*, 1988). However, cAMP-CRP appears to enhance cell division although its exact role has yet to be defined.

CRP was first isolated in 1970 and was one of the first transcriptional regulators to have its crystal structure solved (Kolb *et al*, 1993). CRP has been shown to regulate more than 100 genes in *E. coli* and is best known for its role in catabolite repression. CRP is a 47.2 kDa protein consisting of two identical subunits of 209 amino acids each (Gonzalez-Gil *et al.*, 1998). The CRP monomer consists of two functional domains; the N-terminal domain (residues 1-133) is involved in dimerisation and forms a cAMP binding site; this is joined via a flexible hinge to the C-terminal domain (residues 139-209) that contains a helix-turn-helix motif which binds to DNA (Figure 1.2.1.1a; Harman *et al.*, 2001).

CRP alone binds DNA weakly in a non-sequence specific manner. However when bound to its effector molecule cAMP, the cAMP-CRP complex binds to specific DNA sequences with high affinity (Busby, 1999). The consensus sequence for cAMP-CRP binding consists of a 22 bp palindrome (Figure 1.2.1.1b), however few CRP binding sites match this consensus entirely (Harman, 2001). In fact, the CRP binding site at

the $P_{lac}$ promoter, which is perhaps the best studied, differs from the consensus by 7 nucleotides and exhibits 450 fold less affinity for the cAMP-CRP complex than the consensus sequence. (Botsford & Harman 1992).

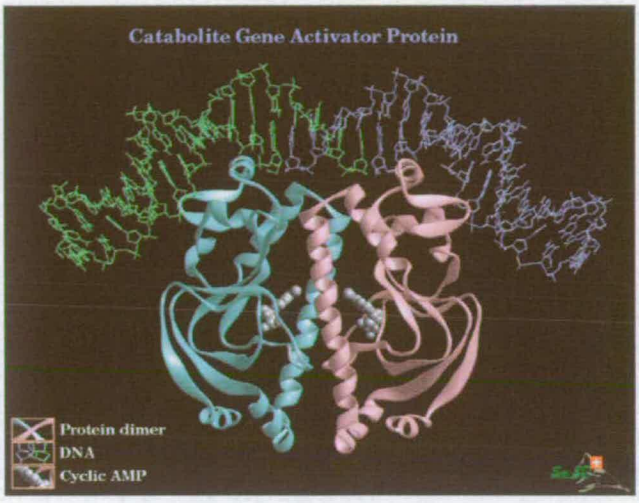


**a.**

**aaaTGTGA-N6-TCACAttt**

**b.**

**Figure 1.2.1.1: Structure of CRP bound to DNA.**
**a.** 3-Dimensional image of CRP bound to DNA in the presence of cAMP. Image from www.ca.expasy.org/ (Swiss-prot 3D Image P03020).
**b.** DNA consensus sequence to which CRP has been shown to bind.

Binding of cAMP to CRP induces small but significant changes in the protein structure. It causes realignment of the subunits by adjustments in the flexible hinge region which results in protrusion of helix F that enhances site-specific interactions with DNA (Harman *et al.*, 2001) When the cAMP-CRP complex binds to target DNA it can generate a bend of 90-180° (Gonzalez-Gil *et al.*, 1998); the degree of this bend depends on how well the target site matches the consensus sequence, which reflects how tightly the DNA is bound to the cAMP-CRP complex (Kolb *et al*, 1993).

As mentioned previously, cAMP and CRP play major roles in the mediation of catabolite repression. When glucose levels in the cell are high, the expression of operons encoding genes necessary for the metabolism of other sugar sources is

repressed (Saier *et al.*, 1997). These operons, including the well studied *lac* operon, require transcriptional activation via the cAMP-CRP complex binding upstream of the promoter region and interactions with RNAP (Tagami & Aiba, 1995).

When glucose is present, cAMP levels in the cell are reduced. This is achieved by cAMP-CRP mediated repression of the *cya* gene, which encodes the cAMP biosynthetic enzyme adenylate cyclase, and also by an increased efflux of cAMP from the cytoplasm (Saier *et al.*, 1997). In addition, CRP levels are also markedly lowered in the presence of glucose, due to negative autoregulation by the cAMP-CRP complex (Ishizuka *et al.*, 1994). Transcription of the *crp* gene is driven by a cAMP-CRP activated promoter directly upstream. The cAMP-CRP complex also activates a divergent promoter which produces a short antisense *crp* transcript. The CRP binding site located at the divergent promoter has greater affinity for cAMP-CRP than the binding site upstream of the *crp* promoter (Hanamura & Alba, 1991). As a result, cAMP-CRP preferentially binds at the divergent promoter and aids recruitment of RNAP. Binding of RNAP to the divergent promoter overlaps the *crp* promoter region, therefore it is not the antisense transcript that represses transcription of *crp*, rather occlusion of the promoter region by the binding of RNAP to the divergent promoter. The transcription of *crp* is also repressed by the pleoitropic regulator FIS (Travers *et al.*, 2001; Nasser *et al.*, 2001).

CRP is usually found to be an activator of transcription, binding to defined areas upstream of promoter regions. At Class I CRP-dependent promoters, the CRP binding site is centred at -61, -71, -81 etc. with the α-CTD interaction occurring in between the cAMP-CRP complex and the bound RNAP (Lloyd *et al.*, 2002). At Class II CRP-dependent promoters the CRP binding site is centred at -41, overlapping the binding region of the core promoter. In this case the α-CTD interacts on the distal side of the cAMP-CRP complex (Lloyd *et al.*, 2002).

In order to activate transcription, the cAMP-CRP complex needs to interact with only one of the α-CTD subunits, this leaves the other subunit free to make interactions with additional regulators (Lloyd *et al.*, 2002). The cAMP-CRP interaction with α-CTD requires activating region 1 (AR1, residues 156-164) which is exposed on the surface of CRP and located near the Helix-Turn-Helix (H-T-H) DNA binding motif. The

activation region of the α-CTD is located in residues 285-290 and 315-318, adjacent to the DNA binding motif (Lloyd *et al.*, 2002). Mutational analysis has identified residue 287 of RNAP to be of particular importance in interactions with cAMP-CRP (Aiyer *et al.*, 2002).

In addition to interactions with RNAP, it has been shown that the cAMP-CRP induced bend at promoter regions is also essential for activation. CRP activated promoters generally have -10 regions that match well with the consensus, however their -35 regions tend to match poorly. The induced bend may enhance RNAP recruitment and binding or may facilitate CRP and α-CTD interactions. It has also been suggested that the energy stored in the bent DNA can be used to facilitate promoter escape of RNAP during transcription elongation (Kolb *et al*, 1993).

### 1.2.2: Transcriptional Regulation by FIS:

FIS (Factor for Inversion Stimulation) is a nucleoid associated, site-specific DNA binding protein, which was first identified by its ability to stimulate DNA inversion reactions by the Hin, Gin and Cin family of recombinases. FIS has subsequently been shown to be involved in processes such as phage λ excision and integration, initiation of DNA replication and as an important pleoitropic regulator of gene expression (Pratt *et al.*, 1997; Zhi *et al.*, 2003). FIS is the most abundant nucleoid associated protein in the cell during exponential phase growth, however its expression fluctuates in a growth phase dependent manner. The level of FIS in the cell peaks following a nutrient up-shift, for example after inoculation into fresh media from a stationary phase culture (Travers *et al.*, 2001; Nasser *et al.*, 2002). This FIS peak occurs within the first 1-2 cell divisions (60-75 mins), at which stage up to 50,000 molecules of FIS can be present in the cell. FIS levels rapidly decrease during exponential phase, until there are fewer than 100 dimers per cell as the cells enter stationary phase growth (Finkel & Johnson, 1992). Bioinformatic studies predict that FIS binds every 232 ± 43 bp in *E. coli*; this represents 4.7 ± 0.9 binding sites per gene. Therefore, during the FIS peak in early exponential phase, every FIS site on the chromosome could be occupied (Hengen *et al.*, 1997). FIS exhibits numerous pleoitropic effects on essential cellular processes, and could potentially have direct or indirect influences on cell division and the regulation of the *mra* region.

FIS is a small 11.2 kDa homodimer, consisting of two identical 98 residue monomers. The monomers contain four distinct α-helical regions, each of which perform specific roles within the protein (Figure 1.2.2.1a; Hengen *et al.*, 1997). The N-terminal helix A is important for the DNA inversion and recombination activities of FIS. Helix B is involved in protein dimerisation. This long, largely hydrophobic helix interacts in the opposite orientation with the corresponding helix B from the other monomer, creating a compact and stable FIS dimer (Topping *et al.*, 2004). The C and D helices of FIS form the helix-turn-helix DNA binding motif. The two D helices of the FIS dimer recognise and interact with the major groove of the DNA binding site. However, due to the small size of FIS, these two helices are only separated by 25Å, rather than the usual 32-34Å in most DNA binding proteins. This distance is too short for the two helices to occupy adjacent major grooves, therefore the DNA must bend in order to accommodate FIS binding (Finkel & Johnson, 1992). FIS binds to DNA in a sequence specific manner, although it has a highly degenerate 15bp consensus sequence (Figure1.2.2.1b) (Bokal *et al.*, 1997; Finkel & Johnson, 1992). When FIS binds to DNA it can induce a bend of 40-90°, which as described previously can facilitate interactions between distantly bound proteins, and improve recruitment of RNAP to promoter regions.

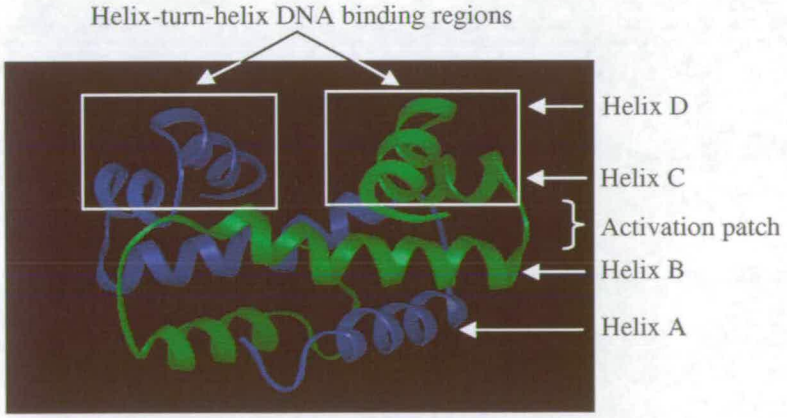


**a.**

GNNYRNN$^{A}/_{T}$NNYRNNC

**b.**

**Figure 1.2.2.1: Structure of FIS and its DNA binding site.**
**a**. Rasmol 3D illustration of a FIS dimer. Each monomer contains 4 α-helices. Helix A is important for recombination and DNA inversion, helix B is involved in dimerisation, while helices C and D form a helix-turn helix DNA binding motif. The activation patch important for interactions with α-CTD is located in the β-turn between helices B and C.
**b**. Degenerate 15bp consensus sequence to which FIS binds.

The expression of FIS is complex since *fis* is highly transcriptionally regulated (Pratt *et al.*, 1997). The *fis* gene is located in an operon, and is predominantly transcribed from a single promoter located 1025bp upstream ($P_{fis}$). Initially six FIS binding sites were identified upstream of the $P_{fis}$ promoter region, two of which overlap the RNAP protected region flanking the promoter. Site II is of particular importance as prebound FIS at this site was shown to prevent RNAP binding, implying an autoregulatory role for FIS (Pratt *et al.*, 1997). Subsequently, a divergent *fis* promoter was identified, located ~100 bp upstream of $P_{fis}$ and transcribed in the opposite orientation (Nasser *et al.*, 2001). RNAP has a higher affinity for this divergent promoter than for $P_{fis,}$ resulting in repression of *fis* transcription due to competition for RNAP binding (Nasser *et al.*, 2001).

FIS represses transcription of *crp*, and CRP in turn regulates transcription of *fis* (Nasser *et al.*, 2001). CRP activates *fis* transcription by binding in a Class I dependent manner at a site centred at -62.5 relative to $P_{fis}$. CRP displaces RNAP from the divergent promoter, attenuating the competition for RNAP and allowing transcription from $P_{fis.}$ This activation of *fis* by CRP only occurs at very low levels of FIS, for example upon nutrient upshift and entry into exponential phase growth. In the presence of both FIS and CRP $P_{fis}$ is repressed as CRP stabilises the binding of FIS to binding Site II enabling FIS to autoregulate its own expression (Nasser *et al.*, 2001).

Additional promoters of *fis* have been identified upstream of $P_{fis}$, these also regulate transcription by competing for binding of RNAP (Nasser *et al.*, 2002). An important IHF (Integration Host Factor) binding site has been located at -114 bp from $P_{fis}$. IHF activates transcription of *fis* 3-4 fold; it is thought that IHF displaces RNAP from the upstream promoters, thereby enhancing transcription from $P_{fis}$ (Pratt *et al.*, 1997).

FIS is involved in the regulation of genes important in cellular metabolism, such as the ribosomal RNA promoters. Interestingly $P_{fis}$ is arranged in a similar fashion to the rRNA promoters, since it contains a GC rich discriminator region, and a poor match to the -35 consensus region. (Muskhelishvili *et al.*, 1997). Transcription from $P_{fis}$ is also similar to that at the rRNA promoters; as in addition to direct interactions with transcriptional regulators, transcription is also modulated by global regulatory factors such as the stringent control system and is particularly sensitive to fluctuations in the superhelical density of the DNA (Muskhelishvili *et al.*, 1997).

FIS can mediate the activation or repression of a promoter in a number of ways. FIS usually represses promoter activity by binding directly to a site overlapping the RNAP recognition sequences (Mcleod *et al.*, 2002). However, FIS can also mediate its effects indirectly as it is intimately linked to other factors in the cell that can affect promoter activity, such as DNA supercoiling (Travers *et al.*, 2001). FIS is known to repress the transcription of the DNA Gyrase genes *gyr*A and *gyr*B, and it also activates transcription of the Topoisomerase I gene *top*A. These effects produce an overall reduction in the average superhelicity of the DNA (Travers *et al.*, 2001). Most $\sigma^{70}$ recognised promoters require high levels of negative supercoiling for efficient activity, this is particularly true of the rRNA promoters and even $P_{fis}$. In addition, FIS has the ability to locally constrain negative supercoils. When FIS binds near a promoter and activates it, it is thought that the local change in DNA topology may play a large role in the activation (Travers & Muskhelishvili, 1997).

FIS also activates transcription from the rRNA promoters and is involved in each stage of the transcription process (Zhi *et al.*, 2003). At *rrn*B P1, FIS binds to a site centred on -71, enabling efficient recruitment of RNAP (Aiyer *et al.*, 2002). FIS also facilitates open complex formation by untwisting the -10 region of DNA, this is a very important step as it counteracts both the negative effect of having a GC-rich discriminator region and the actions of ppGpp. FIS is also believed to subsequently weaken interactions of RNAP with the promoter which enhances promoter escape and elongation of the transcript (Muskhelishvili *et al.*, 1997).

FIS activates transcription in a similar way to CRP at most promoters via interactions with the α-CTD of RNAP. Like CRP activated promoters, Class I FIS promoters have the protein binding site upstream of the α-CTD (centred on -71 at *rrn*B P1), and Class II FIS-dependent promoters have the binding site located between the α-CTD and the RNAP holoenzyme (centred on -41 at *pro*P P2). FIS stimulates transcription through interactions with residues 271-273 of a single α-CTD (Aiyer *et al.*, 2002), via a surface exposed patch spanning the β-turn between helices B and C (Figure 1.2.2.1). In contrast to CRP, FIS bound at Class II promoters does not make additional activating contacts with the σ factor (McLeod *et al.*, 2002).

### 1.2.3: Transcriptional regulation by ppGpp and the Stringent Response.

Guanosine 3′, 5′-bispyrophosphate (ppGpp) has been implicated in a division promoting role because mutants unable to make ppGpp tend to form filaments (Xiao *et al.*, 1991). There have been conflicting reports about ppGpp-mediated regulation of the *fts*QAZ promoters. Navarro *et al* (1998) suggested that the *fts*QAZ promoter pQ1 is activated by ppGpp, however Joseleau-Petit *et al.*, (1999) reported that there was little change in FtsZ expression at elevated ppGpp levels, suggesting that ppGpp is not a major transcriptional regulator of *fts*Z ( Navarro, *et al.*,1998; Joseleau-Petit *et al.*, 1999). Therefore it is possible that transcriptional regulation by ppGpp occurs elsewhere, perhaps at the $P_{mra}$ promoter, where its actions may promote cell division.

ppGpp is a guanine nucleotide derivative produced as part of the cell's stringent response mechanism. The stringent response is induced upon amino acid starvation, where a ribosome binds to an uncharged tRNA molecule, stalling translation (Figure 1.2.3.1; Braeken *et al.*, 2006). This causes an immediate reduction in protein synthesis and a subsequent reprogramming of cellular metabolism, mediated by ppGpp, in order to promote survival of the cell (reviewed by Cashel *et al.*, 1997). The stringent response is conserved in almost all Gram negative and Gram positive organisms, suggesting that it is a key process used by bacteria to confer a selective advantage during nutritional stress (Chatterji & Ojha, 2001).

The synthesis of ppGpp is achieved by the pyrophosphoryl group transfer of the β and γ phosphates from ATP, to the 3′ hydroxyl group of the GDP or GTP acceptor nucleotides, producing ppGpp and pppGpp respectively. These two nucleotides are referred to collectively as (p)ppGpp. The main ppGpp synthetase in the cell is the 84kDa ribosome associated protein RelA (Cashel *et al.*, 1997). The ppGpp synthetase activity of RelA is mediated by the N-terminal 455 residues; this fragment is constitutively active and not ribosome dependent. The C-terminus of RelA is involved in ribosome binding and in RelA oligomerisation. It is thought that conformational changes within the ribosome play an important role in the regulation of RelA dependent ppGpp synthesis (Yang & Ishiguro, 2001). RelA detects blocked ribosomes by the characteristic extrusion of a 3′ extension of mRNA, it then interacts with the large 50S ribosomal subunit. In order to trigger ppGpp synthesis, RelA

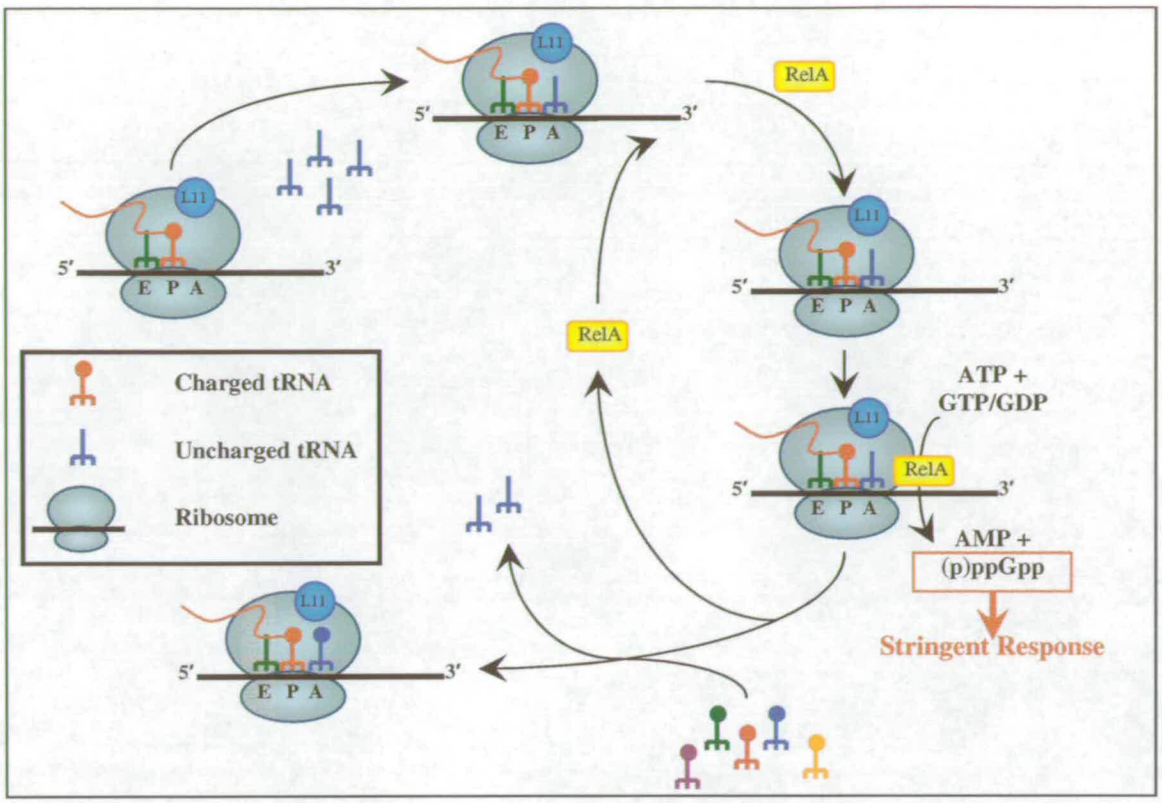


**Figure 1.2.3.1: RelA–mediated (p)ppGpp synthesis.**
When a cell is starved of amino acids, uncharged tRNA molecules rapidly accumulate. The uncharged tRNA binds to the A site of the ribosome, resulting in a block in translation. RelA is thought to recognise the stalled ribosome by the protruding 3′ mRNA extension. RelA binds to the large 50S ribosomal subunit, and is activated by L11 although not through direct contacts. RelA mediates (p)ppGpp synthesis from ATP + GTP/GDP, then it releases its interactions with the ribosome and repeats the cycle of ppGpp synthesis. When the cell is no longer starved of amino acids, the uncharged tRNA is displaced by charged tRNA which binds to the A site with higher affinity, allowing reactivation of translation. E = Exit site, P = binding site for Peptidyl-tRNA, A = binding site for aminoacylated-tRNA. (Figure redrawn with alterations from Braeken et al. 2006.)

requires the binding of an uncharged tRNA to the A site (binding site for aminoacylated-tRNA) of the ribosome and the presence of the ribosomal protein L11 (also known as RelC). RelA binds independently of L11 and the two proteins do not directly interact (Braeken *et al.*, 2006), however the N-terminal domain of L11 is involved in RelA activation, possibly mediated via 23S rRNA with which it is known to interact (Yang & Ishiguro, 2001).

Synthesis of ppGpp decreases the affinity of RelA for ribosome binding. The conversion of ATP and GTP into ppGpp provides the energy for RelA to undergo a conformational change resulting in its reduced affinity for the ribosome (Wendrich *et*

*al.*, 2002). Release of RelA allows it to be recycled in subsequent rounds of ppGpp synthesis. It also ensures that ppGpp synthesis accurately reflects the number of stalled ribosomes in the cell at any particular time. In addition, ppGpp has a short half-life of <1minute (Chang *et al.*, 2002), therefore its pleiotropic effects on the cell can be rapidly reversed upon replenishment of amino acids or upon a shift to more favourable growth conditions. The blocked ribosomes can be re-bound by RelA until amino acid levels return to normal, at which time charged tRNA will displace the uncharged molecules as they have greater affinity for the A site (Braeken *et al.*, 2006).

The synthesis of ppGpp can also be achieved through the actions of SpoT. SpoT is a 79kDa bifunctional cytosolic enzyme (Cashel *et al.*, 1997). Its main function is as a ppGpp 3′-pyrophosphatase (ppGppase) and this is the primary mechanism for ppGpp degradation during recovery from starvation (Yang & Ishiguro, 2003). SpoT contains two overlapping catalytic regions. Residues 1-203 are involved in ppGpp degradation, while 85-375 are necessary for ppGpp synthesis. The C-terminus of SpoT is not involved in the catalysis of ppGpp, but has been shown to be important in regulating the ppGppase activity of the enzyme (Gentry & Cashel, 1996). The ppGppase activity of SpoT is mediated by amino acid starvation, while ppGpp synthesis activity is controlled by growth rate, carbon and phosphate starvation (Rodionov & Ishiguro, 1995; Joseleau-Petit *et al.*, 1999).

During the stringent response, expression of rRNA rapidly decreases due to the transcriptional repression mediated by ppGpp. The *rel*A gene received its name because mutations in it were linked to a continued rRNA accumulation that only slowly decreased upon amino acid starvation. This response was termed "relaxed" when compared to wild type strains (Cashel, *et al* 1997).

The best studied ppGpp regulated promoters are the rRNA promoters. During rapid growth there are around 20,000 ribosomes present in the cell, this requires the synthesis of large amounts of rRNA (Lengeler & Postma, 1998). *E. coli* carries seven copies of the rRNA genes located around the chromosome. The promoters of these genes are particularly strong and it has been estimated that up to 50 RNAP molecules can be transcribing each rRNA operon simultaneously (Snyder & Champness, 1997). The rRNA promoters contain a GC rich discriminator region between the -10 region

and the transcription start site, which is characteristic of promoters negatively controlled by ppGpp. In contrast, promoters with AT rich discriminator regions are generally activated by the presence of ppGpp (Cashel *et al.*, 1997). This form of transcriptional regulation is mediated by the propensity of ppGpp to destabilise promoter open complexes (Nickel & Hochschild, 2004).

All promoters are directly inhibited by ppGpp, even by the basal levels produced in the absence of the stringent response. However, only promoters exhibiting an open complex with a short half-life are significantly repressed by ppGpp (Barker *et al.*, 2001b). Stringently controlled promoters with their GC rich discriminator regions have intrinsically short lived open complexes. This is due to the high energy required to melt the GC rich promoter region and the speed with which the single stranded DNA reanneals.

The mechanism by which ppGpp causes open complex destabilisation has only recently been discovered (Nickel & Hochschild, 2004). Access to the active centre of RNAP is significantly blocked by DNA during transcription, but it had previously been shown that mutations in RNAP β and β′ subunits could mimic the effects of ppGpp by decreasing the promoter/RNAP half-life (Barker *et al.*, 2001a). High resolution crystal structures of RNAP identified a secondary channel, situated adjacent to the β subunits, providing access to the RNAP active centre (Nickels & Hochschild, 2004). This channel has been shown to allow access of iNTP to the RNAP active centre, and it is also a major binding site for a number of transcriptional regulators and accessory factors. ppGpp travels through the secondary channel and binds to a site adjacent to, but not overlapping the RNAP active site. Here it coordinates with a catalytic $Mg^{2+}$ ion causing destabilisation of the RNAP:Promoter complex (Paul *et al.*, 2004; Perederina *et al.*, 2004). Crystal structures identified two oppositely orientated ppGpp complexes bound at the bottom of the secondary channel, these may represent positive and negative stimulatory orientations (Nickels & Hochschild, 2004).

In addition to ppGpp, open complex destabilisation requires the accessory factor DksA. DksA (DnaK suppressor A) has been implicated in many cellular activities including the stringent response, quorum sensing and also cell division (Perederina *et*

*al.*, 2004). DksA interacts with RNAP by inserting its coiled-coil domain into the secondary channel, where it interacts with the catalytic $Mg^{2+}$ ion bound to ppGpp. DksA can interact with RNAP in the absence of both ppGpp and promoter DNA, however its presence was found to reduce the concentration of ppGpp required to inhibit transcription. This suggests that DksA might stabilise the interactions of ppGpp with RNAP. DksA itself causes an increase in the rate of open complex decay at all promoters. This lowers the open complex half-life to a level at which it becomes sensitive to changes in ppGpp concentration (Paul *et al.*, 2004).

Recently the ω subunit of RNAP has also been implicated in ppGpp-mediated transcriptional regulation (Vrentas, *et al.*, 2005). The ω subunit, encoded by *rpoZ*, is the smallest RNAP subunit. It facilitates holoenzyme assembly but does not appear to have a role in RNAP function, however, RNAP lacking ω are unresponsive to the presence of ppGpp. Co-crystal structures show that the ppGpp binding site and ω are too far apart to interact directly, but it is thought that two small regions in β′ may directly connect ω and the ppGpp binding site to enable important structural communication between the two (Vrentas *et al.*, 2005).

Amino acid starvation is overcome due to the expression of ppGpp, however ppGpp has not been shown to directly activate transcription from promoters of operons involved in amino acid biosynthesis (Barker *et al.*, 2001b). During rapid growth, around 80% of RNAP is sequestered in the transcription of stable rRNA and tRNA. During the stringent response ppGpp destabilises promoter open complexes, causing a dramatic increase in the number of free RNAP holoenzymes. Amino acid promoters are therefore activated by passive regulation due the increase in RNAP availability, rather than by direct interactions with ppGpp (Barker *et al.*, 2001b; Jishage *et al.*, 2002).

Regulation by ppGpp affects numerous cellular processes - many involved in cellular survival, in addition to altering cellular metabolism as part of the stringent response. For example, UspA (Universal stress protein A) which is almost ubiquitous in bacteria is usually negatively regulated by FadR. The presence of ppGpp causes a derepression of UspA that is mediated by the increase in free RNAP, which binds with higher affinity to the promoter than FadR (Kvint *et al.*, 2000; Kvint *et al.*, 2003).

ppGpp is also intimately linked to the *maz*EF toxin/anti-toxin system which is involved in programmed cell death under stressful conditions (Gross *et al.*, 2006). MazEF and ppGpp strongly inhibit the *maz*EF promoter. Inhibition of *maz*EF expression results in rapid degradation of the antitoxin MazE and activation of the toxin MazF. MazF is an endoribonuclease with a structure similar to RNaseA, when it cleaves RNA it results in cell death or growth arrest. *maz*G expression is inhibited by MazEF, but upon degradation of MazE, MazG is expressed and limits the effects of MazF. MazG has nucleotide pyrophosphohydrolase activity which causes depletion of ppGpp by up to 70%. This allows reactivation of the *maz*EF promoter and synthesis of the anti-toxin MazE (Gross *et al.*, 2006).

In addition, ppGpp has been shown to be essential for the virulence of a number of pathogenic bacteria. In *Salmonella typhi* for example, systemic infection requires ppGpp for the coordinated expression of virulence genes including *hil*A; the central virulence regulator. *Salmonella* strains unable to make ppGpp (Δ*rel*A,Δ*spo*T) were found to be almost avirulent, and when used as a live vaccine conferred full antibody and cell-mediated immunity against a subsequent infection with a virulent parent strain (Hee Sam Ha *et al.*, 2005; Vinella *et al*, 2005).

The levels of ppGpp in the cell increase as growth slows during exit from exponential phase, due to the growth-rate controlled induction of SpoT ppGpp synthetase activity (Rodionov & Ishiguro *et al.*, 1995). At this time, one of the most important functions of ppGpp in the cell is the regulation of *rpoS* expression. The σ factor RpoS has been referred to as the master regulator of the general stress response in *E. coli* and has been shown to regulate over 50 genes (Brown *et al.*, 2002). RpoS requires ppGpp for transcriptional activation, while the translational efficiency of *rpo*S transcripts has also been shown to be enhanced by the presence of ppGpp (Brown *et al.*, 2002). In addition, all RpoS recognised promoters require ppGpp (Kvint *et al.*, 2000; Chang *et al.*, 2002; Jishage *et al.*, 2002). This is thought to be due to a ppGpp induced conformational change within the RNAP core enzyme, which helps RpoS (and other alternate σ factors) compete more efficiently for RNAP binding (Chatterji & Ojha, 2001).

## 1.3: Project Aims

The primary aim of this project was to investigate the transcriptional regulation of the *mra* region in *E. coli*. We hoped to determine the individual contributions that each of the $P_{mra}$ promoters makes to the transcription of the *mra* region, in addition to examining potential mechanisms of regulation at these promoters. We hypothesised that growth rate control may play an important role in the regulation of the $P_{mra}$ promoters, as a mechanism to increase the expression of cell division proteins at slower growth rates. In order to achieve these aims we intended to study the effects that changes in growth rate or growth conditions had on activity from the $P_{mra}$ promoters. We also looked more directly at potential mediators of growth rate, such as the transcriptional regulators FIS and CRP by investigating potential protein:DNA interactions. In addition, the cellular alarmone ppGpp has been shown to be an indirect effector of growth rate control and we also wished to determine whether it played a role in the regulation of the $P_{mra}$ promoters.

We also investigated whether other additional promoters were present within the *mra* region that may also contribute to its transcription. Many such promoters had been predicted, both bioinformatically and genetically, however none have been confirmed. Finally, we wanted to determine the length of transcripts that originated from the $P_{mra}$ promoters. We hoped that this data would identify the major promoter, or promoters, required for *ftsZ* expression. This would enable us to confirm whether or not the $P_{mra}1$ promoter is the major source of transcription for *ftsZ* transcription as has been previously predicted (Flärdh *et al.*, 1998).

# Chapter 2: Materials and methods

## 2.1 Growth media:

| | | |
|---|---|---|
| **L-broth:** | Difco Bacto-Tryptone | 10g/l |
| | Difco Bacto-yeast extract | 5g/l |
| | NaCl (85mM) | 5g/l |
| | pH to 7.2 with NaOH | |
| | Distilled $H_2O$ to 1 litre | |

**L-agar:** L-broth + 15g/l Oxoid agar

**LC Top agar:** L-broth + 7g/l Oxoid agar

**$H_2O$ agar:** $H_2O$ + 20g/l Oxoid Agar

| | | |
|---|---|---|
| **M9 minimal medium (4x):** | $Na_2HPO_4$ | 200mM |
| | $KH_2PO_4$ | 90mM |
| | NaCl | 35mM |
| | $NH_4Cl$ | 75mM |
| | Distilled $H_2O$ to 1 litre. | |

Working solutions use a final concentration of 1x M9 supplemented with:

| | |
|---|---|
| Casamino acids | 5mg/ml |
| $MgSO_4$ | 2mM |
| $CaCl_2$ | 0.1mM |
| Sugar source | 0.4 % w/v |

| | | |
|---|---|---|
| **M9 minimal medium agar:** | 1x M9 Minimal medium | |
| | Casamino acids | 5mg/ml |
| | $MgSO_4$ | 0.1mM |
| | $CaCl_2$ | 0.5mM |
| | Sugar source | 0.2 % w/v |

Made up to volume with $H_2O$ agar.

| | | |
|---|---|---|
| **Phage Buffer:** | $Na_2HPO_4$ | 50mM |
| | $KH_2PO_4$ | 25mM |
| | NaCl | 90mM |
| | $MgSO_4$ | 1mM |
| | $CaCl_2$ | 1mM |
| | Gelatin | 0.001 % w/v |

Made up to volume with distilled $H_20$.

## 2.2 Antibiotics and Reagents

**Table 2.1 List of antibiotics and reagents**

| Antibiotic/reagent | Stock solution | Working concentration |
|---|---|---|
| Ampicillin | 100mg/ml (in $dH_2O$) | 50μg/ml |
| Chloramphenicol | 34mg/ml (in ethanol) | 20μg/ml |
| Kanamycin | 50mg/ml (in $dH_2O$) | 30μg/ml |
| Tetracycline | 15mg/ml (in 50% v/v ethanol) | 10μg/ml |
| Streptomycin | 20mg/ml (in $dH_2O$) | 20μg/ml |
| Rifampicin | 100mg/ml (in dimethyl formamide) | 100μg/ml |
| Nalidixic acid | 20mg/ml (in 0.1M NaOH) | 20μg/ml |
| Lysozyme | 1mg/ml (in cell lysis buffer) | 100μg/ml |
| IPTG | 0.5M (in $dH_2O$) | 1mM |
| X-GAL | 20mg/ml (in dimethyl formamide) | 40μg/ml |
| ONPG | 4mg/ml (in lacZ buffer) | 0.64mg/ml |
| PMSF | 250mM (in ethanol) | 1mM |

All antibiotics and IPTG were sterilised before use by passing through a 0.22μM filter.

All antibiotics and reagents were stored at -20°C.

## 2.3 Strains

**Table 2.2 List of strains used, their genotypes and their sources.**

| Strain | Genotype | Source |
|---|---|---|
| DH5α | F⁻ Φ80*lac*ZΔM15Δ(*lac*ZYA-*arg*F)U169 *rec*A1 *end*A1 *hsd*R17($r_k^-$, $m_k^+$) *pho*A *sup*E44 *thi*-1 *gyr*A96 *rel*A1 $\lambda^-$. | Invitrogen |
| BL21 (DE-3) | F⁻ *omp*T *hsd*$S_\beta$ ($r_\beta^-$, $m_\beta^-$) *gal dcm* (DE3). | Novagen. |
| XL-1 Blue | *rec*A1 *end*A1 *gyr*A96 ($Nal^r$) *thi hsd*R17 ($r_k^-$, $m_k^+$) *gln*V44 *rel*A1 *lac* [F'::Tn10 *pro*$A^+B^+$*lac*$I^q$ Δ(*lacZ*) M15]. | Stratagene. |
| MG1655 | F⁻ LAM⁻ *rph*-1. | *E. coli* Genetic Resource center. |
| MG1655λ600 | EDCM367 λpROB210 | A. Davidson |
| RE101 | MG1655 *fis*::Kan. | This study |
| RE102 | MG1655 *fis*::Cm. | This study |
| RE103 | MG1655 *relA*::Kan. | This study |
| RE104 | MG1655 *rpo*S::Tet. | This study |
| RE105 | MG1655 *rpo*S::Kan. | This study |
| RE106 | MG1655 *fis*::Cm *rpo*S::Kan. | This study |
| EDCM367 | MG1655Δ*lacZ* | C. Merlin |
| EDCM647 | EDCM367, *yab*B::FLKP2 | C.Merlin |
| RE111 | MG1655Δ*lac yabB*::FLKP2 *fis*::Cm. | This study |
| TP8503 | Δ(*lac-pro*B) *leu thi*-1 *sup*E42 *fhu*4. | M. Masters |
| RE201 | TP8503 *fis*::Kan. | This study |
| RE202 | TP8503 *fis*::Cm. | This study |
| RE203 | TP8503 *rel*A::Kan. | This study |
| RE205 | TP8503 *rel*A::Kan *spo*T::Cm. | This study |
| RE206 | TP8503 *dks*A::Tet. | This study |
| RE207 | TP8503 *ihf*::Tet. | This study |
| RE208 | TP8503 *hns*::Kan. | This study |
| VIP407 | MC1061 *fts*Z::pKFV116[Φ(*fts*Z-*lac*Z) *bla lac*$I^Q$ *tacp-fts*Z] | M Vicente |
| RE301 | VIP407 *fis*::Cm | This study |

| | | |
|---|---|---|
| RE302 | VIP407 *dks*A::Tet. | This study |
| BGL1 | MG1655 *hns*::neo | A. Free |
| CF1652 | MG1655 Δ*rel*A251::Km. | M. Cashel |
| CF1693 | CF1652 Δ*spo*T::Cm. | M.Cashel |
| CLG149 | MC4100 *fis*::Cm. | C. Gutierrez |
| JCB38849 | K-12 Δ*nir* Δ*lac narL narP*253::Tn*10*d(Cm) *him*A452::Tn*10*d(Tet) | D. Browning |
| MM38 | *arg*G6 *asn*A31 or *asnB32 his-1 leuB6 metB1 pyrE gal-6 lacY1 xyl-7 supE44 bgl fhuA2 gyrA rpsL104 tsx-1 uhp* | M. Masters |
| RJ1801 | CAG4000 *fis*::Km | R. Johnson |
| RLG6343 | RLG6341 *dks*A::Tet | R.Gourse |
| ZK1000 | W3110 Δ*lac*U169 *tna*-2 *rpo*S::Km. | R. Kolter |

All strains were grown up from single colonies as liquid cultures in L Broth then stored in a final concentration of 50% v/v Glycerol at -80°C.

## 2.4 Plasmids

**Table 2.3 List of plasmids used, their construction and their sources.**

| Plasmid | Description | Source |
|---|---|---|
| pUC19 | Cloning vector, $Amp^R$ | C. Yanisch-Perron *et al.* (1985) *Gene* 33, 103-119. |
| pBR322 | Cloning vector, $Amp^R$ $Tet^R$ | Bolivar,F. *et al.* (1977) *Gene* 2, 75-91. |
| ptrc99 | Derivative of pKK233-2 expression vector carrying inducible $P_{trc}$ promoter, $Amp^R$ | Amersham |
| pUC4K | Cloning vector carrying *aph* from Tn903 within a restriction site mobilizing element, $Amp^R$ $Kan^R$ | Amersham |
| pUC600 | pUC19 [EcoRI-BamHI: 601 bp $P_{mra}$ region (89033-89634)]. | G. Blakely |
| pUC600 $P_{mra}$1 -10 | As pUC600, with site directed mutation in the $P_{mra}$1 -10 promoter region. | G. Blakely |

| | | |
|---|---|---|
| pUC600 $P_{mra}3$ -10 | As pUC600, with site directed mutation in the $P_{mra}3$ -10 promoter region. | G. Blakely |
| pUC600 $P_{mra}1$ -10, $P_{mra}3$ -10 | As pUC600, with site directed mutations in the $P_{mra}1$ & $P_{mra}3$ -10 promoter regions. | This study |
| P3 DIS MUT | As PUC600, with all G/C's between -10 and +1 of $P_{mra}3$ replaced with A/T by site directed mutation. | G. Blakely |
| pSR | Cloning vector containing λ oop transcriptional terminator. $Amp^R$ | A. Kolb *et al.* (1995) *Nuc. Ac. Res.* 23:819-826. (D.Browning) |
| pSR*Bgl*II | As pSR, with HindIII site changed to BglII by site directed mutagenesis. | This study |
| pSR600 | pSRBglII [EcoRI-BglII: 601 bp $P_{mra}$ region (89033-89634)]. | This study |
| pSP73 | *In vitro* transcription cloning vector using SP6 or T7 RNA polymerase. $Amp^R$ | Promega |
| pSP73-600 | pSP73 [EcoRI-BamHI: 601bp $P_{mra}$ region (89033-89634)]. | This study |
| pSPT18 | pUC based cloning vector using SP6/T7 RNA polymerase to make probe for Northern blot. $Amp^R$ | Roche |
| pSPT18 *fts*I | pSPT18 [PstI-EcoRI: 312 bp region of *fts*I (91498-91810)]. | This study |
| pSPT18 *fts*Z | pSPT18 [PstI-EcoRI: 250 bp region of *fts*Z (105385-105635)]. | This study |
| pET33b | Expression vector for N/C-terminal protein fusion to 6-histidine tag under control of T7 promoter, $Kan^R$ | Novagen |
| pROB101 | pET33b [NdeI-EcoRI: entire 633 bp *crp* gene (3483757-3484389)]. | This study |
| pMAL-c2x | Expression vector for N-terminal fusion of protein to Maltose Binding Protein under inducible control by $P_{tac}$. $Amp^R$ | New England Biolabs |
| pROB102 | pMAL-c2x [EcoRI-BamHI: entire 633 bp | This study |

| | | |
|---|---|---|
| | *crp* gene (3483757-3484389)]. | |
| pROB103 | pMAL-c2x [EcoRI-BamHI: entire 297 bp *fis* gene (3408908-3409204)]. | This study |
| pRS551 | *lacZ*; operon fusion vector. $Amp^R$ $Kan^R$ | R.W. Simons *et al.*. (1987) *Gene* **53**, 85-96. |
| pAD152 | pRS551 [EcoRI-BamHI: 217 bp $P_{mra}$ region (89219-89436) containing $P_{mra}3$ promoter]. | A. Davidson |
| pAD153/pRS3M | pRS551 [EcoRI-BamHI: 135 bp $P_{mra}$ region (89301-89436) containing $P_{mra}3$ promoter]. | A. Davidson |
| pROB201 | pRS551 [EcoRI-BamHI: 217 bp $P_{mra}$ region (89219-89436) P3 DIS MUT as PCR template]. | This Study |
| pROB202 | pRS551 [EcoRI-BamHI: 415 bp $P_{mra}$ region (89219-89634) using pUC600 $P_{mra}1$ -10 as PCR template]. | This study |
| pROB203 | pRS551 [EcoRI-BamHI: 601 bp $P_{mra}$ region (89033-89634) using pUC600 $P_{mra}1$ -10 as PCR template]. | This study |
| pROB204 | pRS551 [EcoRI-BamHI: 415 bp $P_{mra}$ region (89219-89634) using pUC600 $P_{mra}3$ -10 as PCR template. | This study |
| pROB205 | pRS551 [EcoRI-BamHI: 601 bp $P_{mra}$ region (89033-89634) using pUC600 $P_{mra}3$ -10 as PCR template]. | This study |
| pROB206 | pRS551 [EcoRI-BamHI: 566 bp $P_{mra}$ region (89068-89634) using pUC600 $P_{mra}1$ -10 as PCR template]. | This study |
| pROB207 | pRS551 [EcoRI-BamHI: 519 bp $P_{mra}$ region (89115-89634) using pUC600 $P_{mra}1$ -10 as PCR template]. | This study |
| pROB208 | pRS551 [EcoRI-BamHI: 475 bp $P_{mra}$ region (89159-89634) using pUC600 $P_{mra}1$ | This study |

| | | |
|---|---|---|
| | -10 as PCR template]. | |
| pROB209 | pRS551 [EcoRI-BamHI: 601 bp $P_{mra}$ region (89033-89634) using pUC600 $P_{mra}1$ -10, $P_{mra}3$ -10 as PCR template]. | This study |
| pROB210 | pRS551 [EcoRI-BamHI: 601 bp $P_{mra}$ region (89033-89634)] | This study |
| pRS*yab*C | pRS551 [EcoRI-BamHI: 222 bp *yabB-yab*C (89993-90215)]. | This study |
| pRS*fts*L | pRS551 [EcoRI-BamHI: 239 bp *yab*C-*fts*L (90851-91090)]. | This study |
| pRS*fts*I | pRS551 [EcoRI-BamHI: 174 bp *fts*L-*fts*I (91291-91465)]. | This study |
| pRS*mur*E | pRS551 [EcoRI-BamHI: 199 bp *fts*I-*mur*E (93006-93205)]. | This study |
| pRS*mur*F | pRS551 [EcoRI-BamHI: 161 bp *mur*E-*mur*F (94549-94710)]. | This study |
| pRS*mra*Y | pRS551 [EcoRI-BamHI: 201 bp *mur*F-*mra*Y (95831-96032)]. | This study |
| pRS*mur*D | pRS551 [EcoRI-BamHI: 177 bp *mra*Y-*mur*D (96988-97084)]. | This study |
| pRS*fts*W | pRS551 [EcoRI-BamHI: 169 bp *mur*D-*fts*W (98256-98425)]. | This study |
| pRS*mur*G | pRS551 [EcoRI-BamHI: 177 bp *ftsW-mur*G (99526-99703)]. | This study |
| pRS*mur*C | pRS551 [EcoRI-BamHI: 198 bp *mur*G-*mur*C (100663-100861)]. | This study |
| pRS*ddl*B | pRS551 [EcoRI-BamHI: 154 bp *mur*C-*ddl*B (102115-102269)]. | This study |
| pRS*fts*L-2 | pRS551 [EcoRI-BamHI: 309 bp *fts*I-*fts*L (92896-93205)]. | This study |
| pRS*mur*D-2 | pRS551 [EcoRI-BamHI: 306 bp *mra*Y-*mur*D (96859-97165)]. | This study |
| pRS*ddl*B-2 | pRS551 [EcoRI-BamHI: 507 bp *mur*C- | This study |

| | | |
|---|---|---|
| | *ddl*B (101762-102269)]. | |
| pRS400-600For | pRS551 [EcoRI-BamHI: 208 bp $P_{mra}$ region (89033-89241)]. | This study |
| pRS400-600Rev | pRS551 [BamHI-EcoRI: 208 bp $P_{mra}$ region (89033-89241)]. | This study |
| pTOF24 | pKO3 [HinCII-HinCII: 1252 bp *aph* from pUC4K]; $Cm^R$ $Kan^R$ Ts $Suc^R$ | C.Merlin |
| pTOF73 | pTOF70 [HinCII-HinCII: 1252 bp *aph* from pUC4K] $Amp^R$ $Kan^R$ | C.Merlin |
| pGB150 | pACYC [$P_{sfiA}$-GFP] $Cm^R$ | G. Blakely |
| pJM511 | pBR328 derivative [EcoRI-HinDIII: 5.3 kb *pcn*]. $Amp^R$. | M. Masters |
| pZAQ | pBR322 derivative [*fts*QAZ cluster]. $Amp^R$. | Ward, J.E. and Lutkenhaus, J.F. (1985) *Cell* 42:941-949. (W. Donachie) |

All plasmids were stored in strain DH5α as glycerol stocks at -80°C.

## 2.5 Primers

**2.4 List of primers used in this study**

| Primer | Sequence |
|---|---|
| crpFOR | TTTGCATATGGTGCTTGGCAAACCGC |
| crpREV | ACAAGGATCCTTAACGAGTGCCGTAAAACGACG |
| crpEcoFOR | TTTGAATTCATGGTGCTTGGCAAACCG |
| fisEcoFOR | TTTGAATTCATGTTCGAACAACGCG |
| fisREVBam | TCGGATCCTTAGTTCATGCCGTATTTTTTC |
| fisFORNdeI | TTCATATGTTCGAACAACGCGTAAATTC |
| hnsFOR | TATTACCTCAACAAACCACCC |
| hnsREV | GCCGCTGGCGGGATTTTAAGC |
| ihfAFOR | GCATCATTGCGGGATTGAACC |
| ihfAREV | CGGCCTTTTTAGTTAGATCAG |
| lrpFOR | GTAGGGAAGGAATACAGAGAG |
| lrpREV | CGATTTTGCACCTGTTCCGTG |

| | |
|---|---|
| dksAFOR | TGCGTGTTAAGGAGAAGCAAC |
| dksAREV | GTAAACGTGATGGAACGGCTG |
| relAFOR | TGGTCCCTAAAGGAGAGGACG |
| relAREV | TAGATACGAGCAAATTTCGGC |
| spoTFOR | TAATCACAAAGCGGGTCGCCC |
| spoTREV | ATGCGTGCATAACGTGTTGGG |
| Lac crp FOR | TTTCCCGACTGGAAAGCGGG |
| Lac crp REV | CCACACAACATACGAGCCGG |
| lacZ-veC FOR | CCCGGTGCAGTATGAAGG |
| lacZ-veC REV | ACCGCCAAGACTGTTACC |
| fruRFOREco | TAGAATTCTGGAAAGATGATCCGCGCG |
| fruRREVBam | ATGGATCCGCGTATTTTTGTTCGCGGC |
| fruRBamFOR2 | CGGGATCCCAGTTATTCGAAAAATGGCTGGAAACGC |
| yabBPE1 | GCTGTCGAGATTGACTAACG |
| yabBPE2 REV | CACTGATAAGCGCCCTTTGCTGTCG |
| yabBREV2 | TAGAGACAAGTCCTGCAGTC |
| enoFOR | GAAATCATCGACTCCCGTGGT |
| enoREV | ATATCAACGTTGTTGTCAGCG |
| Z2-REV | GACCAGCAAGCTTAATCAGCTTGCTTACGCAG |
| PmraEco | CGAATTCACGGTGATGACGATGAGGG |
| PmraBam | GTGGATCCACCTAGCAGCCTCACCCCTTATTCC |
| PmraFor1 | TTGGATCCACGGTGATGACGATGAGGG |
| Pmra100FOR | CAGAATTCATATTAGCCGTAAACATCGGG |
| Pmra300FOR | CAGAATTCGCCACACAGACGTAACAAGG |
| Pmra400FOR | CAGAATTCATTATTTTGTTACATGCGGCG |
| Pmra450FOR | TTTGAATTCCGTTAATTAACTCACCAGCTG |
| Pmra500FOR | TTTGAATTCAAGACTATTCCTGAC |
| Pmra550FOR | TTTGAATTCATGTTCGAACAACGCG |
| Pmra600FOR | CAGAATTCGCCGCGAACAAAAATACGCG |
| Pmra300REV | AAAGGATCCTTCCCCGGTTAACAGTCC |
| P3400REV | TTGGATCCTCCCTCATCGTCATCACCG |
| 450REV | GCTGGTGAGTTAATTAACGGG |
| 500REV | GTCAGGAATAGTCTTATTTAC |
| 550REV | CCCGTACTCTACGCGCCAGAG |
| pRS551trpREV | TAACTGCGCGTCGCCGCTTTCATCG |
| pSP73REV | GCAGGTCGACTCTAGCGGATCCACC |

| | |
|---|---|
| 600FORBam | CAGGATCCGCCGCGAACAAAAATACGCG |
| 600REVBam | CAGGATCCCGCCGCATGTAACAAAATAATGC |
| 600REVEco | CAGAATTCCGCCGCATGTAACAAAATAATGC |
| PyabBEco | CCCGAATTCGGGATGAAACAACCTGGC |
| PyabBBam | AAAGGATCCCAGACGTGAGTGACCACC |
| PyabCEco | CCCGAATTCATGCGTGAAAACAGCCGC |
| PyabCBam | AAAGGATCCGTGGCTTCCCATCGATCC |
| PftsLEco | ACCGAATTCGAAGAGAATGCGCTCGGC |
| PftsLBam | CAAGGATCCGGCATGTTCTTCCTGACG |
| PftsIEco | GGGGAATTCTATCAACGATCCGCAGGC |
| PftsIBam | AAAGGATCCCACGGAGCAAGAAGGTCG |
| PmurEEco | ACAGAATTCACTGGTCGCGGGCAAAGG |
| PmurEBam | AAAGGATCCGCACCTTGCAGTTCACCG |
| PmurFEco | CCCGAATTCAGCCATGCTATCAGCACC |
| PmurFBam | AAAGGATTCCCAAATGTTCGGCCAGCC |
| PmraYEco | AGGGAATTCGAACTGAAAGGCTGGCCG |
| PmraYBam | ACAGGATCCGGAAAAAGTCCACGCAGG |
| PmurDEco | AGGGAATTCCTATGGAACAGGCGATGC |
| PmurDBam | ACAGGATCCCGAGGGAGAGATAAACGC |
| PftsWEco | CGAGAATTCGCCGCTGATCAGTTACGG |
| PftsWBam | ACAGGATCCTACATGTCCACCGGTTCC |
| PmurGEco | ACAGAATTCATGCCACCGAGCGAGTGG |
| PmurGBam | AAAGGATCCTACCGGCACCACCAATGC |
| PmurCEco | CGAGAATTCCGGTATTAACCGGTAACG |
| PmurCBam | ACAGGATCCGTCCCACCCAACAGGACC |
| PftsIEco2 | CAGGAATTCCCGGTACGCGAAAAAGG |
| PmraYEco2 | CAGGAATTCCTGCTGGTGATTATGGGG |
| PmurCEco2 | CCCGAATTCCCGCTGGAGCCAGTGAATGG |
| PmurCEcoREV | CCCGAATTCGTCCCACCCAACAGGACC |
| PmurCBglEco | CCCAGATCTGTCCCACCCAACAGGACC |
| ftsIPstFOR | AAACTGCAGGGCTGTATTCTCCTGGCG |
| ftsIEcoREV | AGGGAATTCCGGGTTGGCGTTAATGCG |
| ftsZPstFOR | CTACTGCAGAACACATGGTGCGCGAGC |
| ftsZEcoREV | CCTGAATTCTGTACCGGTACCACCACC |
| ftsWivFOR | GCATCTGGTTTAGCTTCCAGG |
| murGivREV | TATACCTTTTCCACGCAGACC |

| | |
|---|---|
| P1 MUT TOP | GCTTTTCCTCAGCTCCGTAGGCTCCTTTCAGTGGG |
| P1 MUT BOT | CCCACTGAAAGGAGCCTACGGAGCTGAGGAAAAGC |
| Bgl-SDM For | CCATCCATGATACAGCATAAAGATCTCTCCCCATCCCCTCAG |
| Bgl-SDM Rev | CTGGAGGGGATGGGGAGAGATCTTTATCTGTATCATGGATGG |
| pSRseq | CACCTGACGTATAAGAAACC |
| NoPmra | AAAAACTGCAGCCACCTTTGGCGATAACGAACTGC |
| NiPmra | CGCTCTTGCGGCCGCTTGGAACGGAGCCAGTCACAAGGCATACCGAGG |
| NiPmra2 | CGCTCTTGCGGCCGCTTGGAACGGAAAGTGTCAGTTTGCGACGCGAGC |
| NiPmra3 | CGCTCTTGCGGCCGCTTGGAACGGTACGTCTGTGTGGCGCTTGATGCC |
| CoPmra | AAAAAGTCGACGTCTCCGGTAGCCAACTGCTCTGC |
| CiPmra | CCGTTCCAAGCGGCCGCAAGAGCGGGGTGAGGCTGGCATGTTCCGGGG |
| CiPmra2 | CCGTTCCAAGCGGCCGCAAGCGCGATCGGGTTTTTTACCTCGGTATGC |
| CiPmra3 | CCGTTCCAAGCGGCCGCAAGCGAGTTAAAACGGTGATGACGATGAGGG |

All primers were supplied by MWG-Biotech. Primers were resuspended in 1xTE at 100pmol/µl. These stocks were then diluted in $dH_2O$ to give a working stock of 10pmol/µl. Primers were stored at -20°C.

## 2.6 Bacterial Methodology

### 2.6.1 Preparation of Competent Cells.

**Calcium Chloride Method:**

This method was used to prepare competent cells that were to be transformed on the same day. 5ml LB were inoculated with the appropriate strain and grown overnight, with shaking, at 37°C. A 1/100 dilution of the overnight culture was made into 10ml prewarmed LB in a 100ml flask. Cells were grown at 37°C in a shaking water bath (167rpm) to an $OD_{600}$ of 0.4. 1ml of cells were pelleted by centrifugation at 16,100 x *g* (Eppendorf 5415 D centrifuge) for 1 minute. The supernatant was discarded and the pellet resuspended in 1ml ice-cold 50mM $CaCl_2$, the cells were then pelleted by centrifugation as before. The supernatant was discarded and the pellet was resuspended in 0.1ml ice-cold 50mM $CaCl_2$. The cells were incubated on ice and were ready for transformation after approximately 1 hour.

**Rubidium Chloride Method:**

This method was used for the preparation of competent frozen stocks, usually of strain DH5α. 5ml LB were inoculated with the appropriate strain and grown overnight with shaking at 37°C. A 1/100 dilution of the overnight culture was made into 250ml prewarmed LB + 20mM $MgSO_4$ in a 1 litre flask. The cells were grown with on a flatbed shaker (160rpm) at 37°C until they had reached an $OD_{600}$ of 0.4. The cells were pelleted by centrifugation at 4,500 x *g* (Sorvall RC-5B centrifuge, with GSA rotor) for 5 minutes at 4°C. The supernatant was discarded and the pellet was gently resuspended in 100ml ice-cold TFB1 before incubation on ice for 5 minutes. The cells were pelleted by centrifugation as before, the supernatant was discarded and the pellet was resuspended in 10ml ice-cold TFB2. The cells were incubated on ice for 1 hour, then aliquoted (200µl/tube) before snap-freezing in liquid nitrogen and storing at -80°C.

**TFB1:** 30mM potassium acetate, 10mM $CaCl_2$, 50mM $MnCl_2$, 100mM RbCl, 15% v/v glycerol. Final pH adjusted to 5.8 with 1M acetic acid and filter sterilised with a 0.22µm filter.

**TFB2:** 10mM MOPS, 75mM $CaCl_2$, 10mMRbCl, 15% v/v glycerol. Final pH adjusted to 6.5 with 1M KOH and filter sterilised with a 0.22µm filter.

### 2.6.2 Heat Shock Transformation of Plasmid DNA.

When using frozen competent cells, these were first slowly thawed on ice. 2-10µl of plasmid DNA (freshly mini prepped or from a ligation) was added to 50µl of competent cells and incubated on ice for 30 minutes. The cells were heat shocked at 37°C for 2 minutes followed by 5 minutes incubation on ice, 500µl LB was added to the cells prior to incubation at 37° for 1 hour. The transformed cells were pelleted by centrifugation at 16,100 x *g* (Eppendorf 5415 D centrifuge) for 1 minute. The supernatant was discarded and the pellet resuspended in 100µl LB, which was spread on selective plates and incubated at 37°C overnight.

### 2.6.3 P1 Transduction.

The recipient strain was grown overnight at 37°C and 100µl was used to inoculate 10ml LB (1/100 dilution) in a 100ml flask. The culture was grown to an $OD_{600}$ of 0.4 and 1ml was centrifuged at 16,100 x *g* for 1 minute. The pellet was resuspended in 1ml LB and 100µl of cells were transferred into each of 3 tubes containing 100µl 50mM $CaCl_2$ and 100µl 100mM $MgSO_4$. 10, 1 and 0.1µl of the appropriate P1 lysate was added to the tubes and mixed before incubation at 37°C. After 20 minutes, 200µl 1M Na Citrate and 500µl LB was added. The cells were incubated for a further 30 minutes at 37°C, then pelleted as before. The pellet was resuspended in 100µl LB and plated on selective medium, which was incubated at a suitable temperature until colonies appeared.

### 2.6.4 Preparation of a P1 Lysate.

The donor strain was grown overnight at 37°C, and a 1/100 dilution was made into 10ml LB in a 100ml flask. The culture was grown to an $OD_{600}$ of 0.8 and 1ml of cells were pelleted by centrifugation at 10,000 x *g* for 5 minutes, before resuspension in 1ml LB. 100µl of resuspended cells was added to 100µl 50mM $CaCl_2$, 100µl 100mM $MgSO_4$ and 1µl P1 phage; this infection mix was vortexed then incubated at 37°C for 25 minutes.

Fresh LB agar plates containing 0.5mM $CaCl_2$ were poured and allowed to set but not to dry. The infection mix was added to 3ml molten top agar which was poured onto the LB agar plate. Following overnight incubation at 37°C, plaque formation was observed. 2.5ml phage buffer was used to cover the surface of the plate; this was left at room temperature for 15 minutes. A sterilised glass spreader was used to scrape up the soft agar layer and phage buffer, which were transferred to a universal bottle. 500µl $CHCl_3$ was added and the bottle was vortexed vigorously for 30 seconds before standing at room temperature for 30 minutes. Following re-vortexing, the agar and cell debris were removed by centrifugation at 3,000 x *g* (in a MSE Mistral 1000 centrifuge) for 10 minutes. The supernatant was transferred to a bijou bottle, 200µl $CHCl_3$ was added and it was centrifuged as before. The lysate was then ready for use, and stored at 4°C.

### 2.6.5 Transposon Mutagenesis.

Transposon mutagenesis of MG1655λ600 was performed in order to search for possible regulators of the $P_{mra}$ promoters. This strain contains a single copy λ prophage carrying DNA from pRS551 (601bp $P_{mra}$ region (89033-89634) fused to *lacZ*). MG1655λ600 was grown to an $OD_{600}$ of 0.4 and 1ml of cells were pelleted by centrifugation at 16,100 x *g* (Eppendorf 5415 D Centrifuge) for 1 minute. The pellet was resuspended in 500µl 10mM $MgSO_4$, 200µl of cells were then added to 10µl λNK1324 (λ lysate carrying mini-Tn10 with $Cm^R$) and the mixture was incubated at 37°C for 20 minutes. 500µl LB was added and incubation at 37°C was continued for 1 hour. The infection mix was plated onto selective media containing X-GAL to detect the mutants, and incubated at 37°C overnight.

### 2.6.6 Growth Curves.

Growth curves to determine doubling times of particular strains were performed in 250ml flasks containing 20ml LB (or appropriate liquid media) inoculated 1/100 from an overnight culture. 1ml samples were taken every 20 minutes (or at appropriate regular intervals for slow growing strains) and the optical density was measured at 600nm (Hitachi U-2000). Since spectrophotometer readings above an $OD_{600}$ of 1 are not accurate, cultures were diluted in LB in the cuvette and thoroughly mixed before a reading was taken. The readings were then multiplied by the dilution factor to give a true optical density.

Growth curves in association with β-galactosidase assays of reporter strains such as VIP407 were performed in a similar way. However, as β-galactosidase is very stable, levels are particularly high in cells exiting stationary phase. In some cases it was necessary to perform a series of 1/10 dilutions into new media as the cells reached mid-log phase growth to dilute out excess β-galactosidase.

### 2.6.7 β-galactosidase Assays.

β-galactosidase assays performed on reporter strains used 0.1ml of the sample culture taken at each time point added to 0.9ml Z Buffer in a 2ml tube. 50µl

$CHCl_3$ was added and the tube was vortexed for 30 seconds to lyse the cells. 200µl of freshly prepared 4mg/ml ONPG was added and vortexed, then the reaction was then incubated in a 30°C water bath. When a yellow colour was visible, 0.5ml 1M $Na_2CO_3$ was added to stop the reaction and the exact time was noted. The reaction was centrifuged at 16,100 x *g* (Eppendorf 5415 centrifuge) for 1 minute then 1ml was transferred to a plastic cuvette and both the $OD_{420}$ and $OD_{550}$ were measured. A reaction using LB instead of culture was treated in the same way and used as a control.

For β-galactosidase assays performed on cells harbouring a reporter plasmid, varying amounts of culture were used in the reactions. For cells with plasmids carrying a weak promoter up to 0.5ml of culture were used; however as pRS551 is a multi-copy plasmid only 0.1ml of culture were required in most cases.

β-galactosidase activity is expressed as Miller Units; these are calculated using the following formula:

$$\frac{OD_{420} - (1.75 \times OD_{550})}{OD_{600} \times 0.1 \times T} \times 1000$$

T = Time in minutes for colour change, 0.1 = Volume of culture in reaction.

**Z Buffer:** 60mM $Na_2HPO_4$, 45mM $NaH_2PO_4$, 10mM KCl, 1mM $MgSO_4.H_2O$, 50mM β-mercaptoethanol, 0.005% w/v Sodium Dodecyl Sulphate.

## 2.7 DNA Techniques

### 2.7.1 DNA Purification.

**Plasmid DNA:**

Plasmid DNA was prepared from 1–5ml of an overnight culture using the Qiagen QIAprep Spin Mini Prep Kit and eluted into 30-50µl Elution Buffer, as per manufacturer's instructions. When a large volume of plasmid was required, 100ml

of overnight culture were used with a Qiagen QIAfilter Plasmid Midi Kit and eluted into 500µl 1x TE Buffer. Plasmid DNA was stored at -20°C.

**1 x TE Buffer:** 10mM Tris-HCl, 1mM EDTA pH8.

**Chromosomal DNA:**
Chromosomal DNA was prepared from 5ml of an overnight culture using the Promega WIZARD Genomic DNA Purification Kit. DNA was resuspended in 100µl DNA Resuspension Buffer yielding approximately 1µg/µl and stored at 4°C.

### 2.7.2 Ethanol Precipitation of DNA

To purify DNA by ethanol precipitation, 0.3M NaOAc was added to DNA in solution, then 2 volumes of 100% ethanol was added and the mix was chilled at -80°C for 30 minutes. The DNA was pelleted by centrifugation at 16,100 x *g* (Eppendorf Centrifuge 5415 D) for 30 minutes, and then the supernatant was discarded and 2 volumes of 70% ethanol were used to resuspend the pellet. The mix was centrifuged as before, the supernatant was discarded and the DNA pellets were dried by spinning at the highest drying rate in a Savant DNA Speed Vac DNA110. The dried DNA pellets were resuspended in appropriate volumes of $dH_2O$ or 1 x TE Buffer, then stored at -20°C.

### 2.7.3 Quantification of DNA

DNA concentration was quantified by measuring the absorption of diluted solutions at 260nm in a spectrophotometer (Hitachi U-2000). For double stranded DNA, an $OD_{260}$ value of 1.0 is equivalent to a DNA concentration of 50µg/ml. The purity of DNA can be determined by measuring absorption at 260 and 280nm, a 260/280 ratio of 1.8 represents protein-free double stranded DNA.

### 2.7.4 Polymerase Chain Reactions

All PCR reactions contained 1 x Polymerase Buffer, 200µM dNTPS (dATP, dCTP, dGTP, dTTP) (Promega), 25 pmol forward primer, 25 pmol reverse primer, 100ng

chromosomal DNA template (unless otherwise stated), 2.5U T*aq* Polymerase (NEB) or 1.5U P*fu* Polymerase (Promega), with the volume made up to 50µl with $dH_2O$.

The PCR program consisted of 3 stages. Stage 1 was a denaturing step with a 3 minute incubation at 94°C to produce a single stranded template. Stage 2 consisted of 30 cycles of the following steps; 94°C denaturing step for 1 minute, 50-60°C (depending on primers used) annealing step for 1 minute, 72°C extension step for 1 minute/kb of expected product. Stage 3 was a final elongation step with a 10 minute incubation at 72°C to finish off the synthesis of any uncompleted product.

All PCR reactions were performed in a Techne Progene Thermal Cycler, or in an Eppendorf Mastercycler Gradient. T*aq* Polymerase was used for analytical PCRs, however for PCR products which were to be used for cloning it was necessary to use a proof-reading polymerase, in this case P*fu* Polymerase. PCR products were purified using the Qiagen PCR Purification Kit and analysed by running 5-10µl on an agarose gel.

### 2.7.5 Agarose Gel Electrophoresis

The separation and visualisation of DNA molecules was performed by Agarose gel electrophoresis. Gels were prepared by adding 1% w/v Agarose (Invitrogen) to 1 x TAE and heating in a microwave (although this did vary from 0.8-2% w/v depending on the size of DNA fragments being resolved). Gels were cast in trays appropriate for the size of Bio-rad electrophoresis tank being used (mini, midi or subcell GT) and lane combs were positioned last. Once set, the gels were transferred to the electrophoresis tank and immersed in 1 x TAE. DNA samples were prepared by the addition of 5 x Loading Dye to the DNA sample of usually 10µl in volume; DNA size ladders were prepared in the same way. DNA samples were loaded onto the gel, which was then run at 80V for 1 hour. The DNA in the gel was stained with 1µg/ml ethidium bromide for 20 minutes followed by destaining in $dH_2O$ for 10 minutes. The gel was transferred to a UV transilluminator connected to a digital CCD detector, and the bands of DNA were photographed.

**50 x TAE Buffer:** 2M Tris, 0.95M glacial acetic acid, 50mM EDTA pH8.

**5 x Loading Buffer:** 15% w/v Ficoll, 100mM EDTA pH8, 0.25% w/v Bromophenol Blue, 0.25% w/v Xylene Cyanol.

### 2.7.6 Digestion of DNA with restriction endonucleases

Endonuclease digestion of DNA was usually performed in a reaction volume of 50µl. Each reaction contained 1 x Restriction Buffer as recommended by the supplier (NEB, Promega, Roche) and 1-10µg DNA with reaction volume made up with $dH_2O$. Enzymes was added at concentrations recommended by the manufacturer and volumes were kept below 10% total volume to reduce star activity. Bovine Serum Albumin was added when recommended at a final concentration of 0.1µg/µl. Digests were incubated at 37°C for 1 hour, and then purified using the Qiagen PCR purification kit. Digests were analysed by running 10µl of the product on an agarose gel.

### 2.7.7 Dephosphorylation of DNA

It was sometimes necessary to dephosphorylate a digested fragment of DNA if it was subsequently to be used in a ligation reaction. After the 1 hour 37°C incubation, 1 unit of calf intestinal Alkaline Phosphatase (Promega) was added to the restriction digest reaction which was then incubated for a further 30 minutes at 37°C. The reaction was subsequently purified using the Qiagen PCR purification kit.

### 2.7.8 Recovery of DNA from an agarose gel

Digested DNA was sometimes purified directly from an agarose gel. The gel was stained as described previously in ethidium bromide, and the bands produced by the restriction digest were visualised on a UV transilluminator. Appropriate bands were excised from the gel and the DNA was extracted using the Qiagen QIAquick gel extraction kit following the supplier's protocol.

### 2.7.9 Ligation of DNA

Ligations of DNA were performed in 10µl reaction volumes. The reactions usually contained 1µg total DNA and a series of vector:insert ratios with a 2-20 fold molar excess of insert to vector were usually set up in parallel. Reactions also contained 1 x T4 DNA Ligase Buffer, 1.5 Units T4 DNA Ligase (Promega) with the reaction volume made up with $dH_2O$. Reactions were incubated at room temperature for at least 2 hours prior to transformation into competent DH5α cells.

### 2.7.10 Single Colony Gels

To determine whether a ligation had worked it was necessary to extract plasmid DNA from single colony transformants. When multiple transformants required screening it was not sensible to perform multiple minipreps, instead a crude lysis buffer was prepared and used to lyse cells from a single patched out colony. A toothpick was used to transfer cells from a patched out colony into 100µl of SCFS buffer. The toothpick was left to stand in the buffer for 15 minutes at room temperature, it was then removed and the tube was centrifuged at 16,100 x *g* (Eppendorf centrifuge 5415 D) for 30 minutes. 20µl of the supernatant containing the DNA was run on a 0.8% w/v agarose gel with vector DNA run alongside as a control. The DNA was stained and visualised as described previously.

**SCFS Buffer**: 2.5% w/v Ficoll, 1.25% w/v SDS, 0.015% w/v Bromophenol Blue, 10µg/ml RNaseA, made up in 1 x TAE Buffer.

### 2.7.11 Single colony PCR

Sometimes it would not be possible to detect an insert on a single colony gel if the vector was too large or the insert too small. In these cases a single colony PCR would be performed using one primer which annealed to the insert and one primer which annealed to the vector. The PCR protocol previously described was followed except that a single colony was inoculated into the PCR reaction using a toothpick, instead of purified DNA as a template.

### 2.7.12 DNA Sequencing

Sequencing reactions were performed in a Techne Progene Thermal Cycler using the ABI PRISM Big Dye™ Ready Reaction Cycle Sequence Kit. 20µl reactions were set up containing: 8µl Big Dye Sequencing mix, 3.2pmol of the appropriate primer, 50-400ng of DNA, with the volume made up with $dH_2O$. The thermal cycling program consisted of 25 cycles of; 96°C for 30 seconds, 50°C for 15 seconds and a 4 minute extension at 60°C. The reactions were sent for processing by the ICMB sequencing service on an ABI PRISM 3100 DNA sequencer.

### 2.7.13 Radiolabelling of DNA

**5′ end-labelling of DNA with $^{32}P$.**

DNA was 5′ labelled using Redivue [$^{32}P$] γ-ATP (Amersham 0.37MBq/µl) and T4 Polynucleotide Kinase (Promega). If both strands of the DNA were to be 5′ labelled then a purified PCR fragment was used in the labelling reaction. If only one end was to be 5′ labelled then a primer was labelled and subsequently used in a radioactive PCR reaction to generate a single-end labelled PCR product. The labelling reaction was performed in a Techne Progene Thermal Cycler in reaction volume of 20µl. The reaction contained 1 x Polynucleotide Kinase buffer, 1.85MBq Redivue [$^{32}P$] γ-ATP, 10pmol ends of DNA (1µl primer, or 10µl PCR product), 5 Units T4 Polynucleotide Kinase, and the volume was made up with $dH_2O$. The reaction was incubated at 37°C for 45 minutes before the addition of 25mM EDTA pH8. The reaction was stopped by incubating at 72°C for 10 minutes, then the labelled DNA was spun through a MicroSpin G25 column (Amersham) at 0.8 x *g* (Eppendorf centrifuge 5415 D) for 2 minutes to remove any unincorporated radionuclide. The labelled DNA/primer was stored at -20°C.

**Random priming of DNA with $^{32}P$.**

When labelled DNA probes were required for hybridisation to RNA on a Northern blot it was necessary to random prime label them, using the Rediprime™II random prime labelling system (Amersham). The DNA to be labelled was diluted to 2.5-25ng in 45µl TE buffer. The DNA was denatured by incubating at 95°C for 5 minutes in a Techne Progene Thermal Cycler, and then snap cooled on ice for 5

minutes. The denatured DNA was added to the Rediprime reaction tube and then 5µl of Redivue [$^{32}$P] dCTP (0.37MBq/µl) was added and mixed in thoroughly. The reaction was incubated at 37°C for 10 minutes and stopped with the addition of 20mM EDTA pH8. The reaction was spun through a MicroSpin G25 column (Amersham) at 0.8 x *g* (Eppendorf centrifuge 5415 D) for 2 minutes to remove any unincorporated radionuclide. The labelled DNA/primer was stored at -20°C.

### 2.7.14 Radioactive PCR

To generate single-end labelled DNA products, PCRs were performed using either a labelled forward or reverse primer. PCRs were performed as described previously, except the entire 20µl primer labelling reaction was used in place of the 2.5pmol of the appropriate unlabelled primer. The radioactive PCR reaction was resolved on a non-denaturing 4% w/v acrylamide gel and then gel extracted.

### 2.7.15 Non-denaturing Acrylamide Gel Electrophoresis

Non-denaturing Acrylamide gels were used to resolve any impurities from radioactive PCR reactions prior to gel extraction, and to resolve the products of EMSAs. Gels were prepared in a volume of 40ml containing: 1 x TBE Buffer, 4% w/v Acrylamide, made up to volume with $dH_2O$ and then polymerised by the addition of 350µl 10% w/v APS and 30µl TEMED. Gels were cast between two glass plates (approx. 17cm x 20cm) that fit within a Sigma vertical electrophoresis tank; finally a comb was positioned to create the wells. When the gel has set it was clamped to the electrophoresis tank. Top and bottom reservoirs were filled with 1 x TBE, and the wells were flushed out to remove any unpolymerised acrylamide. The gel was pre-run at 200V for around 30 minutes until the current remained constant. Samples from EMSAs could be loaded directly onto the gel, however radioactive PCRs required the addition of 50% v/v glycerol, one reaction per gel had 1µl bromophenol blue added to follow the progress of the samples. Gels were run at 200V for 3-4 hours at room temperature (up to 5 hours when gels were run at 4°C) until the bromophenol blue reached the bottom of the gel.

**10 x TBE:** 0.9M Tris-HCL pH8, 0.9M Boric acid, 20mM EDTA.

### 2.7.16 Gel Extraction and Purification of Radioactive PCR products

Radioactive PCR products were run on a non-denaturing acrylamide gel as described previously. The gel plates were split behind a screen and reusable luminescent markers were placed directly onto the sides of the gel as reference points. The gel, still attached to the back plate was wrapped in Saran Wrap, placed in an auto-radiography cassette and exposed to Hyperfilm™ (Amersham) for 5 minutes. The film was developed using a Konica SRX-101A developer and a band representing the Radioactive PCR product was visible. The gel was unwrapped and placed on top of the developed film. The markers were lined up so that the radioactive PCR band on the film corresponded to radioactive PCR product on the gel above. The PCR product was excised and transferred to an Eppendorf tube containing 500µl 1 x STE and incubated overnight at 37°C for the salt to displace the DNA from the gel.

Following incubation, the gel fragment and STE were transferred to a Spin-X (Costar) tube and centrifuged at 0.8 x *g* (Eppendorf centrifuge 5415 D) for 5 minutes. The radiolabelled DNA was ethanol precipitated and the final pellet was resuspended in 10µl 1 x TE.

**1 x STE Buffer**: 100mM NaCl, 10mM Tris-HCl, 1mM EDTA pH8.

## 2.8 RNA Techniques

### 2.8.1 RNA Purification

Total RNA was extracted from cultures using a Qiagen RNeasy Mini prep kit. Cells of the appropriate strain were grown to an $OD_{600}$ of 0.4, and then 1ml was pelleted by centrifugation at 5,000 x *g* (Eppendorf Centrifuge 5415 D) for 5 minutes. A 400µg/ml Lysozyme solution was prepared in TE buffer, 100µl of this was used to resuspend the cell pellet which was incubated at room temperature for 5 minutes, to allow lysis of the cells. The manufacturer's bacterial mini prep protocol was followed with the RNA finally being eluted in 100µl of RNase-free $H_2O$.

It was necessary to remove any DNA from the purified RNA by DNaseI treatment. We found that the Qiagen on-column DNaseI digestion wasn't always sufficient for complete DNA cleavage, so RQ DNaseI Buffer and 10Units of RQ DNaseI (Promega) was added to the 100µl of purified RNA. The reaction was gently mixed, as DNaseI is very sensitive to physical denaturation, and incubated at 37°C for 30 minutes. 1µl of RQ DNaseI Stop Solution was added and the reaction was incubated at 65°C for 10 minutes. The reaction was applied to an RNeasy mini column and the mini prep protocol was followed from step 6 onwards. The DNA free RNA was resuspended in 100µl of RNase-free $H_2O$. RNA was stored long term at -70°C, but was kept in small aliquots at -20°C when frequently in use.

### 2.8.2 Quantification of RNA

RNA concentration was quantified by measuring the absorption of diluted solutions at 260nm in a spectrophotometer (Hitachi U-2000). An $OD_{260}$ value of 1.0 is equivalent to a RNA concentration of 40µg/ml. The purity of RNA can be determined by measuring absorption at 260 and 280nm, a 260/280 ratio of 2.0 represents protein-free RNA.

### 2.8.3 DEPC treatment of solutions.

RNA is easily degraded by RNases, therefore before working with RNA all surfaces were treated with RNaseZAP® (Sigma) and all solutions were treated with DEPC (diethylpyrocarbonate). 0.1% v/v DEPC was added to solutions in a fume hood, they were incubated at 37°C overnight, and the solutions were then autoclaved before use.

### 2.8.4 Reverse-Transcription Polymerase Chain Reaction.

RT-PCRs were performed with the Qiagen OneStep RT-PCR Kit, which contains a mix of Omniscript and Sensiscript Reverse Transcriptases and HotStarTaq DNA Polymerase. RT-PCR reactions were prepared on ice in a 50µl volume containing 1 x OneStep RT-PCR Buffer, 400µM dNTPs, 25pmol both forward and reverse primers, 20Units rRNasin (Promega), 1µg template total RNA, 2µl of OneStep RT-

PCR Enzyme Mix and the volume was made up with RNase-free $H_2O$. A Techne Progene Thermal Cycler was used to perform the RT-PCR reaction. The thermal cycler was first heated to 50°C before the reaction tubes were placed inside; they were then incubated at 50°C for 30 minutes for the reverse-transcription reaction to take place. A 15 minute initial PCR activation step was performed which inactivated the reverse transcriptases, activated the HotStarTaq DNA Polymerase and denatured the newly formed cDNA template. A traditional PCR cycle was then followed as described previously. RT-PCR products and their appropriate controls were resolved by agarose gel electrophoresis.

When attempting to reverse transcribe large transcripts it was necessary to separate the reverse transcription and PCR reactions. The cDNA synthesis was performed using a Qiagen Omniscript™ Reverse Transcriptase Kit following the manufacturer's protocol; this was then used as the template for a PCR using 2 units of the long range DNA Polymerase LA Taq™ (TaKaRa) with an extension time of 1 minute/kb of expected product.

### 2.8.5 Phenol Extraction of RNA

RNA was purified from solution using phenol extraction. The RNA in solution was made up to at least 150µl in volume with RNase-free $H_2O$. An equal volume of phenol was added, the mixture was vortexed and centrifuged at 16,100 x *g* (Eppendorf Centrifuge 5415 D) for 5 minutes. The aqueous layer was retained and transferred into a new tube, an equal volume of 24:1 $CHCl_3$: isoamylethanol was added and the mixture was vortexed and centrifuged as before. The aqueous layer was retained and transferred into a new tube, an equal volume of Phenol: CHCl3 was added and the mixture was vortexed and centrifuged as before. The aqueous layer was retained and transferred to a new tube, an equal volume of $CHCl_3$ was added and the mixture was vortexed and centrifuged as before. The aqueous layer containing purified RNA was retained.

### 2.8.6 *In vitro* Transcription Reactions

The first method of *in vitro* transcription attempted in this work used the plasmid pSP73-600. A 50µl reaction was set up containing 2µg of supercoiled pSP73-600, 200nM RNA Polymerase (USB), and made up to volume in IVT Buffer 1. The reaction was incubated at 30°C for 30 minutes in a Techne Progene Thermal Cycler. The reaction was stopped by the addition of 300µl IVT Buffer 2 containing 10µg/ml Proteinase K and incubation at 42°C for 30 minutes. RNA transcripts were purified by phenol extraction followed by 2 ethanol precipitations and resuspension in 20µl RNase-free $H_2O$. Primer extensions were performed using labelled primer and resolved on a 6% w/v acrylamide sequencing gel.

**IVT Buffer 1:** 10mM Tris-HCl pH8, 2mM DTT, NaCl, 10mM $MgCl_2$, 2.5mM rATP, 2.5mM rGTP, 2.5mM rCTP, 2.5mM rUTP.

**IVT Buffer 2:** 10mM Tris-HCl pH7.4, 1mM EDTA, 50nM NaOAc, 0.2% w/v SDS.

**Single round *in vitro* transcription:**

Single round *in vitro* transcription was performed using the plasmid pSR600, it involves the incorporation of labelled rUTP into the transcript therefore doesn't require a labelled primer extension step. A 10µl reaction was set up containing 1 x Transcription Buffer, 10nM pSR600 DNA, 1µg/ml BSA, 2mM DTT, made up to volume with $dH_2O$. Finally 200nM RNA Polymerase (USB) was added and the reaction was incubated at 37°C for 10 minutes. 5µl of a pre-warmed polymerisation mix containing: 1 x Transcription buffer, 300µM rATP/rCTP/rGTP, 30µM rUTP, 250µg/ml Heparin, 0.07MBq [$\alpha$ -$^{32}$P] UTP was added to the reaction and incubated at 37°C for 5 minutes. The reaction was stopped by the addition of 2 x formamide loading buffer and incubation at 65°C for 5 minutes. The products were denatured by heating to 95°C for 2 minutes then loaded onto a 6% w/v acrylamide sequencing gel for analysis.

Cold single round transcription assays were also performed on pSR600, they were set up in the same way except 300µM rUTP was used per reaction and the [$\alpha$ -$^{32}$P]

UTP was omitted. Following the addition and incubation of the polymerisation mix, 10 units of RQ RNase-free DNaseI (Promega) was added and incubated at 37°C for 15 minutes. The mRNA transcripts were purified by phenol extraction followed by 2 ethanol precipitations and resuspension in 20µl RNase-free $H_2O$. Primer extensions were performed using labelled primer and resolved on a 6% w/v acrylamide sequencing gel.

**10 x Transcription Buffer:** 200mM Tris-HCl pH8, 1M NaCl, 150mM $MgCl_2$.

**Formamide Loading Buffer:** 95% v/v Formamide, 20mM EDTA, 0.05% w/v Bromophenol Blue, 0.05% w/v Xylene Cyanol

**Run-off *in vitro* transcription:**

Run-off *in vitro* transcription using pSR600 was performed to try and increase the amount of transcript produced (protocol based on that used in Gonzalez-Gil *et al.*, 1998, EMBO **17** (10): 2877-2885). Unlike single round assays, run off *in vitro* transcription does not include Heparin in the reaction mix which prevents RNA Polymerase from re-binding to the promoter and producing successive rounds of transcription. A 50µl reaction was set up containing: 1 x Transcription Buffer, 2µg pSR600 DNA, 2mM DTT, 2.5mM rNTPs and 200nM RNA Polymerase (USB), it was incubated at 30°C for 30 minutes in a Techne Progene Thermal Cycler. The mRNA transcripts were purified using a Qiagen RNeasy mini prep kit and eluted into 50µl elution buffer. The transcripts were converted into cDNA by primer extension using a labelled primer, and the products were resolved on a 6% w/v acrylamide sequencing gel.

### 2.8.7 Primer Extension Reactions

Primer extension reactions were performed on total RNA or on *in vitro* transcription products to determine the 5′ end of a particular transcript. 50µl reactions were set up on ice, they contained; 1 x MMLV RT Buffer (Promega), 2.5mM dNTPs, 2µg total RNA/10µl *in vitro* transcription product, ~0.1MBq (2µl of ≤450 cps/µl) labelled reverse primer, made up to volume with RNase-free $H_2O$. The reactions were performed in a Techne Progene Thermal Cycler. The RNA was

initially denatured with a 3 minute incubation at 70°C; the labelled primer was then annealed to the denatured template at 42°C for 10 minutes. 100 Units of MMLV Reverse Transcriptase (Promega) were then added to the reaction, which was incubated at 42°C for 60 minutes to allow extension of the cDNA. The labelled cDNA products were ethanol precipitated and resuspended in 3µl RNase-free Elution Buffer (Qiagen) and 3µl formamide loading buffer. These products were either stored at -20°C, or denatured by heating to 95°C for 2 minutes and loaded onto a 6% w/v acrylamide sequencing gel for analysis.

### 2.8.8 Northern Blots

**Northern Blot using radio-labelled probe**

Northern blots using radio-labelled probe were performed using the Northern Max-Gly Northern Blotting Kit (Ambion). A 1% w/v agarose gel was prepared in Gel running buffer diluted with RNase-free water, as per manufacturer's protocol. A Bio-rad mini subcell electrophoresis tank was cleaned with RNaseZAP before the set gel and running buffer were placed in it. An equal volume of Glyoxal load dye was added to the RNA samples and incubated at 50°C for 30 minutes, before loading onto the gel. The gel was run at 80V for 90 minutes, and the RNA was visualised with a UV-transilluminator while the gel was still in the gel tray.

The gel was transferred to Hybond-N membrane (Amersham) overnight by capillary blot, following the manufacturer's protocol. The membrane was transferred to a hybridisation tube, 10-15 ml of Ultra-hyb which had been preheated to 68°C was added, and then the membrane was prehybridised at 42°C for 30 minutes in a Techne hybridiser HB-1D. A probe for the RNA that had been labelled with $^{32}P$ by random priming was added to the hybridisation tube incubated overnight at 42°C. The radioactive Ultra-hyb was discarded and the membrane was immersed in 10-15ml low stringency wash solution at 22°C for 10 minutes, followed by two washes in high stringency wash solution at 42°C for 15 minutes, these washes were to remove any probe bound to non-specific RNA. The membrane was wrapped in Saran Wrap and exposed to Hyperfilm (Amersham) overnight, prior to developing in a Konica SRX-101A developer.

**Northern Blot using fluorescently labelled probe.**

Fluorescent labelled probes were made using a DIG RNA labelling kit (Roche) and the plasmids pSPT18*ftsI* and pSPT18 *ftsZ*. The probes were ethanol precipitated (in ethanol containing 100mM LiCl), and the pellets were resuspended in 100µl RNase-free $H_2O$. A 1.5% w/v MOPS-formaldehyde-agarose gel was prepared. The agarose was melted in 1 x MOPS buffer and cooled to 50-60°C before addition of 6.3% v/v formaldehyde in a fume hood; the gel was cast and allowed to set for 1 hour. RNA samples were denatured in 3 volumes of: 500µl formamide, 162µl 37% v/v formaldehyde, 100µl 10 x MOPS, at 65°C for 5 minutes. The samples were chilled on ice then 0.4 volumes RNA loading buffer was added before loading the samples on the gel. The gel was run in 1 x MOPS at 70V for 1.5-2 hours, it was then rinsed in RNase-free $H_2O$ and a capillary blot was set up. The gel was transferred to Hybond-$N^+$ membrane (Amersham) in 20 x SSC overnight. The membrane was baked at 65°C for 20 minutes, and then crosslinked on a UV-transilluminator for 3 minutes. The membrane was prehybridised in 50ml RNA hybridisation buffer at 68°C for 3-4 hours. A 1/50 dilution of the RNA probe was made into hybridisation buffer, and it was denatured by boiling for 10 minutes then quick chilling on ice. The denatured probe was added to the membrane and they were hybridised overnight at 68°C with shaking. Two high salt/low temperature washes of the membrane were performed at room temperature for 15 minutes in 50ml 2 x SSC + 0.1% w/v SDS, followed by two low salt/high temperature washes at 68°C for 5 minutes in 50ml preheated 0.1% w/v SSC + 0.1% w/v SDS. The membrane was washed and blocked using the DIG wash and block buffer kit (Roche). This kit contains the Anti-DIG antibody, which is linked to alkaline phosphatase, and which binds to the DIG attached to the probe. CSPD is a chemiluminescent substrate for alkaline phosphatase, and was used to detect bound DIG labelled probe by the production of visible light that can be recorded on Hyperfilm. The membrane was covered in CSPD, wrapped in Saran Wrap and exposed to film for 2 minutes prior to developing in a Konica SRX-101A developer.

**10 x MOPS:** 0.4M MOPS pH7, 0.1M sodium acetate, 0.01M EDTA

**RNA loading buffer:** 50% v/v glycerol, 1mM EDTA pH8, 0.25% w/v bromophenol blue

**RNA hybridisation buffer:** 50% v/v formamide, 5 x SSC, 2% w/v blocking reagent (from kit), 0.1% v/v N-lauryl-sarcosine, 0.02% w/v SDS

**20 x SSC:** 3M NaCl, 0.3M tri -sodium citrate, pH7.

## 2.9 Protein Techniques

### 2.9.1 SDS-Polyacrylamide Gel Electrophoresis

Protein samples were resolved on a denaturing polyacrylamide gel. Gels were cast between glass plates for use in a Bio-rad Mini Protean 3 electrophoresis tank. A 12ml, 12% w/v acrylamide resolving gel was prepared containing 1 x Resolving buffer, 12% w/v acrylamide, 0.1% v/v SDS made up to volume with $dH_2O$. The gel was polymerised by the addition of 8µl TEMED and 100µl 10% v/vAPS, these were quickly mixed into the gel mix and 3.5ml were poured between each pair of plates. Approximately 250µl of isopropanol were poured on top of the gels while they set to create a level interface for the stacking gel. The isopropanol was poured off before the addition of a 5% w/v acrylamide stacking gel on top. 9ml of stacking gel was prepared containing: 1 x Stacking buffer, 5% w/v acrylamide, 0.1% v/v SDS, made up to volume with $dH_2O$ and polymerised by the addition of 8µl TEMED and 100µl 10% v/v APS. The plates were filled to the top with stacking gel, and a comb was inserted. The set gels were placed in the Bio-rad Mini Protean 3 electrophoresis tank and the tank was filled with Running Buffer to half way up the plates.

Proteins samples were denatured by boiling for 5 minutes in 1 x SDS sample buffer (NEB), they were then loaded onto the gel which was run at 200V for 1 hour, or until the dye front had reached the bottom of the gel. Gels were washed in $dH_2O$ then stained in Coomassie stain for 30 minutes. Gels were destained for 30

minutes in Coomassie destain then left overnight in $dH_2O$ to rehydrate. Gels were dried onto blotting paper at 80°C for 25 minutes using a Bio-rad gel dryer.

**4 x Resolving Buffer:** 1.5M Tris-HCl pH8.8

**4 x Stacking Buffer:** 0.5M Tris-HCl pH6.8

**10 x Running Buffer:** 0.25M Tris-HCl, 1.9M Glycine. 1 x Running Buffer had 0.1% v/v SDS added.

**Coomassie Stain:** 45% v/v Methanol, 10% v/v Glacial acetic acid, 0.25% w/v Coomassie Brilliant Blue

**Coomassie Destain:** 45% v/v Methanol, 10% v/v Glacial acetic acid.

### 2.9.2 Preparation of soluble protein lysates.

A 500ml LB culture of the appropriate strain was grown in a 2 litre flask, with shaking at 37°C, until the cells reached an $OD_{600}$ of 0.4. Cells were pelleted by centrifugation at 6000 x *g*, at 4°C, for 10 minutes (in a Sorvall RC-5B centrifuge, with GSA rotor). The supernatant was discarded, and the 2 x 250ml cell pellets were each resuspended in 5ml 0.1M NaCl-HSB buffer containing 1mg/ml Lysozyme to lyse the cells and 1mM of the protease inhibitor PMSF. The cells were incubated on ice for 30 minutes to allow the cells to lyse; this was followed by sonication (Sanyo Soniprep 150, small probe) at 8 microns for 10 x 10 seconds, with 20 seconds cooling in between. The lysed cells were centrifuged at 20,000 x *g*, at 4°C for 20 minutes (in a Sorvall RC-5B centrifuge, with a S34 rotor) to remove the cell debris, and the soluble protein lysate was then kept on ice or stored at -20°C with the addition of an equal volume of 50% v/v glycerol.

When soluble protein lysates were prepared from a small volume of cells, for example when performing a Western blot on multiple samples taken during a growth curve, it was necessary to first pellet the cells by centrifugation at 6000 x *g*

(Sigma 3-16K centrifuge) at 4°C in an appropriate sized centrifuge rotor for the sample being processed (sample volumes varied from 0.5 – 200ml). The samples were then resuspended in 2ml ice-cold 0.1M NaCl-HSB Buffer. The cell walls were weakened by quick freezing in liquid nitrogen followed by thawing at 37°C. This process was repeated 3 times before sonication as described previously using an exponential microprobe. The lysed cells were centrifuged at 16,100 x *g* (Sigma 3-16K centrifuge) for 10 minutes at 4°C to remove cell debris. The soluble protein lysates were incubated on ice for their protein concentrations to be quantified.

**0.1M NaCl-HSB Buffer:** 100mM NaCl, 20mM Tris-HCl, 0.1mM EDTA, pH 7.5

### 2.9.3 Protein purification

**HIS-tagged protein purification**

The gene for the protein of interest (e.g. *crp*) was cloned into pET33b (Novagen) and transformed into DH5α. The resulting vector (e.g. pROB101) was purified by miniprep and transformed into the strain BL21-DE3 for the protein to be over-expressed. The transformed strain was grown up in 250ml LB in a 2 litre flask at 37°C with shaking, until the $OD_{600}$ reached 0.4. A 1ml sample of the culture was retained before protein expression was induced by the addition of 1mM IPTG for 1 hour. Cells were pelleted by centrifugation at 6,000 x *g* at 4°C, for 10 minutes (in a Sorvall RC-5B centrifuge, with GSA rotor). The supernatant was discarded, and the cells were resuspended in 5ml chilled His-tag Lysis Buffer containing 1mg/ml Lysozyme and 1mM PMSF. The cells were incubated on ice for 30 minutes followed by sonication (Sanyo Soniprep 150, small probe) at 8 microns for 10 x 10 seconds, with 20 seconds cooling in between. The lysed cells were centrifuged at 20,000 x *g*, at 4°C for 20 minutes (in a Sorvall RC-5B centrifuge, with a S34 rotor) to remove the cell debris.

The lysate was applied to a Qiagen 5ml polypropylene column prepared with 1ml Qiagen Ni-NTA Agarose Resin. The column was sealed and incubated horizontally on ice, with shaking, for 1 hour. The column was clamped vertically and the flow through was collected. 10ml of His-tag Wash Buffer were used to wash through the column then the His-tagged protein was eluted by the addition of

5ml His-tag Elution Buffer, 0.5ml fractions were collected. Samples from the column were analysed by SDS-PAGE, and stored at -20°C with the addition of an equal volume of 50% glycerol.

**His-tag Lysis Buffer:** 50mM $NaH_2PO_4$, 300mM NaCl, 10mM imidazole, pH8.

**His-tag Wash Buffer:** 50mM $NaH_2PO_4$, 300mM NaCl, 20mM imidazole, pH8.

**His-tag Elution Buffer:** 50mM $NaH_2PO_4$, 300mM NaCl, 250mM imidazole, pH8.

**Purification of MBP-fusion proteins**

The gene for the protein of interest (e.g. *fis*) was cloned into pMAL-c2x (NEB) and transformed into DH5α. The resulting vector (e.g. pROB103) was purified by miniprep and the protein was overexpressed in DH5α. The MBP fusion protein was induced as for HIS-tagged proteins, however the cells were lysed in MBP Column Buffer; lysis and sonication proceeded as described previously for HIS-tagged proteins. A Qiagen 5ml polypropylene column was prepared with 5ml Amylose Resin (NEB). The column was clamped vertically and the liquid from the amylose suspension dripped through and was discarded. The column was washed in 8 volumes of MBP Column Buffer before addition of the MBP-protein lysate. The column was washed in 10 volumes of MBP Column Buffer, and then the protein was eluted in 5ml MBP Elution Buffer, 0.5ml fractions were collected. Samples from the column were analysed by SDS-PAGE, and stored at -20°C with the addition of an equal volume of 50% glycerol.

**MBP Column Buffer:** 20mM Tris-HCl pH7.4, 200mM NaCl, 1mM EDTA, 1mM sodium azide, 1mM DTT.

**MBP Elution Buffer:** 20mM Tris-HCl pH7.4, 200mM NaCl, 1mM EDTA, 1mM sodium azide, 1mM DTT, 10mM Maltose.

### 2.9.4 Quantification of protein concentration (Bradford Assays)

Protein concentration was measured using the Bio-rad Protein Assay (Bradford Reagent). A series of protein standards were prepared (1.25-25µg/ml) from diluted BSA (10mg/ml) in 800µl $dH_2O$. 200µl Protein Assay was added to the protein standards; they were mixed and incubated at room temperature for 5 minutes. The assays were transferred to 1ml plastic cuvettes and the $OD_{595}$ was measured in a spectrophotometer (Hitachi U-2000). A standard curve was generated by plotting protein concentration against $OD_{595}$. Dilutions of protein solutions of unknown concentration were prepared and assayed in the same way. When the $OD_{595}$ of these was known, protein concentration was determined using the standard curve.

### 2.9.5 Ammonium Sulphate Precipitation

Ammonium sulphate precipitation was used in order to fractionate the large number of DNA binding proteins present in a soluble protein lysate. Table 2.5 was used to determine the amount of ammonium sulphate to be added to the lysates.

**Table 2.5 Final Concentrations of Ammonium Sulphate**

| Initial concentration ammonium sulphate (% saturation at 0°C) | Percentage saturation at 0°C | | | | | | | | | | | | | | | | |
|---|---|---|---|---|---|---|---|---|---|---|---|---|---|---|---|---|---|
| | 20 | 25 | 30 | 35 | 40 | 45 | 50 | 55 | 60 | 65 | 70 | 75 | 80 | 85 | 90 | 95 | 100 |
| | Solid ammonium sulphate (grams) to be added to 1 litre of solution | | | | | | | | | | | | | | | | |
| 0 | 106 | 134 | 164 | 194 | 226 | 258 | 291 | 326 | 361 | 398 | 436 | 476 | 516 | 559 | 603 | 650 | 697 |
| 5 | 79 | 108 | 137 | 166 | 197 | 229 | 262 | 296 | 331 | 368 | 405 | 444 | 484 | 526 | 570 | 615 | 662 |
| 10 | 53 | 81 | 109 | 139 | 169 | 200 | 233 | 266 | 301 | 337 | 374 | 412 | 452 | 493 | 536 | 581 | 627 |
| 15 | 26 | 54 | 82 | 111 | 141 | 172 | 204 | 237 | 271 | 306 | 343 | 381 | 420 | 460 | 503 | 547 | 592 |
| 20 | 0 | 27 | 55 | 83 | 113 | 143 | 175 | 207 | 241 | 276 | 312 | 349 | 387 | 427 | 469 | 512 | 557 |
| 25 | | 0 | 27 | 56 | 84 | 115 | 146 | 179 | 211 | 245 | 280 | 317 | 355 | 395 | 436 | 478 | 522 |
| 30 | | | 0 | 28 | 56 | 86 | 117 | 148 | 181 | 214 | 249 | 285 | 323 | 362 | 402 | 445 | 488 |
| 35 | | | | 0 | 28 | 57 | 87 | 118 | 151 | 184 | 218 | 254 | 291 | 329 | 369 | 410 | 453 |
| 40 | | | | | 0 | 29 | 58 | 89 | 120 | 153 | 187 | 222 | 258 | 296 | 335 | 376 | 418 |
| 45 | | | | | | 0 | 29 | 59 | 90 | 123 | 156 | 190 | 226 | 263 | 302 | 342 | 383 |
| 50 | | | | | | | 0 | 30 | 60 | 92 | 125 | 159 | 194 | 230 | 268 | 308 | 348 |
| 55 | | | | | | | | 0 | 30 | 61 | 93 | 127 | 161 | 197 | 235 | 273 | 313 |
| 60 | | | | | | | | | 0 | 31 | 62 | 95 | 129 | 164 | 201 | 239 | 279 |
| 65 | | | | | | | | | | 0 | 31 | 63 | 97 | 132 | 168 | 205 | 244 |
| 70 | | | | | | | | | | | 0 | 32 | 65 | 99 | 134 | 171 | 209 |
| 75 | | | | | | | | | | | | 0 | 32 | 66 | 101 | 137 | 174 |
| 80 | | | | | | | | | | | | | 0 | 33 | 67 | 103 | 139 |
| 85 | | | | | | | | | | | | | | 0 | 34 | 68 | 105 |
| 90 | | | | | | | | | | | | | | | 0 | 34 | 70 |
| 95 | | | | | | | | | | | | | | | | 0 | 35 |
| 100 | | | | | | | | | | | | | | | | | 0 |

Taken from S. Englard, and S. Seifter., (1990).

For each lysate, 20%, 40%, 60%, 80% and 100% fractions were generated by adding more ammonium sulphate to the lysates. The ammonium sulphate was added slowly to the protein lysate, at 4°C with constant stirring for 20 minutes. When the ammonium sulphate had fully dissolved, the solution was left to stand at 4°C for 10 minutes. Precipitated proteins were pelleted by centrifugation at 10,000 x *g*, at 4°C for 10 minutes (Sorvall RC-5B centrifuge, with a S34 rotor). The supernatant was retained and more ammonium sulphate was added to generate the next fraction. The protein pellet was allowed to air dry before redissolving in 1.5ml 0.1M NaCl-HSB Buffer. The protein fraction was kept on ice prior to dialysis or dilution, which was necessary to reduce excess salt which could interfere with downstream applications.

### 2.9.6 Fast Protein Liquid Chromatography

Affinity chromatography using a 10ml Mono-S column (Pharmacia Biotech) connected to the ÄKTA FPLC system was used to purify an unknown DNA binding protein by running a linear NaCl gradient. The column was equilibrated with 0.1M NaCl-HSB Buffer, and the protein of interest peaked at around 300mM NaCl at a flow rate of 1ml/minute.

### 2.9.7 Dialysis of Proteins

Dialysis was performed in order to remove glycerol or excess salt from protein samples. Dialysis tubing (GIBCO BRL ultraPURE) of an appropriate length (approx. 5cm/ml sample) was prepared by washing thoroughly in $dH_2O$. The tubing contained pores that allowed movement of molecules up to 12kDa in size; therefore most proteins were retained within the tubing after dialysis. Tubing containing the protein sample was immersed in 100 volumes of the appropriate buffer and dialysis proceeded with stirring at 4°C for 30 minutes. Dialysis was repeated with 3 changes of buffer, before the protein sample was recovered from the tubing. As dialysis usually results in dilution of the samples it was often necessary to concentrate them following this step.

### 2.9.8 Concentration of protein samples.

Protein samples were concentrated by reducing the sample volume using a 10 kDa Centricon centrifugal filter device (Millipore) as per manufacturer's instructions. When concentrating small samples, for example cell lysates from a growth curve, it was necessary to use 10kDa Microcon centrifugal filter devices (Millipore) as per manufacturer's instructions. It was possible to concentrate a 2ml crude protein lysate to a volume of $\leq 200\mu l$ without precipitation of the proteins.

### 2.9.9 Western blots.

Western blots were performed on protein samples that had been resolved by SDS-PAGE. An unstained gel was equilibrated in transfer buffer for 15 minutes, during which time a square of Hybond-P PVDF(Amersham) membrane the same size as the gel was washed in methanol for 10 seconds, $dH_2O$ for 5 minutes, then transfer buffer for 10 minutes. The blot was set up using the Bio-rad electroblot apparatus. The electroblot cassette was placed on a flat surface; a fibre pad soaked in transfer buffer was placed on the dark side of the cassette and then 4 pieces of blotting paper also soaked in transfer buffer were placed on top. Then equilibrated gel was laid onto the paper and the membrane was carefully placed on top, a glass pipette was rolled over the top to remove any trapped bubbles. Additional paper and another fibre pad were placed on top, and then the cassette was sealed and placed in the electroblot tank with the dark side towards the electrodes. A Bio-Ice cooling unit was placed in the tank which was then filled with transfer buffer. Transfer proceeded at 100V, 350mA for 1 hour. The membrane was blocked overnight in 5% w/v non-fat dried milk (Marvel) in PBS/T on an orbital shaker.

The membrane was probed with primary and secondary antibodies following the protocol included with the ECL Plus Western Blotting Detection Reagents (Amersham). The secondary antibodies used were conjugated to Horse-Radish-Peroxidase, allowing detection with ECL Plus Detection Reagents as per manufacturer's instructions. The membrane was incubated with ECL reagents for 5 minutes, then wrapped in Saran Wrap and exposed to Hyperfilm (Amersham) in

an auto-radiography cassette for 15 seconds - 5 minutes depending on the level of fluorescent emission. The film was exposed using a Konica SRX-101A developer.

**Anti-FtsZ Blots:** 1° antibody; 1/10,000 anti-FtsZ (T. van Blauuwen)
2° antibody; 1/20,000 anti-Mouse IgG Peroxidase Conjugate (Sigma).

**Anti FtsI Blots:** 1° antibody; 1/5,000 anti-FtsI (D. Weiss)
2° antibody; 1/20,000 anti-Rabbit IgG Peroxidase Conjugate (Sigma).

## 2.10 Analysis of Protein:DNA interactions

### 2.10.1 Electrophoretic Mobility Shift Assays (EMSAs)

Electrophoretic Mobility Shift Assays were used to detect whether a radio-labelled piece of DNA could be bound to a particular purified protein, or to unknown proteins within a soluble protein lysate. A series of binding reactions were set up in a volume of 10µl containing: 1 x Binding Buffer, approximately 0.5Bq $^{32}P$ 5'-labelled DNA (to give 10cps per reaction as measured with a radiation and contamination monitor), an appropriate volume of protein/lysate, 50µg/ml poly dIdC, with volume made up with $dH_2O$. A series of reactions were usually set up in parallel so the protein of interest could be titrated in the binding reactions. The reactions were set up on ice then incubated at 37°C for 10 minutes. The reactions were loaded onto a pre-run 4% non-denaturing acrylamide gel with 1µl bromophenol blue added to one reaction. Gels were usually run for 4-5 hours at 4°C until the bromophenol blue reached the bottom of the gel.

Gels were dried onto blotting paper at 80°C for 25 minutes using a Bio-rad gel dryer. The gel was then placed in an auto-radiography cassette and exposed to Hyperfilm (Amersham) at -80°C overnight. The film was developed using a Konica SRX-101A developer.

A no protein control assay was performed with every group of reactions to prove that the DNA was not contaminated. For purified proteins a positive control of the protein bound to a known binding site was also always included.

**2 x Binding Buffer:** 40mM Tris pH8, 50mM NaCl, 20% v/v Glycerol

### 2.10.2 Sequencing Gels

6% w/v acrylamide sequencing gels were used to resolve the products of primer extensions, *in vitro* transcriptions, and footprinting reactions. The gel was prepared in a volume of 90ml containing 7M Urea, 6% w/v Acrylamide, 1 x TBE made up to volume with $dH_2O$. Sequencing gel plates were prepared by cleaning with ethanol and chloroform, and siliconising the back plate once every 5 gels or so to aid removal of the gel. The gel was polymerised by the addition of 350µl 10% w/v APS and 40µl TEMED, these were briefly mixed in, then the gel was poured and a comb was added. The gel was allowed to set for 1 hour and was then moved to the vertical Base Runner (International Biotechnologies) sequencing apparatus, the top and bottom reservoirs were fitted and filled with 1 x TBE. The gel was pre-run for 30 minutes at 2500V; the wells were then washed out to remove any unpolymerised acrylamide or bubbles and up to 3µl of denatured sample were loaded. The gel was run for 2-5 hours depending on the length of the sample being resolved. The gel plates were split, and then immersed in 2 litres of 5% v/v methanol, 5% v/v acetic acid. The gel was loosened from the back plates and transferred to blotting paper onto which it was dried at 80°C for 25 minutes using a Bio-rad gel dryer. The dried gel was wrapped in Saran Wrap and placed in an auto-radiography cassette to be exposed to Hyperfilm (Amersham) overnight at -80°C, and then the film was developed using a Konica SRX-101A developer.

### 2.10.3 Chain Termination Sequencing Reactions

Sequencing reactions needed to be run in parallel with samples on a sequencing gel to determine, for example, start points of transcription from a primer extension or protein binding sites from a footprinting reaction. Chain termination sequencing reactions were performed using the T7 DNA Sequencing kit (USB) following

manufacturer's instructions. The reactions were stopped by the addition of 1 x formamide loading buffer, and the samples were then denatured by boiling to 95°C for 2 minutes prior to loading onto a 6% w/v acrylamide sequencing gel.

### 2.10.4 Maxam Gilbert AG Ladder

Maxam Gilbert AG ladders were prepared as an alternative to chain termination sequencing reactions. Approximately 0.1MBq of $^{32}P$ single-end labelled DNA was made up to 20µl in volume with $dH_2O$ and incubated on ice. The DNA was moved to a fume hood where 4µl piperidine formate was added, the mix was then incubated at 37°C for 20 minutes. 240µl stop solution was added, followed by 750µl ethanol. The reaction was ethanol precipitated, with the DNA pellet finally resuspended in 90µl $dH_2O$. 10µl of piperidine was added to the DNA and incubated at 90°C for 30 minutes. The DNA was then lyophilised using a Savant DNA Speed Vac DNA110 at the highest drying rate for 1 hour. The DNA pellet was resuspended in 100µl $dH_2O$ and then lyophilisation was repeated as before. DNA was finally resuspended in 10µl 1 x formamide loading buffer, 1-2µl was loaded per lane on a 6% w/v acrylamide sequencing gel following denaturation at 95°C for 2 minutes.

**Stop Solution:** 0.3M NaOAc, 0.1mM EDTA, 10µg/ml yeast tRNA

### 2.10.5 Footprinting of protein bound DNA

**DNaseI Footprinting**

A 10µl binding reaction was set up containing 1 x Binding buffer, 0.05MBq $^{32}P$ single end-labelled DNA, 50µg/ml poly dIdC, an appropriate volume of protein, made up to volume with $dH_2O$. The reactions were incubated at 37°C for 10 minutes, and then 1 x RQ DNaseI Buffer (Promega) was added. RQ DNaseI was diluted in buffer so that 0.1Units could be added to the reaction, DNaseI digestion proceeded at 37°C for 1 minute and was stopped by the addition of 6µl RQ DNaseI Stop Solution. Formamide loading buffer was added to the reactions and then 1-3µl were loaded onto a 6% w/v acrylamide sequencing gel following denaturation at 95°C for 2 minutes.

### *In situ* Copper Phenanthroline Footprinting

A 30µl binding reaction was set up containing 1 x Binding buffer, 50µg/ml poly-dIdC, ≥0.04MBq $^{32}P$ labelled DNA, an appropriate volume of protein, and made up to volume with $dH_2O$. The reaction was resolved on a 4% w/v acrylamide non denaturing acrylamide gel as for standard EMSAs. The shifted band containing the protein bound DNA was excised from the gel and cut into small fragments within an Eppendorf tube. The fragments were immersed in 100µl 50mM Tris pH8, 10µl Solution A was added and mixed followed by 10µl Solution B with incubation at room temperature for 10 minutes. 20µl 2,3 dimethylphenanthroline was added and vortexed followed by 500µl 1 x STE buffer and overnight incubation at 37°C to elute the DNA. Following incubation, the gel fragments and STE were transferred to a Spin-X (Costar) tube and centrifuged at 0.8 x *g* (Eppendorf centrifuge 5415 D) for 5 minutes. The DNA was ethanol precipitated and the final pellet was resuspended in 2-3µl 1 x formamide loading buffer to be denatured and resolved on a 6% w/v acrylamide sequencing gel.

**Solution A:** 2mM 1,10-phenanthroline, 0.45 $CuSO_4$.

**Solution B:** 1/200 dilution of mercaptopropionic acid.

### 2.10.6 Stable complex assays

Stable complex assays were performed to determine whether RNA Polymerase was capable of forming a stable open complex with predicted promoter sequences on labelled regions of DNA, when challenged with Heparin. A series of 10µl reactions were set up containing 1 x Stable Complex Buffer, 0.5Bq $^{32}P$ end labelled DNA, 50µg/ml poly dIdC, 0.5Units RNA Polymerase (USB), made up to volume with $dH_2O$ and incubated at 37°C for 30 minutes. A titration of 5-500µg/ml Heparin was added to the different reaction tubes and incubated for a further 5 minutes at 37°C. Samples were resolved on a 4% w/v acrylamide non-denaturing acrylamide gel as described previously.

**2 x Stable Complex Buffer:** 50mM NaCl, 10mM Tris pH8, 60mM KCl, 2mM DTT, 10% v/v Glycerol.

## 2.11: Microscopy

Phase-contrast images of cells were captured using a Zeiss Axiopian II microscope and a Hamamatsu Orca CCD camera. Cell length measurements were obtained using Improvision OpenLab software.

# Chapter 3: Results - Transcriptional Regulation of the *mra* region in *E. coli.*

## 3.1 Introduction

Bacteria have the ability to adapt to their environment in response to multiple stimuli including changes in temperature, nutrient availability and cell density. When conditions are favourable for proliferation, cells enter balanced (exponential) growth. As growth rate increases, cells rapidly accumulate RNA, DNA and mass. As a result, cells in rich media are large and can divide rapidly – approximately every 20 minutes for *E. coli*. In contrast; when cell growth slows in response to a change in external conditions, cell mass decreases and in the case of *E. coli*, the rod shaped cell becomes smaller (Schaechter *et al.*, 1958).

Such changes in cell size have major implications for the expression of genes involved in peptidoglycan biosynthesis and cell division. Small, slow growing cells have a higher surface area:mass ratio than large, fast growing cells of the same strain. As a result a small, slow growing cell will require more cell division proteins per mass to form a septal ring compared to a large fast growing cell (Donachie, 1968; Dewar & Dorazi, 2000). In addition, more peptidoglycan biosynthesis per mass will be required to elongate the small, slow growing cell and to invaginate the septum prior to division. However, it has been reported that although *ftsZ* transcription levels change with growth rate, FtsZ levels remain constant (Rueda *et al.*, 2003). This would suggest that the cell maintains a constitutive level of FtsZ that is sufficient to support division regardless of cell size and growth rate.

This chapter investigates the transcription of genes located in the *mra* region (which includes genes involved in both cell division and growth of the cell wall) in order to determine whether promoters upstream of the *mra* region may be responsible for a significant amount of FtsZ expression. It also focuses on the role of growth rate in the regulation of the *mra* region, and the potential roles of some of the more abundant transcriptional regulators such as FIS and CRP. In addition, regulation mediated by ppGpp and its accessory factor DksA, both of which are involved in the stringent response, is investigated. This study also attempts to assign a function to the individual promoters on the basis of their activity, transcriptional regulation, and to determine whether they are essential for cell viability.

## 3.2 Expression of the *mra* region in response to growth rate.

### 3.2.1 Effect of growth rate on transcription from the $P_{mra}$ promoters.

The genes of the *mra* region encode proteins involved in both formation of the septal ring and peptidoglycan biosynthesis. The *mra* region is constitutively expressed; therefore any regulation will act to fine tune its expression by the modulation of transcription from the $P_{mra}$ promoters, rather than by completely switching "on" or "off" expression of this cluster of essential genes. We proposed that expression of the *mra* region may be inversely related to growth rate to compensate for the changes in the proportion of cell division proteins produced per mass. To test this hypothesis, we used a β-galactosidase based reporter system to indirectly measure transcription originating from promoters upstream of the *mra* region. In addition to $P_{mra}$, two further promoters were identified upstream of the *mra* region in the 601 bp intergenic region between *fru*R and *yab*B (See Section 1.1.1). These promoters, $P_{mra}2$ and $P_{mra}3$ may be required for full expression of the *mra* region and transcription originating from them may contribute to the expression of β-galactosidase in our reporter system. These experiments measured β-galactosidase activity in samples taken at regular time points from strain EDCM647 (Merlin *et al.*, 2002) cultured at 37°C in two different growth media.

EDCM647 is a derivative of MG1655Δ*lac*, and carries a chromosomal replacement of *yab*B with the FLKP2 reporter cassette containing *lac*Z, *aph* (conferring kanamycin resistance) and the inducible $P_{lac}$ promoter (Figure 3.2.1.1). The combined transcription from the $P_{mra}$ promoters drives expression of *lac*Z, which can be measured and quantified by β-galactosidase assay. The genes downstream of *yab*B are essential; therefore they are under the control of $P_{lac}$ to prevent any polar effects caused by the chromosomal deletion and insertion of the reporter cassette. The reporter cassette is flanked by FRT sites which are recognised by the FLP recombinase, which allows the cassette to be removed from the strain if required, leaving a 93 bp in-frame deletion scar.

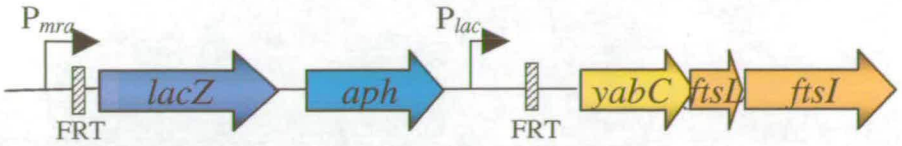


**Figure 3.2.1.1: Illustration of the *yab*B reporter cassette on the EDCM647 chromosome.**
EDCM647 was created by deletion of *yab*B from the MG1655 chromosome and replacement with the FLKP2 cassette carrying *lacZ*, *aph*, and $P_{lac}$. Transcription originating upstream of *yab*B is used to drive expression of *lac*Z. Genes downstream of *yab*B are essential, and are transcribed from the inducible $P_{lac}$. The reporter cassette is flanked by two FRT sites which are recognised by FLP recombinase, this system allows the cassette to be removed from the strain.

Overnight cultures of EDCM647 were used to inoculate fresh LB or M9 Maltose + Casamino Acids (CAA) at 37°C; 1mM IPTG was also added to induce expression from $P_{lac}$. Samples of culture were removed at regular time intervals for measurement of the $OD_{600}$ and β-galactosidase activity. Figure 3.2.1.2a shows the growth curves of EDCM647 in the two different media. A doubling time of 27 minutes was observed for growth in LB, and 36 minutes for growth in M9 Maltose. These growth rates are approximately 20% longer than those measured for MG1655 in the two growth media. This suggests that insertion of the reporter cassette into the MG1655 chromosome causes a slight delay in division, possibly due to changes in expression of the *mra* region when under the control of $P_{lac}$. β-galactosidase activity, measured in Miller Units, was plotted against time to determine how growth phase and growth rate affected expression (See Figure 3.2.1.2b).

When EDCM647 grown in LB entered balanced growth (between 0 and 120 minutes) the expression of β-galactosidase decreased by 63% and then remained at a constant level of approximately 100 Miller Units as the cells grew exponentially. This steady, low level of expression correlates with the cells being large, therefore requiring fewer cell division proteins per mass. As growth slowed and the cultures approached stationary phase, between 240 and 360 minutes, there was a 2.5-fold increase in β-galactosidase expression. The increase in expression may correspond to the predicted decrease in cell size as growth slows and therefore a greater requirement for expression of the genes in the *mra* region.

**a.**

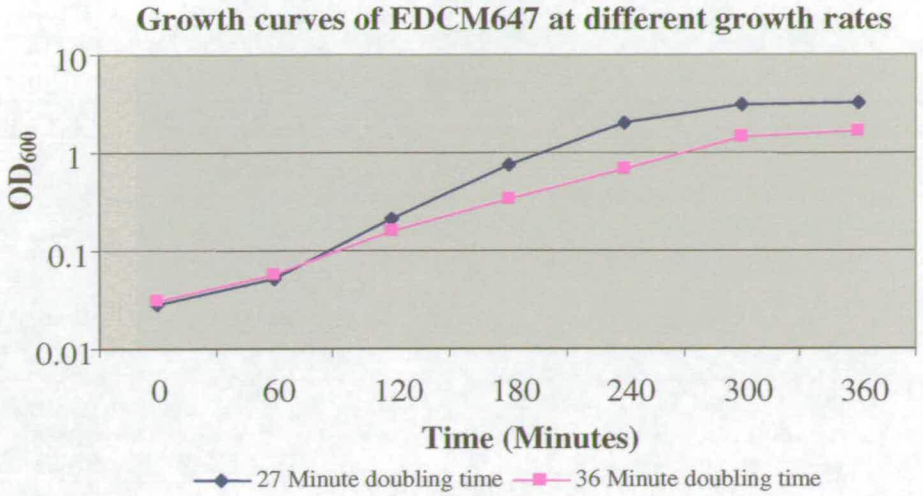


**b.**

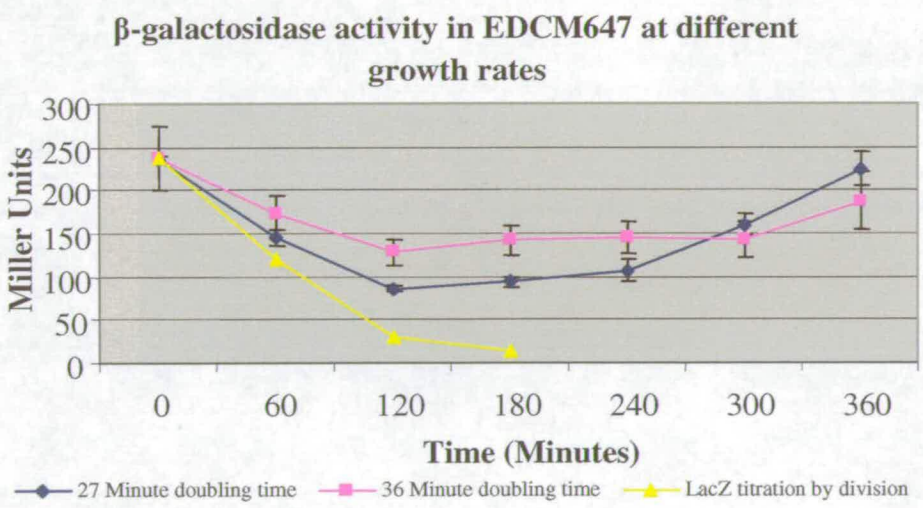


**Figure 3.2.1.2: Optical densities and β-galactosidase activity of EDCM647 at two different growth rates.**

**a**. Graph showing the growth curves of EDCM647 at a fast growth rate (27 minute doubling time in LB) and at a slower growth rate (36 minute doubling time in M9 + Maltose + CAA).

**b**. Graph showing the variation in β-galactosidase expression of EDCM647 at two different growth rates. Faster growing cells express less β-galactosidase during exponential phase growth than slower growing cells of the same strain. Data presented are the averages of measurements from triplicate cultures, error bars of standard deviation are shown. A line depicting the theoretical dilution of β-galactosidase, accumulated during approach to stationary phase in the overnight culture has also been plotted (assuming a doubling time of 30 minutes).

In contrast, EDCM647 grown in M9 Maltose exhibited a decrease in β-galactosidase activity of 40% upon entry into balanced growth (between 0 and 120 minutes). A steady level of expression of around 150 Miller Units was then observed as the cells grew exponentially. This represents a 50% increase in expression compared to

balanced growth in LB. As growth of the cultures slowed between 300 and 360 minutes upon approaching stationary phase, there was a corresponding 25% increase in β-galactosidase expression. The difference in exponential phase β-galactosidase expression between the two growth conditions appears to be quite small in Figure 3.2.1.2b. However, a t-test produced *P* values of 0.005 and 0.007 at $T_{120}$ and $T_{180}$ respectively, indicating that the difference in β-galactosidase expression at the two growth rates was significant.

It is important to consider the limitations of using this form of *lac*Z based reporter system. β-galactosidase is a very stable protein that can accumulate to high levels in the cell, particularly approaching stationary phase. As a result, the detection of low level transcription during early time points following inoculation with such a culture may be masked by the presence of β-galactosidase inherited from parental cells. It can be assumed that with each doubling of cell mass, any accumulated β-galactosidase would be diluted by a factor of two. A line depicting the theoretical average loss of accumulated β-galactosidase from cells with a doubling time of 30 minutes has also been plotted between 0 and 180 minutes in Figure 3.2.1.2b. The slope of this line is steeper than that seen for EDCM647 at growth rates of both 27 and 36 minutes, indicating that additional *de novo* synthesis of β-galactosidase has occurred in EDCM647.

The line representing the theoretical dilution of β-galactosidase, however, does not take into account any potential degradation of the protein, or the dilution of any *de novo* synthesised β-galactosidase. The accumulation of stable β-galactosidase in a stationary culture has important implications for the measurement of *de novo* synthesis following subculture. Therefore results presented in Figure 3.2.1.2b do not provide a fully accurate representation of the β-galactosidase expression being driven by transcription originating from the $P_{mra}$ promoters. This inaccuracy only applies to data corresponding to the first three cell doublings/divisions following inoculation, as during this time the accumulated β-galactosidase levels should have decreased 8-fold to an almost undetectable level.

When the theoretical levels of accumulated β-galactosidase were subtracted from the observed values at 60 and 120 minutes; EDCM647 in LB produced only 25MU and

56MU of β-galactosidase activity respectively, while in M9 Maltose values of 54MU and 99MU were obtained. These values are 74% and 42% lower than the constant β-galactosidase activity levels observed during balanced growth in LB, and 62% and 29% lower than the exponential phase values in M9 Maltose. These results suggest that little transcription is required from the $P_{mra}$ promoters during the growth lag on exit from stationary phase, at which time the cultures are adjusting cell size in response to the new growth rate.

These observations are surprising since it may be expected that cells in balanced growth would exhibit the lowest basal levels of β-galactosidase activity, due to their large size and decreased requirement for the production of cell division proteins. These data may suggest that division proteins accumulate in the cell prior to stationary phase and can be used for division following the resumption of growth, when initially low levels of *de novo* synthesis of division proteins are insufficient to support septation. The increase in *de novo* β-galactosidase activity, followed by constant expression during exponential growth (120-240 minutes in LB, 120-300 minutes in M9 Maltose) may reflect the exhaustion of inherited division proteins and a corresponding increase in transcription from the $P_{mra}$ promoters to allow division during balanced growth.

These experiments have illustrated that growth phase dependent changes in β-galactosidase activity occurred in batch cultures of EDCM647. To determine whether the differences in β-galactosidase expression during balanced growth in LB or M9 Maltose was linked to changes in cell size, the cell lengths and morphologies of EDCM647 and its parent strain MG1655 were analysed by microscopy during growth at 37°C (Figure 3.2.1.3c-f). MG1655 was analysed in addition to EDCM647 because slower growth rates were observed in the reporter strain compared to the parental strain. The reduced growth rate of EDCM647 may be caused by unregulated transcription from $P_{lac}$ that leads to perturbation of doubling time and possible changes to cell morphology.

MG1655 grows to a mean cell length of approximately 4.4μm when cultured in LB with a doubling time of 22 minutes. However, when MG1655 is cultured in M9

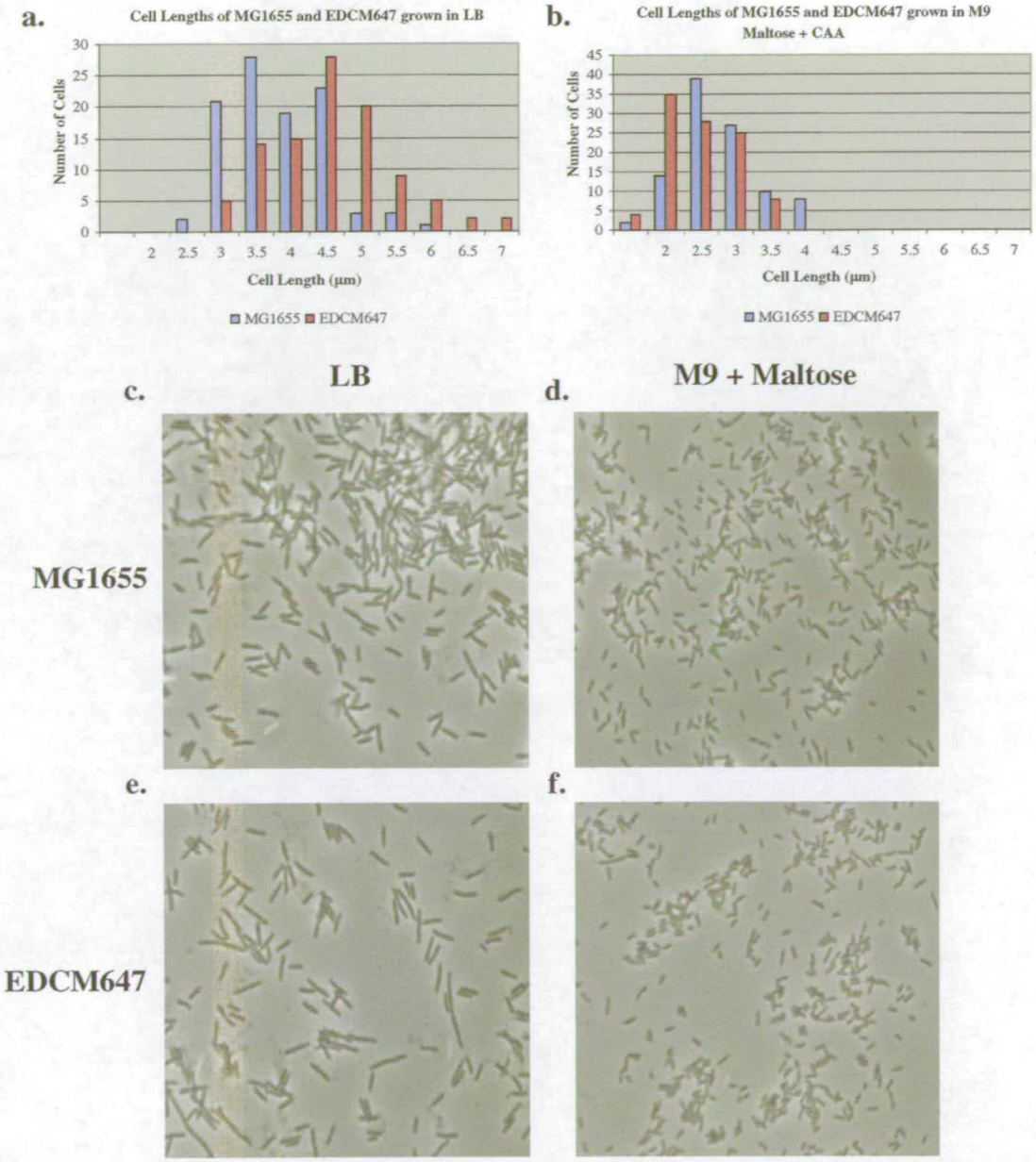


**Figure 3.2.1.3: Cell Length of MG1655 & EDCM647 at different growth rates.**
**a.** Graph showing the frequency in cell length of MG1655 and EDCM647. Cells were grown in LB at 37°C, 200 cells of each strain were measured at an $OD_{600}$ of 0.4.
**b.** Graph showing the frequency in cell length of MG1655 and EDCM647. Cells were grown in M9 Maltose + CAA at 37°C, 200 cells of each strain were measured at and $OD_{600}$ of 0.4.
**c.** MG1655 grown in LB at $OD_{600}$ 0.4. Average cell length 4.35µm. Doubling time 22 minutes.
**d.** MG1655 grown in M9 maltose + CAA at $OD_{600}$ 0.4. Average cell length 2.84µm. Doubling time 30 minutes
**e.** EDCM647 grown in LB at $OD_{600}$ 0.4. Average cell length 4.84µm. Doubling time 27 minutes.
**f.** EDCM647 grown in M9 maltose + CAA at $OD_{600}$ 0.4. Average cell length 2.44µm . Doubling time 36 minutes.

Maltose + CAA with a doubling time of 30 minutes, the average cell length is only 2.8µm during balanced growth (Figure 3.2.1.3a & b). Increased transcription from the

$P_{mra}$ promoters in response to slow growth may contribute to expression of the additional cell division proteins necessary for division. In contrast, EDCM647 exhibited average cell lengths of 4.8μm during balanced growth in LB, and 2.4μm when cultured in M9 Maltose + CAA (Figure 3.2.1.3a & b). In EDCM647, the expression of the *mra* region is driven by $P_{lac}$ and not the $P_{mra}$ promoters. It is unlikely that the level of transcription from $P_{lac}$ will be the same as from the $P_{mra}$ promoters, therefore the expression of cell division proteins may be altered in EDCM647 compared with MG1655. Microscopic examination of EDCM647 showed altered cell morphology during balanced growth in LB, with a heterogeneous population of cells, many of which were elongated (Figure 3.2.1.3 c-f). These observations are particularly significant because during growth in LB, EDCM647 grew around 20% slower than MG1655. We would therefore have predicted EDCM647 cell size to be smaller than that of MG1655; however, cells were on average 10% larger than those measured in MG1655. These data may be interpreted as $P_{lac}$ producing lower levels of transcription compared to the $P_{mra}$ promoters during growth in LB. The EDCM647 cells are not filamentous – there is a sub-population of filaments suggesting that altered transcription of the *mra* region from $P_{lac}$ during growth in LB causes a delay in division. This phenotype may also be caused by some effect of deleting *yab*B, however this gene is non-essential and no previous observation of altered morphology in *yab*B mutants has been reported (Merlin *et al.*, 2002). Since the difference in cell size between MG1655 and EDCM647 is more pronounced in LB than M9 Maltose, it may be that $P_{lac}$ activity is repressed by catabolite repression in LB but not in M9 Maltose.

EDCM647 cells grown in M9 Maltose + CAA were slightly smaller than MG1655, and grew slower with a doubling time of 36 minutes, compared to 30 minutes for MG1655. It might be expected that the high levels of transcription originating from $P_{lac}$ would have less effect on cell morphology at this slower growth rate, as the cells would require a higher expression of cell division genes. However, transcription from $P_{lac}$ will be upregulated during growth in M9 Maltose + CAA, due to the presence of cAMP and the binding of CRP upstream of the $P_{lac}$ promoter. This increase in transcription from $P_{lac}$, and an increase in expression of *fts*Q, A, and Z in response to the slow growth rate (mediated by pQ1 which is inversely controlled by growth rate (Navarro *et al.*, 1998; Joseleau-Petit *et al.*, 1999)), may be causing the formation of

extra septal rings in EDCM647, and consequently early divisions. The presence of mini-cells (which are indicative of over-production of FtsQ, A and Z or a deficient *min* system) was not observed in EDCM647 grown in M9 Maltose + CAA; however the cells were generally small and mini-cells are generally difficult to visualise.

As described previously, differences were observed in the β-galactosidase activity from EDCM647 at two different doubling times (Figure 3.2.1.2b), suggesting that the $P_{mra}$ promoters are inversely regulated by growth rate. However, both EDCM647 and MG1655 alter their cell size in response growth rate (Figure 3.2.1.3a & b), indicating that regulation of the $P_{mra}$ promoters is not absolutely required for the determination of cell length. This conclusion can be drawn because the transcription of the *mra* region in EDCM647 is not controlled by the $P_{mra}$ promoters and yet cell size in this strain changes in response to the rate of growth. The results indicate however, that the regulation of the $P_{mra}$ promoters is important for efficient septation, as a delay in division was observed in EDCM647 grown in LB when compared to MG1655.

### 3.2.2 Comparison of *yab*B and *fts*Z transcription

Published results have suggested that $P_{mra}1$ is responsible for the expression of genes at least as far as *fts*W, and there has been speculation that it may also contribute to the expression of *fts*Q, A and Z at the distal end of the *mra* region (Hara *et al.*, 1997; Mengin-Lecreulx *et al.*, 1998). $P_{mra}2$ and 3 had not been identified at the time of these previous studies but they may also contribute to expression of these cell division genes. If transcripts from the $P_{mra}$ promoters span from *yab*B to *fts*Z, then the pattern of transcription of both genes may be similar during growth in batch culture.

In order to test this hypothesis, the growth curves and β-galactosidase expression in strains EDCM647 and VIP407 (Flärdh *et al*, 1997) were compared during batch culture in LB. VIP407 is a derivative of MC1061 and contains a transcriptional Φ(*fts*Z-*lac*Z) reporter fusion integrated into the chromosome at the *fts*A-*fts*Z junction (Figure 3.2.2.1). VIP407 provides an indirect measure of transcription originating upstream of *fts*Z, which will drive expression of β-galactosidase. The displaced *fts*Z and *lpxC* genes are transcribed from $P_{tac}$ following induction with IPTG. Experiments using this strain, containing a polar insertion in *ddl*B, provided the data suggesting

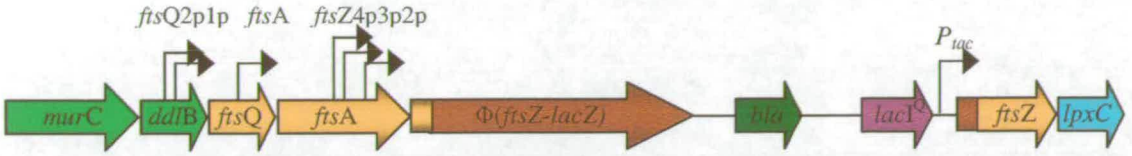


**Figure 3.2.2.1: Illustration of the transcriptional Φ(*ftsZ-lacZ*) reporter fusion integrated into the chromosome of VIP407.**
VIP407 is a MC1061 derivative carrying the plasmid pKFV116, integrated into the chromosome by homologous recombination at the *ftsA-ftsZ* junction. Transcription from upstream promoters drives the expression of the Φ(*ftsZ-lacZ*) fusion, which can be measured by β-galactosidase activity. Transcription of the displaced *ftsZ* and *lpx*C genes is controlled by the inducible $P_{tac}$. The 6 known promoters that provide ~33% of *ftsZ* transcription are shown. (Redrawn with alterations from Flärdh *et al*, 1998).

that up to 66% of *ftsZ* expression originates upstream of the known promoters for *ftsZ* (Flärdh *et al.*, 1998).

During this experiment, EDCM647 had a mass doubling time of 29 minutes and exhibited a 5-fold decrease in β-galactosidase activity between exiting stationary phase and entry into balanced growth. This decrease in β-galactosidase activity from ~500 Miller Units to ~100 Miller Units occurred between 0 and 90 minutes; during which time 3 mass doublings had occurred (Figure 3.2.2.2a). During exponential growth, between 90 and 180 minutes, β-galactosidase activity remained at a constant basal level. Between 180 and 330 minutes, as the culture approached stationary phase, there was a steady increase in β-galactosidase activity resulting in a 5-fold increase returning to the original levels measured immediately following inoculation. As mentioned in section 3.2.1., β-galactosidase accumulation in a stationary phase culture can have a major bearing on the activity levels measured at early time points in a freshly inoculated culture. When the theoretical levels of accumulated β-galactosidase were subtracted from the observed levels, between 30 and 90 minutes, there was an average *de novo* production of 48 Miller Units of β-galactosidase activity. This reinforces the data from section 3.2.1, which suggested that a low level of β-galactosidase activity was produced on exit from stationary phase, which increased approximately 2-fold to a steady state level during balanced growth.

These data reinforce the notion that the $P_{mra}$ promoters are inversely regulated by growth rate and that a low level of transcription originating from them is required for

**a.**

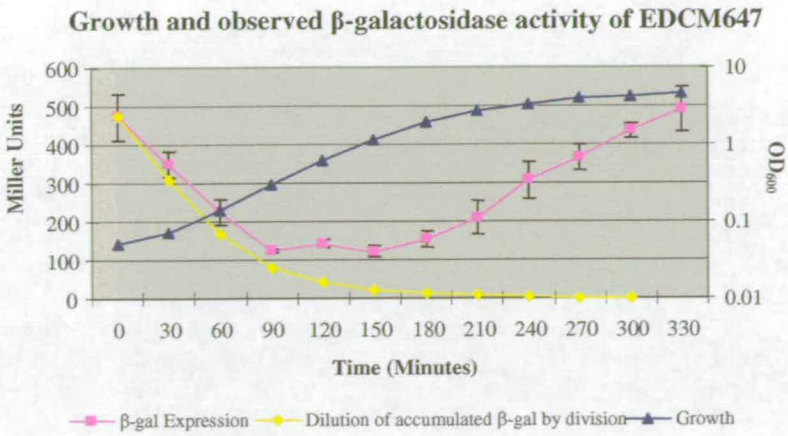


**b.**

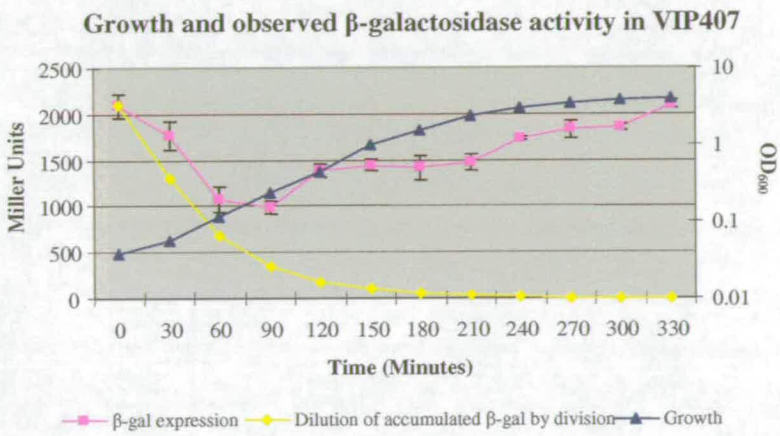


**Figure 3.2.2.2: Comparison of β-galactosidase activity in the reporter strains EDCM647 and VIP407.**

**a.** Graph illustrating the growth and observed β-galactosidase activity of EDCM647 grown in LB at 37°C + 1mM IPTG. A curve depicting the hypothetical dilution of accumulated β-galactosidase by division has also been plotted.

**b.** Graph illustrating the growth and observed β-galactosidase activity of VIP407 grown in LB at 37°C + 50μM IPTG. A curve depicting the hypothetical dilution of accumulated β-galactosidase by division has also been plotted. Data presented are the averages of measurements from triplicate cultures, error bars of standard deviation are shown.

efficient growth and division during balanced growth. The transcription levels increase on approach to stationary phase during which time cell size will be decreasing. This decrease in cell size corresponds to a greater requirement for the expression of cell division proteins. As cells exit stationary phase they must adjust their size to the new growth rate. The data presented here show indirectly that transcription from the $P_{mra}$ promoters was high on exit from stationary phase compared to balanced growth.

The EDCM647 data presented in Figure 3.2.2.2a show a similar pattern of β-galactosidase activity to that seen in Figure 3.2.1.2b. However the maximum activity levels which were measured during, and on exit from, stationary phase are 2-fold lower in Figure 3.2.1.2b compared to Figure 3.2.2.2a. The slight difference in growth rate, and the differences in β-galactosidase activity may have been due to variations in the culture conditions, and demonstrate the necessity for performing all experiments under the same conditions so that expression values are comparable.

Figure 3.2.2.2b shows the growth curve and β-galactosidase activity pattern of VIP407 which doubled every 27 minutes during batch culture in LB. Between 0 and 60 minutes, during which time the cells had doubled in mass twice, there was a 2-fold decrease in β-galactosidase activity, to a basal level of approximately 1000 Miller Units, this level remained constant until 90 minutes. Between 90 and 120 minutes there was a 50% increase in β-galactosidase activity which then remained constant during balanced growth until 210 minutes. As the culture approached stationary phase (210-330 minutes) there was a steady increase in β-galactosidase activity, to a level that was comparable to that which was seen on the exit from stationary phase at 0 minutes.

When the theoretical levels of accumulated β-galactosidase in VIP407 were subtracted from the observed measurements between 30 and 90 minutes, there was an average *de novo* production of 510 Miller Units of β-galactosidase activity. This is 2-fold less than the basal level of ~1000 Miller Units of β-galactosidase activity, observed between 60-90 minutes in VIP407. These data may reinforce the notion that division proteins, in particular FtsZ,A and Q, may be inherited from parental cells to assist in subsequent septation.

The pattern of β-galactosidase activity in VIP407 suggested that *ftsZ* is not highly expressed upon exit from stationary phase. The first increase in β-galactosidase activity in VIP407 was seen at an $OD_{600}$ of around 0.4. At this stage of the batch culture, cells were at their largest and therefore required the least expression of cell division proteins per mass. However, if this coincided with a depletion of recycled FtsZ from parent cells then an increase in *ftsZ* transcription may have been required for successful cell division. As the cells approached stationary phase, β-galactosidase

activity levels in VIP407 increased. This is indicative of increased transcription of *fts*QAZ, in order to provide additional proteins required for more divisions per cell mass. This response to a change in growth rate may be mediated by pQ1 or the $P_{mra}$ promoters, as transcription from both is inversely related to growth rate.

Little is known about the stability of cell division proteins; however, 10,000 to 20,000 monomers of FtsZ are known to be present and uniformly distributed in the cytoplasm in non-dividing cells (Erickson, 1995; Wang *et al.*, 1997). During septation, one-third of the cellular pool of FtsZ is present in the septal ring, but it is constantly remodelled with FtsZ subunits being turned over rapidly (Stricker *et al.*, 2002). Following septation the septal ring disassembles and FtsZ is redispersed throughout the cytoplasm (Erickson, 1995). It is possible that FtsZ subunits which had been polymerised into the septal ring may be biochemically inert and unable to be re-cycled, however there would still be a large pool (around 60%) of FtsZ that could potentially be inherited by progeny cells following cell division.

The patterns of β-galactosidase activity between EDCM647 and VIP407 are different (Figure 3.2.2.2). EDCM647 exhibits a low level of *de novo* β-galactosidase activity upon exit from stationary phase which then doubles and remains constant during exponential growth, increasing between 2 and 5-fold during the approach to stationary phase. These results suggest that transcription from the $P_{mra}$ promoters is regulated, in order to remain at a low level on exit from stationary phase and constant during balanced growth. Upon approaching stationary phase, transcription from the $P_{mra}$ promoters is upregulated in order to increase the number of division proteins, which are required to accommodate division at a smaller cell size. VIP407 also exits stationary phase with a low level of *de novo* β-galactosidase activity. However, this *de novo* level increases 3-fold to a steady activity level during balanced growth. On the approach to stationary phase β-galactosidase activity increased a further 44%, to a level 4-fold greater than the observed basal level. The basal levels of *fts*Z transcription produced on exit from stationary growth may not be sufficient to support cell division during balanced growth. Hence the increase in transcription when entering exponential growth, which is maintained until cell size and growth rate decrease upon the approach to stationary phase.

The general trend in the β-galactosidase activity patterns of EDCM647 and VIP407 during batch culture is the same. Both strains exhibit a decrease in activity upon exiting stationary phase, a low basal level during balanced growth and an increase in activity approaching stationary phase. However differences are evident and are most pronounced during balanced growth. For example, EDCM647 exhibited a steady level of β-galactosidase activity during balanced growth which was 5-fold less than that observed on exit from, and approaching stationary phase. In contrast VIP407 entered balanced growth at a β-galactosidase activity level that was only 2-fold less than that observed on exit from and entry to stationary phase. This level then increased 50% and remained constant until stationary phase was approached. These data suggest that *yab*B, at the start of the *mra* region has a different pattern of transcription compared to *fts*Z located at the distal end of the *mra* region during balanced growth. These data do not rule out the possibility that the $P_{mra}$ promoters may contribute to the transcription of *fts*Z. However, additional sources of transcription and regulation must also be present in order to achieve the β-galactosidase activity observed in VIP407 during batch culture. There are six upstream promoters ( *fts*Q2p1p, *fts*A, *fts*Z4p3p2p) that have been shown to contribute 33% of the transcription of *fts*Z. The β-galactosidase activity patterns of EDCM647 and VIP407 are different and it therefore seems unlikely that the $P_{mra}$ promoters could be solely responsible for the remaining 66% of *fts*Z transcription. This may suggest that additional promoters are present within the *mra* region that contribute to *fts*Z expression.

The β-galactosidase activity levels of EDCM647 and VIP407 cannot be directly compared as the strains originate from different genetic backgrounds, contain different reporter cassettes and use alternative ribosome binding sites which may alter the translational efficiency of β-galactosidase in the two strains. However, the β-galactosidase activity patterns are comparable and highlight the difference in the transcription of genes at the proximal and distal ends of the *mra* region.

### 3.2.3 Comparison of FtsI and FtsZ expression

To determine whether the expression levels measured from the reporter strains EDCM647 and VIP407 reflect *in vivo* gene expression, we monitored cell division protein levels during batch culture. Western blots were performed on soluble protein

lysates prepared from samples of MG1655 during growth in LB at 37°C. The cell samples, extracted at regular time points, were normalised so that 1ml of each sample produced an optical density of 0.4 at $OD_{600}$. Immunodetection was performed on two identical gels that had been transferred to PVDF membrane. Each gel contained protein samples from 0-150 minutes of an MG1655 batch culture (Figure 3.2.3.). This time frame encompassed the lag on exit from stationary growth and the transition from slow to balanced growth. These time points were used since it had been shown that the most significant changes in expression from reporter strains occurred during this period (Figure 3.2.2.2).

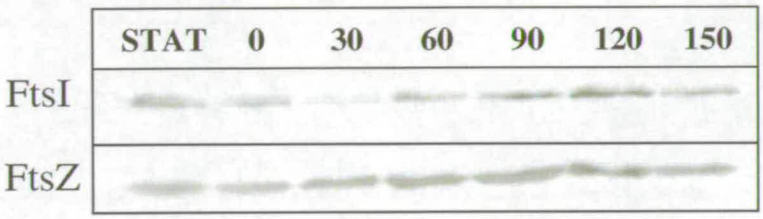


**Figure 3.2.3: Western blots showing levels of FtsI and FtsZ in MG1655 soluble protein lysates.**
Cell samples were taken at regular intervals during a batch culture of MG1655 grown in LB at 37°C. Samples were normalised to an optical density of $OD_{600}$ 0.4. 1ml of cells from each sample was pelleted and resuspended in 100µl 1 x SDS loading buffer, 20µl of which were electrophoresed on a denaturing polyacrylamide gel. The gel was transferred to a PVDF membrane, which was probed with anti-FtsI polyclonal antibody or anti-FtsZ monoclonal antibody. Images are representative results from duplicate experiments.

The membranes were probed with either anti-FtsI polyclonal or anti-FtsZ monoclonal antibodies. FtsI is the fourth gene in the *mra* region. There are no known promoters or transcriptional terminators between *yab*B and *fts*I therefore both genes should exhibit similar levels of transcription. FtsI is a cell division protein known to form part of the septal ring as well as functioning in peptidoglycan biosynthesis (Wang *et al.*, 1998). It was therefore interesting to compare the expression of two cell division proteins, one proximal and the other distal to the $P_{mra}$ promoters, during the batch culture.

FtsI was abundant in the stationary phase sample and at time 0 of the sub-culture. Thirty minutes after inoculation the levels of FtsI had decreased to a level that was at the limit of sensitivity for this method. FtsI expression increased during balanced

growth, seen in time points 60-120 minutes, but then appeared to decrease at 150 minutes. The pattern of FtsI expression superficially reflects the β-galactosidase activity pattern observed for EDCM647. The EDCM647 data suggested that a low level of transcription of the early genes in the *mra* region occurred on exit from stationary phase, followed by a constant level of transcription during balanced growth. The FtsI expression data indicates a rapid decrease in FtsI (low transcription of *ftsI*) followed by a steady increase during balanced growth. This suggests that FtsI is needed from 60 minutes onwards when division at the new cell length is starting to occur. FtsI is not re-used but is synthesised *de novo* prior to resumption of division.

In contrast, the Western blot data suggest that FtsZ expression appears to change less significantly during the growth cycle than FtsI expression. FtsZ levels appear to decrease slightly on exit from stationary phase and then increase during balanced growth between 30-120 minutes. There is a small decrease in FtsZ expression at 150 minutes as was also observed for FtsI, possibly suggesting that this sample may not be representative. The Western blot data indicates that FtsZ expression varies little in response to the changes in growth rate observed during batch culture. This is in agreement with Weart & Levin (2003), who show that average FtsZ levels are constant regardless of growth rate (Weart & Levin, 2003). This is unexpected, not only because the VIP407 transcription data changes significantly during this time period, but also because less FtsZ expression would be required from approximately 60 minutes onwards, when the cells have entered exponential phase growth.

We have observed that FtsZ expression remains relatively constant during batch culture, however *ftsZ* transcription decreases more than 2-fold on exit from stationary phase, increases 50% to a constant level during balanced growth and then returns to the starting level on approach to stationary phase. It has been observed previously that *ftsZ* transcription oscillates in response to growth rate dependent regulation, but that average FtsZ levels remain constant regardless of growth rate (Rueda *et al.*, 2003; Weart & Levin, 2003). This indicates that post-transcriptional mechanisms must exist to control FtsZ levels, and our observations may be explained in part by differential translation during the growth cycle. It has been shown that FtsZ expression is regulated post-transcriptionally by RNaseE cleavage (Cam *et al.*, 1996) and by interference by the small RNAs *stfZ* and DicF (Dewar & Donachie, 1993: Bouché &

Bouché, 1989). It not yet clear how RNaseE and the antisense RNAs are transcriptionally controlled, however RNaseE cleavage does appear to be sensitive to growth-rate dependent regulation (Joseleau-Petit *et al.*, 1999).

The data presented highlight that transcription and expression of genes located proximal in the *mra* region are different to those located at the distal end of this gene cluster. It has been shown that transcription levels originating from the $P_{mra}$ promoters are inversely related to growth rate, and consequently so are the transcription and expression of early genes in the *mra* region. However, when the *mra* region is placed under the control of $P_{lac}$, cell size still alters in response to differences in growth rate suggesting that additional methods of regulation in response to growth rate must also exist. In contrast, the expression of FtsZ - at the distal end of *mra* region, appears to vary little, although the transcription levels for *fts*Z are inversely related to changes in growth rate. The differences in transcription between *yab*B and *fts*Z suggest that both genes may not reside on the same transcript. This would imply that the distal promoters required for the majority of *fts*Z transcription are not the $P_{mra}$ promoters as previously suggested by Hara *et al.*, (1997).

## 3.3 Transcriptional regulation of the $P_{mra}$ promoters.

$P_{mra}$ was first identified in 1997 by Hara *et al.*, and remains the only published promoter identified upstream of *yab*B. Genetics have shown it to be responsible for expression of the *mra* region at least as far as *fts*W, although no direct biochemical evidence to confirm this has yet been presented. There is no data in the current literature regarding the regulation of the promoter $P_{mra}$. Identification of additional promoters ($P_{mra}2$ and $P_{mra}3$) upstream of $P_{mra}$ by the Blakely lab has yet to be published. Transcription originating from the intergenic region between *fru*R and *yab*B, where these promoters are located, has been shown to be necessary for the expression of essential cell division genes (Hara *et al.*, 1997, Mengin-Lecreulx *et al.*, 1998). It is therefore important to investigate how these promoters are regulated and to determine what role they may play with regards to expression of the *mra* region.

### 3.3.1: Construction of $P_{mra}$ - *lacZ* reporter vectors

To determine the activity of the three $P_{mra}$ promoters, a series of $P_{mra}$-*lacZ* reporter vectors were produced. The vectors were made using the multi-copy plasmid pRS551 (Simons *et al.*, 1987). This plasmid enables the directional cloning of promoter DNA between the EcoRI and BamHI restriction sites, upstream of a promoter-less *lacZ* (Figure 3.3.1.1). The plasmids can then be introduced into strains with the appropriate genetic background (Δ*lacZ*) by transformation, and promoter activity measured by β-galactosidase assay.

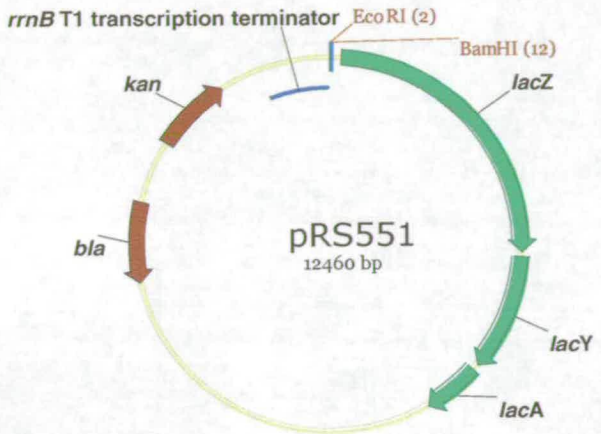


**Figure 3.3.1.1: Illustration of pRS551**
Illustration of the multi-copy *lacZ* reporter vector highlighting the EcoRI and BamHI restriction sites upstream of *lacZ*, into which different lengths of DNA containing combinations of the $P_{mra}$ promoters were cloned. The vector is $Amp^R$ and $Km^R$, and contains the *rrnB* T1 transcriptional terminator to ensure that only transcription originating from the cloned DNA will drive expression of *lacZ*.

Cloned fragments of different lengths were used to determine whether the region upstream of the $P_{mra}$ promoters had any regulatory function. In addition, site-directed mutations were introduced into the -10 regions of $P_{mra}1$ and $P_{mra}3$ (Figure 3.3.1.2). The -10 mutation knocks out promoter function, but unlike a deletion it keeps the promoter region intact and therefore allows read-through from upstream promoters. Individual promoter strength was determined by using combinations of active and knocked out promoters cloned into pRS551, as shown in Figure 3.3.1.3a.

The strain TP8503 which contains a deletion of the entire *lac* operon (Masters *et al.*, 1989) was transformed with each of the $P_{mra}$-*lacZ* reporter plasmids. Transformants were grown overnight in LB at 37°C, they were subcultured 1/100 into fresh LB and grown to an $OD_{600}$ of 0.2 at 37°C. They were then subcultured 1/10 into fresh LB,

WT $P_{mra}1$ -10 = **CAGCTCCGTAAACTCCTTTCAG**

$P_{mra}1$ -10 mutation = **CAGCTCCGTAGGCTCCTTTCAG**

WT $P_{mra}3$ -10 = **ATATGTCCTAAAATGCCGCTCG**

$P_{mra}3$ -10 mutation = **ATATGTCCTAGGATGCCGCTCG**

**Figure 3.3.1.2: Mutations introduced into $P_{mra}1$ and $P_{mra}3$ -10 regions by site directed mutagenesis.**

Site-directed mutagenesis of pUC600, introduced two guanine residues into the AT rich -10 regions of $P_{mra}1$ and $P_{mra}3$, in order to knock out promoter function. The resulting plasmids were used as templates for the PCR amplification of $P_{mra}$ fragments to be cloned into pRS551.

grown again to an $OD_{600}$ of 0.2 at 37°, at which stage β-galactosidase activity was measured. By repeatedly growing the cultures at low $OD_{600}$, any β-galactosidase accumulated in the overnight culture will have been diluted to a negligible level, and the results will reflect constitutive synthesis during exponential growth. The results of these experiments are shown in Figure 3.3.1.3b.

The plasmid pROB210 contains the full length, 601bp, *fru*R-*yab*B intergenic region. Over 10,000 Miller Units of β-galactosidase activity were measured from this plasmid and we assume that this level represents the expression from all active promoters within the intergenic region during exponential growth.

The low β-galactosidase activity (200 Miller Units) measured from pROB209, which contains only a functional $P_{mra}2$ in the full 601bp DNA fragment suggests that this promoter is weak which is in agreement with its poor match to the $\sigma^{70}$ consensus sequence. This is in agreement with preliminary data from primer extension assays (See Figure 1.1.2b) which detected no transcripts originating from this promoter. This also demonstrated that the majority of transcription entering the *mra* region originates from $P_{mra}1$ and $P_{mra}3$.

Expression from pROB204 and pROB205 represents transcription levels originating from $P_{mra}1$. $P_{mra}3$ activity has been knocked out, and as we have seen from the pROB209 data, $P_{mra}2$ contributes little to expression from this region. The presence or absence of the 200 bp upstream of $P_{mra}3$ has little effect on transcription from $P_{mra}1$ (Figure 3.3.1.3.b). This implies that any transcriptional regulation of $P_{mra}1$ occurs in the vicinity of the promoter region. The expression levels also indicate

**a.**

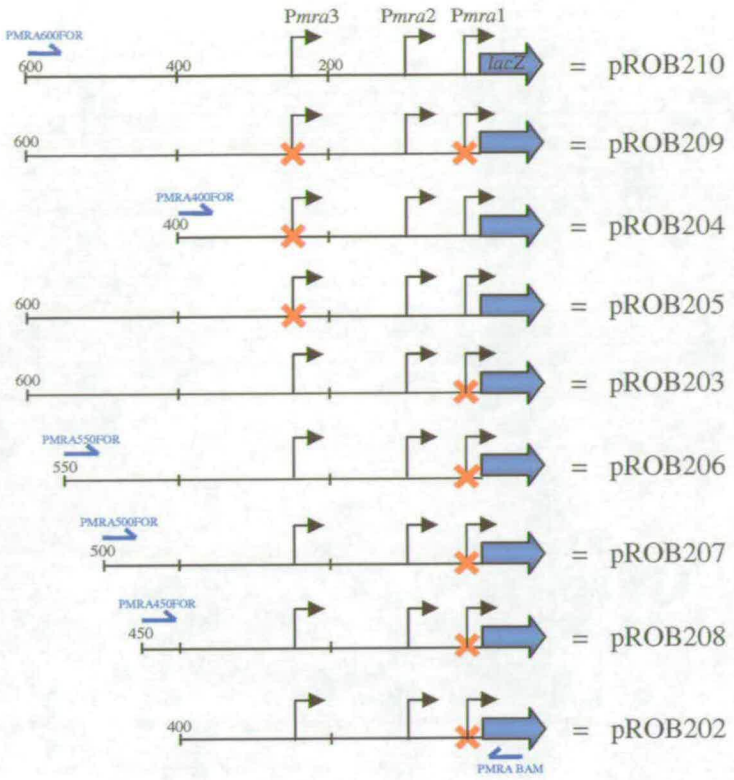


**b.**

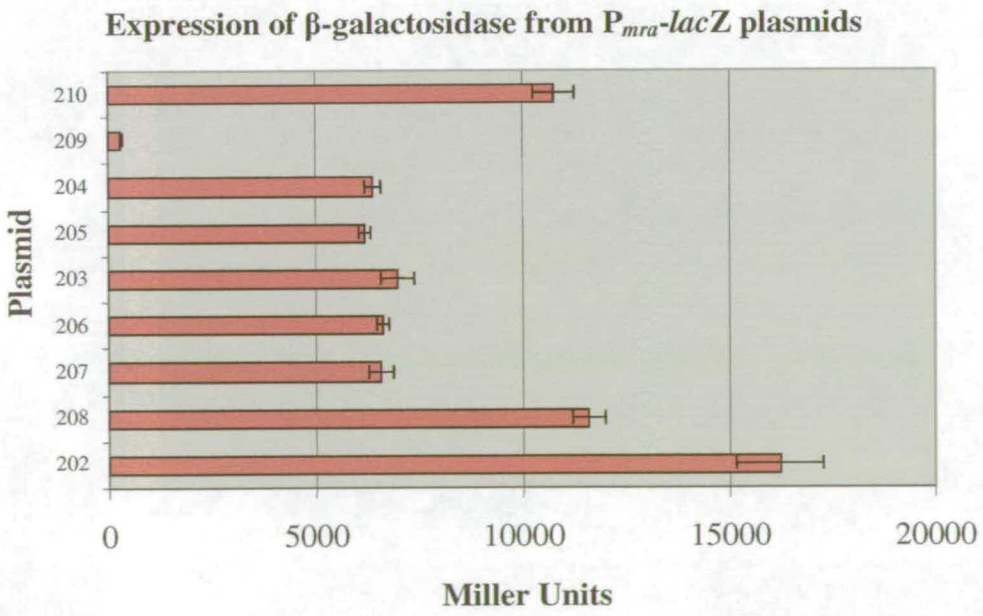


**Figure 3.3.1.3: Construction and expression of $P_{mra}$-*lac*Z reporter plasmids.**

**a.** Illustration of the promoter containing fragments cloned into pRS551 between EcoRI and BamHI. Red crosses indicate a -10 mutation and therefore a functional knock out of that promoter. Numbers represent the distance in bp from the start of transcription of the *mra* region. Primers used in the cloning of these fragments are highlighted in blue.

**b.** Histogram showing the expression of β-galactosidase produced from each of the $P_{mra}$-*lac*Z reporter plasmids in strain TP8503, grown in LB at 37°C. Data represents the average expression from triplicate cultures at an $OD_{600}$ of 0.2; error bars of standard deviation are shown.

.

that $P_{mra}1$ may contribute up to 60% of the total transcription entering the *mra* region, when compared to the data from pROB210.

Plasmids pROB203, 206, 207, 208 and 202 represent expression of β-galactosidase originating from $P_{mra}3$ (in addition to the very low levels from $P_{mra}2$). Figure 3.3.1.3b indicates that $P_{mra}3$ is capable of driving the expression of β-galactosidase at a similar level to $P_{mra}1$ (~7000 Miller Units). However the results for pROB208 show a 1.7-fold increase in expression, and pROB202 shows a 2.5-fold increase in expression when the sequences upstream of $P_{mra}3$ are removed. This result suggests that the region 400-600 bp upstream of *yab*B, causes a ~2-fold decrease in transcription from $P_{mra}3$. This repression is most likely conferred by the binding of a transcriptional repressor somewhere between 400 and 500bp upstream of *yab*B.

The results of these experiments provide some interesting clues to the regulation of the $P_{mra}$ promoters. They show that $P_{mra}2$ is a weak promoter, although it is possible that it was repressed during the conditions in which these experiments were performed. In addition, they show that $P_{mra}3$ has the potential to be a very strong promoter, although it appears repressed under the experimental conditions. It is also possible that high levels of transcription originating from $P_{mra}3$ may result in promoter occlusion of $P_{mra}2$ and even $P_{mra}1$ in its native context on the chromosome. However this does not explain the low levels of β-galactosidase activity observed from pROB209, where no transcription from $P_{mra}3$ would be present. Published work has suggested that $P_{mra}1$ is responsible for transcription of the *mra* region (Mengin-Lecreulx *et al.*, 1998). However the experiments presented here indicate that $P_{mra}3$ may also contribute significantly to expression of the *mra* region.

## 3.4 Identifying Transcriptional Regulators of the $P_{mra}$ promoters.

The experiments presented above suggest that expression from $P_{mra}3$ is highly regulated, and that regions upstream from this promoter are involved in conveying this regulation. It is also possible that $P_{mra}2$ is repressed as it exhibits very low transcription levels despite a good match to the promoter recognition sequence.

Bioinformatic analysis of DNA binding sites on a genome wide scale suggested the *fru*R-*yab*B intergenic region contains sequence motifs for many common transcriptional regulators (Robison *et al.*, 1998). This section investigates the potential regulation of the $P_{mra}$ promoters by some of the more common transcriptional regulators and nucleoid associated proteins such as CRP, FIS, H-NS and IHF.

### 3.4.1: A Role for CRP in the regulation of the $P_{mra}$ promoters?

CRP regulates many genes in *E. coli* and has previously been implicated in the regulation of cell division. Strains carrying *cya* and *crp* mutations show altered morphology and are resistant to the antibiotic mecillinam which acts on PBP2 and prevents lateral cell wall growth. In addition, transcription of *fts*Z is higher in a *cya* mutant although actual FtsZ levels were shown to remain the same as a wild type strain, leading to the conclusion that *fts*Z is not directly regulated by CRP (D'Ari *et al.*, 1988). However, cAMP-CRP appears to enhance cell division although its exact role has yet to be defined. We observed in section 3.1 that β-galactosidase activity in EDCM647 was higher during growth in M9 Maltose compared to LB. In M9 Maltose there will be a large pool of cAMP due to the absence of glucose, therefore the increase in expression of the *mra* region may potentially be caused by cAMP-CRP mediated activation.

To determine whether CRP plays a role in the regulation of the $P_{mra}$ promoters, the intergenic region was analysed for potential CRP binding sites. Three possible sites were identified (Figure 3.4.1.1); one centred on -156 upstream of $P_{mra}3$, one centred on -111 upstream of $P_{mra}2$ and one centred on -41, overlapping $P_{mra}1$, which could make this a Class II CRP-activated promoter. The Harvard *E. coli* DNA-Binding site matrices (http://arep.med.harvard.edu/ecoli_matrices/) predicted two CRP binding sites within the *fru*R-*yab*B intergenic region. These potential binding sites were predicted to be located at chromosomal coordinates 89196 and 89382; these correspond to binding sites I and II depicted in Figure 3.4.1.1. Site III was detected by manual searching, and shows the best match to the CRP consensus recognition motif.

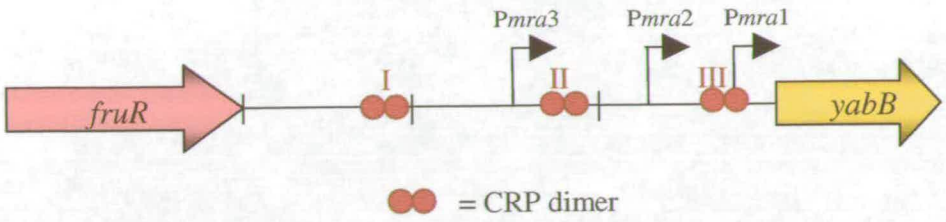


**I = aagTGATATCGACAGCGCGttt**
**II = ataTTTGCTGTGGAAAATAgtg**
**III = cctTGTGACTGGCTTGACAagc**
**Consensus = aaaTGTGA –N6 - TCACAttt**

**Figure 3.4.1.1: Potential CRP binding sites in the 601bp *fru*R-*yab*B intergenic region.**
Illustration depicting three possible CRP binding sites identified within the 601p intergenic region. The sequence of each potential binding site is highlighted. Binding sites I and II were predicted by a bioinformatic search, while Binding site III was identified by a manual search and shows the best match to the CRP consensus recognition sequence.

To determine whether these represent actual CRP binding sites, CRP was purified and used in Electrophoretic Mobility Shift Assays (EMSAs) to detect protein:DNA complexes. The *crp* gene was amplified by PCR using the primers crpFOR and crpREV; these enabled the cloning of *crp* into the NdeI and BamHI sites of the expression plasmid pET33b to create pROB201 (Figure 3.4.1.2a). Cloning into these sites creates an N-terminal fusion of a hexa-histidine tag to the protein. BL21-DE3 was transformed with pROB201. This strain encodes the IPTG inducible T7 polymerase which drives expression of the fusion protein from the T7 promoter. Any basal expression is minimised by the production of LacI, which binds to the *lac* operator placed upstream of the gene encoding T7 polymerase.

A mid-logarithmic culture of BL21-DE3 harbouring pROB101 was induced with 1mM IPTG for 1 hour to overexpress the CRP-HIS fusion protein. CRP-HIS was affinity purified on a Ni-NTA column and eluted with 250mM imidazole (See section 2.9.3). The products of this purification were resolved by SDS-PAGE and can be seen in Figure 3.4.1.2b. Although it was possible to induce high levels of expression of the fusion protein - as seen in the induced cell extract (Figure 3.4.1.2b, lane 3); it was not possible to recover high quantities of CRP-HIS in the elution fractions

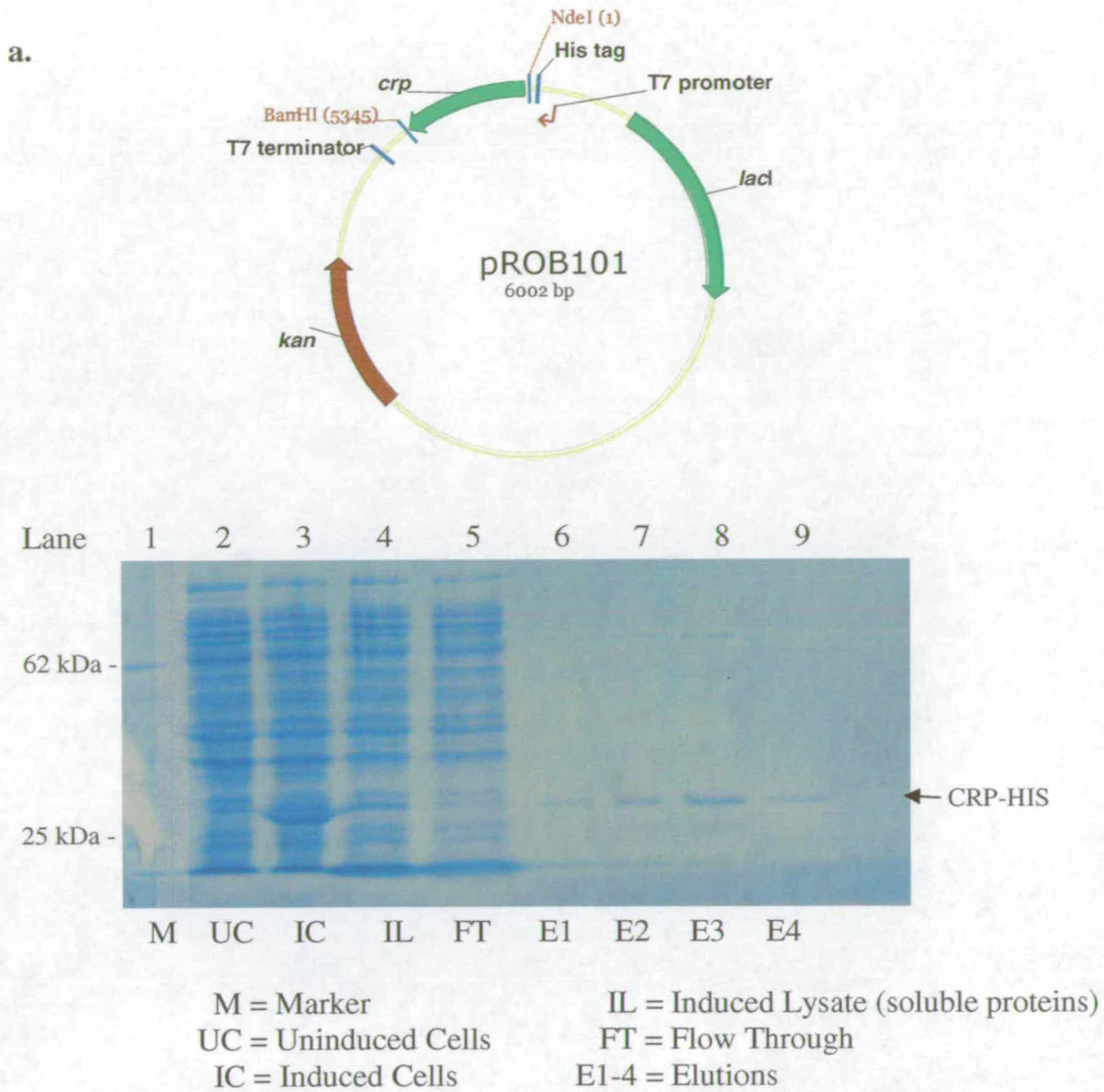


**Figure 3.4.1.2: Purification of HIS-tagged CRP.**
**a**. Illustration of the pET33b based vector used to overexpress CRP with an N-terminal 6xHis fusion. Transcription is controlled by the T7 promoter. Basal expression is minimised by the binding of the Lac repressor (encoded by *lacI)* to the *lac* operator immediately upstream of the gene encoding T7 polymerase which is induced by IPTG.
**b**. SDS-PAGE gel of the products of CRP-HIS purification using a 1ml Ni-NTA agarose column. CRP-HIS has a MW of ~ 28 kDa. 20µl of each fraction resolved per lane.

(Figure 3.4.1.2b lanes 6-9). Little fusion protein was observed in the induced lysate (Figure 3.4.1.2b lane 4), suggesting that this fusion protein may be insoluble.

A different method of affinity purification was performed in an attempt to increase the yield and solubility of purified CRP. The *crp* gene was first amplified by PCR using the primers crpEcoFOR and crpREV; this enabled the cloning of *crp* into the EcoRI and BamHI sites of the expression vector pMAL-c2x to create pROB102 (Figure

3.4.1.3a). Cloning into these sites generates an N-terminal fusion to *mal*E, which codes for Maltose Binding Protein (MBP). The fusion protein is under the transcriptional control of the IPTG inducible $P_{tac}$ promoter. DH5α was transformed with pROB102 in which overexpression of the fusion protein was performed.

A mid-logarithmic LB culture of DH5α harbouring pROB102 was induced with 1mM IPTG for 1 hour to overexpress the CRP-MBP fusion protein. CRP-MBP was affinity purified on an amylose column and eluted with 10mM Maltose. The products of this purification were resolved by SDS-PAGE and can be seen in Figure 3.4.1.3b.

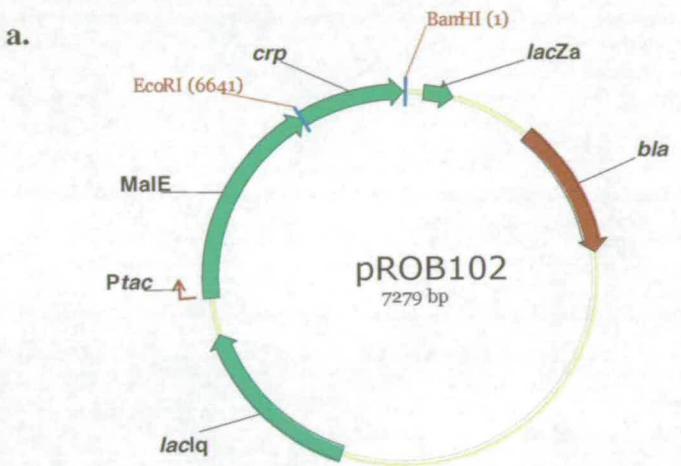


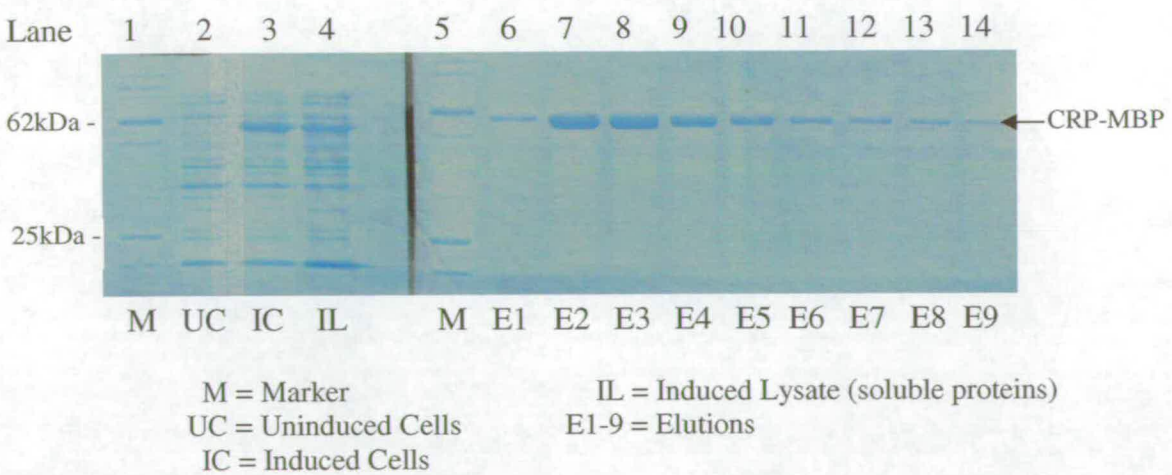


M = Marker
UC = Uninduced Cells
IC = Induced Cells
IL = Induced Lysate (soluble proteins)
E1-9 = Elutions

**Figure 3.4.1.3: Purification of CRP fused to Maltose Binding Protein.**
**a**. Illustration of the pMAL-c2x based vector used to overexpress CRP fused to Maltose Binding Protein at its N-terminus. Transcription is controlled by the inducible $P_{tac}$ promoter. Basal expression is minimised by the binding of the lac repressor (encoded by *lacI*$^q$) to the lac operator immediately downstream of the $P_{tac}$
**b.** SDS-PAGE gel of the products of CRP- MBP purification using a 5ml amylose column. CRP-MBP has a MW of ~ 63.5kDa. 20μls of each fraction resolved per lane.

Using the MBP purification method it was possible to produce large amounts of fusion protein, and to successfully recover the soluble protein with little contamination. In order to remove the MBP from the fusion protein, a Factor Xa site was engineered between the *mal*E gene and the EcoRI site. Cleavage of CRP-MBP was not achieved following incubation with Factor Xa, even following mild denaturation with SDS.

To demonstrate that the MBP-CRP was able to bind DNA, a fragment of the *lac* operator DNA (to which CRP is known to bind) was amplified by PCR using primers Lac-crpFor and Lac-crpRev and subsequently 5′ end-labelled with $^{32}$P. This fragment was used as a positive control for each EMSA to ensure that the assay conditions were appropriate for CRP binding (Figure 3.4.1.4). EMSAs were then performed to determine whether CRP bound to the predicted DNA binding sites in the intergenic region. DNA fragments of approximately 200 bp were amplified by PCR and subsequently 5′ end-labelled with $^{32}$P. The intergenic region was split into three overlapping fragments: 0-200 bp (upstream of *yab*B) amplified using primers PmraEco and PmraBam; 200-400 bp amplified using primers Pmra400 and PmraBam; and 400-600bp amplified using primers Pmra600For and PmraBam.

Binding reactions were performed in the presence of 100μM cAMP. Each DNA fragment was incubated with increasing concentrations of CRP (0 - 4.5μg/ml). The binding reactions were resolved on a non-denaturing polyacrylamide gel containing 100μM cAMP. Successful binding can be recognised as a retardation of the radiolabelled DNA in comparison to the same DNA fragment in the absence of protein. The autoradiograph for one such experiment is shown in Figure 3.4.1.5.

CRP-MBP is active in the presence of 100μM cAMP and capable of binding at a concentration of 4.5μg/ml to the *lac*O DNA. However, the autoradiographs from the experiments show that no retardation of the radiolabelled DNA bands was observed in the presence of increasing CRP for the 0-200, 200-400 and the 400-600 bp (data not shown) fragments. This indicates that CRP does not bind within the intergenic region.

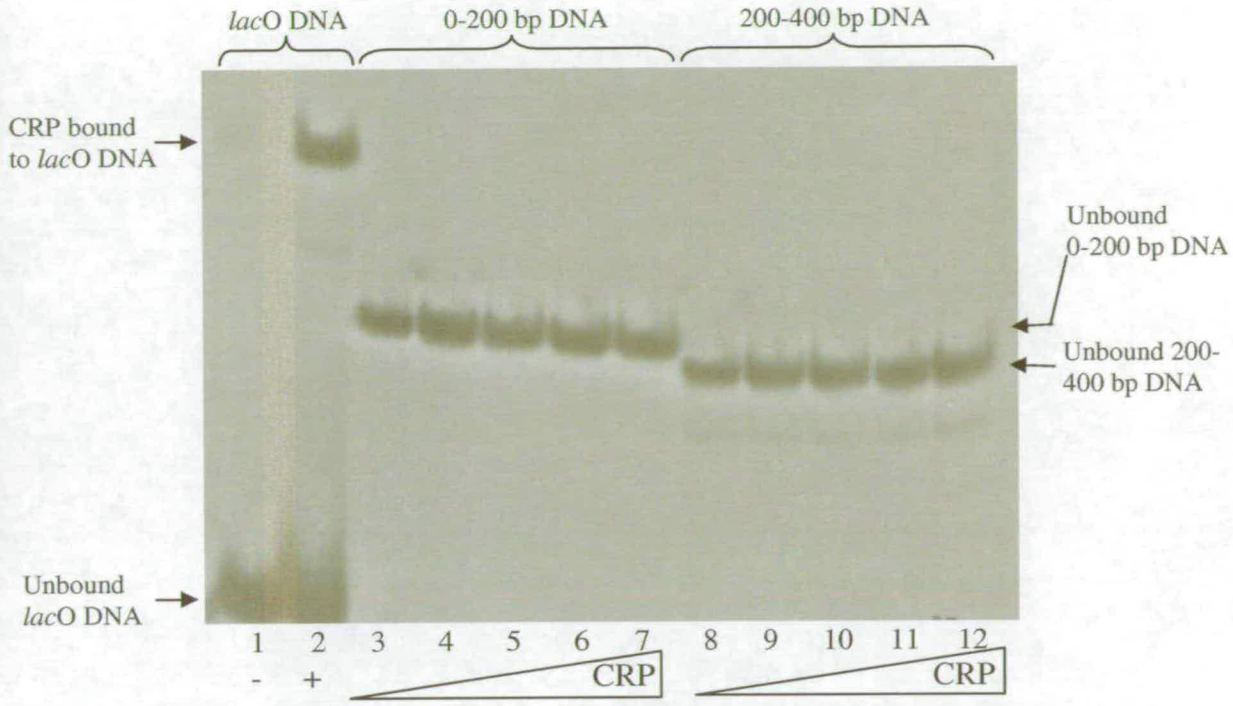


**Figure 3.4.1.4: EMSA to determine whether CRP-MBP binds to DNA.**
Autoradiograph of EMSA performed in the presence of 100μM cAMP (in reaction buffers and gel).
**Lane 1:** Radiolabelled *lac* operator DNA in the absence of CRP-MBP;
**Lane 2:** Radiolabelled *lac* operator DNA in the presence of 4.5μg/ml CRP-MBP. The upper band represents a protein:DNA complex indicating that CRP-MBP is active and capable of binding to CRP sites.
**Lanes 3-7:** Radiolabelled 0-200 bp DNA in the presence of increasing amounts of CRP-MBP (0, 0.8, 1.5, 3, 4.5 μg/ml respectively), no binding was observed with this region of DNA.
**Lanes 8-12:** Radiolabelled 200-400 bp DNA in the presence of increasing amounts of CRP-MBP (as previously), no binding was observed with this region of DNA.

CRP did not form protein:DNA complexes with the potential binding sites I and II which were predicted by bioinformatics. These sites deviate from the CRP consensus sequence and the lack of binding indicates that, in this case, the bioinformatic predictions do not correlate with active sites that might allow biochemical interactions within the cell. CRP also failed to bind to site III, the potential Class II CRP binding site which overlapped the $P_{mra}1$ promoter. This sequence had a good match to the consensus and was positioned at a distance equivalent to sites known to be competent for activation at by CRP (Busby., 1999). It is possible that CRP was unable to bind to this site due to the high GC content of the flanking DNA. Although CRP does not require intrinsically curved DNA; the GC density of the surrounding region may inhibit the significant bend that CRP induces upon binding, and this may have prevented stable interactions between CRP and the DNA.

These data suggest that the difference in expression of the *mra* region between growth in LB and M9 Maltose (observed in section 3.1), is not due to catabolite repression of the $P_{mra}$ promoters. However, CRP is known to regulate the expression of a number of important transcriptional regulators including FIS and IHF. Therefore if these proteins are shown to regulate the $P_{mra}$ promoters, CRP may still mediate regulation of the *mra* region but in an indirect fashion via the actions of other transcriptional regulators.

### 3.4.2: A Role for FIS in the regulation of the $P_{mra}$ promoters.

We reported in section 3.2.3 that FtsI expression was repressed during resumption of growth in lag phase, suggesting that a repressor of the $P_{mra}$ promoters was specifically expressed at this stage in batch culture. An obvious candidate protein was FIS, which is highly expressed in early exponential phase. Additional work in the lab on the *mra* region used a FIS-HIS fusion protein to carry out EMSAs and DNaseI footprinting assays for identification of potential FIS binding sites. Four sites were detected in the intergenic region (Figure 3.4.2.1); two were distally located upstream of $P_{mra}3$ centred on sites -209 and -105, one was found to bind to a very unusual site – directly between the -10 and -35 regions of $P_{mra}3$, while the final site was shown to bind directly over the -10 region of $P_{mra}2$. (G. Blakely, unpublished data). From the positions of the FIS binding sites it may be predicted that FIS would alter transcription mainly through interactions with RNAP at $P_{mra}2$ and $P_{mra}3$. To determine whether FIS binding to these sites has a role in controlling transcription of the $P_{mra}$ promoters, a series of experiments measuring β-galactosidase activity were performed using the pROB plasmids (section 3.2.) in a *fis*$^-$ background.

FIS binding Site IV was the first to be investigated. This binding site is centred directly over the -10 RNAP recognition region of $P_{mra}2$ and as such would be predicted to cause repression of transcription from this promoter. TP8503 and its *fis* derivative RE201 (*fis*::Km) were transformed with pROB209. The β-galactosidase activity was measured from cultures that had been kept in exponential growth for 6 generations. The measured activity of β-galactosidase is presented in Figure 3.4.2.2a. When *fis* is absent from the cell there was an almost 3-fold increase in transcription

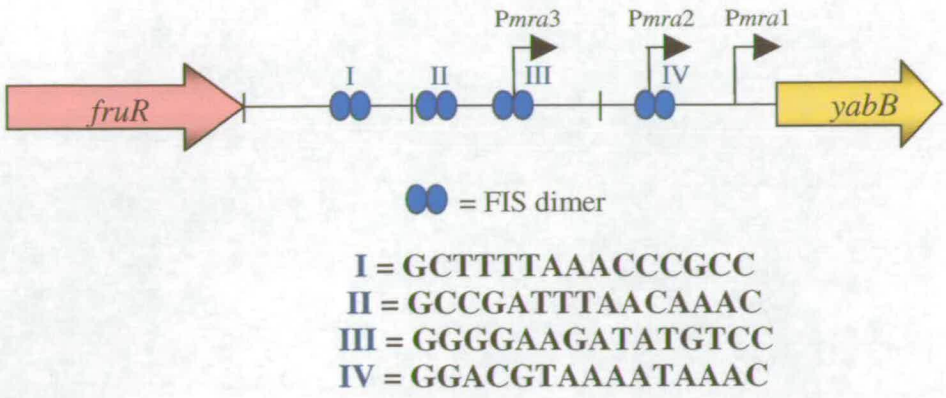


**Figure 3.4.2.1: FIS binding sites identified in the 601bp *fru*R-*yab*B intergenic region.**
Illustration depicting the four observed FIS binding sites located within the 601bp intergenic region. The sequences of each site are also shown. Sites III and IV overlap the $P_{mra}3$ and $P_{mra}2$ promoter regions, respectively.

from $P_{mra}2$; indicating that although this is a weak promoter it is significantly repressed by FIS during early exponential growth.

FIS binding site III is located between the -10 and -35 recognition sequences for RNAP at $P_{mra}3$; this is an unusual position for a transcriptional regulator to bind. It is similar to the position at which MerR binds at the $P_{merT}$ promoter, where it causes activation due to bending of an overly long spacer region, bringing the recognition sequences closer together (Ansari *et al.*, 1992). $P_{mra}3$ however has an optimal spacer region of 17bp, making a bend in this position unnecessary. It would seem more likely that binding of FIS to this region would inhibit subsequent binding of RNAP. Any bend induced by FIS could reduce recruitment of RNAP and make stable interactions with the DNA difficult.

The β-galactosidase activities measured from plasmids containing $P_{mra}3$ in strains TP8503 (*fis*$^+$) and RE201 (*fis*$^-$), are summarised in Figure 3.4.2.2b. Plasmid pRS3M is a pRS551 based vector, containing $P_{mra}3$ in a 135bp fragment cloned upstream of *lac*Z. Expression of β-galactosidase from pROB202 and 203 represents a measure of transcription from $P_{mra}3$ in the 400 or 600 bp fragments of the intergenic region. The expression of β-galactosidase from pROB202 and pROB203 demonstrates that $P_{mra}3$

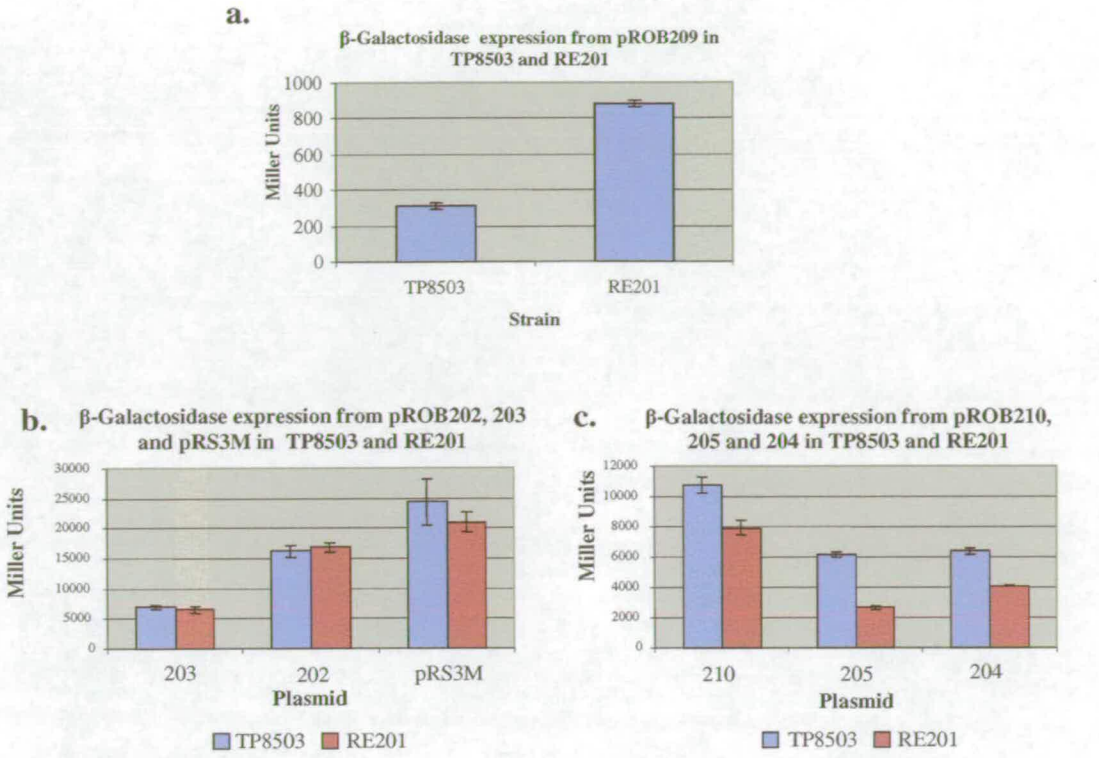


**Figure 3.4.2.2: Effect of FIS on transcription from the $P_{mra}$ promoters.**
**a.** Expression of β-galactosidase from pROB209 ($P_{mra}2$, 600 bp) in TP8503 and its *fis* derivative RE201 (*fis*::Km)
**b.** Expression of β-galactosidase from pROB202 ($P_{mra}3$, 400 bp), pROB203 ($P_{mra}3$, 600 bp) and pRS3M ($P_{mra}3$) in TP8503 and RE201.
**c.** Expression of β-galactosidase from pROB210 (all $P_{mra}$ promoters, 600 bp), pROB205 ($P_{mra}1$, 600 bp) and pROB204 ($P_{mra}1$, 400 bp) in TP8503 and RE201.
All measurements performed on cells grown in LB at 37°C, at an $OD_{600}$ 0.2. Results are from measurements performed on triplicate cultures (or more) error bars of standard deviation are shown.

transcription is not affected by the presence or absence of FIS, particularly when regions upstream of the promoters are present. The pRS3M results indicate however that there is a 20% decrease in β-galactosidase activity in the absence of FIS. A t-test using this data produced a *P* value of 0.04 indicating that the decrease in β-galactosidase activity is statistically significant. It is possible that FIS creates an altered promoter conformation that slightly stimulates transcription from $P_{mra}3$; however as there is only a small decrease in expression in the absence of FIS it seems more likely that the effect is indirect. An important observation was that expression from pRS3M was almost 2-fold higher than that observed from pROB202 and around 5-fold higher than pROB203. This indicates that $P_{mra}3$ is negatively regulated by additional factors, which interact with the intergenic region upstream of $P_{mra}3$.

Expression of FIS is closely linked to DNA supercoiling which is particularly important at promoters with discriminator regions (Travers & Muskhelishvili, 2005). The $P_{mra}3$ promoter appears to have a similar sequence arrangement to the ribosomal promoters and the $P_{fis}$ promoter, as it has a GC rich discriminator region and a poor match to the -35 consensus. These promoters are very sensitive to the level of supercoiling, which may also mean that the same is true at $P_{mra}3$. Therefore in the absence of FIS, the promoter region may not be supercoiled enough for optimal levels of transcription, this may explain the slight decrease in expression of $P_{mra}3$ in the *fis* mutant.

Figure 3.4.2.2c shows the data from experiments using TP8503 and RE201 containing pROB210, pROB205 and pROB204. Plasmid pROB210 contains all three P*mra* promoters, and exhibits a 1.35-fold decrease in expression of β-galactosidase in the absence of FIS. This is much greater than the decrease seen at $P_{mra}3$ and therefore suggests that FIS may activate expression from $P_{mra}1$. This notion is reinforced by the data for pROB205, which gives a measure of transcription from $P_{mra}1$ in a 600 bp fragment and pROB204 which contains $P_{mra}1$ in a 400 bp fragment of the intergenic region. The pROB205 data show a ~2-fold decrease in expression of β-galactosidase from $P_{mra}1$ in the absence of FIS; while pROB204 also exhibits a 1.5-fold decrease in expression. These data imply that the DNA present between 400 and 600bp in the intergenic region may be important for mediating part of this FIS activation, since expression from pROB205 is affected more than pROB204 in the absence of Fis. The requirement for FIS activation at $P_{mra}1$ may be greater than these data initially suggest, since pROB204 and pROB205 both contain a functional $P_{mra}2$ promoter. Figure 3.4.2.2a shows that in the *fis* mutant, β-galactosidase expression from $P_{mra}2$ increases to around 900 Miller Units. This would account for almost one third of the expression observed from pROB205 in a *fis* strain, and one quarter of the expression from pROB204. This means that expression from $P_{mra}1$ alone would be lower than that depicted in Figure 3.4.2.2c.

It is unclear how $P_{mra}1$ would be activated by FIS; it may be an indirect effect mediated via the superhelical density of the DNA or it may be via long range interactions with RNAP. The most proximal FIS binding site (Site IV) which overlaps $P_{mra}2$, is centred on -102. It is feasible that FIS could induce an acute bend

at this site enabling interactions between itself and RNAP or perhaps between RNAP and as yet unidentified regulators binding upstream of the FIS site. The 400-600 bp fragment of DNA from the intergenic region appears to enhance activation of $P_{mra}1$, however it seems unlikely that FIS binding to Site I within this region would play a role in the activation. FIS Site I is located more than 400 bp upstream of $P_{mra}1$ and although the intergenic region is particularly AT rich and therefore very flexible, it seems doubtful that stable interactions could occur between FIS bound at Site I and RNAP bound at $P_{mra}1$.

These results indicate that FIS appears to influence expression from the $P_{mra}$ promoters. This study has presented evidence which suggests that FIS acts as a repressor by binding directly to $P_{mra}2$, we have also shown that FIS slightly modulates $P_{mra}3$ transcription levels, possibly by altering the DNA topology. We observed that $P_{mra}1$ was activated by the presence of FIS and that the combined transcription levels from the three $P_{mra}$ promoters were also activated when FIS was present. This indicates that FIS possibly contributes to fine tuning of the $P_{mra}$ promoters in a growth phase dependent manner.

Since both $P_{mra}1$ and $P_{mra}2$ were affected by the absence of FIS, it was speculated that *fis* mutants may exhibit cell division defects due to altered expression of cell division genes in the *mra* region. Microscopic examination of strain RE201 (*fis*::Km) showed a heterogeneous population of cells with approximately 40% exhibiting filamentation, (defined as cell lengths twice that of MG1655 dividing cells). It was observed that the filamentation phenotype worsened upon continued exponential phase growth (Figure 3.4.2.3). After ten mass doublings, some cells had failed to divide and were more than 100μm in length, while continuous exponential growth eventually resulted in cell lysis. The filaments shown in Figure 3.4.2.3 exhibit a smooth morphology suggesting that the block in cell division occurred at an early stage in septum formation. This may indicate that the expression of FtsZ or FtsA is regulated by the presence of FIS, since temperature sensitive *ftsZ* mutants also produce smooth filaments under non-permissive conditions.


**Figure 3.4.2.3: Filamentation of RE201 (*fis*::Km) with continued exponential phase growth.**

**a**. Cells at $OD_{600}$ 0.2 after approx. 3 mass doublings. Culture grown in LB at 37°C, following inoculation from an overnight culture.
**b**. Cells at $OD_{600}$ 0.2 after approx. 6 mass doublings, following 1/10 dilution of culture sampled in A into fresh LB.
**c**. Cells at $OD_{600}$ 0.2 after approx 10 mass doublings, following 1/10 dilution of culture sampled in B into fresh LB. .

The potential role that FIS plays in transcription during the cell cycle was further investigated to determine why a lack of FIS was detrimental to division. Transcription from the *mra* promoters in a *fis* mutant was first analysed; EDCM647 was again used along with its derivative RE111 (*fis*::Cm) to measure β-galactosidase activity from samples taken at regular time points from a batch culture in LB at 37°C.

RE111 has a doubling time of 36 minutes, compared to 31 minutes for EDCM647, indicating that the *fis*::Cm mutation causes some perturbation of cell growth. Figure 3.4.2.4b shows that the β-galactosidase activity of EDCM647 was high (240 Miller Units) on exit from stationary phase; expression then decreased by 2.5-fold to a basal level of 100 Miller Units during balanced growth, before increasing again as stationary growth was approached. In contrast, β-galactosidase expression in RE111 remained at a low level (~75 Miller Units) until stationary phase growth was approached at which stage expression levels increased, resembling those for EDCM647. These graphs do not take into account the potential β-galactosidase accumulated during stationary phase. It can be assumed that this would have some bearing on the pattern of expression observed at early time points for EDCM647 (See section 3.2). However, RE111 exhibited a low basal level of activity on exit from stationary growth, suggesting that little β-galactosidase had accumulated in this strain.

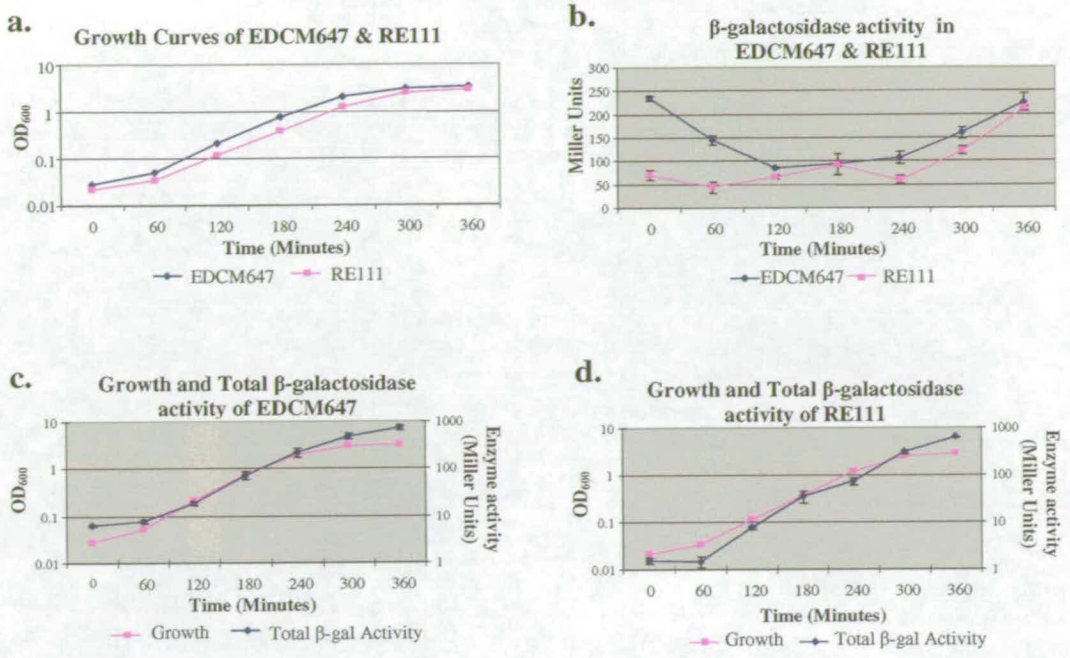


**Figure 3.4.2.4: Growth, β-galactosidase activity and total β-galactosidase activity of EDCM647 & RE111.**

**a**. Comparison of growth curves between EDCM647 and RE111 grown at 37°C in LB. The strains grew with exponential phase doubling times of 31 and 36 minutes respectively

**b**. Comparison of β-galactosidase activity between EDCM647 and RE111. β-galactosidase activity was measured from triplicate cultures; error bars are shown. Results for RE111 show that there is less β-galactosidase expression compared to EDCM647 in cells from early time points, and only when cells are entering stationary phase are the enzyme activities for the two strains similar.

**c & d**. Comparison of Total β-galactosidase Activity between EDCM647 and RE1111. Total β-galactosidase activity represents the Miller units of β-galactosidase as a function of cell mass. Cells exhibiting a constant level of transcription (usually during exponential phase where cells are rapidly dividing and protein levels remain constant) show an activity curve that runs parallel to the growth curve as is seen for EDCM647. However, the total β-galactosidase activity curve for RE111 highlights the significant lag in β-galactosidase activity during early exponential phase growth.

Figures 3.4.2.4c & d, show the total β-galactosidase activities for EDCM647 and RE111. Total β-galactosidase activity represents the amount of β-galactosidase present as a function of cell mass. A steady level of enzyme expression produces a straight line which should run parallel to the growth curve. This is seen for EDCM647 but is never quite achieved by RE111 due to the low levels of expression during early exponential growth. This decrease in expression from the $P_{mra}$ promoters in the *fis* mutant strain agrees with the data from experiments using the pROB plasmids which showed that FIS was necessary to activate $P_{mra}1$ during early exponential phase growth. A deficiency in the transcription of the *mra* region during early exponential growth may be partially responsible for the division defect observed

in the *fis* mutants (Figure 3.4.2.3). If the cells cannot make sufficient division proteins by the time the cell mass has doubled, the cells will continue to elongate. When the culture is maintained in exponential phase, the transcription of the *mra* region will continue to be reduced in a *fis* mutant compared to the control strain. The expression of division proteins to a level sufficient for septation may not occur unless the culture is allowed to approach stationary phase, and cell lengths will continue to increase as long as the culture is maintained in exponential growth, as is shown in Figure 3.4.2.3.

The peak of FIS expression in *E. coli* occurs during early exponential phase growth at around 60-75 minutes (Travers *et al.*, 2001, Nasser *et al.*, 2002), this is the time when cells will be undergoing their first division following subculture into fresh media. We have seen that the absence of FIS alters expression from $P_{mra}1$ and therefore in a *fis*$^-$ strain there may not be sufficient transcription of cell division genes in the *mra* region to support septation. This might explain the large number of filaments observed in exponential phase *fis* cultures. When *fis* cultures are allowed to proceed through batch culture without dilution, the length of filaments does not increase significantly. Therefore cell division can occur successfully later in the growth cycle, suggesting that transcription from the $P_{mra}$ promoters may be activated by factors other than FIS at this time. RE111 however, exhibits the same degree of filamentation as other *fis* mutants, even though transcription of the *mra* region in this strain is driven by the IPTG inducible $P_{lac}$. This suggests that it may not be the lack of FIS activation at the $P_{mra}$ promoters that caused the division defect in *fis* mutants, but rather the action of FIS at distal sites, for example at the *fts*Q, A and Z promoters further downstream in the *mra* region, or perhaps by other indirect effects.

### 3.4.3: Effect of FIS on the expression of *fts*Z.

To determine if FIS had a role in controlling expression of *fts*Z, β-galactosidase activity was measured in the *fts*Z reporter strain VIP407 and its derivative RE301 (*fis*::Cm); results of these experiments are displayed in Figure 3.4.3.1. The VIP407 and RE301 data show that FIS appears to repress expression of *fts*Z during exponential growth. In VIP407 there was a rapid 5-fold decrease in expression of β-galactosidase on exit from stationary phase (0-90 minutes), a constant basal level of

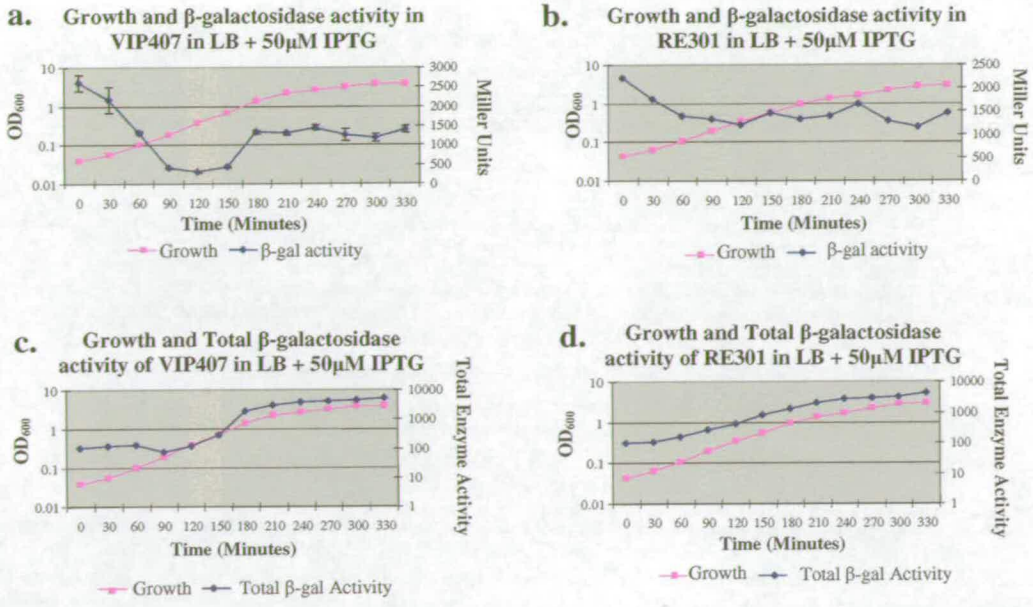


**Figure 3.4.3.1: Growth, β-galactosidase activity and total β-galactosidase activity of VIP407 and RE301.**

**a.** Growth curve and β-galactosidase activity of VIP407, highlighting the rapid decrease in β-galactosidase expression during exponential phase growth.

**b.** Growth curve and β-galactosidase activity of RE301 (*fis*::Cm). There is a relatively constant level of β-galactosidase expression throughout batch culture in the absence of FIS, which is in contrast to the VIP407 (*fis*$^+$) β-galactosidase expression pattern.

**c & d.** Comparison of total β-galactosidase activity, between VIP407 and RE301. The RE301 data show an activity curve running parallel to the growth curve during exponential growth, highlighting the steady level of β-galactosidase activity produced in the absence of FIS. The VIP407 data indicate that FIS lowers the levels of β-galactosidase activity during balanced growth.

expression during exponential growth (90-150 minute), followed by a 3-fold increase to a steady state level as the culture approached stationary phase (180-330 minutes), see Figure 3.4.3.1a. In contrast, RE301 exhibited a fairly steady level of β-galactosidase activity suggesting that transcription of *fts*Z may be constitutive during batch culture in the absence of FIS (See Figure 3.4.3.1b). These results indicate that when FIS levels are at their peak in the cell, there is significant repression of *fts*Z transcription. This may be due to direct interactions between FIS and the *fts*QAZ promoter regions, although no such binding sites have been reported in the current literature.

To determine whether the apparent repression of *fts*Z transcription by FIS caused a corresponding decrease in FtsZ levels in the cell, Western blots were performed on cell samples taken at regular time points during batch culture. MG1655 and its

derivative RE102 (*fis*::Cm) were grown in 1 litre LB at 37°C. Large sample sizes were extracted at early time points so that each sample gave an $OD_{600}$ of around 0.4 when the cells were pelleted and resuspended in 1ml of 0.1M NaCl-HSB buffer.

Lysates containing soluble protein from cells at different time points were produced and then resolved by SDS-PAGE with 5.5μg of protein loaded into each lane. Two polyacrylamide gels with identical samples were electrophoresed for each set of cell lysates. One was stained with Coomassie to check that equal concentrations of lysate had been loaded into each lane, the other was transferred to PVDF membrane for immunoblotting. The membranes were probed with anti-FtsZ monoclonal antibody to detect any changes in FtsZ concentration during the batch culture. The results of this experiment are displayed in Figure 3.4.3.2.

As previously reported, levels of FtsZ appear to vary little in response to changes in growth during batch culture (Rueda *et al.*, 2003), although this contradicts the need for more FtsZ per cell mass during slower growth. Constitutive expression of FtsZ regardless of growth rate is reflected in the results displayed in Figure 3.4.3.2., which show that in MG1655 a fairly steady level of FtsZ was expressed on exit from stationary phase and during balanced growth between 20 and 140 minutes. There was a small increase in expression at 160 minutes as the culture approached stationary phase. The 0 minute sample taken immediately after subculture exhibited a low level of FtsZ expression. It is unclear why such a low level of expression was observed as FtsZ levels in a stationary culture are high (200-240 minutes), therefore it would be expected that a similar level would be seen in cells immediately following dilution. The data for RE102 (*fis*::Cm) also indicates that FtsZ expression changed little in a batch culture of this strain. Figure 3.4.3.2., shows that in RE102 a constant low level of FtsZ was expressed on exit from stationary phase and during early exponential growth (0-120 minutes). There was then a small increase in expression between 140-160 minutes, which decreased upon approach to stationary phase. The results for both MG1655 and RE102 show that the pattern of FtsZ expression is similar for both strains, although overall expression of FtsZ appears, by eye, to be 2-3 fold higher in the wild type MG1655 strain.

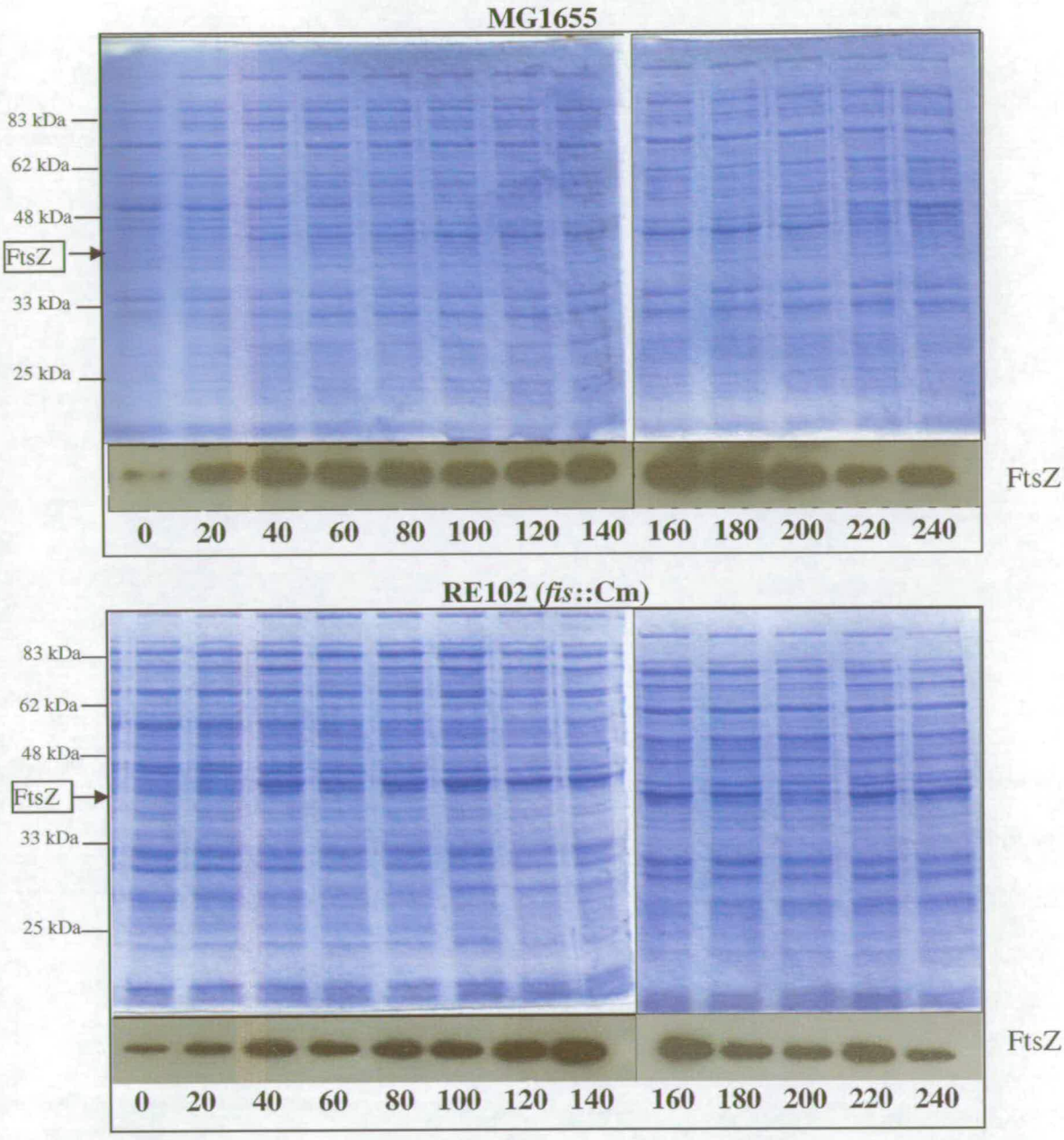


**Figure 3.4.3.2: Western blots of FtsZ in MG1655 and RE102 during batch culture.**

Cell lysates were prepared from MG1655 and RE102 (*fis*::Cm) cell samples, taken every 20 minutes during growth in LB at 37°C. The lysates were concentrated and soluble protein standardised so that 5.5μg of protein was loaded per lane. The stained polyacrylamide gels of samples from each strain can be seen in the above panels. The resolved proteins were transferred to PVDF membrane and probed with anti-FtsZ antibody. Levels of FtsZ at each time point can be seen in the grey panels above.

It is possible that FIS is indirectly affecting the translational efficiency of FtsZ, and this is why an apparent decrease in expression is observed in the *fis* mutant. FIS has been shown to be an important activator of the rRNA promoters. In the absence of FIS, there will be fewer ribosomes in the cell (Muskhelishvili *et al.*, 1997; Zhi *et al.*, 2003), therefore some transcripts may not be translated at their optimal rate and

protein levels may be lower. The decrease in FtsZ expression may be partially responsible for the cell division defect observed in *fis* mutants.

If the filaments observed in the *fis* mutants occur because less FtsZ (and presumably also FtsA and FtsQ) are translated (even though transcription appeared to be higher), then over-expression of these proteins *in trans* may overcome the division defect and restore normal division. The plasmid pZAQ, which is a pBR322 based vector containing the genes *fts*Q, A and Z and all six of their upstream promoters, was used to transform MG1655, RE102 (*fis*::Cm), RE104 (*rpo*S::Km) and RE106 (*fis*::Cm, *rpo*S::Km). We had previously observed filamentation in *rpo*S mutants. *rpo*S is not expressed during exponential phase, however filaments were observed in rpoS mutants at this stage of growth (Figure 3.4.3.3ci.). RpoS may be required to increase the expression of division proteins such as FtsZ as cells approach stationary phase. This would provide sufficient proteins to be recycled when *de novo* synthesis of division proteins is low upon exiting lag phase. In the absence of *rpo*S, filaments may occur in exponential phase due to insufficient division proteins being present to form a septal ring. It was interesting to determine whether this *rpo*S mediated division block could be overcome by overexpression of FtsQ, A and Z. Transformants of each strain were grown overnight then subcultured into fresh prewarmed LB. The cultures were grown at 37°C to an $OD_{600}$ of 0.2, at which stage they were subcultured again into fresh prewarmed LB. This process was repeated and the cell morphologies were analysed by microscopy. Figure 3.4.3.3 shows the morphology of the four strains containing either the control plasmid pBR322, which should have no effect on cell division, or pZAQ which over-expresses FtsQ, FtsA and FtsZ. Since the genes in pZAQ are still under the transcriptional control of their native promoters the ratio of FtsA: FtsZ will be maintained.

Cells harbouring pBR322 exhibited morphologies similar to the untransformed parental strains, confirming that this plasmid does not affect cell division. MG1655 had an average cell length of 4μm, while RE102 showed a heterogeneous population of cells with around 40% considered filamentous since they were longer than 8μm. RE104 and RE106 also exhibited heterogeneous populations with significant cell filamentation present (Figure 3.4.3.3ai-di).

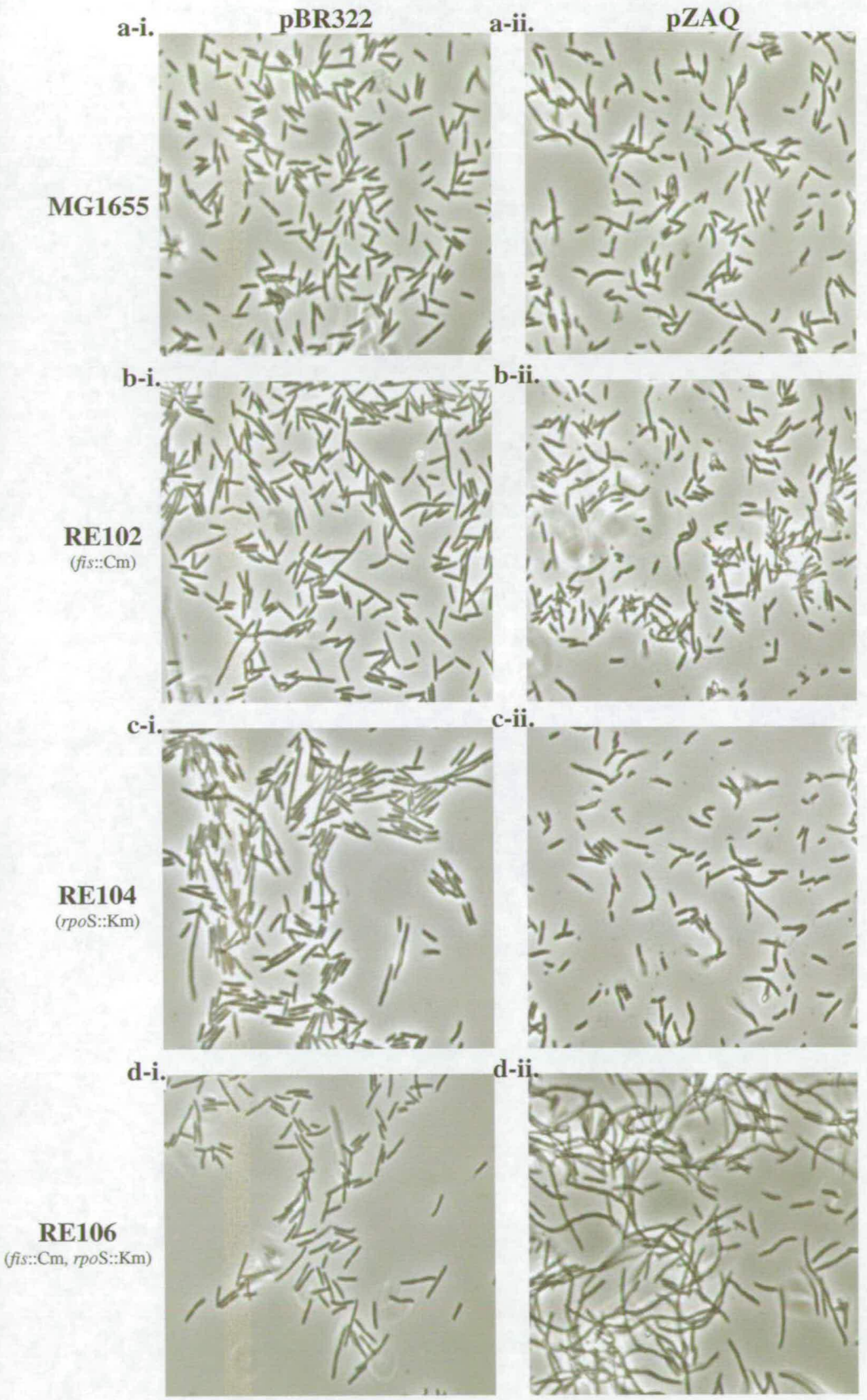


**Figure 3.4.3.3: Morphology of MG1655, RE102, RE104 & RE106 from exponential cultures in LB.**

Images are x400 magnifications of cells grown to an $OD_{600}$ 0.2 from an overnight culture in LB, diluted 1/10 and regrown to $OD_{600}$ 0.2. Cells had been transformed with either pBR322, or the pBR322 based plasmid pZAQ which over-expresses the cell division proteins FtsQ, FtsA and FtsZ.

When pZAQ was present in the cells, very different morphologies were observed. In MG1655, overproduction of FtsZ led to the presence of mini-cells and chains. The presence of chains suggests that septal rings are initiating division with over-expressed FtsZ and FtsA but there are not enough of the other septal ring proteins present in the cell for successful division at each of these sites.

The presence of pZAQ in RE102 and RE104 partially rescued the filamentous phenotype associated with both the *fis* and *rpo*S mutations. However, Figure 3.4.3.3bii-cii. show that both strains exhibited mini-cell production and asymmetric division, which may imply that there is a block to division present at mid-cell. These results suggest that although pZAQ enables the cells to divide, the increase in expression of FtsQ, FtsA and FtsZ does not overcome a possible division block that may result in the filamentation in *fis* and *rpo*S strains.

RE106 transformed with pZAQ exhibited a severe division defect, with more than 80% of cells being filamentous (Figure 3.4.3.3dii). Instead of pZAQ facilitating cell division, in these cells it appeared to cause severe filamentation. The filaments present a smooth morphology without indentations associated with the formation of Z-rings; however they appear to "bulge" in places, suggesting that peptidoglycan synthesis is not uniform along the length of the filament. RE106 containing pZAQ grew slowly with a doubling time of 42 minutes compared to 26 minutes for MG1655 containing pZAQ, and exhibited a very long lag on exit from stationary growth; this was not observed with the single *fis* or *rpo*S mutants RE102 and RE104.

It is difficult to explain the morphology of RE106 containing pZAQ. These cells are growing more slowly and should therefore be smaller in size than wild type MG1655, with a corresponding increase in expression of the genes in the *mra* region. It may be that over-expression of FtsQ, A and Z from pZAQ, in conjunction with increased expression of FtsQ, A and Z from the chromosome, may cause the titration of other division proteins resulting in the formation of non-productive septal rings. Excess FtsZ, A and Q should result in the formation of mini-cells, as observed in RE102 and RE104. However at the slower growth rate exhibited by RE106 this increase in FtsZ, A and Q is no longer enough to support division.

We have shown that over-expression of FtsQ, FtsA and FtsZ from pZAQ in these strains caused a cell division defect. To test the prediction that the filamentation associated with pZAQ is caused by titration of other division proteins, the same strains were grown in M9 Glycerol + CAA, since growing the cells more slowly should increase the expression of division proteins from the chromosome.

When grown in M9 Glycerol + CAA, strains RE102 and RE104 containing pBR322 did not filament; the cells were small and largely homogeneous in morphology (Figure 3.4.3.4bi-ci). This either suggests that an increase in FtsQAZ expression caused by slow growth overcomes the block in cell division, or that the block in division is not present. RE106 harbouring pBR322 still produced filamentous cells and there was no reduction in cell size under these growth conditions (Figure 3.4.3.4di). This implies that division is still blocked in these cells and that expression of the *mra* region in the *fis*, *rpo*S double mutant may be unable to respond to changes in growth rate.

Under this slower growth condition, all four strains exhibited division defects in the presence of pZAQ (Figure 3.4.3.4aii-dii). These data suggest that too much FtsZ, A and Q results in filamentation and mini-cell production in the parental strain, MG1655 (Figure 3.4.3.4aii). Of particular interest was the observation that in the presence of pZAQ RE102, 104 and 106 all showed significant cell chaining when grown in M9 + Glycerol + CAA (Figure 3.4.3.4bii-dii). The presence of chaining suggests that a semi-functional septal ring has formed but that it is incapable of completing the septum; this may be due to titration of available division proteins.

To determine the localisation of DNA in the *fis* filaments, RE102 (*fis*::Cm) was subcultured and grown to an $OD_{600}$ of 0.2 three times in LB at 37°C. The nucleoids were condensed with Chloramphenicol and the DNA was stained with DAPI. In the heterogeneous population, those cells with a normal morphology had well segregated nucleoids (Figure 3.4.3.5). However, in the long filamentous cells, large masses of unsegregated chromosomes were observed. Large regions of DNA could result in the inhibition of division by nucleoid occlusion and may also explain the asymmetric divisions observed in Figure 3.4.3.3.

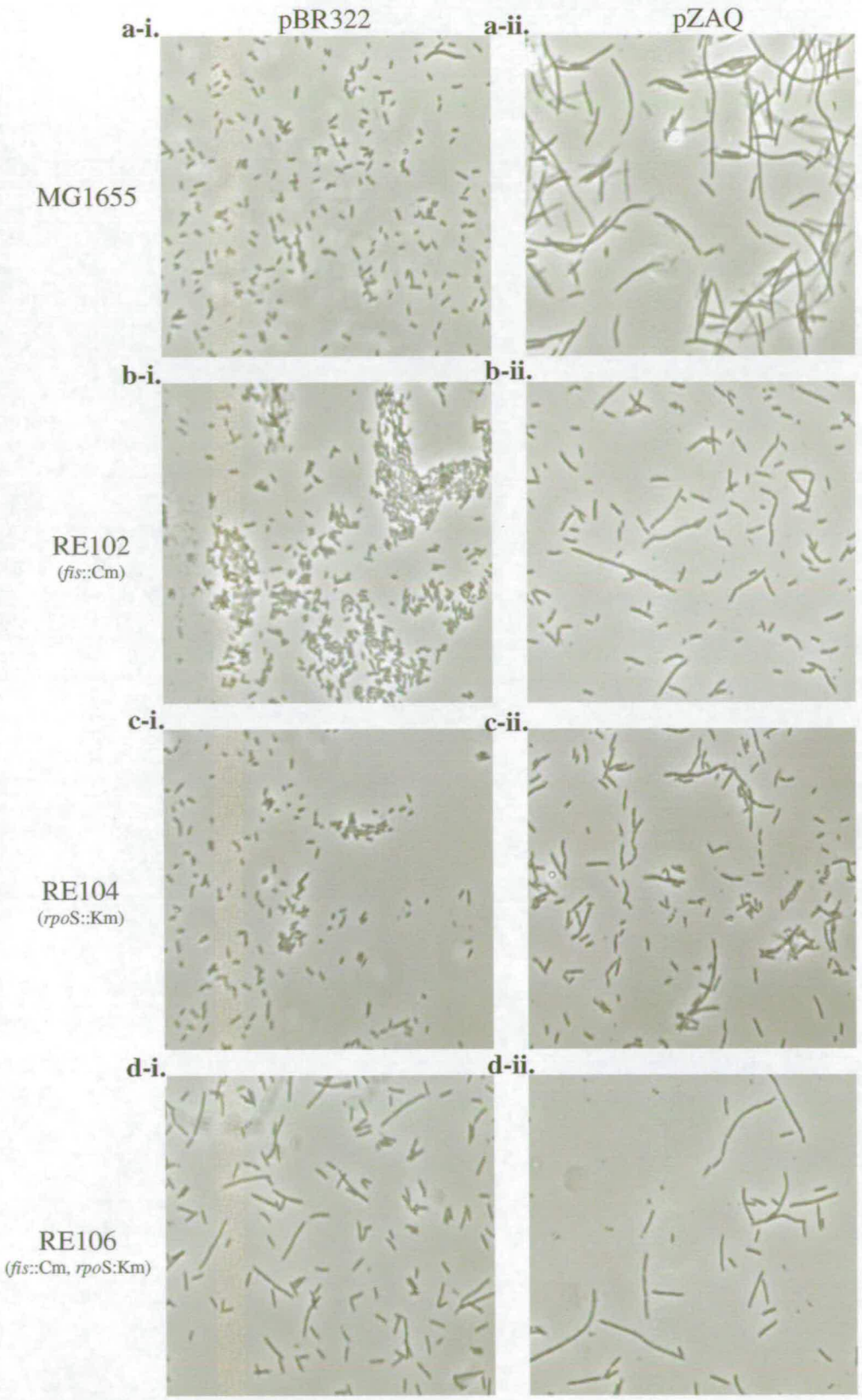


**Figure 3.4.3.4: Morphology of MG1655, RE102, RE104 & RE106 grown in M9 Glycerol + CAA.**

Images are x400 magnifications of cells grown to an $OD_{600}$ 0.2 from an overnight culture in M9 Glycerol + CAA, diluted 1/10 and regrown to $OD_{600}$ 0.2. Cells had been transformed with either pBR322, or the pBR322 based plasmid pZAQ which over-expresses the cell division proteins FtsQ, FtsA and FtsZ.

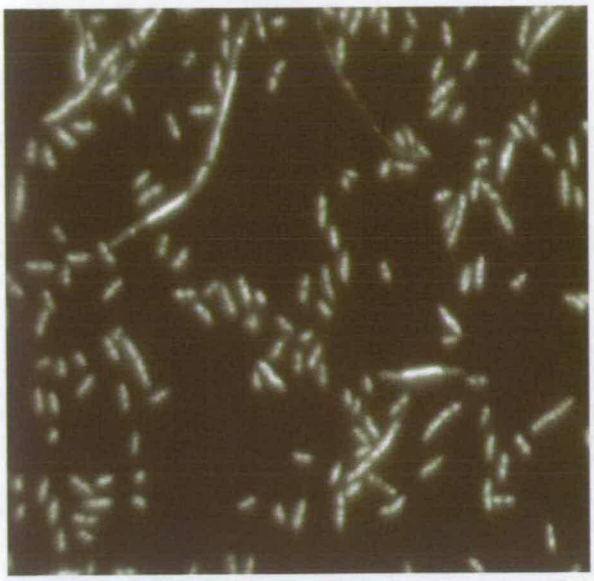

**Figure 3.4.3.5: Mis-segregation of DNA in *fis*⁻ filaments.**
RE102 was repeatedly grown to an $OD_{600}$ of 0.2, in LB at 37°C. The cells were treated with Chloramphenicol to condense the nucleoids which were subsequently stained by the addition of DAPI. RE102 exhibits a mixed phenotype with dividing cells and large number of division inhibited smooth filaments. Large masses of DNA were seen in the filamentous cells; whereas the dividing cells contained well segregated nucleoids.

Aberrant DNA segregation in filamentous *fis*⁻ cells has been previously reported, but only at high temperatures, i.e. 42°C. (Filutowicz *et al.*,1992). The mis-segregation of DNA reported by Filutowicz *et al.*, (1992) was attributed to a lack of DNA replication due to the actions of FIS at *ori*C. However, it seems unclear how DNA could be accumulating if it is not being replicated.

Initiation of DNA replication at *ori*C is tightly regulated, particularly in rapidly growing cells where it must occur from all copies of *ori*C synchronously. DnaA binds to multiple sites at *ori*C generating a nucleoprotein structure that causes unwinding of *ori*C DNA; this binding is enhanced by IHF also binding within *ori*C (Ryan *et al.*, 2004). FIS inhibits DNA replication by binding competitively to sites within *ori*C that overlap the IHF binding site, and also by binding to weak DnaA binding sites forcing an accumulation of DnaA at stronger binding sites required for *ori*C unwinding (Ryan *et al.*, 2004). In exponentially growing *fis* mutants, the mis-segregated DNA present in the filaments may result from unregulated over-initiation of DNA replication. It is also possible that FIS may be involved in the regulation of genes such as *fts*K, *xer*C and *xer*D all of which are important for chromosome dimer resolution during segregation in the cell (Bigot *et al.*, 2004).

FIS is a pleoitropic global regulator and this study has shown it to be important for efficient cell division. Evidence has been presented suggesting that FIS activates the overall expression from the $P_{mra}$ promoters by around 30% and most of this activation occurs at $P_{mra}1$. FIS has also been shown to repress the transcription of *fts*Z in early exponential growth, however, the levels of FtsZ expression were shown to remain relatively constant regardless of the growth rate. This contradicts the need for more FtsZ per cell mass in small cells. This may suggest that FtsZ is expressed constitutively at a level sufficient for septation in small, slow growing cells regardless of growth rate. Average FtsZ levels however are somewhat reduced in a *fis* mutant compared to a wild type cell, possibly due to the reduced number of ribosomes whose expression is normally activated by FIS. Strains carrying a *fis* mutation have a heterogeneous population of cells with around 40% exhibiting filamentation. This filamentation is exaggerated by prolonged exponential growth which eventually results in cell lysis. Filamentation is associated with mis-segregation of DNA within the cell, which might result from unregulated over-initiation of DNA replication from *ori*C in the absence of FIS.

### 3.4.4: Involvement of other DNA-binding proteins in the regulation of the $P_{mra}$ promoters

This study has investigated the role that FIS, the most abundant nucleoid protein during exponential growth, plays in the regulation of the *mra* region. It has also covered potential regulation by CRP which had been speculated to play a role in cell division. However, data in section 3.4.3 suggests that the $P_{mra}$ promoters, in particular $P_{mra}3$, may be regulated by other transcriptional regulators.

To determine whether other DNA binding proteins that interact with the *fru*R-*yab*B intergenic region could be identified, EMSAs were performed on radiolabelled fragments of DNA from the intergenic region using a soluble protein lysate prepared from strain RE201 (*fis*::Km) grown to an $OD_{600}$ of 0.4. Multiple FIS binding sites are known to be present in the intergenic region (see section 3.4.3) and EMSAs performed in the presence of purified FIS produce a characteristic ladder of FIS bands (See Figure 3.4.4.1). Strong binding of FIS to the intergenic region would mask the

binding of other proteins, therefore a lysate prepared from a *fis* mutant strain was used in this experiment.

A single protein:DNA complex was identified (Complex 1), located in the 200-400bp fragment of the intergenic region (Figure 3.4.4.1, lanes 6-8). It is likely that this protein also binds when FIS is present, however retardation of the DNA caused by interactions with the high intracellular level of FIS in a wild type lysate would mask these weaker complexes.

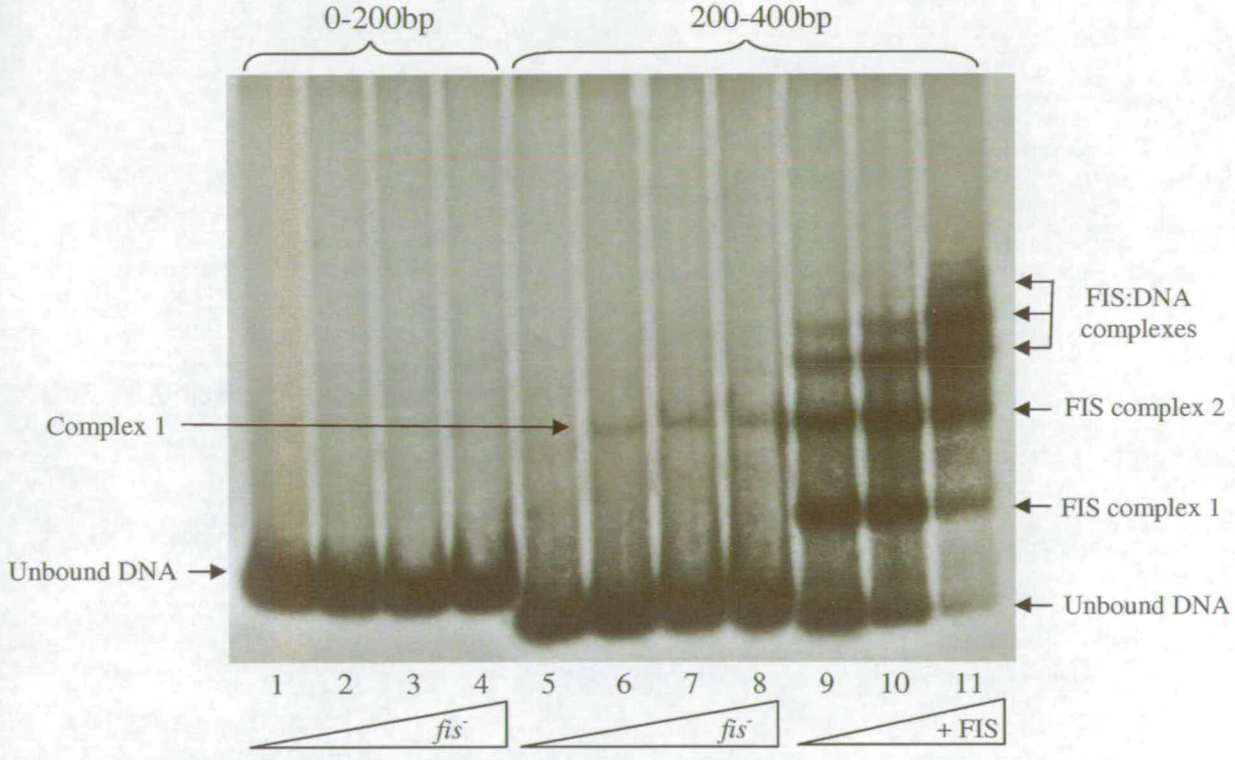


**Figure 3.4.4.1: Autoradiograph of binding reactions containing either purified FIS or a protein lysate from a *fis*⁻ strain with DNA from the *fru*R-*yab*B intergenic region**

**Lanes 1-4** 0-200bp region of DNA incubated with 0, 0.6, 1.2 and 2.4mg/ml *fis*⁻ protein lysate respectively; no protein:DNA complexes were observed.
**Lanes 5-8** 200-400bp region of DNA incubated with 0, 0.6, 1.2 and 2.4mg/ml *fis*⁻ protein lysate. In the absence of FIS a single protein:DNA complex was observed (Complex 1).
**Lanes 9-11** 200-400bp region of DNA incubated with 20, 40 and 80µg/ml of HIS-tag purified FIS. FIS binds to this region of DNA; the characteristic FIS banding pattern demonstrates the presence of 4 high affinity binding sites and at least one low affinity site.

The protein binding to the 200-400bp sequence of the intergenic region in Complex 1 could represent any of the 240 different DNA binding proteins that *E. coli* produces;

of which more than 100 are involved in transcriptional regulation (Azam *et al.*, 2000). Of these transcriptional regulators, 10-20 are involved in condensation of the circular chromosome and are usually referred to as nucleoid or histone-like proteins (Azam & Ishihama *et al.*, 1999). These nucleoid proteins are not structurally similar to eukaryotic histones, however, their DNA-binding ability, low molecular mass and copy number enable them to perform a similar role in prokaryotes.

In addition to FIS, two of the most abundant nucleoid proteins during exponential growth are IHF (Integration Host Factor) and H-NS (Histone-like nucleoid-structuring protein) (Azam *et al.*, 1999). IHF plays an indirect role in cell division since it enhances the initiation of DNA replication (Ryan *et al.*, 2004), and we have seen that perturbation of this process results in division defects, as observed in the *fis* mutants in section 3.4.2. Both IHF and H-NS also assist in maintaining the chromosome in a condensed state suitable for DNA replication, segregation, and for nucleoid occlusion (since Z-rings can assemble on top of decondensed nucleoids) (Sun & Margolin, 1998). No obvious division defects have been observed for *hns* or *ihf* mutants, indicating that other nucleoid proteins can compensate for the absence of HNS and IHF and maintain chromosomal compaction. We were interested in determining whether HNS and IHF play a direct role in the regulation of cell division by acting on the $P_{mra}$ promoters, and whether either protein was present in Complex 1 (Figure 3.4.3.1, lanes 6-8).

IHF was first identified as a host factor required for site-specific integration of phage λ (Drlica, 1999). IHF is a small heterodimer consisting of two ~10kDa subunits encoded by the genes *ihf*A and *ihf*B (Bykowski & Sirko, 1998). The two subunits are 30% identical and are closely related to those found in the nucleoid protein HU. IHF forms a compact dimer with 2 β-ribbon arms protruding to interact with the minor groove of DNA. IHF induces two kinks in the DNA upon binding, resulting in a sharp bend of up to 160°, and a hairpin like structure (Rice *et al.*, 1996). IHF is a sequence specific DNA binding protein, making contacts with around 35bp of DNA. The binding site for IHF is large and considered to have two distinct domains; the 3'-domain is conserved with a 13bp consensus of WATCAANNNNTTR (W = A/T, R = Purine, N = any), while the 5'-domain is degenerate but always A/T rich (Goodman *et al.*, 1999).

IHF is mainly an architectural protein in the cell and is important for numerous long range DNA interactions (McLeod *et al.*, 2001). Microarray data show that IHF also directly or indirectly affects transcription of over 100 genes, and it has been shown to act as both a transcriptional activator and repressor. (Arfin *et al.*, 2000). Although none of the genes in the *mra* region were shown to be significantly regulated by IHF in this report, only those genes whose expression had changed by 3-fold were indicated. Since small changes in the expression of the *mra* region can have significant effects on division it is still possible that IHF may play an important regulatory role at the $P_{mra}$ promoters. IHF is present at around 12,000 dimers per cell during exponential growth, but is most prevalent during early stationary phase when up to 55,000 dimers per cell are present (Azam *et al.*, 1999).

H-NS is a small 15.6kDa homodimer that acts as a global repressor, reducing the transcription of around 5% of the genes in *E. coli* (Dorman & Deighan, 2003). H-NS mainly regulates transcription in response to environmental stimuli - most notably changes in temperature as its expression is induced 3-fold by cold shock (Atlung & Hansen, 2002). H-NS repression can often be overcome by the binding of activators or by changes in DNA supercoiling in response to environmental signals such as changes in osmolarity (Dorman & Deighan, 2003). H-NS is present at around 20,000 dimers per cell in exponential phase, but its expression decreases to around 12,000 dimers per cell in stationary phase growth (Azam *et al.*, 1999).

H-NS binds to DNA in a non-specific manner but exhibits a preference for binding to A/T rich curved DNA, however unlike IHF and FIS; H-NS does not induce a significant bend upon binding to DNA (Drlica, 1999). DNA binding occurs via the C-terminus of each H-NS monomer; while the N-terminus has been shown to be involved in oligomerisation of H-NS mulitmers (Dorman & Deighan, 2003).

The Harvard binding site matrices predicts in excess of 90 IHF binding sites located within the *fru*R – *yab*B intergenic region, however this is probably due to the AT-richness of the intergenic reigon and the degeneracy of the IHF binding site. Purified IHF was used in EMSAs with radiolabelled DNA from the intergenic region (data not shown), however no protein:DNA complexes were observed. This indicates that the binding site predictions were incorrect and that IHF may not play a direct role in the

regulation of the $P_{mra}$ promoters. H-NS binds DNA in a non-specific manner, therefore binding sites cannot be predicted. In addition, interactions between H-NS and DNA would not be detected by EMSAs because poly-dIdC is used in these reactions as a competitive inhibitor of non-specific DNA binding. To determine whether IHF or H-NS play a role in the regulation of the $P_{mra}$ promoters, a series of β-galactosidase assays were performed on *ihf* and *hns* mutant strains using the pROB plasmids.

Strains TP8503, RE202 (*fis*::Cm), RE207 (*ihf*::Tet) and RE208 (*hns*::Km) were each transformed with plasmids pROB210, pROB209 and pROB202-205. The transformants were grown in LB at 37°C and β-galactosidase activity was measured during exponential growth. Activity of β-galactosidase from pROB210 decreased 17% in the absence of FIS, 7% in the absence of H-NS and increased 18% in the absence of IHF when compared to expression in the parental strain TP8503 (Figure 3.4.4.2a). *P* values calculated with these data suggest that the overall transcription from the $P_{mra}$ promoters on a plasmid is not significantly affected by H-NS ($P$ = 0.102), however small but significant changes in transcription occur when FIS ($P$ = 0.012) and IHF ($P$ = 0.039) are absent. This is in agreement with the RE201 (*fis*::Km) data from section 3.4.2 that showed a 26% decrease in β-galactosidase which was interpreted as a slight activation of the $P_{mra}$ promoters by FIS. The results from pROB202 showed a 12% decrease in β-galactosidase expression in the absence of FIS, no difference in the absence of H-NS and a 25% increase in the absence of IHF, compared to expression in the parental strain TP8503. These data suggest there is no significant regulation by H-NS ($P$ = 0.345), slight activation by FIS ($P$ = 0.003), while the presence of IHF may slightly repress $P_{mra}3$ when it is present in the 0-400bp fragment of the intergenic region ($P$ = 0.000018). The pROB203 data show no significant difference in β-galactosidase expression in any of the TP8503 derivatives. The data for pROB204 and pROB205 reiterate the results from section 3.4.2, which showed that FIS is required for activation of $P_{mra}1$ as a 41% and 57% decrease in expression was measured for the 2 plasmids in the *fis* mutant. The data presented in Figure 3.4.4.2a also show that β-galactosidase expression decreased 26% and 37% in the *ihf* mutant in pROB204 and pROB205, suggesting that IHF may also play an indirect role in the activation of $P_{mra}1$. The absence of H-NS appears to have no effect on transcription from $P_{mra}1$ in pROB204 and pROB205.

**a.** **Expression of β-galactosidase from pROB plasmids in derivatives of TP8503**

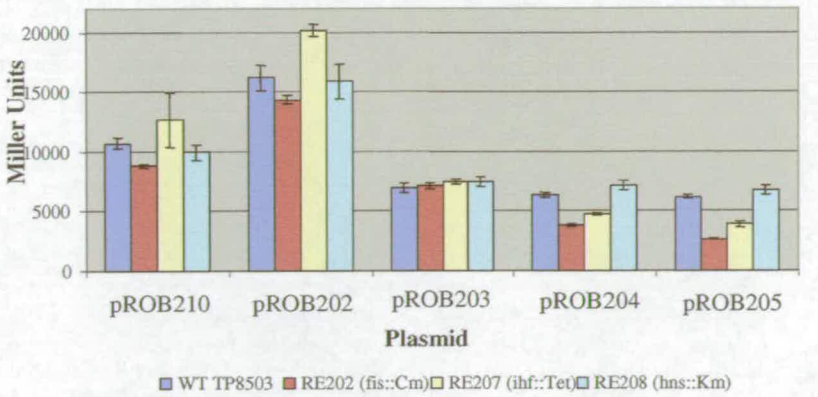


**b.** **Expression of β-Galactosidase from pROB209 in derivatives of TP8503**

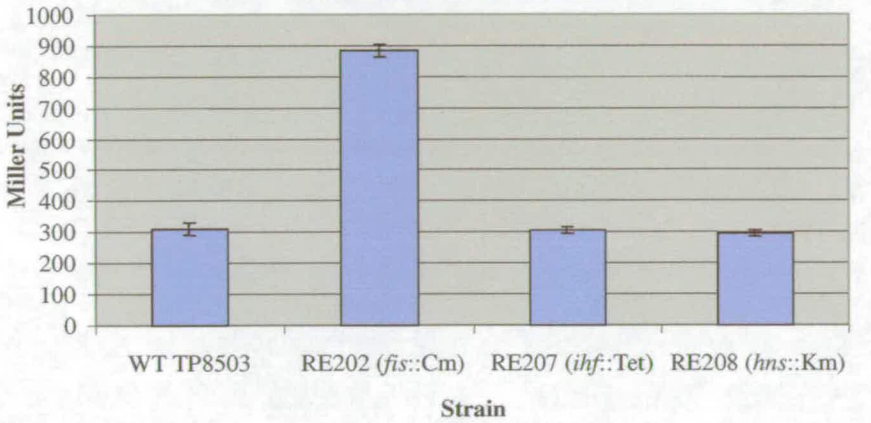


**Figure 3.4.4.2: Expression of β-galactosidase from the $P_{mra}$ promoters in derivatives of TP8503.**

**a.** Histogram illustrating the differences in β-galactosidase activity from pROB plasmids in the absence of particular DNA binding proteins. pROB210 contains the entire 601bp intergenic region with wild type promoters upstream of *lac*Z, pROB202 and 204 have 400bp fragments of the intergenic region with -10 mutations knocking out the functions of $P_{mra}1$ and $P_{mra}3$, respectively. pROB203 and 205 carry 601bp fragments with -10 mutations of $P_{mra}1$ and $P_{mra}3$. The strains used were TP8503, RE202 (*fis*::Cm), RE207 (*ihf*::Tet) and RE208 (*hns*::Km).

**b.** Histogram illustrating the differences in β-galactosidase activity in pROB209, which carries -10 mutations in $P_{mra}1$ and $P_{mra}3$ in a 601 bp fragment of the intergenic region, in the TP8503 mutant strains. β-galactosidase activity was measured from exponential phase cultures grown in LB at 37°C. Results are averages of measurements from triplicate cultures, error bars of standard deviation are indicated.

The β-galactosidase activity from pROB209 in the different TP8503 derivatives is shown on Figure 3.4.4.2b. In the *ihf* and *hns* strains there is no discernable difference in β-galactosidase expression when compared to the parental strains. However, there is a 3-fold increase in the *fis* mutant indicating that FIS represses $P_{mra}2$ (as previously demonstrated in section 3.4.2).

These experiments suggest that H-NS does not play a significant role in the regulation of the $P_{mra}$ promoters. IHF however may play a minor role in the fine tuning of the levels of transcription from $P_{mra}1$. We could not detect binding to the *fru*R-*yab*B intergenic region, therefore this IHF mediated regulation must occur in an indirect manner possible by changes in the downstream nucleoid structure or by altering the supercoiling density of the promoter region (Travers *et al.*, 2001; Zhi *et al.*, 2003). It has also been reported that IHF causes a 3-4 fold activation of *fis* transcription (Pratt *et al.*, 1997), therefore the decrease in expression from $P_{mra}1$ measured from plasmids pROB204 and pROB205 may actually be due to a decrease in FIS activation caused by the absence of IHF.

## 3.5: The effect of changing growth rate on the individual $P_{mra}$ promoters.

This study has previously reported that the combined transcription from the $P_{mra}$ promoters is inversely related to growth rate (Section 3.2.1). To determine which of the promoters were capable of responding to changes in growth rate in this way, TP8503 was transformed with the pROB expression vectors and the strains were grown in LB or M9 Maltose + CAA. Overnight cultures were diluted 1/100 into fresh media and grown to an $OD_{600}$ of 0.2 at 37°C, at which stage the culture was diluted 1/10 into fresh media and grown at 37°C. The β-galactosidase activity was measured at an $OD_{600}$ of 0.2, and the results are illustrated in Figure 3.5.1. If a promoter responds inversely to growth rate, it would be expected that transcription levels would increase when grown in M9 Maltose + CAA. Expression from $P_{mra}3$ in a 400 bp fragment (pROB202) was slightly reduced (11%) at the slower growth rate. A t-test on these data produced a $P$ value of 0.048, indicating that the small change in expression from $P_{mra}3$ at the slower growth rate is statistically significant. However, when present in the full 601bp intergenic fragment, expression from both $P_{mra}1$ (pROB205) and $P_{mra}3$ (pROB203) was increased slightly 20% ($P$ = 0.002) and 18% ($P$ = 0.005) with slower growth. Although the changes in expression were small they were larger than the standard errors within the experiments and statistically significant. These data may suggest that the presence of the 400-600 bp region is involved in mediating the inverse growth rate control.

**a.**

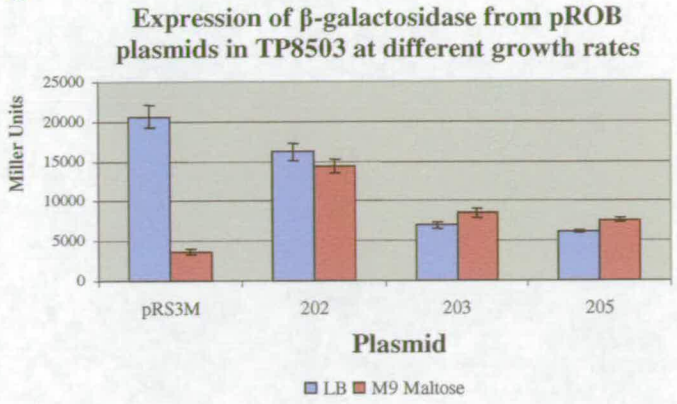


**b.**

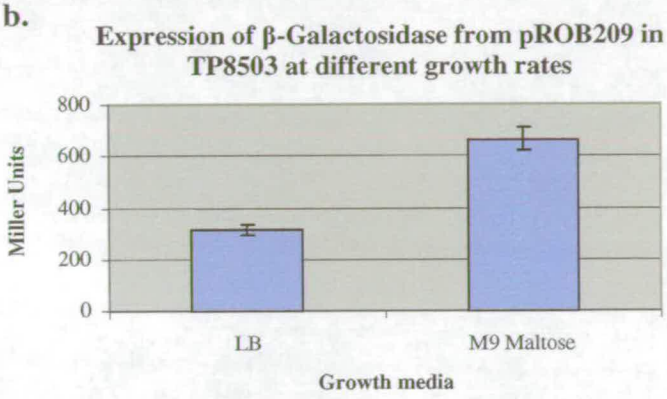


**Figure 3.5.1: Expression of β-galactosidase from the $P_{mra}$ promoters at two different growth rates.**

**a.** Histogram illustrating the changes in expression of β-galactosidase from pROB202 (400 bp fragment $P_{mra}1$ knock out), pROB203 (601 bp fragment $P_{mra}1$ knock out), pROB205 (601 bp fragment $P_{mra}3$ knock out) and pRS3M ($P_{mra}3$ promoter on 100 bp fragment) at two different growth rates.
**b.** Histogram illustrating the differences in β-galactosidase expression from pROB209, which carries -10 mutations in $P_{mra}1$ and $P_{mra}3$ in a 601 bp fragment of the intergenic region, in the TP8503 at different growth rates. Assays were performed on cells grown in LB at 37°C with a doubling time of ~24 minutes, or grown in M9 Maltose + CAA with a doubling time of ~30 minutes; at an $OD_{600}$ of 0.2. Results are averages of measurements on at least triplicate cultures, error bars of standard deviation are indicated.

The $P_{mra}3$ promoter region has a sequence arrangement similar to the *fis* and rRNA promoters, with a GC rich discriminator region and a poor match to the -35 consensus sequence. The regulation of these promoters has been well studied, and they are all positively regulated by growth rate (Cashel *et al.*, 1997; Nasser *et al.*, 2002). Positive regulation requires the presence of FIS which efficiently recruits RNAP, facilitates open complex formation and enhances promoter escape. As growth slows, the promoters are negatively regulated due to the reduction in FIS concentration and an increase in the induction of the transcriptional repressor ppGpp. (See section 3.6).

The response of the minimal $P_{mra}3$ promoter region to different growth rates was measured with the plasmid pRS3M. A 20-fold decrease in transcription from $P_{mra}3$ was observed at the slower growth rate (See Figure 3.5.1). These data suggest that $P_{mra}3$ is positively regulated by growth rate, however the medium may be influencing these results. The cells were grown in M9 Maltose + CAA as these conditions have been shown to be sufficient to slow cell growth and therefore alter cell size. However, Maltose is the sole carbon source in this medium which results in the upregulation of cAMP and CRP. When both CRP and FIS are present in the cell, as they would be under these assay conditions, it results in the negative autoregulation of FIS expression. Therefore FIS may also play a role in the regulation of growth rate control that could be altered in this growth medium.

The 20-fold decrease in expression from pRS3M in M9 Maltose suggests that the $P_{mra}3$ promoter region alone is able to respond to changes in growth rate. However, the expression from pROB202 and pROB203 does not significantly decrease at the slower growth rate, which may suggest that transcriptional regulators bind to the DNA of the *fru*R – *yab*B intergenic region and interact with $P_{mra}3$ making it less responsive to changes in growth rate. We have seen previously that $P_{mra}3$ appears to be highly repressed by factors presumed to interact with the DNA upstream (Section 3.3), and the data here may indicate an additional regulatory mechanism which would enable the cell to maintain inverse growth rate control over the *mra* region.

Figure 3.5.1.b shows the β-galactosidase activity from pROB209 grown in LB or M9 Maltose + CAA. A 2-fold increase in expression was observed at the slower growth rate when compared to growth in LB. This increase in expression is similar to the results from pROB209 measurements in a *fis* mutant where expression was increased 3-fold compared to the parental strain (Figure 3.4.3.2b). The potential alleviation of FIS mediated repression at $P_{mra}2$ could result when cultures are grown in M9 Maltose + CAA due to reduced levels of FIS. It is important to consider, however that $P_{mra}2$ may also be negatively regulated by growth rate.

These experiments suggest that when isolated, the $P_{mra}$ promoters respond independently to changes in growth rate. In particular, the minimal $P_{mra}3$ promoter is positively regulated by growth rate, however when present in the full 601 bp

intergenic region its response to slow growth changes. The expression from each $P_{mra}$ promoter was observed to increase (at varying levels) during slow growth, although this increase in expression was only slight at $P_{mra}1$ and $P_{mra}3$. The presence of the 400-600bp fragment of the intergenic region appeared to be important for inverse growth rate control of $P_{mra}3$, suggesting this may be the site for interactions with regulators which respond to growth rate.

## 3.6: Regulation of $P_{mra}3$ by ppGpp.

Guanosine 3′, 5′ - bispyrophosphate (ppGpp) has been implicated in the regulation of cell division, as demonstrated by filamentation in *rel*A *spo*T double mutants (Xiao *et al.*, 1991). Over-production of ppGpp results in inhibition of peptidoglycan polymerisation, mediated by the Penicillin Binding Proteins (PBPs) (Rodionov & Ishiguro, 1995). Most importantly, one of the more active promoters of the FtsQAZ operon, pQ1, which has inverse growth rate regulation is recognised by RpoS and activated by ppGpp (Navarro *et al.*, 1998). However, FtsZ concentration varies little upon elevation of ppGpp levels, due to the other 5 promoters of the FtsQAZ operon being unresponsive to ppGpp. This suggests that ppGpp is not a major transcriptional regulator of *fts*Z (Joseleau-Petit *et al.*, 1999).

### 3.6.1: The Effect of ppGpp on $P_{mra}3$ Activity.

$P_{mra}3$ contains a GC rich sequence which resembles previously described discriminator regions (Cashel *et al.*, 1997), suggesting that it may be negatively regulated by ppGpp. To determine if altered levels of ppGpp had an effect on transcription from $P_{mra}3$, *rel*A and *rel*A/*spo*T mutants of TP8503 were prepared by P1 transduction and transformed with the reporter plasmid pRS3M. A null mutation of *spo*T alone cannot be made as such strains are non-viable unless a mutation in *rel*A is also present; this is thought to be due to the cell accumulating toxic levels of ppGpp synthesised by RelA, but having no mechanism to reduce these levels (Xiao *et al.*,

1991). The genotypes and phenotypes of the TP8503 derivatives were confirmed by PCR analysis of the deletions and microscopy to confirm filamentation.

β-galactosidase activities were measured in the TP8503 derivatives containing pRS3M during exponential growth ($OD_{600}$ of 0.2) at 37°C in either LB or M9 Maltose + CAA (Figure 3.6.1). The slower growth achieved using M9 Maltose + CAA should be sufficient to induce production of ppGpp from SpoT, whose ppGpp synthesis activity is controlled by growth rate and carbon starvation (Rodionov & Ishiguro, 1995; Joseleau-Petit *et al.*, 1999). We hypothesise that if $P_{mra}3$ is negatively regulated by ppGpp we will observe a decrease in expression from wild type TP8503 when grown in M9 Maltose compared to LB. In the *rel*A strain (RE203) we would expect a lower level of ppGpp as the cell does not make its major ppGpp synthase, however the ppGpp synthetic activity of SpoT should be induced under these conditions. In the *rel*A/*spo*T derivative of TP8503 (RE205) we would expect no production of ppGpp, therefore if $P_{mra}3$ is negatively regulated by ppGpp we would observe an increase in β-galactosidase expression in M9 Maltose compared to LB.

An 80% decrease in β-galactosidase expression was measured from pRS3M in the parental strain TP8503 when grown in M9 Maltose compared to LB (Figure 3.6.1). This is similar to the pRS3M data presented in Figure 3.5.1a, where the decrease was attributed to $P_{mra}3$ being positively regulated by growth rate, when isolated in a 100bp fragment. It has been suggested that ppGpp is linked to growth rate control (Chatterji *et al.*, 2001), therefore the decrease in expression from pRS3M in M9 Maltose may be partially attributable to an increase in ppGpp in TP8503 under the experimental conditions.

A 10-fold increase in β-galactosidase expression was measured from pRS3M in RE203 (*rel*A::Km) upon growth in M9 Maltose when compared to expression from pRS3M in TP8503 under the same conditions, suggesting that $P_{mra}3$ is negatively regulated by ppGpp (Figure 3.6.1). These data imply that when RelA is absent, ppGpp

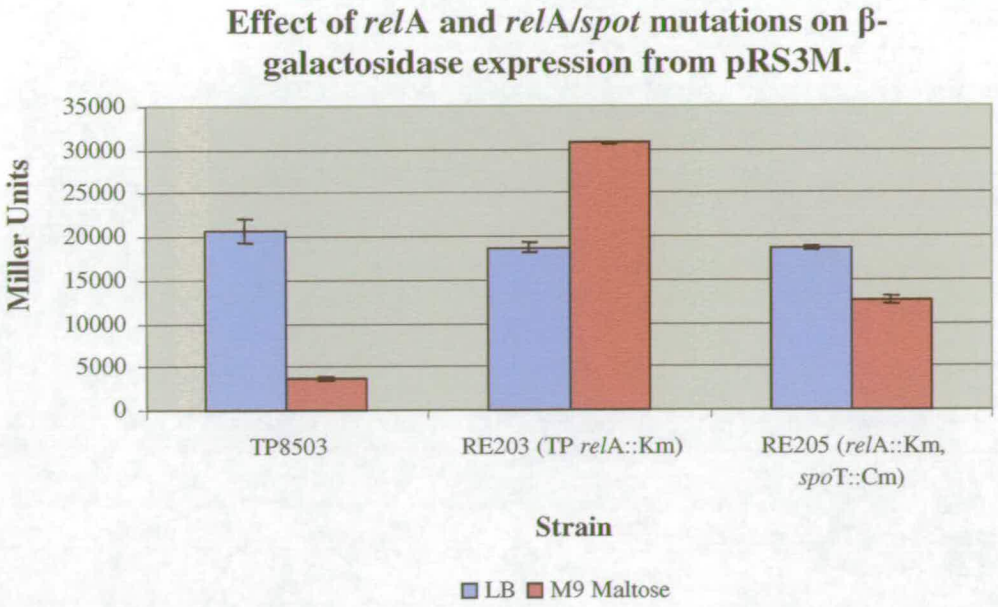


**Figure 3.6.1: The effect of *rel*A and *rel*A/*spo*T mutations on β-galactosidase expression from pRS3M.**

Histogram illustrating the differences in β-galactosidase expression from pRS3M in TP8503 and its derivatives RE203 (*rel*A::Km) and RE205 (*relA*::Km,*spoT*::Cm). Strains were grown at 37°C in LB or M9 Maltose + CAA. and β-galactosidase activity was measured during exponential growth. Results are averages of measurements from at least triplicate cultures, error bars of standard deviation are indicated.

levels are lower allowing increased expression from $P_{mra}3$. This would indicate that the basal levels of ppGpp synthesis from RelA and SpoT during exponential growth, which are thought to be 10-100 fold lower than during a stringent response (Barker *et al.*, 2001), result in a 10-fold reduction in transcription from $P_{mra}3$ during growth in LB. In addition, there was little difference in expression from pRS3M in TP8503 or RE203 grown in LB, suggesting that the basal level of repression of $P_{mra}3$ can be maintained solely by ppGpp synthesised by SpoT. However, it is unclear why in the absence of RelA, the basal expression of ppGpp is sufficient to repress $P_{mra}3$ in LB but not in M9 Maltose, suggesting that other growth rate or medium specific factors may be involved in this repression. The data suggest that production of ppGpp synthesis by SpoT may not be very efficient in M9 Maltose, or that if ppGpp synthesis is being induced it is at a low level not sufficient to compensate for the absence of RelA and to repress $P_{mra}3$ under these conditions.

The RE205 data shows a 30% decrease in expression upon growth in M9 Maltose when compared to LB. This strain should be completely devoid of ppGpp, and we

would therefore have expected expression in M9 Maltose to be at least as high as that observed for RE203. However, the expression in M9 Maltose is 4-fold higher than that observed for TP8503 confirming that expression from $P_{mra}3$ increases in the absence of ppGpp. Also we may have expected the expression in LB to increase since the basal levels of ppGpp, thought to repress $P_{mra}3$, would be absent. The decrease in expression observed in M9 Maltose compared to LB for RE205 is hard to explain and may suggests some medium-specific form of regulation.

RE205 exhibited filamentation when analysed by microscopy (data not shown) and grew slowly with a doubling time of 36 minutes in M9 Maltose, a generation time that was 7 minutes slower than TP8503 in the same conditions. It is possible that the slower growth of this strain could have reduced plasmid copy number, and therefore caused a decrease in β-galactosidase expression. However any changes in ppGpp levels in the cell are likely to have pleiotropic effects due to the many processes in which this alarmone is involved (Traxler *et al.*, 2006). An absence of ppGpp may, for example, alter the cells' ability to respond to changes in growth rate (Chatterji *et al.*, 2001), and we have previously described the growth rate regulation of $P_{mra}3$ (Section 3.5). The absence of ppGpp would also have a significant effect on DNA supercoiling, which can act as an additional form of transcriptional regulation. It has already been noted that $P_{mra}3$ has a sequence structure similar to the rRNA and *fis* promoters, and the data presented here suggests that $P_{mra}3$ may also be negatively regulated by ppGpp. These promoters are particularly sensitive to the level of DNA supercoiling, so it seems plausible that $P_{mra}3$ may be affected by changes in supercoiling due to the absence of ppGpp.

### 3.6.2: The Role of the GC-rich Discriminator region in regulation of $P_{mra}3$

To determine whether the potential response of $P_{mra}3$ to ppGpp could be reversed or abolished, an altered $P_{mra}3$ promoter (referred to as $P_{mra}3dis^-$) was made by site-directed mutagenesis of the GC rich discriminator region, with five of the GC nucleotides replaced with Adenines or Thymines (Figure 3.6.2a). The altered promoter region was cloned into pRS551 to create pROB201, and β-galactosidase activity was measured as previously described.

The β-galactosidase activity of $P_{mra}3dis^-$ was measured from pROB201 in TP8503 grown in LB. The alterations in the discriminator region had caused a 5-fold decrease in expression from $P_{mra}3dis^-$ when compared to $P_{mra}3$ in pRS3M (c.f. Figure 3.6.2b and Figure 3.6.1). This suggests that the sequence of the discriminator region is important for maintaining full activity of $P_{mra}3$. When pROB201 in TP8503 was grown in M9 Maltose there was a 2-fold increase in expression compared to growth in LB. This indicates that changes in the discriminator region have altered the response of $P_{mra}3$ to differences in growth rate. Wild type $P_{mra}3$ in pRS3M exhibited positive growth rate control, whereas pROB201 showed negative growth rate control.

**a.**

| | |
|---|---|
| Wild Type $P_{mra}3$ | **ATATGTCCTAAAATGCCGCTCG** |
| $P_{mra}3$ Discriminator mutant ($P_{mra}3dis^-$) | **ATATGTCCTAAAATAATTTTCG** |

**b.**

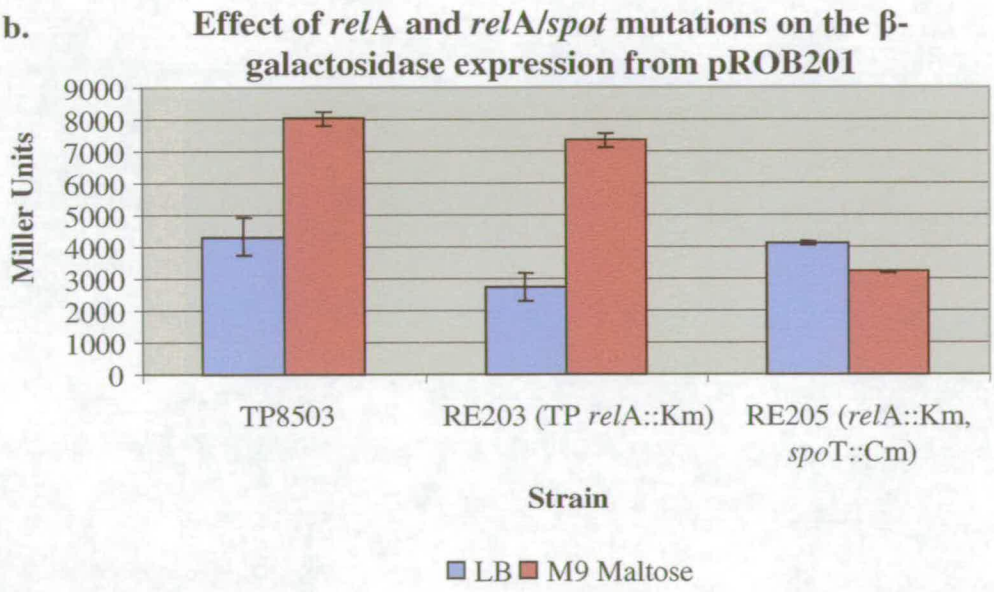


**Figure 3.6.2: The effect of *relA* and *relA/spo*T mutations on transcription from $P_{mra}3dis^-$.**

**a)** Mutations introduced into the discriminator region of $P_{mra}3$ by site-directed mutagenesis. The -10 region is highlighted red, the discriminator region blue, and the transcription start site is green.

**b)** Histogram illustrating the change in β-galactosidase expression from a $P_{mra}3dis^-$ in TP8503 *relA/spoT* mutant strains grown at 37°C in LB or M9 Maltose + CAA. The slower growth rate achieved using M9 Maltose + CAA, should induce ppGpp synthesis from SpoT in addition to basal expression from RelA. Results are averages of measurements from at least triplicate, error bars of standard deviation are indicated.

When β-galactosidase activity of $P_{mra}3dis^-$ from pROB201 was measured in RE203, a 2.5-fold increase in expression was observed in M9 Maltose compared to LB. If the alterations in the $P_{mra}3$ discriminator region had changed this promoter to be positively regulated by ppGpp, then we would expect less β-galactosidase activity from $P_{mra}3dis^-$ during growth in M9 Maltose in RE203 compared to TP8503. pROB201 in both TP8503 and RE203 however, showed comparable levels of expression in M9 Maltose, suggesting that an altered discriminator region makes $P_{mra}3$ unresponsive to ppGpp (Figure 3.6.2b), and that differences in expression between growth in M9 Maltose and LB may be therefore attributable to other forms of growth rate control.

The β-galactosidase activity of $P_{mra}3dis^-$ from pROB201 in RE205 showed a 25% decrease upon growth in M9 Maltose compared to LB. This suggests that in the complete absence of ppGpp there is no activation of $P_{mra}3dis^-$ during growth in M9 Maltose. However, since the RE203 data suggest that $P_{mra}3dis^-$ is unresponsive to ppGpp, the reduced expression measured from RE205 in M9 Maltose may be due to the slower growth rate. These unusual results may be strain specific and possibly due to the indirect pleiotropic effects of a complete absence of ppGpp, similar to the effect described for pRS3M in RE205.

Together, these data have shown that the $P_{mra}3$ promoter appears to be negatively regulated by ppGpp, an effect mediated by the GC rich discriminator region. In addition, the response to ppGpp can be abolished by converting the GC rich discriminator region into an AT rich sequence. In the *rel*A *spo*T double mutant there should be no ppGpp in the cell, and this phenotypic effect may contribute to altered transcription from $P_{mra}3$, and a reduction in its ability to respond to changes in growth rate. These factors may be responsible for the characteristic filamentation of the *rel*A *spo*T double mutants suggesting a role for ppGpp in the regulation of cell division.

### 3.6.3: A role for DksA in the regulation of the $P_{mra}$ promoters?

DksA is an important accessory factor involved in stabilising ppGpp interactions with RNAP (Perederina *et al.*, 2004). In the absence of DksA, ppGpp mediated regulation is reduced (Paul *et al.*, 2004). *dks*A mutants have also been observed to filament in

M9 minimal medium (M. Masters, unpublished results) suggesting a role for DksA in cell division. In order to determine whether regulation of $P_{mra}3$ by ppGpp affected the total transcription of the *mra* region from the $P_{mra}$ promoters, a *dks*A::tet mutation was introduced into EDCM647 by P1 transduction to generate strain RE302. β-galactosidase activity was measured from samples of RE302 during batch culture at 37 °C. It has been demonstrated that $P_{mra}3$ is negatively regulated by ppGpp, therefore in the *dks*A mutant it may be expected that transcription levels from $P_{mra}3$ would increase compared to the control strain.

The growth curves of EDCM647 and its derivative RE302 show that the *dks*A::tet mutation caused a 10% decrease in the growth rate. Doubling times during exponential phase growth were 31 and 34 minutes respectively (Figure 3.6.3a). The transcription levels from the $P_{mra}$ promoters, as measured by β-galactosidase activity, were also different between the two strains (Figure 3.6.3b). RE302 exhibited 40% less expression than EDCM647 on exit from stationary phase followed by a 50% decrease in expression at 60 minutes, before maintaining a basal level of around 100 Miller Units throughout exponential growth. Between 240-300 minutes, as the culture approached stationary phase, there was a 75% increase in β-galactosidase expression. The EDCM647 results are similar to those observed previously, (Section 3.2) with a 2-fold decrease in β-galactosidase activity on exit from stationary phase (0-120 minutes) to a basal level of around 100 Miller Units during balanced growth (120-240 minutes) followed by a 2-fold increase in activity as stationary phase is approached (240-300 minutes). During exponential growth, under these conditions, ppGpp would not normally be expected to play a significant regulatory role, therefore similar levels of expression would be expected from both strains at this time. However the 40% lower expression observed in RE302, compared to EDCM647, on exit from stationary phase is not what we would predict from the interpretation of the ppGpp data experiments. These data may suggest that DksA plays an indirect role in the growth rate regulation of $P_{mra}3$. This would be in agreement with the RE205 data from Section 3.6.2, which suggested that in the absence of ppGpp $P_{mra}3$ was less able to respond to differences in growth rate. However, it is important to consider that here we were measuring activity from all three $P_{mra}$ promoters, not just $P_{mra}3$, and therefore the absence of DksA may also alter activity from $P_{mra}2$ and $P_{mra}1$.

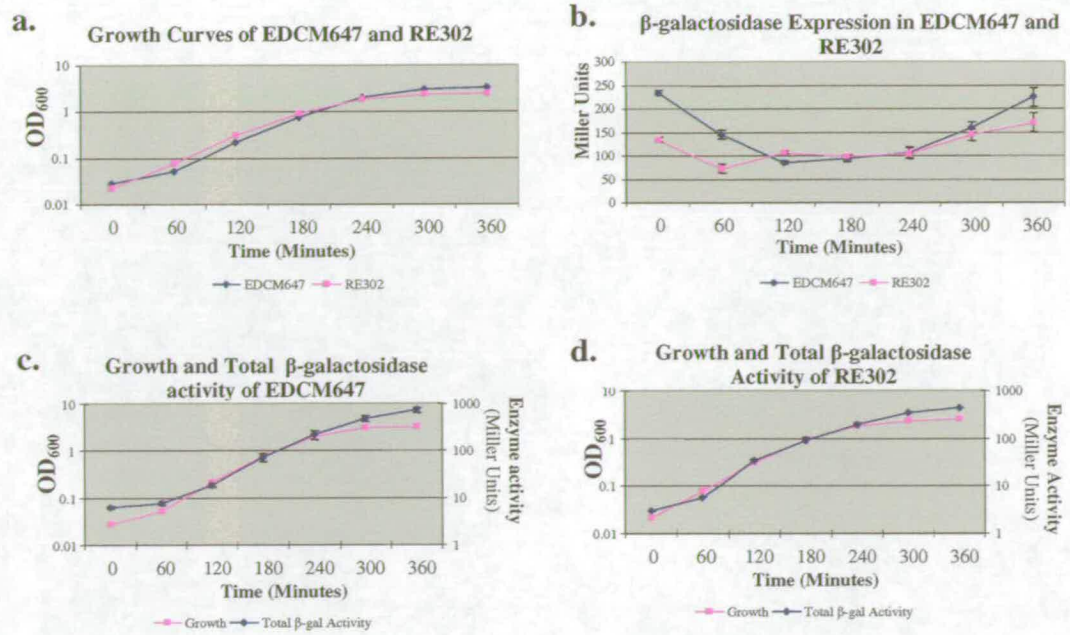


**Figure 3.6.3: Growth, β-galactosidase expression and total β-galactosidase activity of EDCM647 & RE302 during batch culture..**

**a**. Comparison of growth curves between EDCM647 and RE302 grown at 37°C in LB. The strains grew with exponential phase doubling times of 31 and 34 minutes respectively, indicating that the *dksA*::tet mutation in RE302 has a measurable effect on the growth rate of this strain compared to EDCM647.

**b**. Comparison of β-galactosidase expression between EDCM647 and RE302, assays were performed from triplicate cultures with error bars shown. Results for RE302 show that there is less β-galactosidase activity compared to EDCM647 on exit from and entry into stationary phase.

**c & d**. Total β-galactosidase Activities for EDCM647 and RE302. RE302 exhibits a slight lag in Total β-galactosidase Activity during lag phase before exponential growth, but a steady level of expression similar to EDCM647 during balanced growth. Results shown are averages of measurements from triplicate cultures, error bars of standard deviation are shown.

In wild type cells during stationary phase, the expression of $\sigma^{70}$ is not reduced, however alternate σ factors are able to compete more efficiently for binding to RNAP. This is thought to be due to a ppGpp induced conformational change within the core enzyme (Chatterji *et al.*, 2001). In contrast, when DksA is absent, alternate σ factors will be able to compete less well for RNAP during stationary phase, and proteins usually only expressed during balanced growth may continue to be produced. This may suggest that the inverse growth rate regulation of the $P_{mra}$ promoters is mediated by repressors expressed during exponential growth – which may be constitutively produced in the absence of DksA during stationary phase. If this was the case then the repressors may also be negatively regulated by ppGpp under wild type conditions. Alternatively, stationary phase expressed activators may mediate the growth rate regulation; the levels of these activators would be reduced in the *dks*A mutant strain.

Although DksA is involved in numerous cellular functions, its absence has a minor effect on cell growth and transcription from the $P_{mra}$ promoters during exponential phase. However, expression from the $P_{mra}$ promoters is reduced on the approach to stationary phase in RE302 suggesting that DksA, presumably in conjunction with ppGpp, may be indirectly involved in the inverse growth-rate regulation of the $P_{mra}$ promoters.

## 3.7: Determination of Transcript Length from the $P_{mra}$ promoters.

In order to assign a role to each of the $P_{mra}$ promoters it was important to determine both the number of transcripts and the length of transcripts originating from each promoter. Although β-galactosidase activity provided a guide to promoter activity, it would be more useful to directly identify the frequency and lengths of transcripts being produced.

### 3.7.1: Determination of Transcript Length by Primer Extension

RNA transcripts were produced and purified from the *in vitro* transcription vector pSP73-600 (Section 2.8.6), then used in primer extension reactions with radio-labelled pSP73REV primer. The reactions were resolved by electrophoresis on a 6% denaturing acrylamide gel. After repeated attempts, no successful primer extensions were achieved most likely due to the loss of RNA during the purification steps. Primer extension reactions using the radiolabelled primer yabBPE1 were subsequently attempted on total cellular RNA from MG1655 and MM38 (ΔRNaseE). These reactions were also unsuccessful; in this case it was thought to be due to poor annealing of the primer to the transcript as a result of RNA secondary structure, and also due to low concentration of the transcripts. In order to increase the overall concentration of *mra* transcripts, the multi-copy plasmids pROB202 (400 bp $P_{mra}1$ -10 mut), pROB204 (400 bp $P_{mra}3$ -10 mut) and pROB210 (601 bp, all $P_{mra}$ promoters) were used to transform MG1655 and total RNA from the cells was extracted. In an attempt to overcome poor primer annealing, Pmra Bam was radio-labelled with $^{32}P$, as

this primer had repeatedly been shown to anneal to the *yab*B region and result in successful PCR reactions. However, again the reactions were unsuccessful, which led to the conclusion that there may be significant RNA secondary structure within the *yab*B region. This could potentially play a role in transcriptional regulation of the $P_{mra}$ promoters.

### 3.7.2: Determination of Transcript Frequency by *in vitro* Transcription

The *in vitro* transcription vector pSR600 (Section 2.8.6), containing the *fru*R-*yab*B intergenic region was used in single round *in vitro* transcription reactions using the radioactive nucleotide $^{32}$P-rUTP in the polymerisation mix, this overcomes the need for a primer extension step as the transcripts themselves become radiolabelled upon incorporation of $^{32}$P. Very faint bands were produced and because the transcripts from the three promoters are different lengths, the incorporation of radioactivity for each was different, therefore the bands could not be compared to determine the relative number of transcripts from each promoter. To increase the yield of transcripts, run-off *in vitro* transcription was performed. The primer Pmra Bam was radiolabelled with $^{32}$P and used in primer extensions of the mRNA transcripts. Although some bands could be visualised following resolution by electrophoresis on a 6% denaturing acrylamide gel and detection on radiography film, the results were still very faint and consistent results were not achieved.

### 3.7.3: Determination of Transcript Length by Northern Blot.

Total cellular RNA from cells carrying pROB210 was resolved by denaturing agarose gel electrophoresis then transferred to membrane by capillary blot. A probe was prepared by PCR of the constitutively expressed enolase gene *eno*; the PCR was 5'-end labelled with $^{32}$P, then heat-denatured and hybridised to the membrane. Following optimised hybridisation, only a weak signal was detected amidst significant non-specific binding of the probe. A radiolabelled probe to detect *yab*B transcripts was subsequently prepared and used to probe the membrane. No obvious hybridisation of the *yab*B probe was observed suggesting that the RNA may have degraded or that the probe could not hybridise due to RNA secondary structure within these transcripts.

Northern blots using total cellular RNA from cells carrying pROB210 were subsequently performed using fluorescently DIG-labelled probes (Section 2.8.8). RNA Probes were made which would anneal to *fts*I or *fts*Z transcripts, it was hoped that by detecting transcripts further downstream from *yab*B that the RNA secondary structure present in this region would not affect annealing of the probe. *ftsI* and *fts*Z probes were prepared to determine whether both would anneal to the same transcript. RNA was resolved by electrophoresis through a denaturing formaldehyde gel. The gel was transferred to membrane and hybridised to fluorescently labelled probe. Again, no obvious hybridisation of probe and transcript was observed indicating that the transcripts of the *mra* region may be particularly sensitive to degradation.

### 3.7.4: Determination of Transcript Length by RT-PCR

Reverse Transcription PCRs (RT-PCRs) were utilised to confirm that transcripts originating from the $P_{mra}$ promoters extend into the *mra* region. Many commercially available reverse transcriptases are only proficient at extending cDNAs up to 2-3 kb in length. Therefore, although long range DNA polymerases can be used in PCR reactions to amplify the entire 17 kb $P_{mra}$-*fts*Z region (Figure 3.7.4.1a and Figure 3.7.4.1b, Lane 2), it is not possible to reverse transcribe a potential mRNA of the same length. However long-range RT-PCRs were attempted using the primer Z2 REV and the Qiagen Omniscript and Sensiscript Reverse Transcriptases (Section 2.8.4). This was followed by cDNA amplification using the primers PMRA Eco & Z2 REV and the long range DNA polymerase LA Taq™ in a PCR with an extension time of 18 minutes per cycle (Figure 3.7.4.1b, Lane 5).

A series of RT-PCRs were performed using total cellular RNA from MG1655 (growing in exponential phase), to determine the maximum length of transcript from the $P_{mra}$ promoters that could be detected. The RT-PCRs were performed using forward primers which annealed to the *fru*R-*yab*B intergenic region and reverse primers which annealed to sequences within the genes of the *mra* region (Figure 3.7.4.2a).

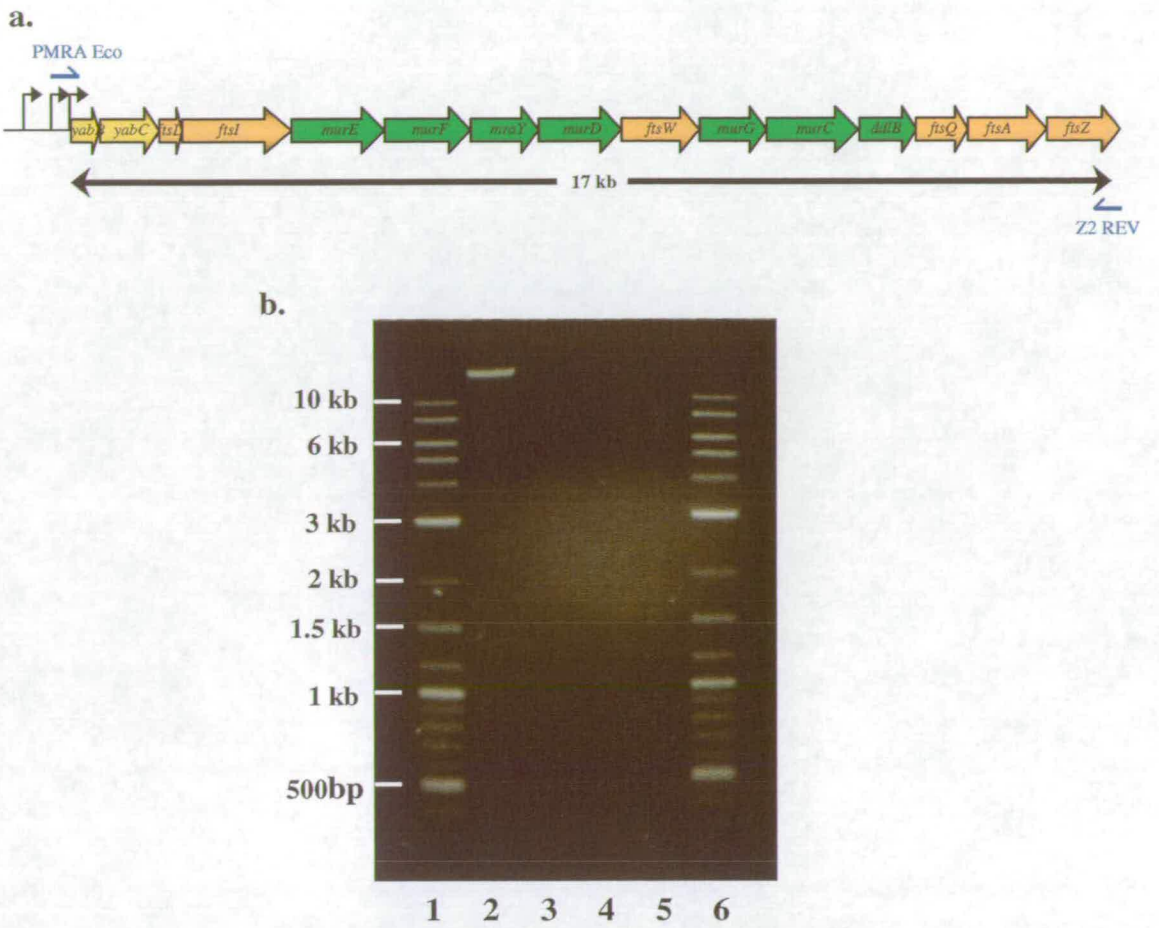


**Figure 3.7.4.1: PCR and RT-PCR spanning $P_{mra}$1-*ftsZ*.**
**a.** Illustration of the region amplified by the $P_{mra}$1-*ftsZ* PCR.
**b. Lane 1 & 6:** DNA size ladder; **Lane 2:** $P_{mra}$1-FtsZ PCR (DNA template); **Lane 3:** $P_{mra}$1-FtsZ PCR control (No template); **Lane 4:** $P_{mra}$1-FtsZ PCR (RNA template); **Lane 5:** $P_{mra}$1-FtsZ RT-PCR. Photograph of a 0.8% agarose gel, with PCR and RT-PCR products electrophoresed for 2 hours and stained with ethidium bromide. Only the PCR using MG1655 chromosomal DNA produced a successful 17kb product (lane 2).

RT-PCR products corresponding to transcripts originating from all possible $P_{mra}$ promoters were detected using primers PyabBEco and PftslBam. The presence of a 1460 bp band in Figure 3.7.4.2b, Lane 4, indicates that transcription originating from the $P_{mra}$ promoters enters the *mra* region and transcribes genes at least as far as *fts*L.

Primers Pmra100FOR and PftsLBam were used in reactions to detect transcripts originating upstream of $P_{mra}$1 (See Figure 3.7.4.2b, Lane 5). Since $P_{mra}$2 has been shown to be a weak promoter, we can assume that most of these transcripts therefore originate from $P_{mra}$3. As a result these data suggest that transcripts originating from $P_{mra}$3 can also span as far as *fts*L. RT-PCR products to detect transcripts originating

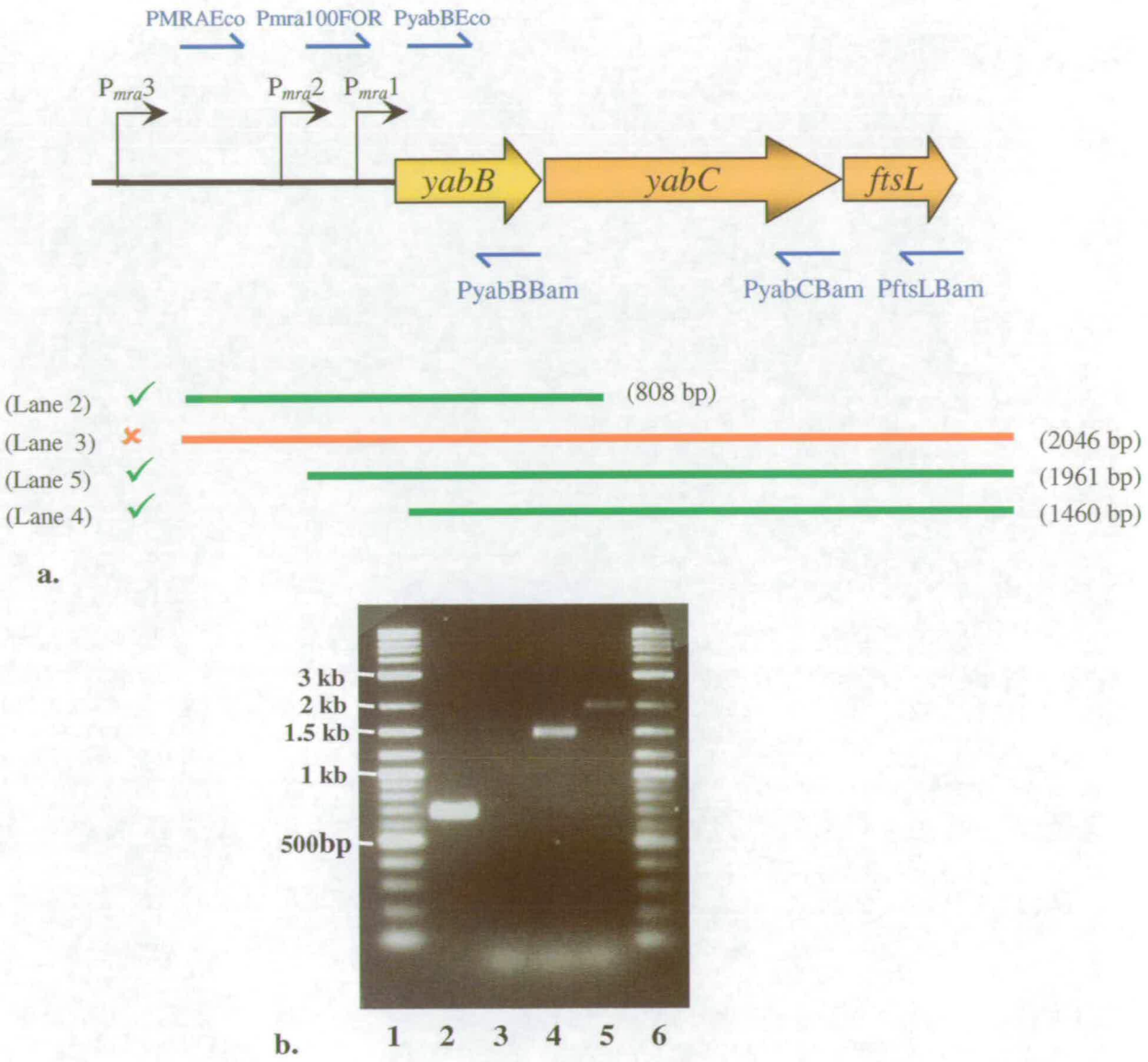


**Figure 3.7.4.2: Maximum transcript lengths detectable by RT-PCR from the $P_{mra}$ promoters.**

**a.** Illustration of the position of primers used in RT-PCRs, the lengths of the amplified transcripts, and whether RT-PCR amplification was successful. Transcripts originating from $P_{mra}3$ were shown to span as far as the distal end of *yabC*. Transcripts spanning $P_{mra}3$-*fts*L could not be amplified, suggesting that the RT-PCR reaction conditions only allow the amplification of ≤ 2Kb. Transcripts originating from $P_{mra}1$ and upstream were shown to extend at least as far as *fts*L, as were transcripts originating from $P_{mra}2$ and upstream.

**b.** Photograph of 1% agarose gel, with RT-PCR products electrophoresed for 100 minutes, and stained with ethidium bromide.

**Lane 1:** 2-log ladder; **Lane 2:** PMRAEco-yabBBam; **Lane 3:** PMRAEco-P*fts*LBam; **Lane 4:** P*yab*BEco-P*fts*LBam; **Lane 5:** Pmra100FOR-P*fts*LBam; **Lane 6:** 2-log ladder.

solely from $P_{mra}3$ were generated as far as *yab*B (Figure 3.7.4.2b, Lane 2) and no products were produced from a reaction to detect $P_{mra}3$ transcripts spanning to *fts*L

(Figure 3.7.4.2b, Lane 3). This does not necessarily indicate an absence of these transcripts, but probably represents the limitations of using this form of reaction (or the limitations of the primers).

It can be seen from Figure 3.7.4.2b that longer regions of amplification result in less RT-PCR product, this may be due to poor annealing or incompatibility of primer pairs. However, in the case of PMRAEco and P*fts*LBam, both primers had successfully been used in separate RT-PCR reactions (Figure 3.7.4.2b, Lanes 2 and 4), and were seen to be compatible when used in a PCR with DNA as a template (data not shown). These results may indicate that the 2046 bp RT-PCR product between PMRAEco and P*fts*LBam is beyond the upper limit of amplification of the RT-PCR reaction. This is most likely due to the processivity limitations of the Reverse Transcriptase. Although the Omniscript and Sensiscript Reverse Transcriptases used in the RT-PCR assays are reported to be capable of synthesising in excess of 3 kb, they appear to only be sensitive enough to copy 2 kb of transcript originating from the $P_{mra}$ promoters. RNA secondary structure thought to be present in the *yab*B region may slow the processivity of the Reverse Transcriptases and reduce the optimum amplification length of the RT-PCR.

Hara *et al.*, (1997) state that $P_{mra}1$ is responsible for transcription at least as far as *fts*W and is important for the expression of downstream genes, however, a transcript spanning the $P_{mra}$-*fts*W region has not been reported. Again, the length of this transcript makes RT-PCR difficult although it was attempted. RT-PCRs were performed as described previously, using the primer FtsWivREV for the reverse transcription and PCR amplification using PMRA Eco & FtsWivREV with an extension time of 10 minutes per cycle. No $P_{mra}$-*fts*W transcript was detected using RT-PCR, however this is most likely due to the limitations of the reaction rather than an absence of the template RNA (data not shown).

If we assume that the genetic data are correct and that transcripts from $P_{mra}1$ span from the intergenic region to *fts*W, it raises the question, where does *mur*G transcription orginate from? If $P_{mra}1$ derived transcription terminates at *fts*W, then there must be a promoter for *mur*G within *fts*W. This would also mean that the two genes would reside on separate transcripts and would not be detected by an RT-PCR

using a forward primer in *fts*W and a reverse primer in *mur*G. No transcriptional terminators have been reported within *fts*W and $P_{mra}1$ has been shown to contribute to the transcription of downstream genes (Mengin-Lecreulx *et al.*, 1998; de la Fuente *et al.*, 2001). Some transcripts should therefore span *fts*W-*mur*G. To determine if *fts*W and *mur*G are co-transcribed therefore could be detected on the same transcript, RT-PCRs were performed using MG1655 total cellular RNA with primers ftsWivFOR and murGivREV.

Figure 3.7.4.3 shows that *fts*W and *mur*G are co-transcribed, however, this does not imply that the transcript originates solely from the $P_{mra}$ promoters. Expression of MurG is not dependent on transcription originating from $P_{mra}1$ (Hara *et al.*, 1997), which suggests that additional promoters may exist upstream of *mur*G. Transcription from such hypothetical promoters may be at a low level, sufficient for transcription of *mur*G, but not enough to transcribe *fts*W in the absence of $P_{mra}1$.

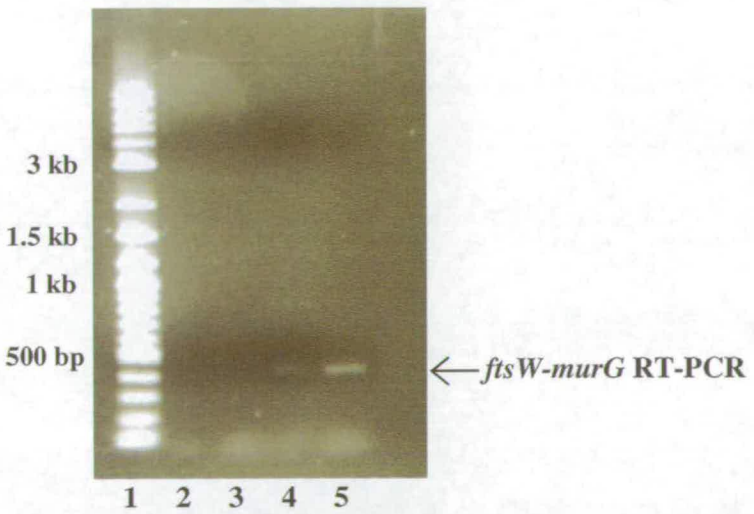


**Figure 3.7.4.3: Detection of transcript spanning *ftsW-murG* using RT-PCR.**
**Lane 1:** 2-log ladder; **Lane 2:** Control PCR (No template); **Lane 3:** Control PCR (RNA template); **Lane 4:** RT-PCR (1µg RNA template); **Lane 5:** RT-PCR (2µg RNA template).
Photograph of 1% agarose gel, with RT-PCR products electrophoresed for 100 minutes, and stained with ethidium bromide.

### 3.7.5: Detection of Additional Promoters in the *fruR-yabB* intergenic region.

In order to confirm the presence of transcripts from each of the $P_{mra}$ promoters and to determine whether there were any additional promoters within the *fru*R-*yab*B

intergenic region, a set of RT-PCR experiments were performed using the reverse primer YabBREV2, in conjunction with a series of forward primers which anneal within the intergenic region (Figure 3.7.5.1). The amplified transcripts varied by only 600 bp and none exceeded 1200 bp in length; therefore the assays would not be severely affected by the limitations of the Reverse Transcriptases.

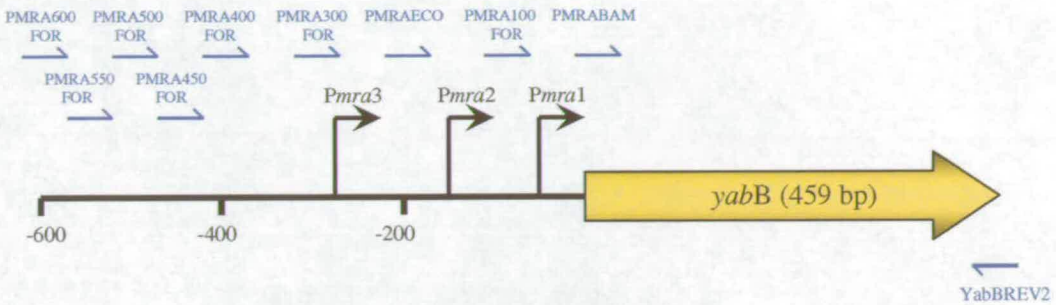


**a.**

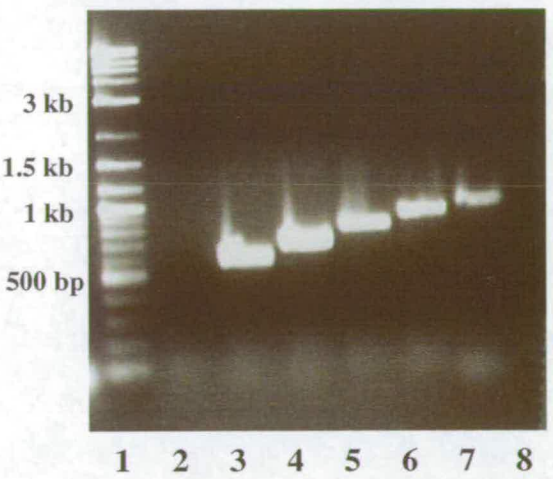


**b.**

**Figure 3.7.5.1.: RT-PCRs to determine which of the $P_{mra}$ promoters contribute to transcription of the *mra* region.**

**a.** Illustration of the positions of primers used in the RT-PCRs.

**b.** Photograph of a 1% agarose gel, with RT-PCR products electrophoresed for 100 minutes, and stained with ethidium bromide.

**Lane 1:** 2-log ladder; **Lane 2:** PmraBam-yabBREV2; **Lane 3:** PMRA100FOR-yabBREV2; **Lane 4:** PMRAEco-yabBREV2; **Lane 5:** PMRA300FOR-yabBREV2; **Lane 6:** PMRA400FOR-yabBREV2; **Lane 7:** PMRA450FOR-yabBREV2; **Lane 8:** PMRA500FOR-yabBREV2.

The RT-PCR between PMRA Bam-yabBREV2 was unsuccessful (Figure 3.7.5.1, Lane 2), probably due to incompatibility of the primers. Lanes 3 and 4 which represent RT-PCRs, using forward primers Pmra100FOR and PmraEco, show bands of 600-700 bps confirming the presence of transcripts originating from upstream of $P_{mra}1$ and $P_{mra}2$. Interestingly an RT-PCR product was detected in the reactions using

the forward primers PMRA300FOR, PMRA400FOR and PMRA450FOR; these primers anneal upstream of $P_{mra}3$. Transcript amplification was not achieved in RT-PCRs using primers which annealed 500 bp or more, upstream of *yab*B. These results indicate the presence of an additional promoter, located 450-500 bp upstream of *yab*B, which contributes to the transcription of the *mra* region.

Although the use of RT-PCRs can be limiting due to the lengths of transcript which they can detect, the RT-PCR experiments performed in this work have shown

1. That the $P_{mra}$ promoters transcribe the early genes of the *mra* region.
2. That *fts*W and *murG* are co-transcribed on the same transcript
3. That an additional promoter of the *mra* region ($P_{mra}4$) is located 450-500 bp upstream of *yab*B.

## 3.8: Is $P_{mra}3$ Essential for Expression of the *mra* region and for Cell Viability?

This study has shown that $P_{mra}3$ contributes significantly to expression of the *mra* region. It is a strong promoter but in most circumstances appears to be highly repressed. To determine whether the contribution of $P_{mra}3$ to transcription of the *mra* region is essential for cell viability we attempted to construct a chromosomal deletion of $P_{mra}3$. Initially a series of chromosomal deletions of each of the $P_{mra}$ promoters was attempted using the pKO3 based pTOF system (Merlin *et al.*, 2002). This system allows insertion of a reporter cassette (FLKP2) into the deleted region on the chromosome. If the deleted region is essential then the cells will be non-viable, however the mutant strains can be maintained by induction of $P_{lac}$ in the reporter cassette which will maintain transcription of downstream genes. After repeated attempts it was not possible to clone the necessary fragments into the pTOF vectors. As a result, an alternate method was followed to generate a chromosomal knock-out of $P_{mra}3$.

Two regions of DNA flanking $P_{mra}3$ were amplified by PCR, using the primers FruRFOREco with FruRREVBam, and PmraFOR1 with yabBREV2 (Figure 3.8.1a) .The amplified PCR products contained restriction sites for the cloning steps.

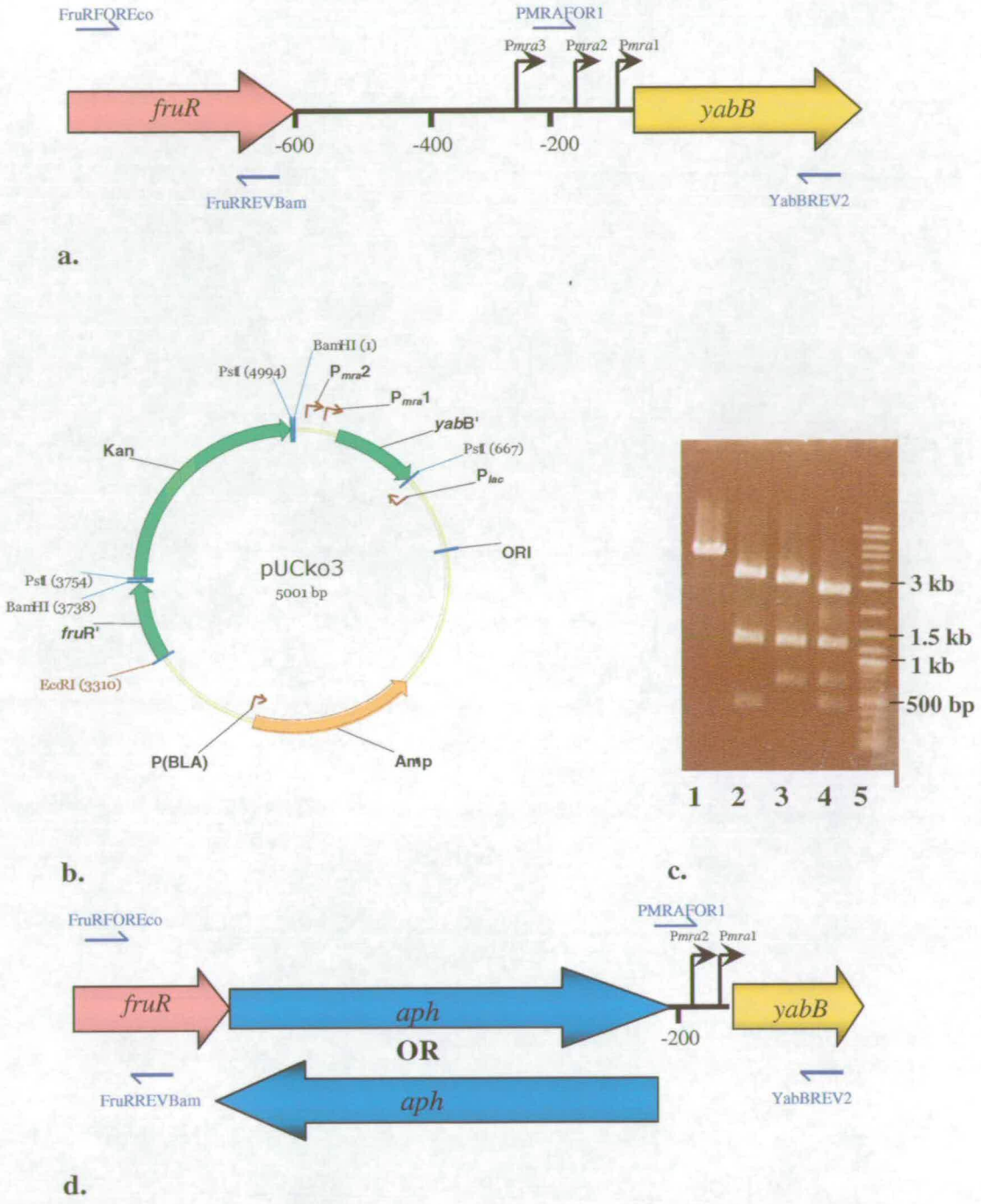


**Figure 3.8.1: Construction of the $P_{mra}3$ knockout vector pUCko3.**

**a.** Illustration of the position of the primers used to amplify DNA flanking $P_{mra}3$.

**b.** Illustration of the vector produced by cloning the DNA fragment which flanked $P_{mra}3$, into pUC19. The kanamycin resistance gene (*aph*) from pUC4K was cloned between the two PCR regions, to generate the $P_{mra}3$ knock-out vector, pUCko3. When this plasmid is transformed into a recombination proficient strain, homologous recombination between the chromosome and the regions of homology on the vector should occur. This will replace $P_{mra}3$ with *aph*.

**c.** Photograph of 1% agarose gel, with restriction digests of pUCko3 electrophoresed for 80 minutes, and stained with ethidium bromide.

**Lane 1:** pUCko3 + EcoRI; **Lane 2:** pUCko3 + EcoRI, BamHI; **Lane 3:** pUCko3 + BamHI, PstI; **Lane 4:** pUCko3 + EcoRI, PstI; **Lane 5:** DNA size ladder.

**d.** Illustration of the chromosome following P*mra*3 replacement with (*aph*), the kanamycin resistant gene which could be inserted in either orientation due to non-directional cloning.

The *fru*R fragment carried an EcoRI site at its 5′ end and BamHI at its 3′ end; while the *yab*B fragment (which also contained $P_{mra}1$ and $P_{mra}2$) had a BamHI site at the 5′ end and a PstI site at the 3′ end. The DNA fragments were digested and sequentially cloned into the multicopy plasmid pUC19 to generate the plasmid pFY.

A kanamycin resistance gene (*aph*) was digested with BamHI and inserted into pFY, between the *fru*R and *yab*B regions to generate the plasmid pUCko3 (Figure 3.8.1.b). Construction of the vector was checked by restriction digest (Figure 3.8.1.c).The knockout vector pUCko3 was introduced into MG1655 by transformation. A P1 lysate was prepared on MG1655 containing pUCko3 and transduction was then used to introduce $Km^R$ into untransformed MG1655. Two hundred colonies were patched onto kanamycin and kanamycin/ampicillin plates to screen for recombinants and detect any double cross-overs (which would be $Km^R$, $Amp^S$, see Figure 3.8.1.d), however, all colonies were $Km^R$, $Amp^R$. A second P1 lysate was prepared from a $Km^R$, $Amp^R$ colony and used for transduction of $Km^R$ into MG1655. 200 recombinants were again screened but no double recombinants were isolated. Two further rounds of transduction and screening failed to produce any $Km^R$, $Amp^S$ double recombinants. These results suggest that $P_{mra}3$ cannot be deleted from the chromosome and may therefore be essential for cell viability.

## 3.9: Summary

This work has identified a number of potential mechanisms of transcriptional regulation of the $P_{mra}$ promoters. These include inverse growth rate regulation, indirect effects of FIS, repression by unidentified regulators, and negative regulation by the cellular alarmone ppGpp. These complex and potentially overlapping mechanisms of regulation may allow the cell to fine-tune the expression of the major cell division locus. Since the genes of the *mra* region are constitutively expressed, we were not expecting to identify mechanisms of regulation at the $P_{mra}$ promoters that produced an "all or nothing" effect, which would effectively switch on or off the activity from the $P_{mra}$ promoters. Instead we had predicted that the promoters would be regulated in a more subtle manner and we have shown that the cell modulates

expression of the *mra* region in response to changes in growth rate, nutrient availability and cell stress.

We have presented evidence indicating that the $P_{mra}$ promoters are inversely regulated by growth rate. Using the reporter strain EDCM647 low expression levels were measured during lag phase and exponential growth compared to the approach to stationary phase. In addition, expression from the $P_{mra}$ promoters on reporter plasmids was also observed to be inversely related to growth rate, however only when all three promoters were active. Individually, the $P_{mra}$ promoters responded differently to changes in growth rate, with $P_{mra}3$ exhibiting positive growth rate control when present in a 100bp fragment of the *fru*R-*yab*B intergenic region. When present in the full intergenic region all $P_{mra}$ promoters exhibited some degree of inverse growth rate regulation, this may suggest that DNA upstream of the promoters is important for the inverse growth rate control and may contain binding sites for proteins that respond to growth rate. Little is known about how growth rate regulation is controlled in *E. coli*, however many proteins and regulatory factors exhibit oscillations in their expression during batch culture. For example, levels of both ppGpp and $\sigma^S$ increase on approach to stationary phase (Kvint *et al.*, 2000), while FIS levels peak upon nutrient upshift in exponential phase (Travers *et al.*, 2001). Changes in the levels of these important regulators may have a significant bearing on the growth rate control of the $P_{mra}$ promoters.

Using reporter strains, we have also shown that the pattern of β-galactosidase expression (as an indirect measure of transcription) in response to growth rate is different for *yab*B the first gene in the *mra* region compared to *fts*Z, the fifteenth gene in this cell division locus. The pattern of FtsI expression (encoded by *fts*I, the fourth gene in the *mra* region) compared to FtsZ was also very different suggesting that the entire *mra* region may not be co-transcribed as previously suggested (Mengin-Lecreulx *et al.*, 1998) and bringing into question the reports that $P_{mra}1$ may be responsible for up to 66% of *fts*Z transcription (Flärdh *et al.*, 1998).

We predicted, due to its abundance during early exponential phase, that FIS may play a role in the regulation of the $P_{mra}$ promoters, particularly during the growth transition from stationary phase into balanced growth. FIS had been shown to interact with the

*fru*R-*yab*B intergenic region and to bind within the promoter regions of both $P_{mra}2$ and $P_{mra}3$. FIS was observed to repress the already weak promoter $P_{mra}2$, but to have little effect on expression from $P_{mra}3$ despite the presence of a binding site between the -10 and -35 region. FIS was also shown to activate expression from $P_{mra}1$, however it is unclear which FIS binding site is responsible for this activation.

*Fis* mutants exhibited a filamentous phenotype upon continuous exponential growth, which indicated an effect on cell division. It was shown that in the absence of FIS, transcription of *fts*Z was altered in comparison to the control strain, and that FtsZ levels appeared to be 2-3-fold lower in the *fis* strain, which was particularly evident during exponential growth. The cell division defect in the *fis* mutants was only partially rescued by increasing the levels of FtsZ *in trans*, which suggested that reduced amounts of FtsZ were not responsible for the filamentation. Upon staining the nucleoids in the filamentous cells, large masses of mis-segregated DNA were observed. FIS is known to be involved in the regulation of DNA replication at *ori*C (Ryan *et al.*, 2004) and we suggest that the mis-segregated DNA may be a result of unregulated over-initiation of DNA replication. We cannot confirm that the mis-segregated DNA caused the filamentation of the cells, since it is also possible that the lack of septation would prevent segregation because of a failure to localise FtsK to the mid-cell (Draper *et al.*, 1998). FIS may also regulate other factors which may then cause the division defect. For example, little is known about potential transcriptional regulation by FIS at the 6 promoters of the *fts*QAZ genes. It is possible that FIS plays numerous roles in the regulation of cell division, but that this regulation is often likely to occur in an indirect manner. For example, through the regulation of DNA supercoiling (Travers *et al.*, 2001) or by the regulation of ribosomal RNA synthesis (Muskhelishvili *et al.*, 1997).

The potential regulation of the $P_{mra}$ promoters by other proteins was also investigated. However, no binding sites could be identified for CRP or IHF within the *fru*R-*yab*B intergenic region. In addition, experiments using *crp*, *ihf*, and *hns* mutants showed little change in expression from the $P_{mra}$ promoters, indicating that they are not directly regulated by these proteins. However, deletion of the intergenic region between 400-500bp upstream of *yab*B resulted in a 3-fold increase in expression from

$P_{mra}3$, indicating that this region may contain the binding site for an unidentified repressor.

$P_{mra}3$ has been shown to be a strong promoter that is highly repressed under most circumstances. It contains sequence similarity to the rRNA and *fis* promoters, which all contain a GC-rich discriminator region and are negatively regulated by ppGpp. We have shown that $P_{mra}3$ also appears to be negatively regulated by this cellular alarmone, and that this regulation can be abolished by altering the GC-rich discriminator region, although this also appears to affect the promoter's response to growth rate. The complex regulation of $P_{mra}3$ that we have begun to uncover suggests that it may make an important contribution to transcription of the *mra* region. This notion is reinforced by our inability to make a $P_{mra}3$ chromosomal knockout suggesting that it may be essential for cell viability.

It was not possible to establish the length of the transcripts originating from the $P_{mra}$ promoters, however we have shown that they span at least as far as *fts*L. We have also identified a transcript spanning *fts*W-*murG,* which may suggest that if *fts*W is solely transcribed from $P_{mra}1$, the transcripts from here span over 10kb to at least as far as *mur*G. However, we cannot confirm this and can only conclude that *fts*W and *mur*G are co-transcribed.

RT-PCR analysis uncovered the presence of an additional $P_{mra}$ promoter located upstream of $P_{mra}3$. $P_{mra}4$ contributes to transcription entering the *mra* region and it is possible that this promoter also contributes to some of the repression of $P_{mra}3$, perhaps by promoter occlusion – a mechanism that has been well documented at the tandemly arranged *rrnB* P1 and P2 promoters (Nasser *et al.*, 2002). However, only $P_{mra}3$ is repressed by the presence of the upstream intergenic region and promoter occlusion would be expected to reduce transcription from all downstream promoters, which was not observed.

The following chapter investigates further the possibility of additional regulators of the $P_{mra}$ promoters, in addition to a study into the presence of unidentified promoters located within the *mra* region itself.

# Chapter 4: Results - Additional Factors Involved in the Regulation of the *mra* region

## 4.1 Introduction

In chapter 3 we presented results which suggest that the $P_{mra}$ promoters were regulated by changes in growth rate, that $P_{mra}3$ was negatively regulated by ppGpp, and that $P_{mra}2$ was repressed by FIS while $P_{mra}1$ was activated in its presence. In addition we found that CRP, IHF and H-NS played no direct role in the regulation of the $P_{mra}$ promoters. However, the deletion of the 400-500 bp sequence in the *fru*R-*yab*B intergenic region caused a 3-fold increase in transcription from $P_{mra}3$ suggesting that a transcriptional repressor interacts with this region of DNA. A single protein:DNA complex was identified from a *fis*⁻ soluble protein lysate when incubated with the 200-400 bp fragment of the *fru*R-*yab*B intergenic region. This complex indicates that other proteins in addition to FIS can bind specifically to this region and may also be involved in the regulation of the $P_{mra}$ promoters. This chapter describes the methods used to screen, purify and identify these potential transcriptional regulators.

In addition, we have noted that there are no reported promoters between $P_{mra}1$ and *fts*Q2p, in the *mra* region (See Figure 1.1.1). However, if we are prepared to question the idea that $P_{mra}1$ is the major contributor to *fts*Z transcription (Flärdh *et al.*, 1998) then we must attempt to identify other potential sources of transcription initiation. Many authors have implicated the presence of additional promoters within the *mra* region. For example, Hara *et al* (1997) noted that promoter-like sequences exist immediately preceding both *fts*I and *fts*L. Boyle *et al* (1997) suggested that *mur*D and *fts*W are co-transcribed and that a potential promoter resides between the EcoRI and BglII restriction sites located in the junction between *mra*Y and *mur*D. Mengin-Lecreulx *et al* (1998) also proposed that a promoter for *mur*G exists somewhere between the EcoRV site in *mur*D and the SnaBI site within *fts*W. However, the position and activity of none of these potential promoters have been confirmed. This chapter includes an investigation into the presence of additional promoters of the *mra* region and measures the contribution that transcription from these promoters may make to the expression of cell division genes.

## 4.2: Identification of Transcriptional Regulators by Transposon Mutagenesis

A genetic screening approach was attempted to isolate repressor mutants of the $P_{mra}$ promoters. A $\lambda P_{mra}600$ MG1655Δ*lac* reporter strain was utilised in this screen. This strain was created using the method of Simons *et al*, (1987), by recombination between pROB210 and λ (following induction of the λ lysogen). The λ was then used to lysogenise MG1655 and was selected for by growth on kanamycin. $\lambda P_{mra}600$ MG1655Δ*lac* was streaked out on M9 Maltose + CAA + XGAL plates. Slow growth on maltose was previously seen to cause a decrease in transcription from $P_{mra}3$ which resulted in low levels of β-galactosidase expression (Section 3.5). In this experiment growth on M9 Maltose + CAA + XGAL plates produced colonies which were very pale blue in colour. This pale colony colour was essential for the next stage of the screen to allow identification of colonies with increased β-galactosidase expression. Transposon mutagenesis was used at this stage to disrupt potential genes encoding the putative repressor thought to bind between 400 and 500 bp of the *fru*R-*yab*B intergenic region, or indeed for any potential repressor of the $P_{mra}$ promoters.

A λ phage carrying mini-Tn10 with a chloramphenicol gene was used to infect $\lambda P_{mra}600$ MG1655Δ*lac* (Kleckner *et al.*, 1991). Infected cells were plated onto M9 + Maltose + CAA + XGAL + Chloramphenicol and incubated overnight at 37°C. Resultant colonies exhibited various levels of β-galactosidase expression as observed qualitatively as differing intensities of blue colour, with around 1 in every 500 being very intense dark blue. This colour suggested that an increase in expression was possibly due to the gene for a repressor of one of the $P_{mra}$ promoters being disrupted by the insertion of the mini Tn10. Colonies were streaked onto kanamycin to ensure the λ600 was still present before β-galactosidase activity was measured to quantify the levels of expression. In general it was found that dark blue colonies showed 3-4-fold higher expression than was measured from the $\lambda P_{mra}600$ MG1655Δ*lac* control cultures.

P1 transductions were used to transfer the insertion mutations back into the $\lambda P_{mra}600$ MG1655Δ*lac* background. The purpose of this was to confirm that increased

expression was due to an insertion into a gene of interest rather than other mutations with a strong effect. P1 lysates were made from the very dark blue colonies and used to infect the λ$P_{mra}$600 MG1655Δ*lac* strain. Following transduction from 30 mutants and measurements of β-galactosidase activity during exponential growth, none of the transductants gave increased enzyme activity compared to the parental strain. This suggested that only gene mutations were isolated rather than gene disruptions caused by insertion of the mini Tn10. A more direct approach to identifying transcriptional regulators was therefore attempted.

## 4.3 Purification and identification of a DNA-binding protein shown to interact with the intergenic region upstream of $P_{mra}3$

In Chapter 3, we saw how at least one protein:DNA complex was formed when a *fis*$^-$ soluble protein lysate was incubated with a radiolabelled 200-400 bp DNA from the *fru*R-*yab*B intergenic region in an EMSA reaction (Figure 3.4.3.1). In addition, it was noted that the absence of the 400-500 bp region of intergenic DNA resulted in a 3-fold increase in transcription from $P_{mra}3$, indicating that a repressor of $P_{mra}3$ may bind within this region. To identify any additional regulators of $P_{mra}3$, and to verify possible protein:DNA interactions in the 200-400 bp and 400-600 bp intergenic regions, further EMSA reactions were performed using soluble protein lysates from TP8503, RE201 (*fis*::Km) and RE202 (*fis*::Cm). The protein:DNA complexes were resolved on acrylamide gels by non-denaturing gel electrophoresis.

A lysate from the parental stain TP8503 produced a single protein:DNA complex when incubated with both the 200-400 bp and 400-600 bp fragments of DNA from the intergenic region (Figure 4.3.1). This complex was not present when *fis*$^-$ lysates were used in the EMSA reactions, indicating that the complex represents binding of FIS to the two regions of DNA. In the absence of FIS there is also enhanced binding of other proteins to the DNA fragments, this is illustrated by protein:DNA complexes 1 and 2. These interactions either represent DNA-binding by proteins which are usually repressed by FIS, or binding is occluded by FIS in a wild type cell. It should be noted

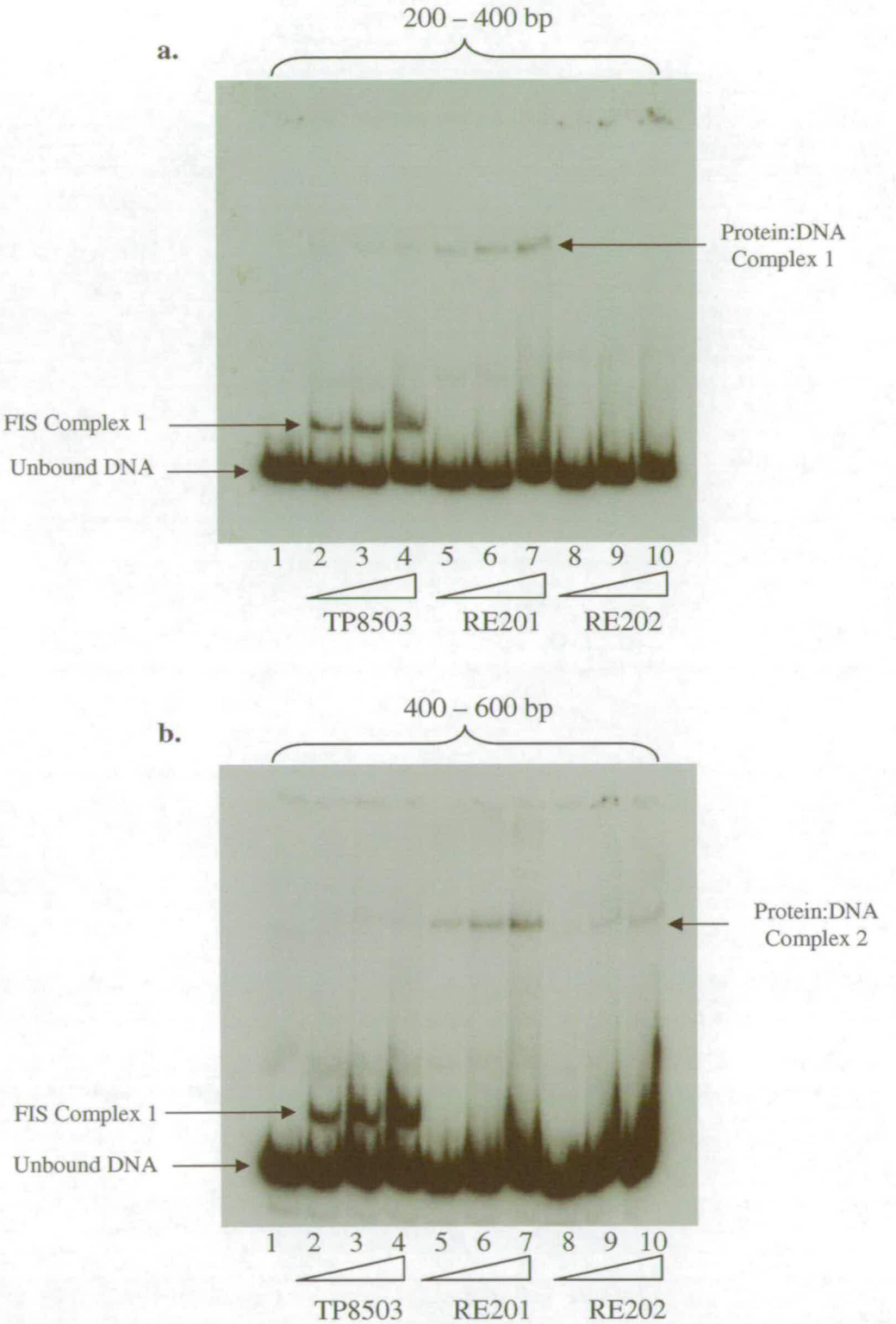


**Figure 4.3.1: Autoradiograph of binding reactions using TP8503, RE201 (*fis*::Km) and RE202 (*fis*::Cm) soluble protein lysates with *fru*R-*yab*B intergenic region DNA.**

**a.** EMSAs with the 200-400 bp intergenic region DNA.

**b.** EMSAs with the 400-600 bp intergenic region DNA.

**Lane 1:** No protein. **Lanes 2-4:** Increasing concentration of TP8503 soluble protein lysate. **Lanes 5-7:** Increasing RE201 (*fis*::Km) soluble protein lysate. **Lanes 8-10:** Increasing RE202 (*fis*::Cm) soluble protein lysate. All gels were electrophoresed at 4°C.

that the lysate for RE202 did not produce the same number of complexes compared to the lysate from RE201, although both strains contain mutations in *fis*. It appears most likely that protein has been lost from the RE202 lysate possibly by degradation as the Protein:DNA complexes observed with the RE201 lysate are barely detectable with the RE202 lysate. These data show however that additional proteins can be observed to interact with the *fru*R-*yab*B intergenic region, particularly in the absence of FIS.

To separate the DNA-binding proteins from the other soluble proteins in the lysate, affinity chromatography using FPLC was performed. A soluble protein lysate was prepared from a exponential phase culture of RE201 (*fis*::Km) in LB, which was then applied to a 5ml Heparin column attached to an FPLC. Heparin acts as a DNA mimic, therefore DNA-binding proteins should bind to the column, while all other proteins should be collected in the flow through. The DNA-binding proteins were eluted with a 0.1M-1M NaCl gradient. Two peaks in protein concentration were observed during the elution, between fractions C6 and C15 (Figure 4.3.2a). This corresponded to a NaCl concentration of approximately 300mM, indicating that this may be the optimum concentration for disruption of Protein:Heparin interactions. The eluted fractions were analysed by SDS-PAGE (Figure 4.3.2b), which showed that the separation was successful and that each fraction appeared to contain different proteins.

To determine which eluted fractions contained DNA-binding proteins capable of interacting with the *fru*R-*yab*B intergenic region, EMSAs were performed using radiolabelled 0-200 bp, 200-400 bp, and 400-600 bp fragments in the presence of each of the protein fractions, C6-C15. The 0-200 bp DNA fragment was slightly retarded in lanes 10 and 11 (Figure 4.3.3a), indicating that a protein in fractions C13 and C14 interacted specifically with this region of DNA. Since only a faint band shift was observed, this may either indicate that the protein is of low abundance in the cell, or that it has a low affinity for the DNA. Multiple protein:DNA complexes were detected formed with the 200-400 bp region of DNA (Figure 4.3.3.b), at least six different complexes were observed in lanes 5 and 12, however it appeared that most of the DNA-binding proteins capable of interacting with the intergenic region were present in the later fractions (C13-C14), since the most prominent band shifts were observed

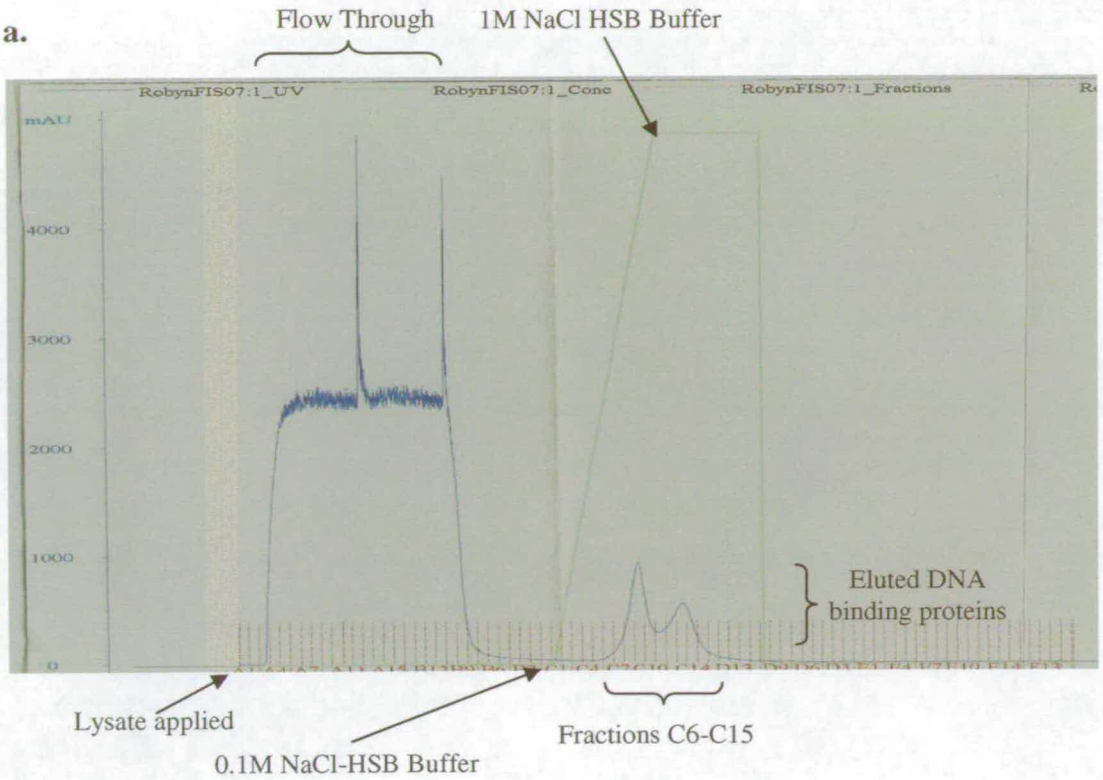


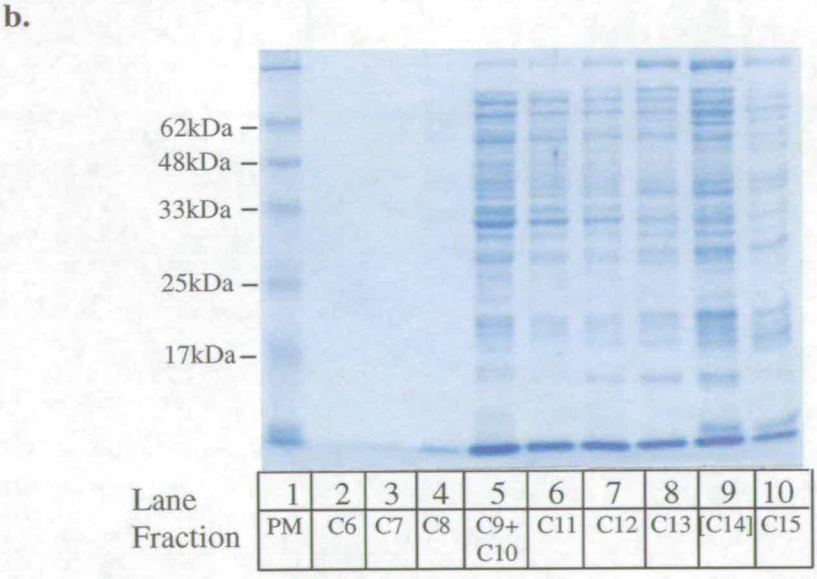


**Figure 4.3.2.: Fractionation of DNA-binding proteins from a RE201 (*fis*::Km) soluble protein lysate using FPLC.**

**a.** UV spectrophometric trace of eluted proteins from a RE201 soluble protein lysate using FPLC. A 5ml Heparin column was equilibrated with 0.1M NaCl-HSB Buffer. Filtered lysate was applied to the column; proteins unable to bind Heparin were lost in the flow through. A 5ml 0.1M-1M NaCl gradient at a flow rate of 1ml/min was used to elute proteins bound to the column. Proteins were collected in 0.5ml fractions. Two peaks in protein concentration were observed between fractions C6 and C15, at approximately 300mM NaCl.

**b.** SDS-PAGE of eluted protein fractions. Fractions C9 and C10 were pooled as they corresponded to the largest protein peak. Fraction C14 was concentrated as it was shown to produce the most significant binding in subsequent EMSA experiments.

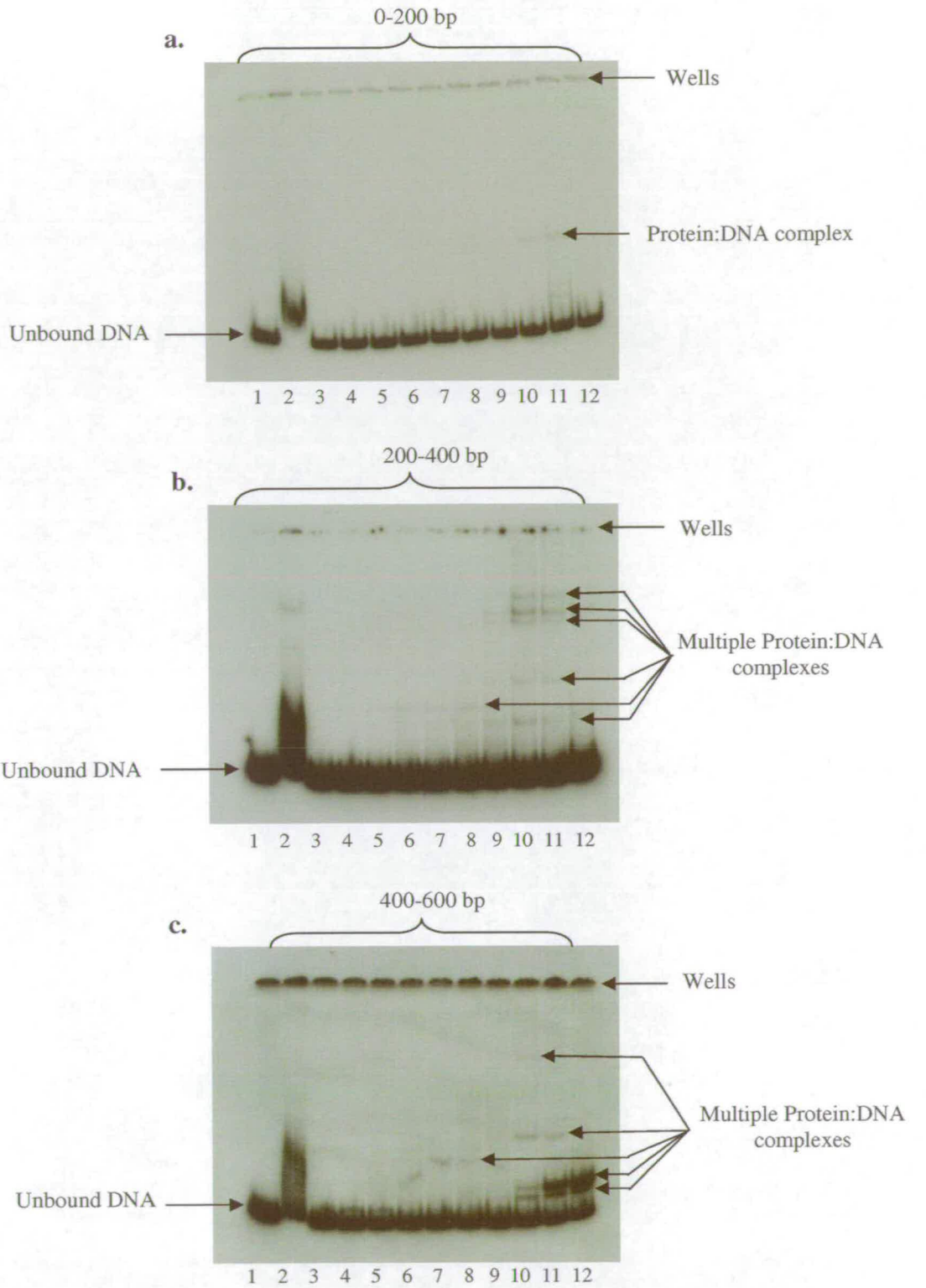


**Figure 4.3.3: Autoradiographs of interactions between DNA-binding proteins from a RE201 (*fis*::Km) lysate and fragments of the *fru*R-*yab*B intergenic region.**
**a.** Protein:DNA interactions between a fractionated RE201 lysate and the 0-200 bp intergenic region.
**b.** Protein:DNA interactions between a fractionated RE201 lysate and the 200-400 bp intergenic region.
**c.** Protein:DNA interactions between a fractionated RE201 lysate and the 400-600 bp intergenic region.
**Lane 1:** No protein; **Lane2:** Soluble protein lysate; **Lane 3:** C6; **Lane 4:** C7; **Lane5:** C8; **Lane 6:** C9; **Lane 7:** C10; **Lane 8:** C11; **Lane 9:** C12; **Lane 10:** C13; **Lane 11:** C14; **Lane 12:** C15.

in lanes 10 and 11 (Figure 4.3.3.b). The results from EMSAs using the 400-600 bp DNA produced the most interesting results (Figure 4.3.3c). Retardation of the DNA was observed across lanes 5-8 and 10-12, indicating multiple protein:DNA interactions with this region of DNA. In lanes 10-12, which represent fractions C13-15, approximately 50% of total DNA was present in two protein:DNA complexes.

These experiments demonstrate that the *fru*R-*yab*B intergenic region contains binding sites for numerous DNA-binding proteins that are present during exponential growth in a *fis*$^-$ strain. Retardation of radiolabelled DNA was observed for each of three fragments from the intergenic region, however, the 200-400 bp fragment exhibited the greatest number of protein:DNA complexes. This was encouraging since we were searching for potential regulators of $P_{mra}3$, which also resides within this DNA fragment. Many of the protein:DNA complexes were detected as faint bands of retarded DNA. This may either suggest that the proteins have low affinity for the DNA fragment, or that the proteins were at a low concentration. It was therefore possible that these interactions could be enhanced by concentrating the protein fractions. We also observed that protein fractions C13 and C14 produced the greatest number of protein:DNA complexes, indicating that they contain several DNA binding proteins capable of interacting with the intergenic region.

The protein:DNA complexes that produced the 50% shift in the 400-600bp fragment of DNA (Figure 4.3.3.c) indicated the presence of two DNA-binding proteins with high affinity for this region of DNA. Alternatively it may suggest that proteins with low affinity for the 400-600 bp region are present at high concentrations in fractions C13-C15. These data were interesting because we were also searching for a transcriptional repressor(s) which binds between 400 and 500 bp. To determine whether the percentage of bound DNA could be increased to a level sufficient to perform DNaseI footprinting, fraction C14 was concentrated 2-fold and EMSAs were performed with the 400-600 bp fragment.

The proteins in the concentrated fraction C14 produced two distinct complexes with the 400-600 bp DNA as observed in Lanes 3-6 (Figure 4.3.4). As the concentration of C14 increased, there was a corresponding increase in intensity of the retarded DNA

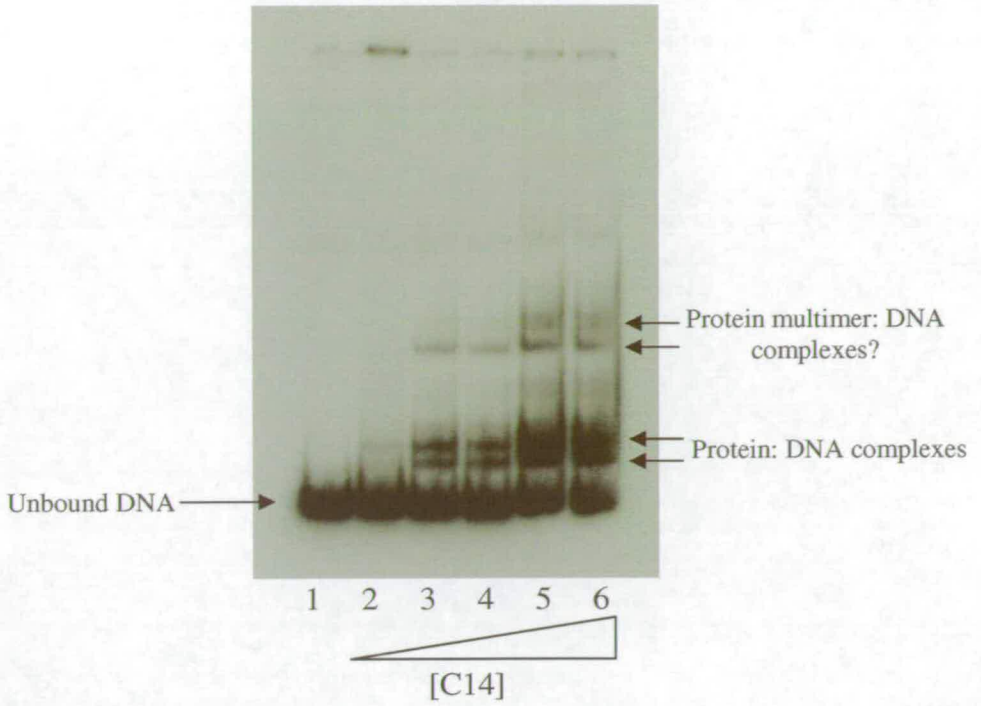


**Figure 4.3.4: Autoradiograph of interactions between DNA-binding proteins in the C14 fraction, with the 400-600 bp DNA of the *fru*R-*yab*B intergenic region.**
Increasing volumes of the concentrated C14 fraction were used in EMSAs. Two protein:DNA complexes were present, as observed in Lanes 3-6. These may represent two separate DNA binding proteins, or a DNA-binding protein and a proteolytic fragment of the same protein that has retained its binding ability. As concentration of C14 increased, extra bands that were more retarded in the gel became evident. These may be additional binding proteins which exhibit lower affinity for the DNA in this region, or they may represent multimeric protein complexes of the same proteins with the DNA.

bands located higher in the gel. This may reflect an increase in concentration of a protein which binds with low affinity, or the bands may represent multimeric protein:DNA complexes of the same proteins.

To identify the binding sites of these proteins, DNaseI footprinting was performed using the radiolabelled 400-600 bp fragment of DNA and the concentrated [C14] protein fraction (data not shown). Although a 50% shift in the DNA was observed in the EMSAs with [C14] (Figure 4.3.4) there was no significant protection of the DNA observed following DNaseI digestion. This result may indicate that the proteins are of high abundance, but with low affinity for the DNA. Since DNaseI footprinting reactions were performed in solution, the high dissociation for a low affinity DNA binding protein may enable DNaseI to gain access to the binding site and cleave the DNA backbone. This would result in an absence of protection, even though the DNA-binding protein was present in solution. It may have been possible to determine the

protein binding site by increasing the protein concentration further. However, we observed in Figure 4.3.2b that fraction C14 contains in excess of 50 proteins, therefore any further concentration of this fraction may have resulted in precipitation of the proteins. As a result, a new strategy for the separation of DNA binding proteins from a soluble protein lysate was followed.

To reduce the total number of DNA-binding proteins eluted following affinity chromatography, ammonium sulphate precipitation was used to fractionate the soluble protein lysate prior to the chromatographic steps. A series of 20%, 40%, 60%, 80% and 100% ammonium sulphate cuts were performed on a 10ml soluble protein lysate prepared from a 500ml exponential phase culture of RE201 (*fis*::Km). The precipitated proteins were resuspended and dialysed to remove excess salt. Figure 4.3.5 shows the SDS-PAGE analysis of the ammonium sulphate fractions. Few proteins were precipitated in the 20% and 40% fractions, however the 60% and 80% fractions appeared to contain most of the cellular proteins and were more concentrated than the original soluble protein lysate. As a result, each fraction was diluted prior to performing EMSAs with the DNA fragments from the intergenic region.

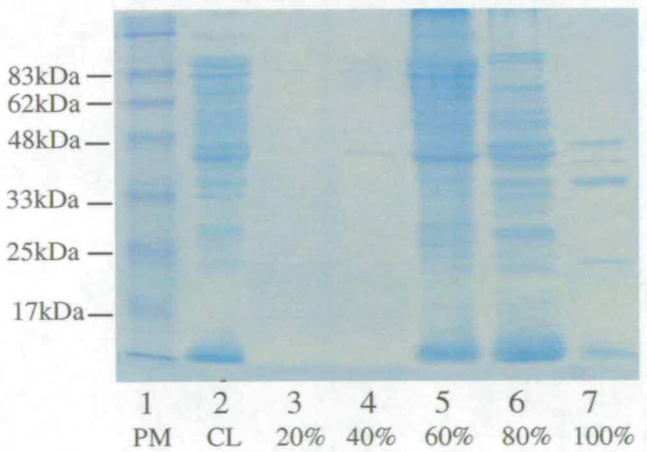


**Figure 4.3.5: SDS-PAGE of the protein fractions produced by Ammonium sulfate precipitation of an RE201 (*fis*::Km) soluble protein lysate.**
A 10ml soluble lysate was prepared from a 500ml exponential culture of RE201(*fis*::Km), 20µl of this was electrophoresed in Lane 2. The lysate was fractionated by the addition of ammonium sulphate. Precipitated proteins were pelleted by centrifugation from solutions of 20%, 40%, 60%, 80% and 100% ammonium sulphate. The pelleted proteins were resuspended in 1.5ml 0.1M NaCl-HSB buffer and dialysed to remove excess salts. The 60% and 80% fractions contained most of the soluble cellular protein

Figure 4.3.6 shows the autoradiographs of EMSAs using the 0-200 bp, 200-400 bp and 400-600 bp fragments of the intergenic region, in reactions with diluted 20%, 40%, 60%, 80% and 100% ammonium sulphate fractions. No defined protein:DNA complexes could be observed with the 0-200 bp and 200-400 bp fragments when the fractions were diluted 1/10 (Figure 4.3.6a). However, significant smearing was seen particularly for the 60-80% fraction, which may be due to the protein fractions being too concentrated or still containing too much salt for resolution of the retarded DNA. Similar smearing was observed for the 1/10 diluted 60-80% fractions with the 400-600bp fragment of DNA (Figure 4.3.6b). However, when the ammonium sulphate fractions were diluted 1/50, a defined protein:DNA complex was observed in the 60% fraction (Figure 4.3.6b, Lane 10). The mobility of this protein:DNA complex resembled that of one of the protein:DNA complexes that we had seen previously in Figure 4.3.4 (Lanes 3-6).

To scale up the protein preparation, a series of ammonium sulphate cuts were performed on a soluble protein lysate, prepared from a 1 litre exponential phase culture of RE201 (*fis*::Km) in LB. A final 60% ammonium sulphate cut was prepared, and a dilute lysate of this was made by resuspending the precipitated protein in 20ml 0.1M NaCl-HSB buffer. This dilute lysate was applied to a 10ml MonoS column attached to an FPLC. MonoS is negatively charged, like DNA; therefore DNA-binding proteins should bind to the column, while all other proteins should be collected in the flow through. To achieve greater separation of the proteins, the DNA-binding proteins were eluted with a NaCl gradient, at a flow rate of 1ml/min over 50 ml. A peak of protein concentration was observed at approximately 350mM NaCl in fraction 25 (Figure 4.3.7a), however the UV spectrophometric trace illustrates that fractions 23-31 also contained eluted proteins.

To determine if fractions 23-31 contained DNA-binding proteins EMSAs were performed using the 400-600 bp fragment of DNA with fractions 23-31 (Figure 4.3.7.b). Lane 2, which represents the 400-600 bp region in a reaction with a 1/20 dilution of the 60% ammonium sulphate cut of soluble protein lysate, illustrates the protein:DNA complex of interest. This same protein:DNA complex was observed in lanes 6-8 which correspond to fractions 25-27. Lane 8 shows the two distinct

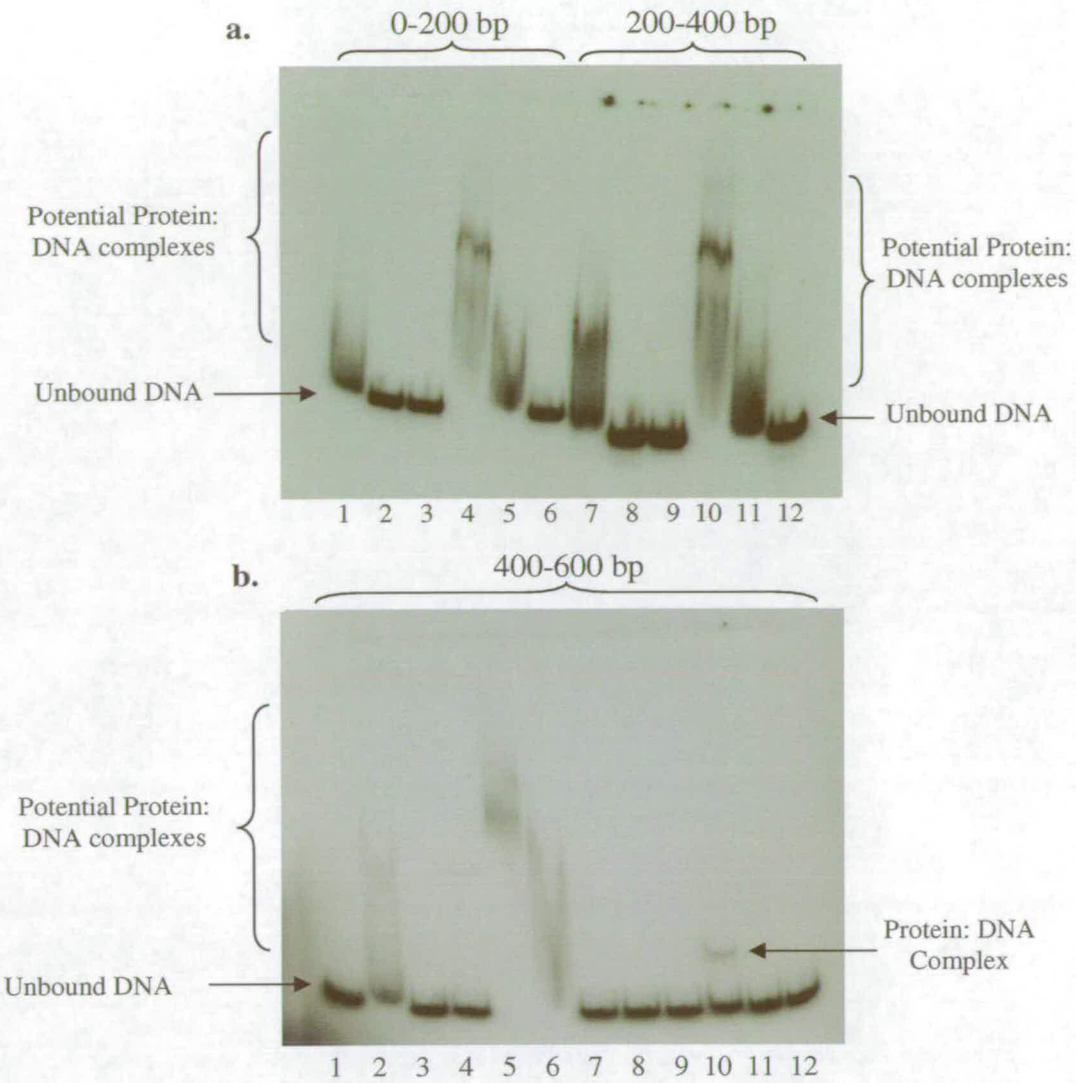


**Figure 4.3.6: Autoradiographs of binding reactions between DNA from the *fru*R-*yab*B intergenic region with DNA-binding proteins from an RE201 (*fis*::Km) soluble protein lysate, fractionated by ammonium sulphate precipitation.**

**a. Lanes 1-6:** Reactions containing the 0-200 bp fragment of the *fruR-yabB* intergenic region. **Lanes 7-12:** Reactions containing the 200-400 bp fragment of the *fruR-yabB* intergenic region. **Lanes 1&7:** Soluble lysate; **Lanes 2&8:** 1/10 dilution of 20% fraction; **Lanes 3&9:** 1/10 dilution of 40% fraction; **Lanes 4&10:** 1/10 dilution of 60% fraction; **Lanes 5&11:** 1/10 dilution of 80% fraction; **Lanes 6&12:** 1/10 dilution of 100% fraction.

**b.** Autoradiograph of binding reactions with 400-600 bp fragment of the *fru*R-*yab*B intergenic region. **Lane 1:** No protein; **Lane 2:** Soluble lysate; **Lane 3:** 1/10 dilution of 20% fraction; **Lane 4:** 1/10 dilution of 40% fraction; **Lane 5:** 1/10 dilution of 60% fraction; **Lane 6:** 1/10 dilution of 80% fraction; **Lane 7:** 1/10 dilution of 100% fraction; **Lane 8:** 1/50 dilution of 20% fraction; **Lane 9:** 1/50 dilution of 40% fraction; **Lane 10:** 1/50 dilution of 60% fraction; **Lane 11:** 1/50 dilution of 80% fraction; **Lane 12:** 1/50 dilution of 100% fraction.

No defined protein:DNA complexes were observed with the intergenic region using the 1/10 dilution of the fractionated lysate. However the smearing observed suggests that interactions may have been occurring but forming unstable complexes due to the fractionated lysate being too concentrated, or still containing too much salt for resolution of the retarded DNA. When the fractions were diluted further (1/50), smearing was not observed and a observed protein:DNA complex with the 400-600 bp region was detected in the 60% fraction.

protein:DNA complexes observed previously (Figures 4.3.3, and 4.3.4), however lanes 6 and 7 exhibited only a single complex. This indicated that the combined methods of fractionation had enabled the separation of these two proteins. Lane 7 also indicates a 60-70% shift of the unbound DNA band, suggesting that the purification methods had also increased the concentration of the unknown DNA-binding protein.

Consequently, fraction 26 (2.5 ml), was concentrated by centrifugal filtration to a final volume of 1ml without any precipitation of protein. This concentrated fraction 26 was used in further EMSAs to identify the potential binding site of the unknown DNA binding protein. No retardation of DNA was detected when either the 400-450 bp or the 400-500 bp fragments were included with fraction 26, indicating that the binding site for the unknown protein was not present between 400-500 bp (Figure 4.3.8, Lanes 1-4). However, proteins in fraction 26 were shown to interact with both the 400-550 bp and 400-600 bp region and resulted in a complete shift in the DNA band. This indicated that the binding site for the protein was within the 500-550 bp region.

To determine the binding site of the unknown protein, DNaseI footprinting reactions were performed using fraction 26 and the 500-600 bp fragment of DNA. As seen previously, no protection of DNA was observed by the unknown protein (data not shown). This was unexpected since figure 4.3.8 suggested that the protein was at a high enough concentration in fraction 26 to transiently bind every DNA molecule in a reaction.

*In situ* Copper Phenanthroline footprinting of the bound complex in the polyacrylamide matrix was also attempted to define the binding site. This form of footprinting cleaves DNA through the minor groove, and is useful for footprinting proteins which alter the geometry of the DNA. No protection of the DNA was observed by this form of footprinting (data not shown). This result was unexpected particularly considering the evidence from numerous EMSAs that indicated the unknown protein binding to the 400-600 bp region of DNA. One possible conclusion is that the protein does not occlude the minor groove and does not cause significant alteration in the geometry of the DNA

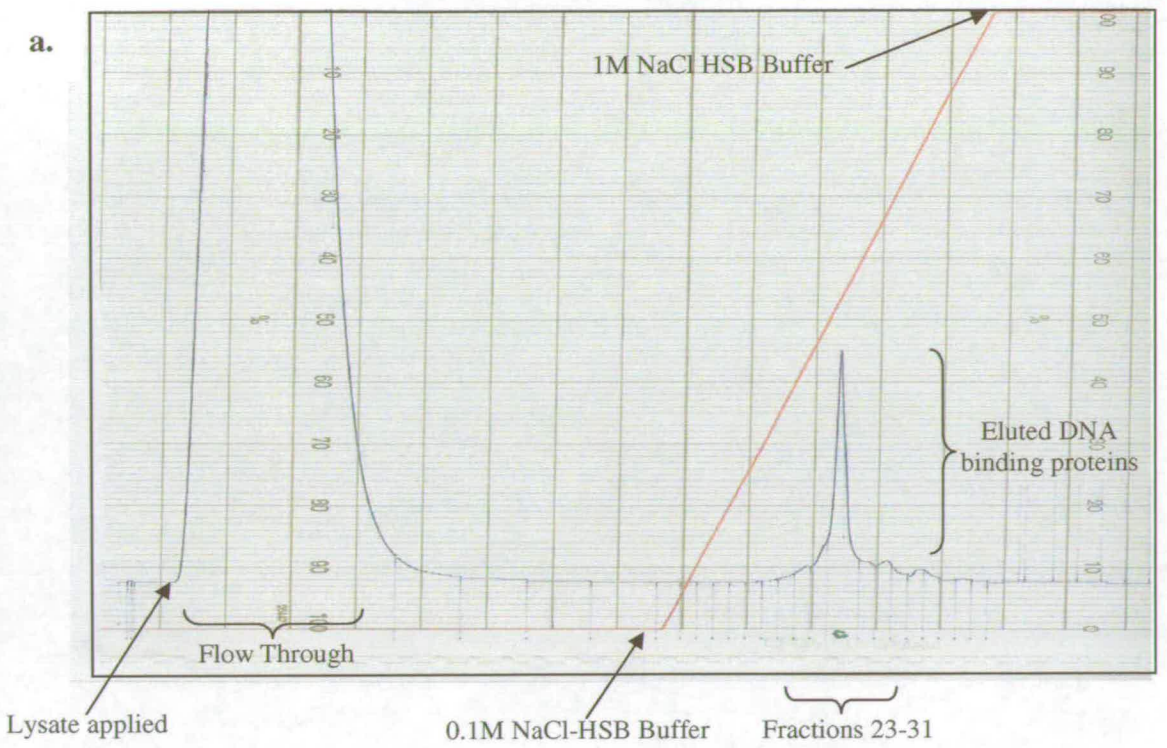


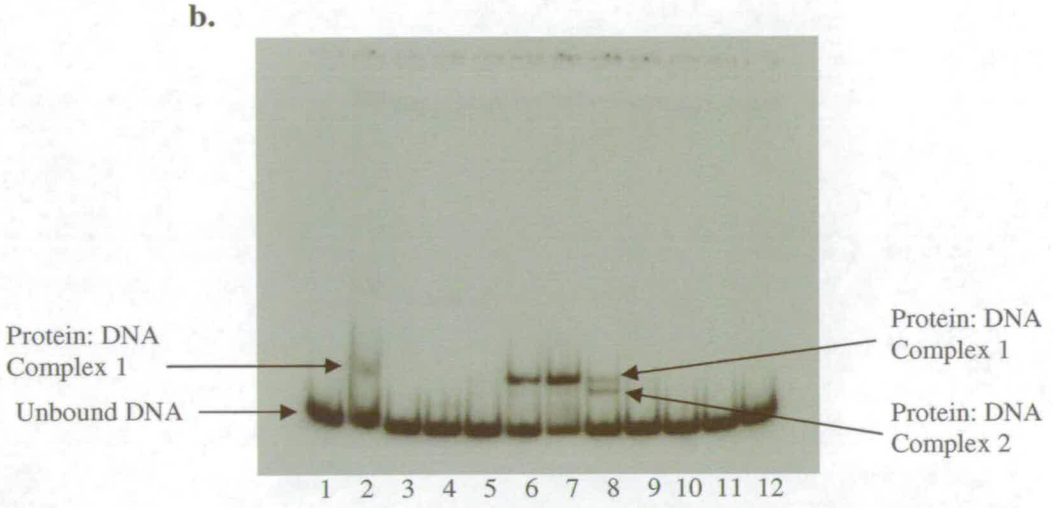


**Figure 4.3.7: Fractionation of DNA-binding proteins from a 60% ammonium sulphate cut of a RE201 (*fis*::Km) soluble protein lysate.**

**a.** UV spectrophometric trace of fractionated proteins from a 60% Ammonium sulphate cut of a RE201(*fis*::Km) soluble protein lysate, using FPLC. A 10ml MonoS column was equilibrated with 0.1M NaCl-HSB Buffer. A 1/20 dilution of the 60% cut was dialysed, filtered and then applied to the column; proteins unable to bind to MonoS were lost in the flow through. A 50ml 0.1M-1M NaCl gradient was run at 1ml/min to elute the proteins bound to the column. Proteins were eluted in 2.5ml fractions. A single peak in protein elution was observed between fractions 23 and 31, at a concentration of approximately 300mM NaCl. Fraction 26 appeared to contain the most protein.

**b.** Autoradiograph of reactions between fraction 23-31 and the 400-600 bp fragment of the *fru*R-*yab*B intergenic region. **Lane 1:** No protein; **Lane 2:** 1/20 dilution of 60% cut; **Lane 3:** Flow Through; **Lane 4:** 23; **Lane 5:** 24; **Lane 6:** 25; **Lane 7:** 26; **Lane 8:** 27; **Lane 9:** 28; **Lane 10:** 29; **Lane 11:** 30; **Lane 12:** 31.

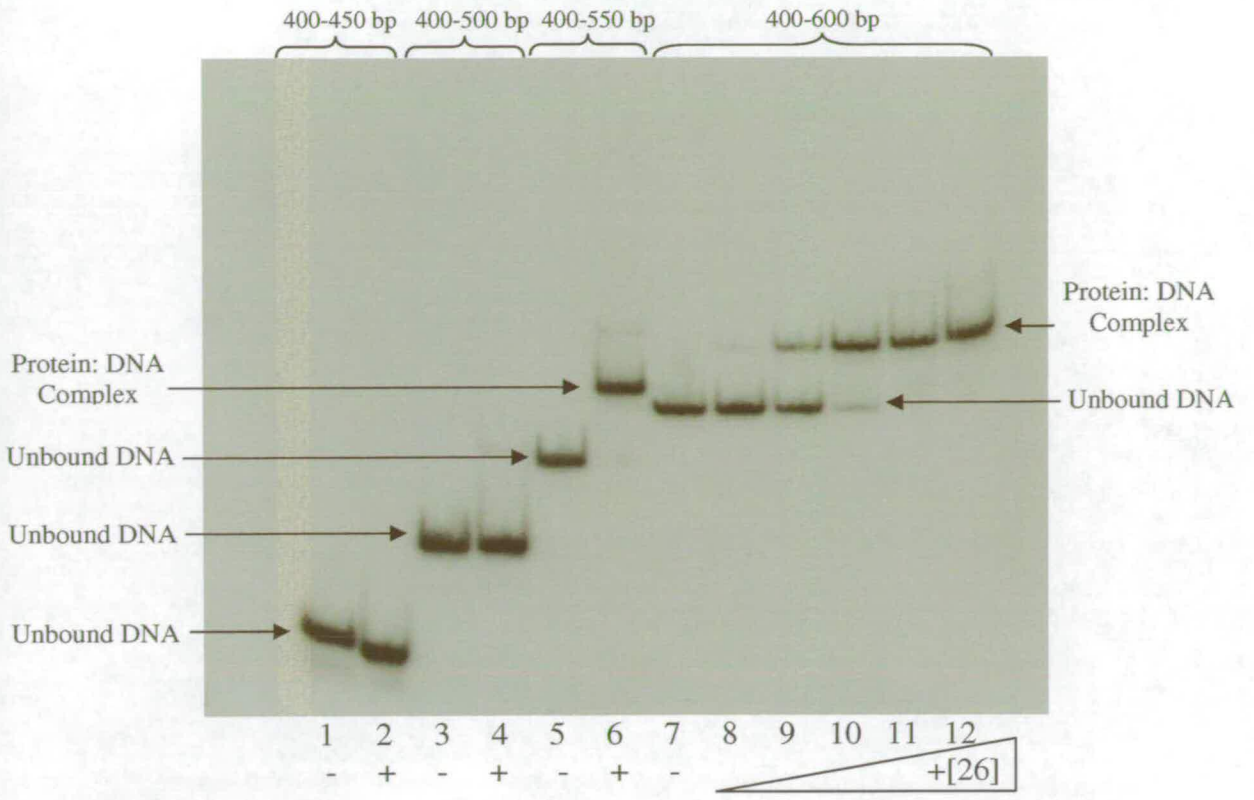


**Figure 4.3.8: Autoradiograph of binding reactions between concentrated protein fraction 26 and the 400-600 bp DNA of the *fru*R-*yab*B intergenic region.**
Fraction 26 was concentrated 2-fold and used in EMSA reactions with fragments of the 400-600 bp DNA of the *fru*R-*yab*B intergenic region. **Lanes 1&2:** Represent reactions with the 400-450 bp region of DNA; **Lanes 3&4:** Represent reactions with the 400-500 bp region of DNA; **Lanes 5&6:** Represent reactions with the 400-550 bp region of DNA, an almost 100% shift in DNA is observed in the presence of fraction 26; **Lanes 7-12:** Represent reactions with the 400-600 bp region of DNA. A complete shift in DNA was observed with an increase in the concentration of fraction 26.

Fraction 26 was resolved by SDS-PAGE which showed that there were only 3 major protein species within the fraction (Figure 4.3.9). Protein A was approximately 10kDa in mass and was particularly abundant, Protein B was around 17 kDa, and Protein C was around 25 kDa in mass. The three proteins were extracted from the gel and identified by MALDI-TOF Mass Spectrometry. The most abundant protein in fraction 26, Protein A, was identified as Lysozyme. This was used for lysis of the cells prior to sonication and is not present in *E. coli*. The results for proteins B and C are illustrated in Figure 4.3.10. The peptide analyses following trypsin digestion of the proteins are shown, as are the best matches to the proteins as determined by the probability based Mowse score. Both proteins B and C showed a match to the 50S subunit ribosomal protein L3 which has a molecular mass of around 22 kDa, this is approximately the

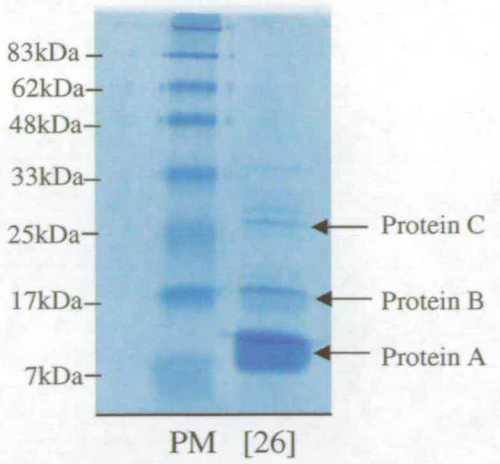


**Figure 4.3.9: SDS-PAGE of the proteins present in fraction 26.**
SDS-PAGE of the detectable proteins present in fraction 26. Protein bands A, B and C were extracted from the gel and identified by MALDI-TOF Mass Spectrometry.

size of Protein C (Figure 4.3.9). Protein B may represent a proteolytic fragment of this protein since it migrates further through in a polyacrylamide gel than Protein C.

Ribosomal protein L3 is highly conserved in prokaryotes (Herwig *et al.*, 1992). L3 is one of the central components of the 50S subunit and is one of the first ribosomal proteins to be assembled into the ribosome (Roth *et al.*, 1980) and is required for the ribosome's peptidyltransferase activity (Petrov *et al.*, 2004). L3 has been reported to bind to both single stranded and double stranded DNA (Soultanas *et al.*, 1998), however it has never been reported as a transcriptional regulator. Our data suggest that L3 may interact with the DNA in the 500-550 bp fragment of the *fru*R-*yab*B intergenic region during exponential growth. We predicted that the unknown protein would be highly abundant but with low affinity for the 500-600 bp fragment of DNA. This would be in agreement with the identification of ribosomal protein L3 as our unknown protein.

We suggested in section 3.5 that the presence of the 400-600 bp region was important for the inverse growth rate control of the $P_{mra}$ promoters and that this region may be the site for interactions with important mediators of growth rate. Little is known about the mechanisms of growth rate regulation in *E. coli*. The first response a cell makes to a change in growth rate is to alter its number of ribosomes by modulating levels of total RNA and protein production (Cashel *et al.*, 1997). Rapidly growing cells in rich medium can contain up to 20,000 ribosomes, while a slow growing culture in poor

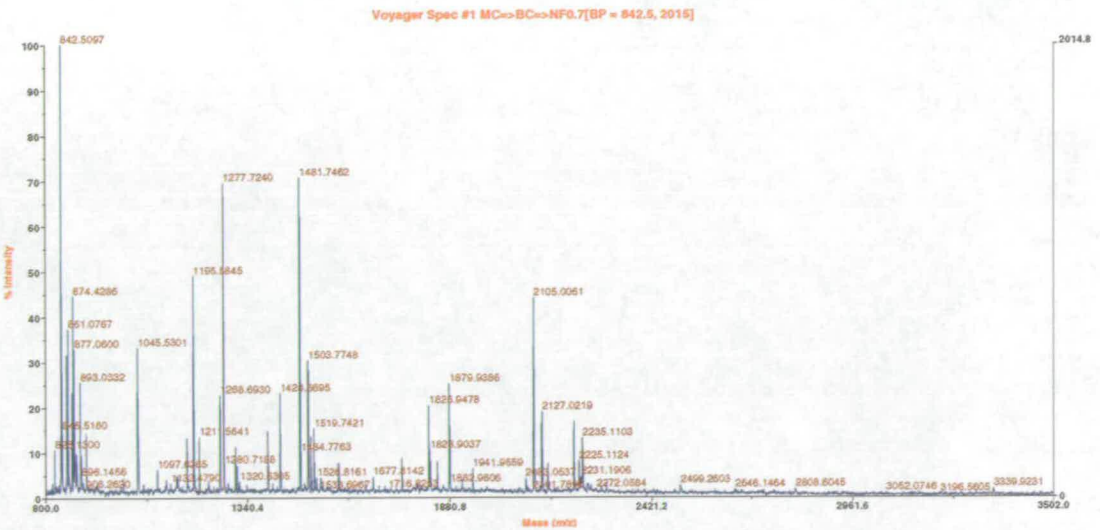


Sample B

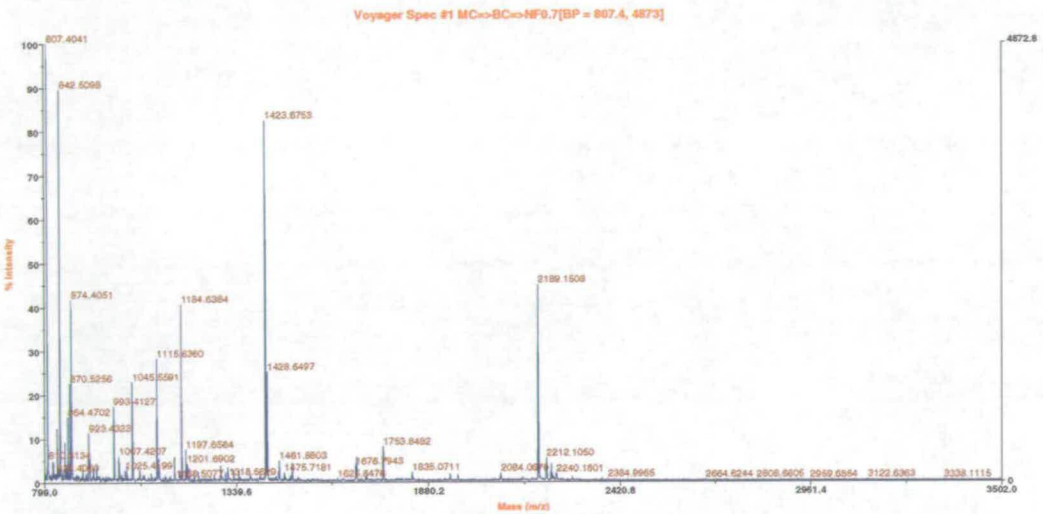


Sample C

**Results**

| Sample | MALDI-TOF | | | | |
|---|---|---|---|---|---|
| | MOWSE Score* | Peptide coverage | Protein MW(Da)/pI | Accession | Protein name |
| B | 3.46e+004 | 13/54 (24%) | 22243.7 / 9.90 | 24114598 | 50S ribosomal subunit protein L3 [Shigella flexneri 2a str. 301] |
| C | 1 1.41e+004 | 15/142 (10%) | 22243.7 / 9.90 | 24114598 | 50S ribosomal subunit protein L3 [Shigella flexneri 2a str. 301] |

**Figure 4.3.10: Identification of proteins present in fraction 26 by Mass Spectrometry.**

Protein A was determined to be Lysozyme, which would have been a contaminant from the lysis of the cells. The peptide analysis following Trypsin digestion is illustrated for both Protein samples B and C. The best match to both these proteins was the 50S ribosomal subunit protein L3, which has a molecular weight of 22 kDa, therefore protein B may represent a proteolytic fragment of L3.

medium may contain as few as 2,000 ribosomes (Lengeler & Postma, 1998). During exponential growth there will be many ribosomes and therefore high levels of expression of L3. It can be assumed that the majority of L3 will be sequestered in the ribosomes however there may be sufficient free L3 to interact with the *fru*R-*yab*B intergenic region and cause repression of the $P_{mra}$ promoters. As growth slows approaching stationary phase, the number of ribosomes and free L3 would decrease therefore the L3 repression of the $P_{mra}$ promoters would be alleviated. Ribosomal protein L3 could potentially maintain the inverse growth rate control exhibited by the $P_{mra}$ promoters. Since the number of ribosomes reflect the growth rate (and therefore cell size) of the cell, it would seem prudent for bacteria to exploit this as a mechanism of cell size control. The data presented here may be the first evidence for a ribosomal protein mediated control of cell size.

## 4.4 Identification of additional promoters of the *mra* region.

We have provided evidence to show that transcripts originating from the $P_{mra}$ promoters span the proximal genes in the *mra* region (Section 3.7). However, we have not been able to verify whether transcription from the *fru*R-*yab*B intergenic region spans as far as *fts*Z, or whether the $P_{mra}$ promoters contribute 66% of *fts*Z transcription as suggested by Flärdh *et al* (1998). Our data suggest that this is unlikely since the transcription patterns of proximal genes during batch culture are very different to the transcription patterns of *fts*Z (Section 3.2). Expression of the *fts*QAZ operon does appear to require transcription originating from upstream (Flärdh *et al.*, 1998), but if this is not originating from the $P_{mra}$ promoters it must be coming from unidentified promoters within the genes of the *mra* region.

We used the Regulon DB database (http://regultondb.ccg.unam.mx:80/index.html) which provides a computational model of mechanisms of transcriptional regulation, to identify all potential $\sigma^{70}$ recognised promoter regions between *fru*R and *ddl*B. Thirteen potential promoters were identified, all of which are located within ~100 bp upstream of a gene in the *mra* region. In addition, each gene between *yab*B and *ddl*B potentially appears to have its own promoter. The potential promoter sequence details

are shown in Table 4.1. None of the potential promoters contain GC rich discriminator regions which may have made them sensitive to regulation by ppGpp, and there are no obvious FIS or CRP binding sites in or around the potential promoter regions.

| Promoter? | -35 Sequence | Spacing | -10 Sequence | Ability to form Stable Complex with RNAP | Promoter Activity (Miller Units) |
|---|---|---|---|---|---|
| $\sigma^{70}$ Consensus | TTGACA | 17-19 bp | TATAAT | N/A | N/A |
| $P_{yab}$C? | TCGACG | 18 bp | GAGACT | +++ | 93 ± 2.5 MU |
| $P_{fts}$L3? | TTACCG | 20 bp | AAAACT | - | 10 ± 3 MU |
| $P_{fts}$L2? | CCGTCA | 20 bp | TAATGC | - | 10 ± 3 MU |
| $P_{fts}$L1? | TGCCCG | 15 bp | TATTGC | - | 10 ± 3 MU |
| $P_{fts}$I? | TCGCCA | 17 bp | CAGCAT | +++++ | 33 ± 5.5 MU |
| $P_{mur}$E? | TGCCAT | 18 bp | TACCAT | +++++ | 39 ± 1.7 MU |
| $P_{mur}$F? | TTACCA | 20 bp | TGGACT | - | 18 ± 1 MU |
| $P_{mra}$Y? | CTGATT | 17 bp | TACGAT | ++ | 293 ± 32 MU |
| $P_{mur}$D? | TGGATT | 17 bp | TCTGAT | + | 35 ± 1.2 MU |
| $P_{fts}$W? | TTCAGC | 15 bp | TGCTCT | - | 12 ± 2.5 MU |
| $P_{mur}$G? | CTTACT | 15 bp | CATCAT | + | 129 ± 5.7 MU |
| $P_{mur}$C? | TTGTAG | 17 bp | TATGAA | + | 84 ± 2.5 MU |
| $P_{ddl}$B? | CTGATT | 17 bp | TAATAT | + | 1665 ± 160 MU |
| $P_{ddl}$B2? | CTGATT | 17 bp | TAATAT | + | 2049 ± 167 MU |
| $P_{mra}$4for? | Undefined | Undefined | Undefined | +++ | 316 ± 6 MU |
| $P_{mra}$4rev? | Undefined | Undefined | Undefined | +++ | 151 ± 4 MU |

**Table 4.1: Promoter sequences, affinities for RNAP and relative activities of potential promoters of the *mra* region.**
Potential promoter sequences were identified from the Regulon DB database, their respective positions in the mra region are illustrated in Figure 4.4.3b. Their ability to form stable complexes with RNAP was determined from the autoradiographs depicted in Figure 4.4.2a. Promoter activity was determined by cloning each promoter region into pRS551 and measuring the β-galactosidase activities, these data are illustrated graphically in Figure 4.4.3a.

To determine whether these predictions represented functional promoters, a series of RNA Polymerase stable complex assays were performed. In these experiments radiolabelled DNA was incubated with RNAP and then challenged with the competitive inhibitor Heparin. A negative control for the RNAP stable complex assay using *lac*Z DNA, which is known to contain no promoter sequences, was used to allow differentiation between specific and non-specific binding of RNAP (Figure 4.4.1a). In Lane 2, where the DNA was in the presence of RNAP but no heparin,

smearing was observed. This represents the repetitive binding and release of RNAP as it searches for a promoter recognition sequence. In Lanes 3-5 the was no smearing and no RNAP:promoter complexes since all free RNAP had been sequestered by Heparin. A positive control for the RNAP stable complex assay used the $P_{mra}1$ and $P_{mra}2$ sequences from the 0-200 bp fragment of DNA from the *fru*R-*yab*B intergenic region. This DNA fragment contains two promoter regions and stable complexes can be observed across lanes 2-5. The Heparin resistant RNAP:Promoter stable complex observed in lanes 3-5 probably represents RNAP binding to $P_{mra}1$. RNAP has high affinity for $P_{mra}1$ and therefore exhibits a very low dissociation rate. As a result, the stable complex is maintained and there is no release of RNAP for Heparin to sequester.

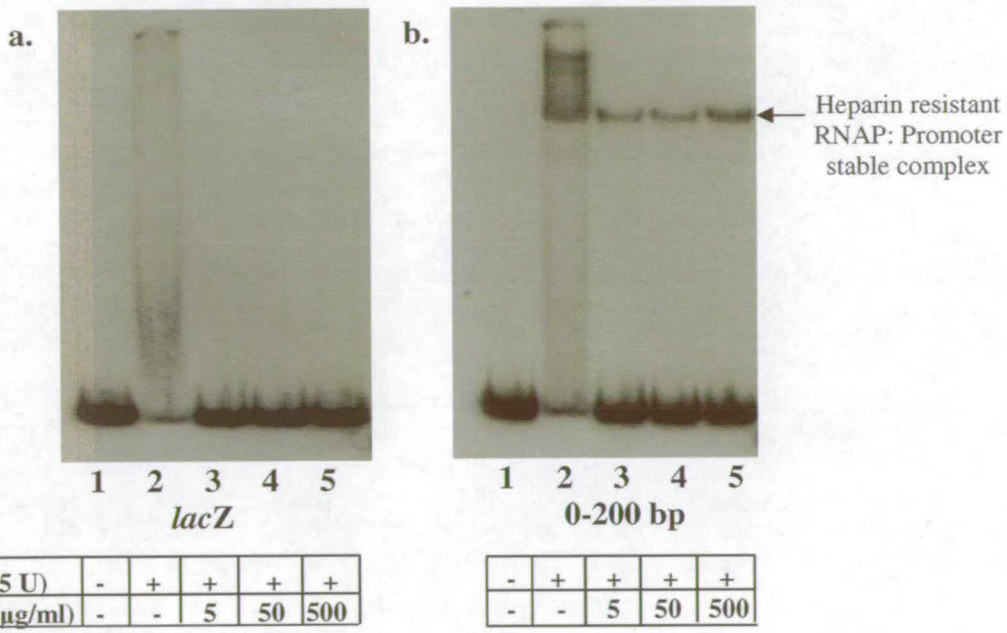


**Figure 4.4.1.: Autoradiographs of stable complex assays using DNA with and without promoter regions**

**a.** In a binding reaction with *lac*Z DNA, RNA Polymerase fails to make any stable protein:DNA interactions. This would be expected since *lac*Z contains no promoters. The smearing observed in Lane 2 reflects transient interactions as RNA Polymerase binds and releases the DNA until it encounters a binding site at a promoter region to which it will bind with high affinity. These transient interactions are not observed in Lanes 3-5 as the competitive inhibitor Heparin sequesters any unbound RNAP.

**b.** In a binding reaction with the 0-200 bp fragment of the *fru*R-*yab*B intergenic region DNA, RNAP forms a stable complex, even in the presence of an increasing concentration of the competitive inhibitor Heparin. This complex probably represents RNAP bound at $P_{mra}1$.

Each of the potential promoter sequences located in the *mra* region were amplified by PCR, radiolabelled with $^{32}P$ and used in RNAP stable complex assays (Figure 4.4.2).

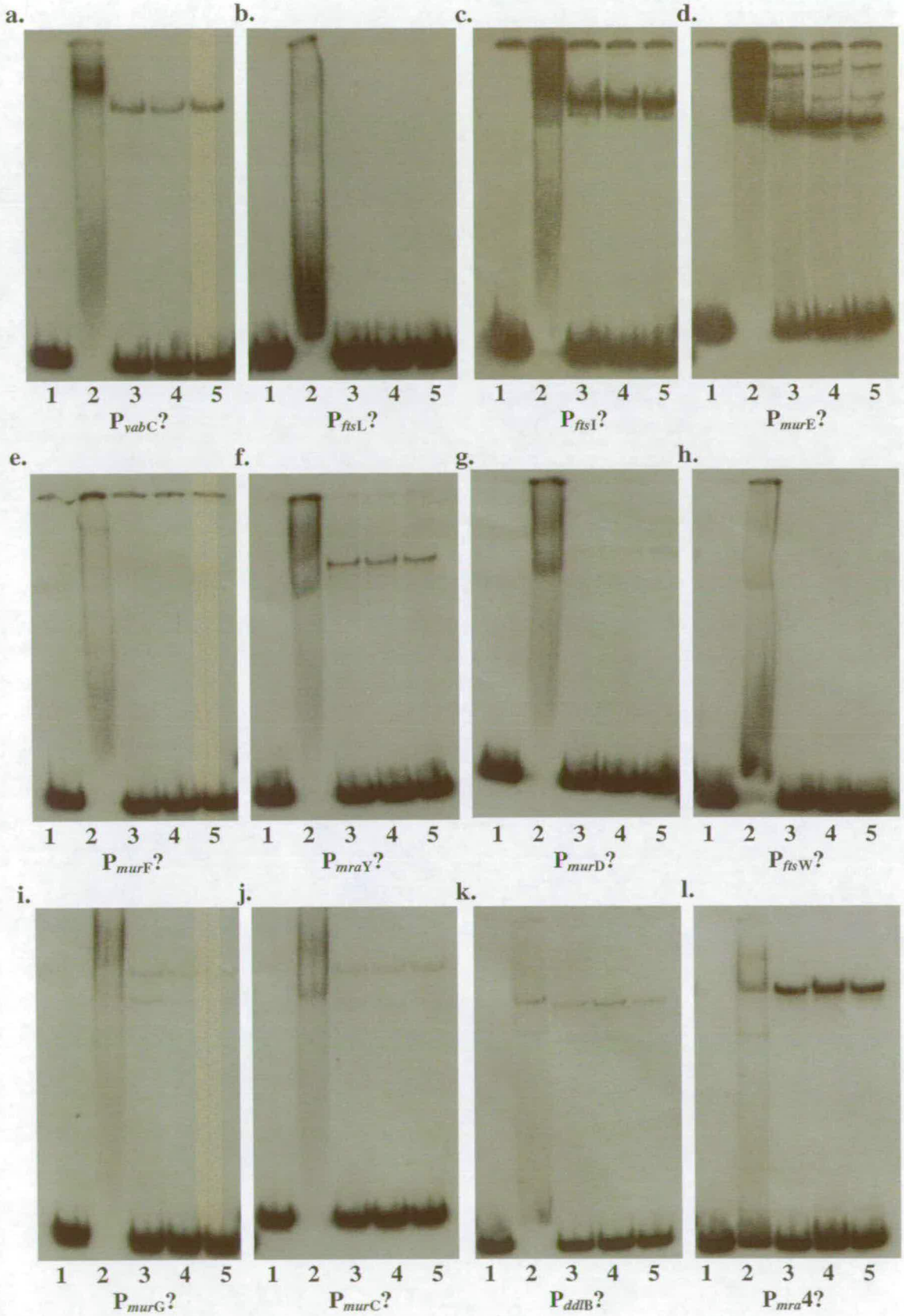


**Figure 4.4.2: Autoradiographs of stable complex assays using DNA fragments containing potential promoter sequences in the presence of RNA Polymerase.**
The stable complex assays for each potential promoter contained; **Lane 1:** No protein; **Lane 2:** 0.5U RNAP; **Lane 3:** 0.5U RNAP, 5µg/ml Heparin; **Lane 4:** 0.5U RNAP, 50µg/ml Heparin; **Lane 5:** 0.5U RNAP, 500µg/ml Heparin.

$P_{yabC}$ exhibited a good match to the -35 consensus sequence, but a poor match to the -10, with an optimal spacing of 18 bp. It is capable of producing a stable complex with RNAP which suggests that it is a functional promoter (Figure 4.4.2a). There were three potential promoters identified upstream of *ftsL*, $P_{ftsL1}$, $P_{ftsL2}$,and $P_{ftsL3}$. Hara *et al.*, (1997) had also predicted a possible promoter within this region. All three promoters exhibited good matches to both the -10 and -35 consensus sequences, however they had 20 bp, 20 bp and 15 bp spacing respectively. RNAP stable complexes were not observed with this potential promoter region, indicating that none of the potential $P_{ftsL}$ promoters are functional and that *ftsL* does not possess its own promoter (Figure 4.4.2b). $P_{ftsI}$, which was also predicted by Hara *et al* (1997), exhibits a good match to the -35 consensus sequence with optimal spacing of 17 bp, however its -10 sequence is GC rich. A strong RNAP stable complex was observed with this DNA fragment indicating that $P_{ftsI}$ is a functional promoter (Figure 4.4.2c). $P_{murE}$ shows a good match to both the -35 and -10 consensus sequences, and has a optimal spacing of 18 bp between the two recognition regions. Multiple RNAP stable complexes were observed indicating this $P_{murE}$ is also a functional promoter (Figure 4.4.2d). $P_{murF}$ shows a good match to the -35 consensus but the -10 region is GC rich and there is long 20 bp spacing between the two. An RNAP stable complex was not seen for $P_{murF}$ indicating that it is not functional (Figure 4.4.2e). $P_{mraY}$ exhibits a poor match to the -35 consensus, but there is an optimal 17bp spacing between the -35 and well matched -10 region. An RNAP stable complex was observed for $P_{mraY}$ suggesting that it is a functional promoter (Figure 4.4.2f). $P_{murD}$ was also predicted by Boyle *et al.*, (1997), it has a good match to both the -35 and -10 and an optimal spacing of 17 bp. However, only a faint RNAP stable complex was observed indicating that $P_{murD}$ may not be a functional promoter (Figure 4.4.2g). $P_{ftsW}$ may represent the promoter for *murG* that Mengin-Lecreulx *et al* predicted in 1998. It shows a good match to the -35 consensus but a short spacing of 15 bp with a poor match to the -10. It is therefore not surprising that $P_{ftsW}$ did not form a stable complex with RNAP and is not a functional promoter (Figure 4.4.2h). $P_{murG}$ exhibits a good match to the -10 consensus sequence but a short spacing of 15 bp with a poor match to the -35 sequence. However, two faint RNAP stable complexes were observed suggesting that $P_{murG}$ is functional (Figure 4.4.2i). $P_{murC}$ shows a good match to the -35 and -10 consensus sequences with optimal spacing of 17 bp, however it produced only a faint stable complex with RNAP indicating that it may not be a functional promoter (Figure 4.4.2j). $P_{ddlB}$ shows a good

match to the -35 consensus sequence and optimal spacing of 17 bp with an excellent match to the -10 sequence. A stable complex formed with RNAP suggesting that P*ddl*B is functional (Figure 4.4.2k). $P_{mra4}$ was predicted to be located in the 400-600 bp fragment of the intergenic region by RT-PCR analysis of the transcripts entering the *mra* region (Section 3.7). The production of an RNAP stable complex in the 400-600 bp region confirms the presence of $P_{mra}4$ in this region (Figure 4.4.2l).

The RNAP stable complex results indicate that $P_{ftsL1/2/3}$, $P_{murF}$ and $P_{ftsW}$ do not represent functional promoters, which suggests that the bioinformatic prediction of promoter sequences by the Regulon DB database is flawed. It should also be noted that a strong RNAP stable complex is not directly indicative of a highly active promoter, it is just a measure of the affinity of RNAP for the promoter region. In order for a promoter to be highly active it must also allow RNAP to rapidly form an open complex and subsequently escape the promoter region following transcription initiation.

To validate the assignment of promoters and to determine their activity, each potential promoter region was cloned into the reporter vector pRS551. TP8503 and RE201(*fis*::Km) were transformed with each of the pRS vectors and β-galactosidase activity was measured during early exponential phase. Activity in RE201 was measured in addition to that from WT TP8503 because FIS is the most abundant nucleoid protein during exponential phase and is a pleiotropic transcriptional regulator that may have direct or indirect effects on each of these promoters.

The β-galactosidase activity derived from the potential promoters $P_{yabC}$, $P_{ftsL1/2/3}$, $P_{ftsI}$, $P_{murE}$, $P_{murF}$, $P_{murD}$, $P_{ftsW}$ and $P_{murC}$ was observed to be very low, with less than 100 Miller Units of β-galactosidase activity detected (Figure 4.4.3a). This result was predicted for sequences $P_{ftsL1/2/3}$, $P_{murF}$ and $P_{ftsW}$ because they possessed poor matches to the $\sigma^{70}$ promoter consensus and failed to form a stable complex with RNAP. However, the other low activity promoters $P_{yabC}$, $P_{ftsI}$, $P_{murE}$, $P_{murD}$, and $P_{murC}$ each possessed good matches to the promoter consensus sequences, with optimal spacing and formed stable complexes with RNAP. In the cases of $P_{ftsI}$ and $P_{murE}$, particularly strong stable complexes were also formed with RNAP, indicating that these promoters are very good at recruitment of RNAP polymerase. These results may suggest that the

high affinity of RNAP for $P_{ftsI}$ and $P_{murE}$ prevents promoter escape and transcription elongation. This explanation could also apply to $P_{yabC}$ and $P_{murD}$, although neither of these potential promoters exhibited such strong stable complexes with RNAP. Another possible explanation is that these promoters are repressed during the experimental conditions. FIS is not a major regulator of any of the potential promoters (Figure 4.4.3a), however there are other regulatory mechanisms that could be repressing transcription from these promoters. For instance, we have seen that the $P_{mra}$ promoters are negatively regulated by growth rate, therefore if these promoters are contributing to transcription of the cell division genes of the *mra* region we might also expect them to be negatively regulated by growth rate, and subsequently repressed during exponential growth. The activities of $P_{mraY}$ and $P_{murG}$ were a little higher than the other potential promoters with 293 Miller Units and 129 Miller Units respectively. However, when compared to the activities observed from the $P_{mra}$ promoters (Figure 3.3.1.3) these still represent weak promoters.

The only significant promoter identified within the *mra* region was $P_{ddlB}$. The $P_{ddlB}$ promoter sequence has a good match to the -35 and -10 consensus sequences (3/6 and 4/6 bases, respectively), and optimal spacing of 17 bp. Only a weak stable complex was observed with RNAP, however this promoter exhibited 1600 Miller Units of β-galactosidase activity, which increased to over 2000 Miller Units when the upstream region was extended in the reporter vector. $P_{ddlB}$ is still a weak promoter compared to $P_{mra}1$ and $P_{mra}3$, however it exhibited 10-fold higher activity than $P_{mra}2$ under the same experimental conditions. The data in Figure 4.4.3 indicate that FIS may play a small role in the regulation of $P_{ddlB}$, however this may be mediated by indirect effects for instance, on promoter topology. $P_{ddlB}$ is the most proximal potential promoter to the *fts*QAZ operon (Figure 4.4.3b), and its activity levels may be enough to make a contribution to transcription of this cluster of cell division genes.

In addition to potential promoters in the *mra* region, Figure 4.4.3 also illustrates the β-galactosidase activity data for $P_{mra}4$ located in the 400-600 bp fragment of the intergenic region. We know nothing about the promoter sequence of $P_{mra}4$, however we know that transcripts entering the *mra* region can be detected from the 400-600 bp fragment by RT-PCR. The stable complex experiments with RNAP confirmed the presence of a promoter in this region of DNA, however it is possible that RNAP

a.

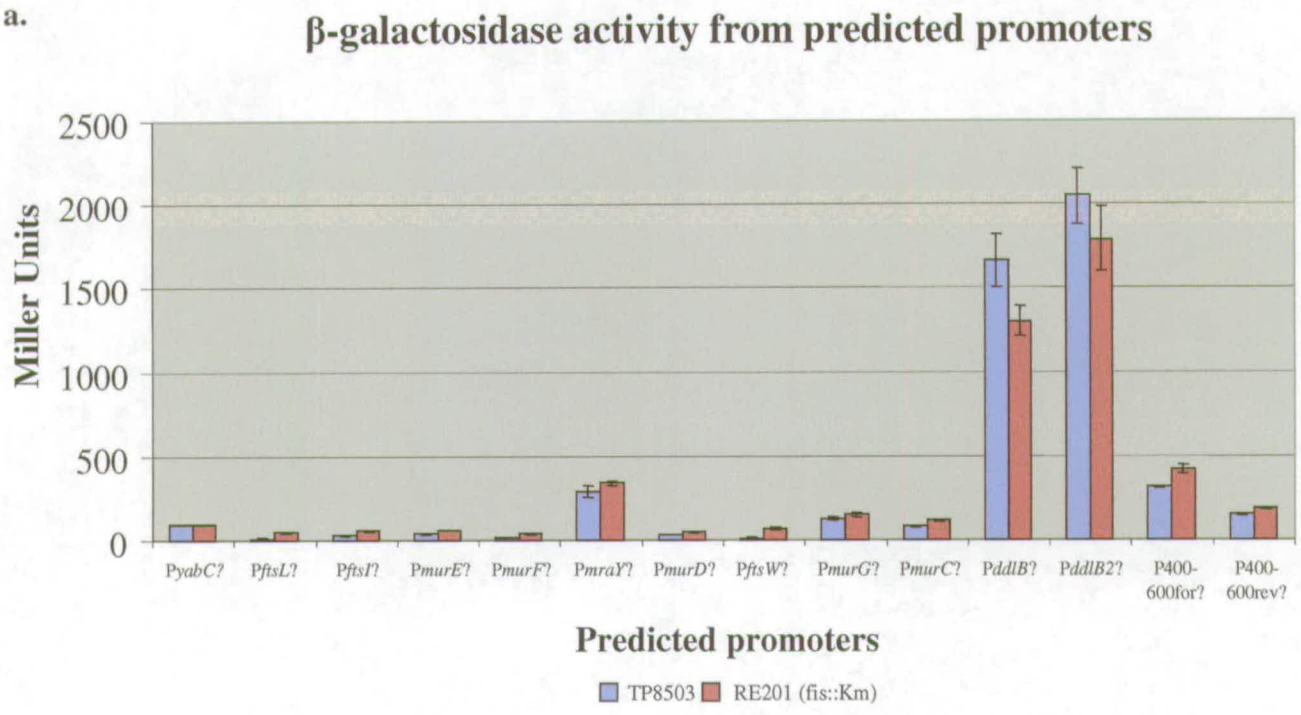


b.

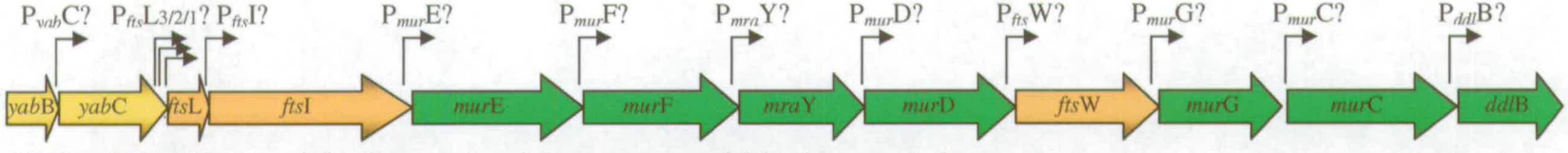


**Figure 4.4.3: β-galactosidase activity from potential promoters within the *mra* region.**

**a.** Histogram showing expression from the pRS series of reporter plasmids, which each contain a potential promoter for the *mra* region cloned upstream of *lac*Z in pRS551. The plasmids were used to transform TP8503 and RE201 (*fis*::Km) ,β-galactosidase activity was measured during exponential growth in LB at 37°C. $P_{ddlB}2$ represents the $P_{ddlB}$ promoter with 50bp of extra DNA included upstream of the promoter. Results are averages of measurements from triplicate cultures, error bars are shown.

**b.** Illustration showing positions of potential promoters within the *mra* region.

binding in this region could transcribe in the opposite direction and produce an antisense transcript of *fru*R. To test this hypothesis, the 400-600 bp fragment was cloned into pRS551 in both orientations. In the forward orientation, 316 Miller Units of β-galactosidase activity were detected. This confirms that $P_{mra}4$ drives transcription in the direction of the *mra* region, but it appears to be a relatively weak promoter under these experimental conditions, which may suggest that it makes little contribution to transcription of the *mra* region. In the reverse orientation, 151 Miller Units of β-galactosidase activity were measured, indicating that a promoter orientated in the reverse direction produces a low level of antisense *fru*R transcription.

The promoter activity data illustrated in Figure 4.4.3 suggest that although each of the genes of the *mra* region appears to have its own promoter, these promoters are mostly inactive or repressed during exponential growth. It is plausible that the cumulative transcription from each of these promoters could contribute to transcription of *fts*Z however these data indicate that only $P_{ddlB}$ is likely to make a significant contribution to transcription of this essential cell division gene. Therefore our analysis of potential promoters within the *mra* region, leads us to the conclusion that (with the exception of $P_{ddlB}$) $P_{mra}1$ and $P_{mra}3$ represent the only promoters that produce high enough levels of transcription to contribute to the transcription of *fts*Z. However, their considerable distance from the gene may suggest that these contributions would be relatively minor.

## 4.5: Summary

This chapter has detailed the methods used to identify possible regulators of the $P_{mra}$ promoters. A genetic screen using transposon mutagenesis to identify mutations in repressors of the $P_{mra}$ promoters proved unsuccessful. Therefore, a more direct biochemical strategy was employed. The separation of DNA-binding proteins from a mixed soluble protein lysate produced interesting results when used in EMSAs with radiolabelled DNA from the *fru*R-*yab*B intergenic region. The purification, concentration and identification of a single protein which interacted with the 400-600 bp fragment of DNA was achieved. It should be noted that at least 10 other protein:DNA complexes were observed and the proteins that are involved in these interaction could potentially be identified by using similar methods to those described.

The 50S subunit ribosomal protein L3 was identified as the protein which interacted with the 500-550 bp fragment of DNA. We have previously seen that this fragment of the intergenic region appears to be important for the negative growth rate regulation of the $P_{mra}$ promoters. The number of ribosomes in a cell correlates with the growth rate of that cell, with high numbers of ribosomes present during rapid growth, and up to 10-fold fewer during slow growth. We have seen that L3 appears to bind with low affinity but interactions were detected due to the high concentration of the protein. If binding of L3 caused repression of transcription this is likely to only occur during exponential growth, when a high concentration of free L3 may be present in the cell. As a result, L3 may mediate inverse growth rate regulation by repression of $P_{mra}3$ during balanced growth.

This chapter has also investigated whether additional promoters exist within the *mra* region, and what contribution these may make to transcription of genes at the distal end of the gene cluster. Thirteen potential promoters were identified by bioinformatic analysis of the *yab*B-*ddl*B *mra* region, the positions of these promoters suggested that each gene of the *mra* region may have its own promoter. Of these promoters, five were shown to be incapable of forming a stable complex with RNAP. When the sequence data for these promoters was analysed, suboptimal spacing was observed between the -10 and -35 regions indicating that the bioinformatic predictions were flawed. Subsequently, the promoter activities were determined by measurement of β-galactosidase activity from reporter plasmids. Only one promoter from the thirteen predicted sequences was significantly active. This promoter, $P_{ddlB}$, is the most proximal to the *fts*QAZ operon and is potentially active enough to contribute to transcription of these genes. Although it is possible that a small amount of cumulative transcription from the weak promoters may contribute to transcription of *fts*Z, the data suggest that $P_{mra}1$, $P_{mra}3$ and $P_{ddlB}$ represent the promoters which make significant contributions to transcription of *fts*Z.

These conclusions assume that the bioinformatic prediction of promoter sequences by the Regulon DB database is accurate. We have however identified flaws in relying on the system used to predict potential promoters. For instance, not all the predicted promoters formed stable complexes with RNAP ($P_{ftsL}$, $P_{murF}$ and $P_{ftsW}$). In addition, a potential promoter sequence may be recognised by RNAP, which may then bind with

high affinity ($P_{ftsI}$ and $P_{murE}$). However, if the RNAP cannot escape the promoter region to allow transcription elongation, the activity of the promoter will be very low – which contradicts the predictive sequence data and stable complex results. Of most concern, however, is the fact that bioinformatic predictions failed to recognise $P_{mra}3$. This promoter has an excellent match to the -10 consensus sequence (5/6 bases) with 17bp spacing between the -10 and the albeit poor match to the -35 sequence (2/6 bases). $P_{mra}3$ is a strong promoter which plays a significant role in the regulation of the *mra* region, but was not identified in the bioinformatics database search. This highlights the fact that although bioinformatic predictions can be very useful, they cannot be relied on as fact and each prediction must be confirmed by "wet" experiments which still remain the fundamental source of new factual data.

# Chapter 5: Discussion

# 5: Discussion.

This thesis has investigated the transcriptional regulation of the *mra* region – a major locus of genes involved in cell growth and division in *E. coli*. The main aim of this work was to determine the role and transcriptional contribution that each of the $P_{mra}$ promoters makes to the expression of the *mra* region. We also wanted to investigate how the $P_{mra}$ promoters were regulated, particularly in response to changes in growth rate. In addition we hoped to determine whether $P_{mra}1$ was responsible for the majority of *fts*Z transcription, as had previously been suggested (Flärdh *et al.*, 1998).

## 5.1: Regulation of the $P_{mra}$ promoters by Growth Rate.

We had hypothesised that the $P_{mra}$ promoters may be regulated by growth rate, as a potential mechanism for the cell to alter expression of division proteins in response changes in growth and therefore cell size. We also hypothesised that alterations in expression would be minor, since the genes of the *mra* region are essential and must be constitutively expressed. Therefore we predicted that any mechanisms of regulation would result in modulation of promoter activity rather than a simple switching "on" or "off" of transcription. Growth rate regulation of cell division genes has previously been investigated at the *fts*Q, A and Z promoters (Aldea *et al.*, 1990), where it was shown that pQ1 was inversely regulated by growth rate. We observed that transcription originating from all three $P_{mra}$ promoters on the chromosome was also inversely regulated by growth rate. This conclusion was drawn from β-galactosidase activity data from a *yab*B transcriptional reporter strain grown in L Broth, which was lower during exponential growth compared to that measured on the approach to stationary phase. When the *yab*B reporter strain was cultured at a lower growth rate in M9 Maltose, higher expression was measured during exponential growth compared to that during growth in LB which validated our conclusion. These results indicated that the inverse growth rate regulation of the $P_{mra}$ promoters, observed during batch culture, did not simply occur in response to increased cell density or the presence of stationary phase regulators, since increased transcription of the *mra* region was also observed during exponential phase at a slower growth rate. Our findings may therefore suggest that the $P_{mra}$ promoters are repressed by a growth

rate responsive protein expressed during exponential phase. These data are also consistent with catabolite repression (reviewed by Saier *et al.*, 1997). However, we could not detect CRP binding to the intergenic region. The individual $P_{mra}$ promoters each exhibited some degree of inverse growth rate regulation when present in the full 601 bp *fru*R-*yab*B intergenic region. However, when $P_{mra}3$ was present in a 100 bp fragment of the intergenic region it exhibited positive growth rate regulation, suggesting that DNA upstream of the $P_{mra}3$ promoter contains potentially important binding sites for proteins that respond to growth rate and which may mediate the inverse growth rate control of the $P_{mra}$ promoters. These results further supported our hypothesis that the $P_{mra}$ promoters were regulated by growth rate in order to increase expression of division proteins at a slower growth rate and smaller cell size.

## 5.2: Regulation of the $P_{mra}$ promoters by FIS.

FIS binds to four sites within the *fru*R-*yab*B intergenic region and was shown to bind within the promoter regions of both $P_{mra}2$ and $P_{mra}3$. We speculated that FIS may play a regulatory role at the $P_{mra}$ promoters that was linked to the inverse growth rate control, since FIS is expressed transiently during batch culture and is the most abundant transcriptional regulator during exponential growth (Travers *et al.*, 2001; Nasser *et al.*, 2002). FIS represses expression from the weak $P_{mra}2$ promoter, but had little effect on the expression from $P_{mra}3$, despite the presence of a FIS binding site between the -10 and -35 sequences of this promoter. We observed that FIS weakly activated expression from $P_{mra}1$, however we have been unable to predict a mechanism for the activation of this promoter since all four FIS binding sites are situated a considerable distance upstream. We therefore believe that FIS activation of $P_{mra}1$ is likely to be indirect, perhaps via FIS mediated changes in the supercoiling density of the $P_{mra}1$ promoter region. Although FIS repressed expression from $P_{mra}2$, it did not cause a major reduction in expression from $P_{mra}3$. We would have predicted that a mediator of inverse growth rate control would have repressed at least one of the $P_{mra}1$ or $P_{mra}3$ promoters since we determined these two promoters drive the majority of expression of the *mra* region, with each making a relatively equal contribution, during exponential growth. Our data suggest that FIS does not play a direct role in the inverse growth rate regulation of the $P_{mra}$ promoters. However, an indirect role in inverse growth rate regulation could be imagined, where FIS functions to repress the

expression of an activator, or to activate the expression of a repressor of the $P_{mra}$ promoters during exponential phase.

Although the expression data suggests that FIS does not play a significant, or direct role in the regulation of the two strongest promoters of the *mra* region ($P_{mra}1$ and $P_{mra}3$) it was observed that *fis* mutants exhibited a filamentous phenotype upon continued exponential growth, indicating a potentially important role in cell division. We determined that the transcription of *ftsZ* in a *fis* mutant was reduced compared to the control strain and that FtsZ levels were lower, particularly during exponential phase. However, when FtsZ levels were increased *in trans* the division defect was only partially rescued, suggesting that lower FtsZ levels were not responsible for the filamentation. We observed that the nucleoids in the filamentous *fis* cells were mis-segregated, the large masses of DNA that were produced may cause the observed filamentation due to nucleoid occlusion of potential division sites. Nucleoid mis-segregation may be a result of over-initiation of DNA replication, since FIS has been shown to be involved in the regulation of initiation of DNA replication at *oriC* (Ryan *et al.*, 2004). However, FIS is a pleiotropic global regulator and may regulate other factors that could also result in a division defect (Pratt *et al.*, 1997). For example, FIS may regulate the *ftsQAZ* promoters and any perturbation in the transcription of this region may result in a lack of division. In addition, if the expression of proteins recruited early to the septal ring (such as ZipA or FtsA) were altered by FIS-mediated transcriptional repression, then the septal ring may not form and FtsK may fail to localise to midcell where it is required to assist in DNA segregation (Bigot *et al.*, 2004).

## 5.3: Repression of $P_{mra}3$.

Of the three $P_{mra}$ promoters, the transcriptional regulation of $P_{mra}3$ was found to be the most interesting and complex. We discovered that $P_{mra}3$ was a very active promoter but was strongly repressed during exponential phase in the experimental conditions tested. We determined that the DNA upstream of $P_{mra}3$ was responsible for repressing transcription. Deletion of the DNA in the 400-500 bp region of the *fruR-yabB* intergenic sequence resulted in a 3-fold increase in transcription from $P_{mra}3$, indicating that an unidentified repressor binding site may be located in this region. We

investigated whether some of the most abundant transcriptional regulators were responsible for repression of $P_{mra}3$. However, there was little change in the expression from $P_{mra}3$ in *crp*, *ihf*, and *h-ns* mutants and no CRP or IHF binding sites were found within the entire *fru*R-*yab*B intergenic region despite several being suggested by bioinformatic predictions.

A search for proteins which could bind to the DNA of the intergenic region was utilised to identify potential regulators of the $P_{mra}$ promoters. At least 10 different protein:DNA complexes were observed from EMSAs using fractionated soluble protein lysate from a *fis* mutant, with *fru*R-*yab*B intergenic region DNA. The purification and identification of a single protein which bound to the 400-600 bp region was achieved. The protein was identified as the 50S subunit Ribosomal Protein L3, and we narrowed down the binding site to the 500-550 bp region, although it was not possible to footprint the protected region in the protein:DNA complex. We believe that ribosomal protein L3 binds specifically, but with low affinity to the intergenic region DNA. We therefore suggest that the interaction of L3 with the intergenic region is highly dynamic, with rapid dissociation and re-occupation of the binding site due to the predicted high concentration of L3 in the cell during rapid growth.

## 5.4: Ribosomal Protein L3 – A Potential Mediator of Growth Rate Regulation?

Ribosomal protein L3 has previously been shown to bind to DNA (Soultanas *et al*, 1998), however it has never been reported as a transcriptional regulator. Our data indicate that the binding site for L3 (between 500-550 bps) is located upstream of $P_{mra}3$, in a region which we have demonstrated is important for mediating the inverse growth rate regulation of the $P_{mra}$ promoters. Relatively little is known about how growth rate regulation is mediated in *E. coli* (Weart & Levin, 2003). However the number of ribosomes in the cell correlates with the growth rate of that cell, with high numbers during rapid growth and up to 10-fold fewer during slow growth (Lengeler and Postma, 1998). We assume that the majority of L3 is sequestered in the ribosomes, however during exponential phase there will be greater expression of ribosomal proteins and therefore potentially more 'free' L3 in the cell. We propose that during this phase of rapid growth, there may be sufficient ribosomal protein L3 to bind to the intergenic region DNA and repress transcription from the $P_{mra}$ promoters. The

mechanism of this transcriptional repression is unclear however the L3 binding site is located closest to $P_{mra}3$, therefore this may be the main target for repression. As growth slows on the approach to stationary phase, the expression of ribosomal proteins will be reduced. This may alleviate repression of the $P_{mra}$ promoters, resulting in greater transcription of the *mra* region - allowing increased expression of cell division proteins which are required to enable a decrease in cell size. We propose that ribosomal protein L3 may act as a growth rate controlled transcriptional repressor, which could represent the first identified factor directly linking growth rate and cell division in *E. coli*.

## 5.5: Regulation of the $P_{mra}3$ by ppGpp

The $P_{mra}3$ promoter region contains sequence similarity to the *r*RNA and *fis* promoter regions which are negatively regulated by the cellular alarmone ppGpp as part of the stringent response (Travers & Muskhelishvili, 2005). We showed that ppGpp repressed the transcriptional activity of $P_{mra}3$ 20-fold, as we had predicted from the presence of a GC-rich discriminator region within the promoter sequence. We have previously described that when $P_{mra}3$ is present in a 100 bp fragment it exhibits positive growth rate control. Since ppGpp increases on the approach to stationary phase, it is likely that ppGpp mediated repression is at least partly responsible for the positive growth rate regulation of $P_{mra}3$. However, when present in the full length intergenic region, $P_{mra}3$ is regulated inversely by growth rate. This may suggest that binding of a protein upstream makes RNAP bound at $P_{mra}3$ unresponsive to the effects of ppGpp – possibly by blocking entry of ppGpp into the RNAP holoenzyme.

## 5.6: Do the P*mra* promoters drive transcription of *fts*Z?

It has been suggested that the entire *mra* region may be co-transcribed (Mengin-Lecreulx *et al.*, 1998) and that 66% of *fts*Z transcription originates from $P_{mra}1$ (Flärdh *et al.*, 1998), however these experiments did not take into account any transcription originating upstream of $P_{mra}1$. Therefore we hoped to determine whether the majority of *fts*Z transcription originated from any of the three $P_{mra}$ promoters. Using reporter strains, we compared β-galactosidase expression patterns during batch culture, which indirectly measured the transcription of *yab*B (the first gene in the *mra* region) and

*ftsZ* (the fifteenth gene in the *mra* region). The patterns appeared to be different, particularly in exponential phase, suggesting that the two genes may not be co-transcribed. We also analysed FtsI and FtsZ expression patterns during batch culture, and again noticed a pronounced difference during exponential phase. These results indicated that the entire *mra* region may not be co-transcribed as previously suggested and that the $P_{mra}$ promoters may not contribute significantly to the majority of *ftsZ* transcription.

In an attempt to define the major promoter for *ftsZ* transcription we wanted to determine transcript lengths originating from the $P_{mra}$ promoters. We identified that all three $P_{mra}$ promoters produce transcripts that entered the *mra* region, and these were shown to span at least as far as *ftsL*. RT-PCR analysis also enabled us to detect an additional source of transcription originating from the 450-500 bp area of the *fruR-yabB* intergenic region, indicating that a fourth promoter ($P_{mra}4$) was located here. We could not detect a transcript spanning from the $P_{mra}$ promoters to *ftsZ*, therefore we attempted to find other sources of *ftsZ* transcription by determining whether other promoters existed within the *mra* region. Thirteen potential promoter regions were predicted by bioinformatic analysis of the *mra* region between *yabB* and *ddlB*. Only one of these potential promoters – $P_{ddlB}$, exhibited both binding to RNAP *in vitro* and significant promoter activity *in vivo*. $P_{ddlB}$ is situated immediately upstream of the *ftsQAZ* promoters and may make an important contribution to the transcription of *ftsQ*, A and Z. This work has been unable to confirm whether the $P_{mra}$ promoters contribute significantly to transcription of *ftsZ*, however we have shown that all four $P_{mra}$ promoters contribute to transcription entering the *mra* region. The identification of $P_{ddlB}$ also raises new questions about the regulation of *ftsZ*.

## 5.7: Project overview

Cell division in *E. coli* is a complex process requiring intricate regulation in order to co-ordinate the spatial and temporal initiation of septation with cell growth and the termination of DNA replication. We have investigated the regulation of the $P_{mra}$ promoters, which we have shown drive the transcription entering the *mra* region and have identified many direct and indirect forms of regulation at these promoters.

Many of the genes in the *mra* region are essential and it is therefore imperative that sufficient basal, constitutive expression of this region is maintained. The presence of multiple promoters upstream of the *mra* region may allow constitutive basal expression from one promoter, in addition to regulated expression from other promoters. This may enable the cell to fine tune expression of the *mra* region in response to external signals such a changes in growth rate or cell density whilst maintaining constitutive expression of the region. We have shown that the promoters $P_{mra}1$-3, are independently regulated, with $P_{mra}1$ and $P_{mra}3$ contributing the majority of transcription entering the *mra* region. We did not investigate the regulation of $P_{mra}4$ in depth since it was identified late in this work, however transcription from $P_{mra}4$ could repress the activity of downstream promoters by promoter occlusion - although initial experiments indicate that it is a relatively weak promoter. We have observed that $P_{mra}3$ is highly repressed by ppGpp and unidentified regulators. It may also be the target for potential growth rate regulation by ribosomal protein L3. We have shown that $P_{mra}2$ is a weak promoter that is repressed by FIS, while the activity of $P_{mra}1$ is constitutive with only slight changes in promoter activity in response to activation by FIS and inverse growth rate control. Our model for the transcriptional regulation of the $P_{mra}$ promoters is presented in Figure 5.7.

While it would be convenient to assign $P_{mra}1$ as a constitutive promoter, with $P_{mra}3$ providing the fine tuning and modulation of expression of the *mra* region, our data has shown that this simple scenario is not the case. We were unable to delete $P_{mra}3$ from the chromosome, indicating that its transcriptional contribution may be essential for cell viability. Therefore basal expression from $P_{mra}1$ may not be sufficient to support expression of the *mra* region and transcription originating from $P_{mra}3$ is also required. It is unclear why $P_{mra}3$ is so highly repressed, since its maximum activity could produce transcription levels greater than the combined transcription from all three $P_{mra}$ promoters when regulated. If $P_{mra}3$ was not repressed, the high level of transcription may cause promoter occlusion of downstream promoters and therefore regulation at these downstream promoters would be masked.

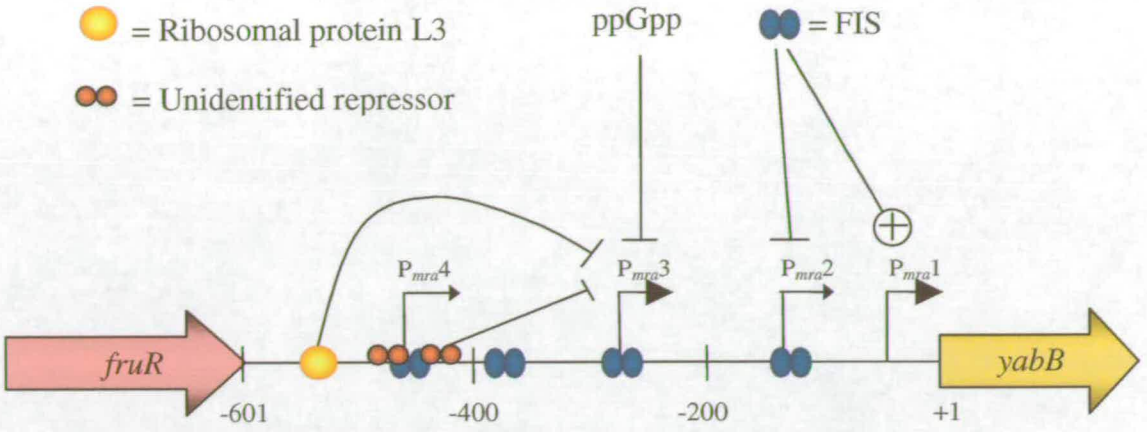


**Figure 5.7: Transcriptional Regulation of the $P_{mra}$ Promoters.**
All four $P_{mra}$ promoters contribute to transcription entering the *mra* region. $P_{mra}1$ is activated by FIS but responds inversely to growth rate, however neither of these forms of regulation cause a large change in $P_{mra}1$ promoter activity. $P_{mra}2$ is a weak promoter that is repressed by FIS. $P_{mra}3$ is a very strong promoter that is repressed under most circumstances. Transcription from $P_{mra}3$ is repressed by ppGpp and by an unidentified repressor which binds within the 400-500 bp fragment of the *fru*R-*yab*B intergenic region. Ribosomal protein L3 was shown to bind upstream of $P_{mra}3$ (between 500-550 bp) and we believe this may repress $P_{mra}3$ – or possibly any of the $P_{mra}$ promoters during exponential phase when there is sufficient free L3 protein in the cell. This may represent an important mechanism for mediating inverse growth rate regulation at the $P_{mra}$ promoters.

The multiple forms of regulation that we have identified at the $P_{mra}$ promoters indicate that a complex network of regulation governs the transcription entering the *mra* region (Figure 5.7). Each of the individual regulatory mechanisms has a potentially overlapping role in the growth rate control of the $P_{mra}$ promoters. Growth rate regulation is poorly understood in *E. coli*. Regulatory factors such as ppGpp and RpoS, which are transiently produced during batch culture, have previously been shown to be involved in growth rate regulation. This has been best studied at the rRNA promoters, where ppGpp represses the *rrn*B P1 promoter during the stringent response and on the approach to stationary phase (Josiatis *et al.*, 1995). However, when the *rrn*B P1 promoter was mutated and made insensitive to ppGpp it still exhibited growth rate control (Josiatis *et al.*, 1995). This indicates that although ppGpp contributes to growth rate control it is not the main effector of this mode of regulation. Regulation at the *rrnB* P1 promoter is under positive growth rate control which contrasts with our observations of the $P_{mra}$ promoters. In particular it raises the question, why is $P_{mra}3$ repressed by ppGpp when transcription from the $P_{mra}$ promoters is inversely regulated by growth rate? We have found that $P_{mra}3$ may be essential for viability, therefore we would imagine that transcription originating from

here is important during both fast and slow growth. We have also shown that $P_{mra}3$ exhibits inverse growth rate control when present in the full length *fru*R-*yab*B intergenic region. One possible explanation is that RNAP bound at $P_{mra}3$ is made unresponsive to ppGpp, perhaps by binding of an additional protein near $P_{mra}3$ which interacts with RNAP and blocks the access of ppGpp to the holoenzyme.

Inverse growth rate control has previously been investigated at the promoters of *fts*Q, A and Z (Aldea, *et al.*, 1990). It had been observed that transcription of *fts*Q, A and Z increased on the approach to stationary phase, indicative of inverse growth rate regulation (Aldea, *et al.*, 1990; Vicente *et al.*, 1991). It was found that the so called "gearbox" promoter pQ1 was recognised by $\sigma^S$ in addition to $\sigma^{70}$ and was induced during the growth transition on approach to stationary phase (Aldea *et al.*, 1990; Vicente *et al.*, 1991). The mediator of growth rate control at pQ1is RpoS. RpoS expression is upregulated during the growth transition between exponential and stationary phase by quorum sensing, changes in nutrient availability, and multiple other cellular stresses (Hengge-Aronis, 2002). Like ppGpp, RpoS plays an important role in growth rate control but is itself induced by the change of growth rate. RpoS therefore does not represent the direct link between the change in growth rate and regulation of the *fts*Q, A, Z promoters.

Although growth rate regulation at the rRNA and pQ1 promoters has been well studied, a direct mediator of this regulation, that is produced solely in response to a change in growth rate rather than in response to nutrient availability or cell density, has yet to be identified. We believe that this work may have identified such a factor in Ribosomal protein L3. Our hypothesis is that during exponential growth, when there are over 20,000 ribosomes in the cell, there may be sufficient "free" L3 in the cell to transiently bind to the intergenic region and repress transcription from the $P_{mra}$ promoters. We suggest that this repression is most likely to occur at the highly regulated promoter $P_{mra}3$ which is proximal to the L3 binding region. Ribosomal protein L3 is encoded by *rpl*C, the second gene in the S10 operon - a conserved operon of 11 genes encoding ribosomal proteins (Zurawski & Zurawski, 1985; Allen *et al.*, 2004). Unlike the intricate regulation at the rRNA promoters, the S10 operon is transcribed from a single promoter and is autoregulated by ribosomal protein L4, encoded by *rpl*D (Worbs *et al.*, 2000; Allen *et al.*, 2004). Ribosomal protein L4

inhibits both the transcription and translation of the S10 operon via interactions with the 172 bp un-translated leader sequence of the S10 mRNA (Allen *et al.*, 2004). Whenever L4 concentration exceeds that required for ribosome synthesis, it binds to a hairpin structure in the S10 leader sequence which promotes transcription termination and inhibits translation initiation (Yanofsky, 2000). This tight regulation of r-protein synthesis may contradict our hypothesis, since only enough ribosomal proteins are made to meet the ribosomal demand of the cell. Therefore there may not be sufficient L3 available, even during rapid growth, at a concentration high enough for interactions with the intergenic region DNA, due to the low affinity of L3 for its binding site. However, *rplC* is not overlapped by its flanking genes and it contains its own RBS, therefore it is not translationally coupled to upstream genes (Zurawski & Zurawski, 1985). This might ensure that there is significant production of L3 for some time following repression of the S10 operon by L4. Ribosomal protein L3 has previously been shown to bind DNA (Soultanas, *et al.*, 1998) and since there have been no reports of the concentration of "free" L3 in the cell during batch culture, our prediction that L3 may represent the first mediator of growth rate that is directly linked to the growth rate and size of the cell is feasible and is potentially very exciting.

This work has only focused on the transcriptional regulation of the *mra* region – in particular at the $P_{mra}$ promoters. However there are many other forms of regulation likely to be important within this region that we have not investigated. For example, each of the $P_{mra}$ promoters ($P_{mra}$1-3) is located a significant distance from the translational start site of *yab*B, resulting in long leader sequences (44, 135, 271 bp respectively). Leader sequences are well known to be involved in attenuation of transcription in bacteria, one of the best studied is the *trp* operon leader sequence (Yanofsky *et al.*, 1996). Depending on the $tRNA^{Trp}$ availability, appropriate RNA structures form in the *trp* operon leader transcript to determine whether transcription is either terminated or allowed to continue into the *trp* operon (Yanofsky, 2004). When sufficient tryptophan is present, the leader sequence is rapidly translated and sections of the leader mRNA form a transcriptional terminator, reducing further expression of the operon. If tryptophan is lacking, the translating ribosome stalls at one of two Trp codons in the leader sequence. This prevents the formation of an intrinsic terminator, allowing transcription to proceed into the operon (Yanofsky, 2004). There are no obvious transcriptional terminators within the $P_{mra}$ leader

sequences or in *yab*B – the first gene of the *mra* region. However, we experienced problems with both PCR and primer extension reactions using this region of DNA, suggesting there may be a problem with annealing of primers or extension of the reactions. This may indicate that some RNA secondary structure may be present in this region. Therefore attenuation of transcription may potentially play a role in regulation of the *mra* region. A potential feedback mechanism, maybe mediated by the as yet undefined product of *yab*B, could exist to maintain expression of the *mra* region in particular during exponential growth when a basal level of expression appears to be maintained.

This thesis has only begun to unravel the complex network of regulation that controls transcription from the $P_{mra}$ promoters and it has raised many new questions and potential avenues for future work. It would be of particular interest to determine whether ribosomal protein L3 is a *bona fide* mediator of growth rate control, since regulation by growth rate is so poorly understood in *E. coli*. In addition, it would be very useful to replace $P_{mra}1$ and $P_{mra}3$ on the chromosome with inducible promoters – as attempted in chapter 3, to investigate their individual roles during batch culture. The regulation of $P_{ddlB}$ may have important implications for the transcription of *fts*Q, A and Z and the relative contribution it makes to transcription of these genes should be determined. We identified 10 different protein:DNA complexes between the *fru*R-*yab*B intergenic region and soluble proteins in an exponential phase lysate. Identification of these proteins could provide interesting insights into potential mechanisms of regulation at the $P_{mra}$ promoters. Identification of proteins which bind to the *fru*R-*yab*B intergenic region, in a lysate prepared from a culture during the exponential to stationary phase growth transition, may also prove fruitful in identifying important regulators of the $P_{mra}$ promoters.

**Aarsman, M. E. G., A. Piette, C. Fraipont, T. M. F. Vinkenvleugel, M. Nguyen-Distèche, and T. den Blaauwen.** (2005) Maturation of the *Escherichia coli* divisome occurs in two steps. *Mol Microbiol* **55** (6): 1631-1645.

**Addinall, S. G., and J. Lutkenhaus.** (1996) FtsA Is Localized to the Septum in an FtsZ-Dependent Manner. *J Bacteriol* **178** (24): 7167-7172.

**Addinall, S. G., E. Bi, and J. Lutkenhaus.** (1996) FtsZ Ring Formation in *fts* Mutants. *J Bacteriol* **178** (13): 3877-3884.

**Addinall, S. G., C. Cao, and J. Lutkenhaus.** (1997) FtsN, a late recruit to the septum in *Escherichia coli. Mol Microbiol* **25** (2): 303-309.

**Aiyer, S. E., S. M. McLeod, W. Ross, C. A. Hirvonen, M. S. Thomas, R. C. Johnson, and R. L. Gourse.** (2002) Architecture of Fis-activated Transcription Complexes at the *Escherichia coli rrnB* P1 and *rrnE* P1 Promoters. *J Mol Biol* **316**: 501-516.

**Aldea, M., T. Garrido, J. Pla, and M. Vicente.** (1990) Division genes in *Escherichia coli* are expressed co-ordinately to cell-septum requirements by gearbox promoters. *EMBO J* **9** (11): 3787-3794.

**Allen, T. D., T. Watkins, L. Lindahl, and J. M. Zengel.** (2004) Regulation of Ribosomal Protein Synthesis in *Vibrio cholerae*. *J Bacteriol* **186** (17): 5933-5937.

**Anderson, D. E., F. J. Gueiros-Filho, and H. P. Erickson.** (2004) Assembly Dynamics of FtsZ Rings in *Bacillus subtilis* and *Escherichia coli* and Effects of FtsZ-Regulating Proteins. *J Bacteriol* **186** (17): 5775-5781.

**Ansari, A., M. L. Chael, and T. V. O'Halloran.** (1992) Allosteric underwinding of DNA is a critical step in positive control of transcription by Hg-MerR. *Nature* **355**: 87-89.

**Arfin, S. M., A. D. Long, E. T. Ito, L. Tolleri, M. M. Riehle, E. S. Paegle, and G. W. Hatfield.** (2000) Global gene expression profiling in *Escherichia coli* K12. The effects of integration host factor. *J Biol Chem* **275** (38): 29672-29684.

**Auner, H., M. Buckle, A. Deufel, T. Kutateladze, L. Lazarus, R. Mavathur, G. Muskhelishvili, I. Pemberton, R. Schneider, and A. Travers.** (2003) Mechanism of Transcriptional Activation by FIS: Role of Core Promoter Structure and DNA Topology. *J Mol Biol* **331**: 331-344.

**Azam, T. A., and A. Ishihama.** (1999) Twelve species of the nucleoid-associated protein from *Escherichia coli*. Sequence recognition specificity and DNA binding affinity. *J Biol Chem* **274** (46): 33105-13.

**Azam, T. A., S. Hiraga, and A. Ishihama.** (2000) Two types of localization of the DNA-binding proteins within the *Escherichia coli* nucleoid. *Genes Cells* **5** (8): 613-626.

**Ballesteros, M., S. Kusano, A. Ishihama, and M. Vicente.** (1998) The *ftsQ1p* gearbox promoter of *Escherichia coli* is a major sigma S-dependent promoter in the *ddlB-ftsA* region. *Mol Microbiol* **30** (2): 419-430.

**Barker, M. M., T. Gaal, C. A. Josaitis, and R. L. Gourse.** (2001a) Mechanism of Regulation of Transcription Initiation by ppGpp. I. Effects of ppGpp on Transcription Initiation *in Vivo* and *in Vitro*. *J Mol Biol* **305**: 673-688.

**Barker, M. M., T. Gaal, and R. L. Gourse.** (2001b) Mechanism of Regulation of Transcription Initiation by ppGpp. II. Models for Positive Control Based on Properties of RNAP Mutants and Competition for RNAP. *J Mol Biol* **305**: 689-702.

**Begg, K. J., B. G. Spratt, and W. D. Donachie.** (1986) Interaction between Membrane Proteins PBP3 and RodA Is Required for Normal Cell Shape and Division in *Escherichia coli*. *J Bacteriol* **167** (3): 1004-1008.

**Begg, K. J., S. J. Dewar, and W. D. Donachie.** (1995) A New *Escherichia coli* Cell Division Gene *ftsK*. *J Bacteriol* **177** (21): 6211-6222.

**Begg, K. J., Y. Nikolaichik, N. Crossland, and W. D. Donachie.** (1998) Roles of FtsA and FtsZ in activation of division sites. *J Bacteriol* **180** (4): 881-884.

**Bernhardt, T. G., and P. A. J. de Boer.** (2003) The *Escherichia coli* amidase AmiC is a periplasmic septal ring component exported via the twin-arginine transport pathway. *Mol Microbiol* **48** (5): 1171-1182.

**Bernhardt, T. G., and P. A. J. de Boer.** (2004) Screening for synthetic lethal mutants in *Escherichia coli* and identification of EnvC (YibP) as a periplasmic septal ring factor with murein hydrolase activity. *Mol Microbiol* **52** (5): 1255-1269.

**Bernhardt, T. G., and P. A. J. de Boer.** (2005) SlmA, a Nucleoid-Associated, FtsZ Binding Protein Required for Blocking Septal Ring Assembly over Chromosomes in *E. coli*. *Mol Cell* **18**: 555-564.

**Bigot, S., J. Corre, J.-M. Louarn, F. Cornet, and F.-X. Barre.** (2004) FtsK activities in Xer recombination, DNA mobilization and cell division involve overlapping and separate domains of the protein. *Mol Microbiol* **54** (4): 876-880.

**de Boer, P. A. J., R. E. Crossley, and L. I. Rothfield.** (1989) A Division Inhibitor and a Topological Specficity Factor Coded for by the Minicell Locus Determine Proper Placement of the Division Septum in *Escherichia. coli*. *Cell* **56**: 641-649.

**de Boer, P. A. J., R. E. Crossley, A. R. Hand, and L. I. Rothfield.** (1991) The MinD protein is a membrane ATPase required for the correct placement of the *Escherichia coli* division site. *EMBO J* **10** (13): 4371-4380.

**Bokal, A. J., W. Ross, T. Gaal, R. C. Johnson, and R. L. Gourse.** (1997) Molecular anatomy of a transcription activation patch: FIS-RNA polymerase interactions at the *Escherichia coli rrnB* P1 promoter. *EMBO J* **16** (1): 154-162.

**Bolivar, F., R. L. Rodriguez, M. C. Betlach, H. W. Boyer.** (1977) Construction and characterization of new cloning vehicles. I. Ampicillin-resistant derivatives of the plasmid pM9. *Gene* **2** (2): 75-93.

**Botsford, J. L. and J. G. Harman.** (1992) Cyclic AMP in Prokaryotes. *Microbiol Revs* **56** (1): 100-122.

**Bouché, F., and J.-P. Bouché.** (1989) Genetic evidence that DicF, a second division inhibtor encoded by the *Escherichia coli dic*B operon, is probably RNA. *Mol Microbiol* **3** (7): 991-994.

**Boyle, D.S., M. M. Khattar, S. G. Addinall, J. Lutkenhaus, and W. D. Donachie.** (1997) *fts*W is an essential cell-division gene in *Escherichia coli*. *Mol Microbiol* **24** (6): 1263-1273.

**Bramhill, D., and C. M. Thompson.** (1994) GTP-dependent polymerisation of *Escherichia coli* FtsZ protein to form tubules. *Proc Natl Acad Sci USA* **91**: 5813-5817.

**Braeken, K., M. Moris, R. Daniels, J. Vanderleyden, and J. Michiels.** (2006) New horizons for (p)ppGpp in bacterial and plant physiology. *Trends Microbiol* **14** (1): 45-54.

**Brown, L., D. Gentry, T. Elliott, and M. Cashel.** (2002) DksA Affects ppGpp Induction of RpoS at a Translational Level. *J Bacteriol* **184** (16): 4455-4465.

**Browning, D. F., and S. J. W. Busby.** (2004) The Regulation of Bacterial Transcription Initiation. *Nature Revs* **2**: 1-9.

**Buddelmeijer, N., and J. Beckwith.** (2002) Assembly of cell division proteins at the *E. coli* cell center. *Curr Op Microbiol* **5**:553-557.

**Buddelmeijer, N., N. Judson, D. Boyd, J. J. Mekalanos, and J. Beckwith.** (2002) YgbQ, a cell division protein in *Escherichia coli* and *Vibrio cholerae*, localizes in codependent fashion with FtsL to the division site. *Proc Natl Acad Sci USA* **99** (9): 6316-6321.

**Buddelmeijer, N., and J. Beckwith.** (2004) A complex of the *Escherichia coli* cell division proteins FtsL, FtsB and FtsQ forms independently of its localization to the septal region. *Mol Microbiol* **52** (5): 1315-1327.

**Busby, S., and R. H. Ebright.** (1994) Promoter Structure, Promoter Recognition, and Transcription Activation in Prokaryotes. *Cell* **79**: 743-746.

**Busby, S.** (1999) Repressors and activators. Chapter 4: Prokaryotic Gene Expression. Edited by B.D. Hames and D. M. Glover. Oxford University Press.

**Bykowski, T., and A. Sirko.** (1998) Selected phenotypes of *ihf* mutants of *Escherihchia coli*. *Biochimie* **80** (12): 987-1001.

**Cam, K., G. Rome, H. M. Krisch, and J.-P. Bouché.** (1996) RNaseE processing of essential cell division genes mRNA in *Escherichia coli*. *Nuc Ac Res* **24** (15): 3065-3070.

**Caramel, A. and K. Schnetz.** (2000) Antagonistic control of the *Escherichia coli bgl* promoter by FIS and CAP *in vitro*. *Mol Microbiol* **36** (1): 85-92.

**Carson, M. J., J. Barondess, and J. Beckwith.** (1991) The FtsQ Protein of *Escherichia coli*: Membrane Topology, Abundance, and Cell Division Phenotypes Due to Overproduction and Insertion Mutations. *J Bacteriol* **173** (7): 2187-2195.

**Cashel, M., D. R. Gentry, V. J. Hernandez, and D. Vinella.** (1997) The Stringent Response. *E. coli & Salmonella – Cellular and Molecular Biology.* Edited by Neidhardt. 2nd Edition, Volume 1.

**Chang, D.-E., D. J. Smalley, and T. Conway.** (2002) Gene expression profiling of *Escherichia coli* growth transitions: an expanded stringent response model. *Mol Microbiol* **45** (2): 289-306.

**Chatterji, D., and A. K. Ojha.** (2001) Revisiting the stringent response, ppGpp and starvation signalling. *Curr Op Microbiol* **4**: 160-165.

**Chen, J. C., M. Minev, and J. Beckwith.** (2002) Analysis of *ftsQ* Mutant Alleles in *Escherichia coli*: Complementation, Septal Localization, and Recruitment of Downstream Cell Division Proteins. *J Bacteriol* **184** (3): 695-705.

**Clements, J. M., F. Coignard, I. Johnson, S. Chandler, S. Palan, A. Waller, J. Wijkmans, and M. G. Hunter.** (2002) Antibacterial Activities and Characterization of Novel Inhibitors of LpxC. *Antimicrob Agents Chemother* **46**(6): 1793-1799.

**Cooper, S., and C. E. Helmstetter.** (1968) Chromosome Replication and the Division Cycle of *Escherichia coli* B/r. *J Mol Biol* **31**: 519-540.

**Dai, K., and J. Lutkenhaus.** (1991) *ftsZ* Is an Essential Cell Division Gene in *Escherichia coli*. *J Bacteriol* **173** (11): 351 00-3506.

**Dai, K., and J. Lutkenhaus.** (1992) The proper Ratio of FtsZ to FtsA Is Required for Cell Division To Occur in *Escherichia coli*. *J Bacteriol* **174** (19): 6145-6151.

**Daniel, R. A., and J. Errington.** (2003) Control of Cell Morphogenesis in Bacteria: Two Distinct Ways to Make a Rod-Shaped Cell. *Cell* **113**: 767-776.

**D'Ari, R., A. Jaffe, P. Bouloc, and A. Robin.** (1988) Cyclic AMP and cell Division in *Escherichia coli*. *J Bacteriol* **170** (1): 65-70.

**Dewar, S. J., K. J. Begg., and W. D. Donachie.** (1992) Inhibition of Cell Division Initiation by and Imbalance in the Ratio of FtsA to FtsZ. *J Bacteriol* **174** (19): 6314-6316.

**Dewar, S. J., and W. D. Donachie.** (1993) Antisense Transcription of the *ftsZ-ftsA* Gene Junction Inhibits Cell Division in *Escherichia coli*. *J Bacteriol* **175** (21): 7097-7101.

**Dewar, S. J., and R. Dorazi.** (2000) Control of division gene expression in *Escherichia coli*. *FEMS Microbiol Letts* **187**: 1-7.

**Di Lallo, G., M. Fagioli, D. Barionov, P. Ghelardini, and L. Paolozzi.** (2003) Use of a two-hybrid assay to study the assembly of a complex multicomponent protein machinery: bacterial septosome differentiation. *Microbiol* **149**: 3353-3359.

**Donachie, W. D.** (1968) Relationship between Cell Size and Time of Initiation of DNA Replication. *Nature* **219**: 1077-1079.

**Donachie, W. D. , K. J. Begg, and M. Vicente.** (1976) Cell Length, cell growth, and cell division. *Nature* **264**: 328-333.

**Donachie, W. D.** (2001) Co-ordinate regulation of the *Escherichia coli* cell cycle or *The cloud of unknowing. Mol Microbiol* **40** (4): 779-785.

**Dorazi, R., and S. J. Dewar.** (2000) Membrane topology of the N-terminus of the *Escherichia coli* FtsK division protein. *FEBS Letts* **478**: 13-18.

**Dorman, C. J., and P. Deighan.** (2003) Regulation of gene expression by histone-like proteins in bacteria. *Curr Op Gen & Dev* **13**:179-184.

**Draper, G. C., N. McLennan, K. Begg, M. Masters, and W. D. Donachie.** (1998) Only the N-Terminal Domain of FtsK Functions in Cell Division. *J Bacteriol* **180** (17): 4621-4627.

**Eberhardt, C., L. Kuerschner, and D. S. Weiss.** (2003) Probing the Catalytic Activity of a Cell Division-Specific Transpeptidase In Vivo with β-Lactams. *J Bacteriol* **185** (13): 3726-3734.

**Edwards, D. H., and J. Errington.** (1997) The *Bacillus subtilis* DivIVA protein targets to the division septum and controls the site specificity of cell division. *Mol Microbiol* **24** (5): 905-915.

**Englard, S., and S. Seifter.** (1990) Precipitation techniques. *Methods Enzyymol* **182**: 285-300.

**van den Ent, F., L. Amos, and J. Löwe.** (2001) Bacterial ancestry of actin and tubulin. *Curr Op Microbiol* **4**: 634-638.

**Erickson, H. P.** (1995) FtsZ, a Prokaryotic Homolog of Tubulin? *Cell* **80**: 367-370.

**Errington, J., R. A. Daniel, and D.-J. Scheffers.** (2003) Cytokinesis in Bacteria. *Micro & Mol Biol Revs* **67** (1): 52-65.

**Feucht, A., I. Lucet, M. D. Yudkin, and J. Errington.** (2001) Cytological and biochemical characterization of the FtsA cell division protein of *Bacillus subtilis. Mol Microbiol* **40** (1): 115-125.

**Figueroa-Bossi, N., M. Guérin, R. Rahmouni, M. Leng and L. Bossi.** (1998) The supercoiling sensitivity of a bacterial tRNA promoter parallels its responsiveness to stringent control. *EMBO J* **17** (8): 2359-2367.

**Filutowicz, M., W. Ross, J. Wild, and R. L. Gourse.** (1992) Involvement of Fis protein in replication of the *Escherichia coli* chromosome. *J Bacteriol* **174** (2): 398-407.

**Finkel, S. E., and R. C. Johnson.** (1992) The Fis protein: it's not just for DNA inversion anymore. *Mol Microbiol* **6** (22): 3257-3265.

**Flärdh, K., T. Garrido, and M. Vicente.** (1997) Contribution of individual promoters in the *ddlB-ftsZ* region to the transcription of the essential cell-division gene *ftsZ* in *Escherichia coli*. *Mol Microbiol* **24** (5): 927-936.

**Flärdh, K., P. Palacios, and M. Vicente.** (1998) Cell Division genes *ftsQAZ* in *Escherichia coli* require distant *cis*-acting signals upstream of *ddl*B for full expression. *Mol Microbiol* **30** (2): 305-315.

**Francis, F., S. Ramirez-Arcos, H. Salimnia, C. Victor, and J. R. Dillon.** (2000) Organization and transcription of the division cell wall (*dcw*) cluster in *Neisseria gonorrhoeae*. *Gene* **251**: 141-151.

**Frantz, B., and T. V. O'Halloran.** (1990) DNA Distortion Accompanies Transcriptional Activation by the Metal-Responsive Gene-Regulatory Protein MerR. *Biochem* **29** (20): 4747-4751.

**Fu, X., Y.-L.Shih, Y. Zhang, and L. I. Rothfield.** (2001) The MinE ring required for proper placement of the division site is a mobile structure that changes its cellular location during the *Escherichia coli* division cycle. *Proc Natl Acad Sci USA* **98** (3): 980-985.

**de la Fuente, A., P. Palacios, and M. Vicente.** (2001) Transcription of the *Escherichia coli dcw* cluster: Evidence for distal upstream transcripts being involved in the expression of the downstream *ftsZ* gene. *Biochimie* **83**: 109-115.

**García-Lara, J., L. H. Shang, and L.I. Rothfield.** (1996) An Extracellular Factor Regulates Expression of *sdiA*, a Transcriptional Activator of Cell Division Genes in *Escherichia coli*. *J. Bacteriol* **178** (10): 2742-2748.

**Garrido, T., M. Sánchez, P. Palacios, M. Aldea, and M. Vicente.** (1993) Transcription of *ftsZ* oscillates during the cell cycle of *Escherichia coli*. *EMBO J* **12** (10): 3957-3965.

**Geissler, B., D. Elraheb, and W. Margolin.** (2003) A gain-of-function mutation in *fts*A bypasses the requirement for the essential cell division gene *zip*A in *Escherichia coli*. *Proc Natl Acad Sci USA* **100** (7): 4197-4202.

**Geissler, B., and W. Margolin.** (2005) Evidence for functional overlap among multiple bacterial cell division proteins compensating for the loss of FtsK. *Mol Microbiol* **58** (2): 596-612.

**Gentry, D. R., and M. Cashel.** (1996) Mutational analysis of the *Escherichia coli spoT* gene identifies distinct but overlapping regions involved in ppGpp synthesis and degradation. *Mol Microbiol* **19** (6): 1373-1384.

**Gervais, F. G., P. Phoenix, and G. R. Drapeau.** (1992) The *rcsB* Gene, a Positive Regulator of Colanic Acid Biosynthesis in *Escherichia coli*, Is Also an Activator of *ftsZ* Expression. *J Bacteriol* **174** (12): 3964-3971.

**Ghigo, J. –M., and J. Beckwith.** (2000) Cell Division in *Escherichia coli*: Role of FtsL Domains in Septal Localization, Function, and Oligomerization. *J Bacteriol* **182** (1): 116-129.

**Gill, D. R., G. F. Hatfull, and G. P. C. Salmond.** (1986) A new cell division operon in *Escherichia coli*. *Mol Gen Genet* **205**: 134-145.

**Gitai, Z., and L. Shapiro.** (2003) Bacterial cell division spirals into control. *Proc Natl Acad Sci USA* **100** (13): 7423-7424.

**Goehring, N. W., and J. Beckwith.** (2005) Diverse Paths to Midcell: Assembly of the Bacterial Cell Division Machinery. *Current Biology* **15**:R514-R526.

**González-Gil, G., R. Kahmann, and G. Muskhelishvili.** (1998) Regulation of *crp* transcription by oscillation between distinct nucleoprotein complexes. *EMBO J* **17** (10): 2877-2885.

**Goodman, S. D., N. J. Velten, Q. Gao, S. Robinson, and A. M. Segall.** (1999) *In vitro* selection of integration host factor binding site. *J Bacteriol* **181** (10): 3246-3255.

**Goosen, N., and P. van de Putte.** (1995) The regulation of transcription initiation by integration host factor. *Mol Microbiol* **16** (1): 1-7.

**Gross, M., I. Marianovsky, and G. Glaser.** (2006) MazG – a regulator of programmed cell death in *Escherichia coli*. *Mol Microbiol* **59** (2): 590-601.

**Gruber, T. M., and C. A, Gross.** (2003) Multiple Sigma Subunits and the Partitioning of Bacterial Transcription Space. *Ann Rev Microbiol* **57**: 441-466.

**Gueiros-Filho, F. J., and R. Losick.** (2002) A widely conserved bacterial cell division protein that promotes assembly of the tubulin-like protein FtsZ. *Genes & Dev.* **16**: 2544-2556.

**Hale, C. A., and P. A. J. de Boer.** (1997) Direct Binding of FtsZ to ZipA, an Essential Component of the Septal Ring Structure That Mediates Cell Division in *E. coli*. *Cell* **88**: 175-185.

**Hale, C. A., and P. A. J. de Boer.** (1999) Recruitment of ZipA to the Septal Ring of *Escherichia coli* Is Dependent on FtsZ and Independent of FtsA. *J Bacteriol* **181** (1): 167-176.

**Hale, C. A., A. C. Rhee, and P. A. J. de Boer.** (2000) ZipA-Induced Bundling of FtsZ Polymers Mediated by an Interaction between C-Terminal Domains. *J Bacteriol* **182** (18): 5153-5166.

**Hale, C. A., H. Meinhardt, and P. A. J. de Boer.** (2001) Dynamic localization cycle of the cell division regulator MinE in *Escherichia coli*. *EMBO J* **20** (7): 1563-1572.

**Hanamura, A., and H. Aiba.** (1991) Molecular mechanism of negative autoregulation of *Escherichia coli crp* gene. *Nuc Ac Res* **19** (16): 4413-4419.

**Hara, H., S. Yasuda, K. Horiuchi, and J. T. Park.** (1997) A Promoter for the First Nine Genes of the *Escherichia coli mra* Cluster of Cell Division and Cell Envelope Biosynthesis Genes, Including *fts*I and *fts*W. *J Bacteriol* **179** (18): 5802-5811.

**Hara, H., S. Narita, D. Karibian, J. T. Park, Y. Yamamoto and Y. Nishimura.** (2002) Identification and characterization of the *Escherichia coli envC* gene encoding a periplasmic coiled-coil protein with putative peptidase activity. *FEMS Microbiol Letts* **212**: 229-236.

**Harman, J. G.** (2001) Allosteric regulation of the cAMP receptor protein. *Biochim Biophys Acta* **1547**:1-17.

**Helmann, J. D.** (1999) Promoters, sigma factors, and variant RNA polymerases. Chapter 3: Prokaryotic Gene Expression. Edited by B. D. Hames and D. M. Glover. Oxford University Press.

**Hengen, P. N., S. L. Bartram, L. E. Stewart, and T. D. Schneider.** (1997) Information analysis of FIS binding sites. *Nuc Ac Res* **25** (24): 4994-5002.

**Hengge-Aronis, R.** (1999) Integration of control devices: A global regulatory network in *Escherichia coli*. Chapter 7: Prokaryotic Gene Expression. Edited by B. D. Hames and D. M. Glover. Oxford University Press.

**Hengge-Aronis, R.** (2002) Signal transduction and regulatory mechanisms involved in control of the sigma (S) (RpoS) subunit of RNA Polymerase. *Microbiol Mol Biol Rev* **66** (3): 373-95.

**Herwig, S., V. Kruft, and B. Wittman-Liebold.** (1992) Primary structures of ribosomal proteins L3 and L4 from *Bacillus stearothermophilus*. *Eur J Biochem* **207** (3): 877-885.

**Höltje, J.-V.** (1998) Growth of the Stress-Bearing and Shape-Maintaining Murein Sacculus of *Escherichia coli*. *Microbiol Mol Biol Revs* **62** (1): 181-203.

**Höltje, J.-V., and C. Heidrich.** (2001) Enzymology of elongation and constriction of the murein sacculus of *Escherichia coli*. *Biochimie* **83**: 103-108.

**Hsu, L. M.** (2002) Promoter clearance and escape in prokaryotes. *Biochim Biophys Acta* **1577** (2): 191-207.

**Hu, Z., and J. Lutkenhaus.** (1999) Topological regulation of cell division in *Escherichia coli* involves rapid pole to pole oscillation of the division inhibitor MinC under the control of MinD and MinE. *Mol Microbiol* **34** (1): 82-90.

**Hu, Z., A. Mukherjee, S. Pichoff, and J. Lutkenhaus.** (1999) The MinC component of the division site selection system in *Escherichia coli* interacts with FtsZ to prevent polymerisation. *Proc Natl Acad Sci USA* **96** (26): 14819-14824.

**Hu, Z., and J. Lutkenhaus.** (2000) Analysis of MinC Reveals Two Independent Domains Involved in Interaction with MinD and FtsZ. *J Bacteriol* **182** (14): 3965-3971.

**Hu, Z., and J. Lutkenhaus.** (2001) Topological Regulation of Cell Division in *E. coli*: Spatiotemporal Oscillation of MinD Requires Stimulation of Its ATPase by MinE and Phospholipid. *Mol Cell* **7**: 1337-1343.

**Hu, Z., and J. Lutkenhaus.** (2003) A conserved sequence at the C-terminus of MinD is required for binding to the membrane and targeting MinC to the septum. *Mol Microbiol* **47** (2): 345-355.

**Ichimura, T., M. Yamazoe, M. Maeda, C. Wada, and S. Hiraga.** (2002) Proteolytic Activity of YibP Protein in *Escherichia coli*. *J Bacteriol* **184** (10): 2595-2602.

**Ishizuka, H., A. Hanamura, T. Inada, and H. Aiba.** (1994) Mechanism of the down-regulation of cAMP receptor protein by glucose in *Escherichia coli*: role of autoregulation of the *crp* gene. *EMBO J* **13** (13): 3077-3082.

**Jishage, M., K. Kvint, V. Shingler, and T. Nyström.** (2002) Regulation of σ factor competition by the alarmone ppGpp. *Genes & Dev* **16**:1260-1270.

**Joseleau-Petit, D., D. Vinella, and R. D'Ari.** (1999) Metabolic Alarms and Cell Division in *Escherichia coli*. *J Bacteriol* **181** (1): 9-14.

**Khattar, M. M., S. G. Addinall, K. H. Stedul, D. S. Boyle, J. Lutkenhaus, and W. D. Donachie.** (1997) Two Polypeptide Products of the *Escherichia coli* Cell division Gene *fts*W and a Possible Role for FtsW in FtsZ Function. *J Bacteriol* **179** (3): 784-793.

**Kleckner, N., J. Bender, and S. Gottesman.** (1991) Uses of transposons with emphasis on Tn10. *Methods Enzymol* **204**: 139-180.

**Kolb, A., S. Busby, H. Buc, S. Garges, and S. Adhya.** (1993) Transcriptional Regulation by cAMP and its receptor protein. *Annu. Rev. Biochem* **62**: 749-95.

**Kolb, A., D. Kotlarz, S. Kusano, and A. Ishihama.** (1995) Selectivity of the *Escherichia coli* RNA polymerase E sigma 38 for overlapping promoters and ability to support CRP activation. *Nuc Ac Res* **23** (5): 819-26.

**Koppelman, C.-M., M. E. G. Aarsman, J. Postmus, E. Pas, A. O. Muijsers, D.-J. Scheffers, N. Nanninga, and T. den Blaauwen.** (2004) R174 of *Escherichia coli* FtsZ is involved in membrane interaction and protofilament bundling, and is essential for cell division. *Mol Microbiol* **51** (3): 645-657.

**Kvint, K. , C. Hosbond, A. Farewell, O. Nybroe, and T Nyström.** (2000) Emergency derepression: stringency allows RNA polymerase to override negative control by an active repressor. *Mol Microbiol* **35** (2): 435-443.

**Kvint, K., L. Nachin, A. Diez, and T. Nyström.** (2003) The bacterial universal stress protein:function and regulation. *Curr Op Microbiol* **6**:140-145.

**Lara, B., and J. A. Ayala.** (2002) Topological characterization of the essential *Escherichia coli* cell division protein FtsW. *FEMS Microbiol Letts* **2002**: 23-32.

**Lengeler, J. W., and P. W. Postma.** (1998) Chapter 20.3: The RelA/SpoT Modulon Controls Anabolic Pathways and Macromolecule Biosynthesis. Biology of Prokaryotes. Edited by J. Lengeler, G. Drews, and H. Schlegel. Blackwell Science.

**Li, M., H. Moyle, and M. M. Susskind.** (1994) Target of the Transcriptional Activation Function of Phage λ cI Protein. *Science* **263**: 75-77.

**Lloyd, G. S., W. Niu, J. Tebbutt, R. H. Ebright, and S. J. W Busby.** (2002) Requirement for two copies of RNA polymerase α subunit C-terminal domain for synergistic transcription activation at complex bacterial promoters. *Genes & Dev* **16**: 2557-2565.

**Löwe, J., and L. A . Amos.** (1998) Crystal structure of the bacterial cell-division protein FtsZ. *Nature* **391**: 203-206.

**Lu, C., J. Stricker, and H. P. Erickson.** (1998) FtsZ From *Escherichia coli, Azotobacter vinelandii,* and *Thermotoga maritima* – Quantitation, GTP Hydrolysis, and Assembly. *Cell Motil Cytoskel* **40**: 71-86.

**Lu, C., M. Reedy, and H. P. Erickson.** (2000) Straight and Curved Conformations of FtsZ Are Regulated by GTP Hydrolysis. *J Bacteriol* **182** (1): 164-170.

**Lui, Z., A. Mukherjee, and J. Lutkenhaus.** (1999) Recruitment of ZipA to the division site by interaction with FtsZ. *Mol Microbiol* **31** (6): 1853-1861.

**Lutkenhaus, J.** (1993) FtsZ ring in bacterial cytokinesis. *Mol Microbiol* **9** (3): 403-409.

**Lutkenhaus, J., and A. Mukherjee.** (1997) Cell Division. *Escherichia coli* and *Salmonella typhimurium* Cellular and Molecular Biology. (Edited by G. C. Neidhardt) pp1615-1626. American Society for Microbiology, Washington, DC.

**Lutkenhaus, J.** (2002) Dynamic proteins in bacteria. *Curr Op Microbiol* **5**: 548-552.

**Ma, H. S., H. J. Kim, H.-C. Lee, Y. Hong, J. H. Rhee, and H. E. Choy.** (2006) Immune response induced by *Salmonella typhimurium* defective in ppGpp synthesis. *Vaccine* **24** (12): 2027-2034.

**Ma, X., and W. Margolin.** (1999) Genetic and Functional Analyses of the Conserved C-Terminal Core Domain of *Escherichia coli* FtsZ. *J Bacteriol* **181** (24): 7531-7544.

**Malan, T. P., A. Kolb, H. Buc, and W. R. McClure.** (1984) Mechanism of CRP-cAMP Activation of *lac* Operon Transcription Initiation Activation of the P1 Promoter. *J Mol Biol* **180**: 881-909.

**Margolin, W.** (2000) Themes and variations in prokaryotic cell division. *FEMS Microbiol Revs* **24**: 531-548.

**Margolin, W.** (2001) Spatial regulation of cytokinesis in bacteria. *Curr Op Microbiol* **4**: 647-652.

**Marston, A. L., and J. Errington.** (1999) Selection of the midcell division site in *Bacillus subtilis* through MinD-dependent polar localization and activation of MinC. *Mol Microbiol* **33** (1): 84-96.

**McLeod, S. M., J. Xu, and R. C. Johnson.** (2000) Coactivation of the RpoS-Dependent *proP* P2 Promoter by Fis and Cyclic AMP Receptor Protein. *J Bacteriol* **182** (15): 4180-4187.

**McLeod, S. M., and R. C. Johnson.** (2001) Control of transcription by nucleoid proteins. *Curr Op Microbiol* **4**: 152-159.

**McLeod, S. M., S. E. Aiyar, R. L. Gourse, and R. C. Johnson.** (2002) The C-terminal Domains of the RNA Polymerase α Subunits: Contact Site with FIS and Localization during Co-activation with CRP at the *Escherichia coli proP* P2 Promoter. *J Mol Biol* **316**: 517-529.

**Mercer, K. L. N., and D. S. Weiss.** (2002) The *Escherichia coli* Cell Division Protein FtsW is Required To Recruit Its Cognate Transpeptidase, FtsI (PBP3), to the Division Site. *J Bacteriol* **184** (4): 904-912.

**Mengin-Lecreulx, D., J. Ayala, A. Bouhss, J. van Heijenoort, C. Parquet, and H. Hara.** (1998) Contribution of the $P_{mra}$ Promoter to Expression of Genes in the *Escherichia coli mra* Cluster of Cell Envelope Biosynthesis and Cell Division Genes. *J Bacteriol* **180** (17): 4406-4412.

**Merlin, C., S. McAteer, and M. Masters.** (2002) Tools for Characterization of *Escherichia coli* Genes of Unknown Function. *J Bacteriol* **184** (16): 4573-4581.

**Mingorance, J., S. Rueda, P. Gómez-Puertas, A. Valencia, and M. Vicente.** (2001) *Escherichia coli* FtsZ polymers contain mostly GTP and have a high nucleotide turnover. *Mol Microbiol* **41** (1): 83-91.

**Mooney, R. A., S. A Darst, and R. Landick.** (2005) Sigma and RNA Polymerase: An On-Again, Off-Again Relationship? *Mol Cell* **20**: 335-345.

**Mulder, E., and C. L. Woldringh.** (1989) Actively Replicating Nucleoids Influence Positioning of Division Sites in *Escherichia coli* Filaments Forming Cells Lacking DNA. *J Bacteriol* **171** (8): 4303-4314.

**Mukherjee, A., and W. D. Donachie.** (1990) Differential Translation of Cell Division Proteins. *J Bacteriol* **172** (10): 6106-6111.

**Mukherjee, A., and J. Lutkenhaus.** (1999) Analysis of FtsZ Assembly by Light Scattering and Determination of the Role of Divalent metal Cations. *J Bacteriol* **181** (3): 823-832.

**Muskhelishvili, G., M. Buckle, H. Heumann, R. Kahmann, and A. A. Travers.** (1997) FIS activates sequential steps during transcription initiation at a stable RNA promoter. *EMBO J* **16** (12): 3655-3665.

**Nanninga, N.** (1998) Morphogenesis of *Escherichia coli*. *Micro Mol Biol Revs* **62** (1): 110-129.

**Nasser, W., R. Schneider, A. Travers, and G. Muskhelishvili.** (2001) CRP Modulates *fis* Transcription by Alternate Formation of Activating and Repressing Nucleoprotein Complexes. *J Biol Chem* **276** (21): 17878-17886.

**Nasser, W., M. Rochman, and G. Muskhelishvili.** (2002) Transcriptional regulation of *fis* operon involves a module of multiple coupled promoters. *EMBO J* **4**: 715-724.

**Navarro, F., A. Robin, R. D'Ari, and D. Joseleau-Petit.** (1998) Analysis of the effect of ppGpp on the *ftsQAZ* operon in *Escherichia coli*. *Mol Microbiol* **29** (3): 815-823.

**Nguyen-Distèche, M., C. Fraipont, B. Buddelmeijer, and N. Nanninga.** (1998) The structure and function of *Escherichia coli* penicillin-binding protein 3. *Cell Mol Life Sci* **54**: 309-316.

**Nickels, B. E., and A. Hochschild.** (2004) Regulation of RNA Polymerase through the Secondary Channel. *Cell* **118**: 281-284.

**Ohlsen, K. L., and J. D. Gralla.** (1992) Interrelated effects of DNA supercoiling, ppGpp, and low salt on melting within the *Escherichia coli* ribosomal RNA *rrnB* P1 promoter. *Mol Microbiol* **6** (16): 2243-2251.

**Paget, M. S. B., and J. D. Helmann.** (2003) The $\sigma^{70}$ family of sigma factors. *Genome Biology* **4**:203.

**Pastoret, S., C. Fraipont, T. den Blaauwen, B. Wolf, M. E. G. Aarsman, A. Piette, A. Thomas, R. Brasseur, and M. Nguyen-Distèche.** (2004) Functional Analysis of the Cell Division Protein FtsW of *Escherichia coli*. *J Bacteriol* **186** (24): 8370-8379.

**Paul, B. J., M. M. Barker, W. Ross, D. A. Schneider, C. Webb, J. W. Foster, and R. L. Gourse.** (2004) DksA: A Critical Component of the Transcription Initiation Machinery that Potentiates the Regulation of rRNA Promoters by ppGpp and the Initiating NTP. *Cell* **118**: 311-322.

**de Pedro, M. A., J. C. Quintela, J.-V. Höltje, and H. Schwarz.** (1997) Murein Segregation in *Escherichia coli*. *J Bacteriol* **179** (9): 2823-2834.

**de Pedro, M. A., W. D. Donachie, J.-V. Höltje, and H. Schwarz.** (2001) Constitutive Septal Murein Synthesis in *Escherichia coli* with Impaired Activity of the Morphogenetic Proteins RodA and Penicillin-Binding Protein 2. *J Bacteriol* **183** (14): 4115-4126.

**Pemberton, I. K., G. Muskhelishvili, A. A. Travers, and M. Buckle.** (2000) The G+C-rich discriminator region of the *tyr*T promoter antagonises the formation of stable preinitiation complexes. *J Mol Biol* **299** (4): 859-864.

**Perederina, A., V. Svetlov, M. N. Vassylyeva, T. H. Tahirov, S. Yokoyama, I. Artsimovich, and D. G. Vassylyev.** (2004) Regulation through the Secondary Channel – Structure Framework for ppGpp-DksA Synergism during Transcription. *Cell* **118**: 297-309.

**Petrov, A., A. Meskauskas, J. D. Dinman.** (2004) Ribosomal Protein L3. *RNA Biol* **1** (1): 59-65.

**Pichoff, S., and J. Lutkenhaus.** (2002) Unique and overlapping roles for ZipA and FtsA in septal ring assembly in *Escherichia coli*. *EMBO J* **21** (4): 685-693.

**Pichoff, S., and J. Lutkenhaus.** (2005) Tethering the Z ring to the membrane through a conserved membrane targeting sequence in FtsA. *Mol Microbiol* **55** (6): 1722-1734.

**Pla, J., A. Dopazo, and M. Vicente.** (1990) The Native Form of FtsA, a Septal Protein of *Escherichia coli*, Is Located in the Cytoplasmic Membrane. *J Bacteriol* **172** (9): 5097-5102.

**Pla, J., P. Palacios, M. Vicente, and M. Aldea.** (1991) Preferential cytoplasmic location of FtsZ, a protein essential for *Escherichia coli* septation. *Mol Microbiol* **5** (7): 1681-1686.

**Pratt, T. S., T. Steiner, L. S. Feldman, K. A. Walker, and R. Osuna.** (1997) Deletion Analysis of the *fis* Promoter Region in *Escherichia coli*: Antagonistic Effects of Integration Host Factor and Fis. *J Bacteriol* **179** (20): 6367-6377.

**Rafaelle, M., E. I. Kanin, J. Vogt, R. R. Burgess, and A. Z. Ansari.** (2005) Holoenzyme Switching and Stochastic Release of Sigma Factors from RNA Polymerase In Vivo. *Mol Cell* **20**: 357-366.

**Raskin, D. M., and P. A. J. de Boer.** (1999a) Rapid pole-to-pole oscillation of a protein required for directing division to the middle of *Escherichia coli*. *Proc Natl Acad Sci USA* **96**: 4971-4976.

**Raskin, D. M., and P. A. J. de Boer.** (1999b) MinDE-Dependent Pole-to Pole Oscillation of Division Inhibitor MinC in *Escherichia coli*. *J Bacteriol* **181** (20): 6419-6424.

**Redick, S. D., J. Stricker, G. Briscoe, and H. P. Erickson.** (2005) Mutants of FtsZ Targeting the Protofilament Interface: Effects on Cell Division and GTPase Activity. *J Bacteriol* **187** (8): 2727-2736.

**Ricard, M., and Y. Hirota.** (1973) Process of Cellular Division in *Escherichia coli*: Physiological Study on Thermosensitive Mutants Defective in Cell Division. *J Bacteriol* **116** (1): 314-322.

**Rice, P. A., S. Yang, K. Mizuuchi, and H. A. Nash.** (1996) Crystal structure of an IHF-DNA complex: a protein-induced DNA U-turn. *Cell* **87** (7): 1295-1306.

**Robison, K., A. M. McGuire, and G. M. Church.** (1998) A comprehensive library of DNA-binding site matrices for 55 proteins applied to the complete *Escherichia coli* K-12 genome. *J Mol Biol* **284** (2): 241-254.

**Rodionov, D. G., and E. E. Ishiguro.** (1995) Direct Correlation between Overproduction of Guanosine 3', 5'-Bispyrophosphate (ppGpp) and Penicillin Tolerance in *Escherichia coli. J Bacteriol* **177** (15): 4224-4229.

**Romberg, L., and P. A. Levin.** (2003) Assembly Dynamics of the Bacterial Cell Division Protein FtsZ: Poised at the Edge of Stability. *Ann Rev Microbiol* **57**: 125-154.

**Roth, E. H., and K. H. Nierhaus.** (1980) Assembly map of the 50-S subunit from *Escherichia coli* ribosomes, covering the proteins present in the first reconstitution intermediate particle. *Eur J Biochem* **103** (1): 95-98.

**Rothfield, L., A. Taghbalout, and Y.-L. Shih.** (2005) Spatial control of bacterial division-site placement. *Nat Revs Microbiol* **3**: 959-968.

**Rueda, S., M. Vicente, and J. Mingorance.** (2003) Concentration and Assembly of the Division Ring Proteins FtsZ, FtsA, and ZipA during the *Escherichia coli* Cell Cycle. *J Bacteriol* **185** (11): 3344-3351.

**Ryan, V. T., J. E. Grimwade, J. E. Camara, E. Crooke, and A. C. Leonard.** (2004) *Escherichia coli* prereplication complex assembly is regulated by dynamic interplay among Fis, IHF and DnaA. *Mol Microbiol* **51** (5): 1347-1359.

**Saier, M. H., T. M. Ramseier, and J. Reizer.** (1997) Regulation of Carbon Utilization. *E. coli & Salmonella – Cellular and Molecular Biology.* Edited by Neidhardt. 2nd Edition.

**Saleh, O. A., C. Pérals, F.-X. Barre, and J.-F. Allermand.** (2004) Fast, DNA-sequence independent translocation by FtsK in a single-molecule experiment. *EMBO J* : 1-10.

**Sánchez, M., A. Valencia, M. –J, Ferrándiz. C. Sander, and M. Vicente.** (1994) Correlation between the structure and biochemical activities of FtsA, an essential cell division protein of the actin family. *EMBO J* **13** (20): 4919-4925.

**Schaechter, M., O. Maaloe, and N. O. Kjeldgaard.** (1958) Dependency on medium and temperature of cell size and chemical composition during balanced growth of *Salmonella typhimurium. J Gen Microbiol* **19** (3): 592-606.

**Schmidt, K. L., N. D. Peterson., R. J. Kustusch, M. C. Wissel, B. Graham, G. J. Phillips, and D. S. Weiss.** (2004) A Predicted ABC Transporter, FtsEX, Is Needed for Cell Division in *Escherichia coli. J Bacteriol* **186** (3): 785-793.

**Schneider, R., A. Travers, T. Kutateladze, and G. Muskhelishvili.** (1999) A DNA architectural protein couples cellular physiology and DNA topology in *Escherichia coli. Mol Microbiol* **34** (5): 953-964.

**Schneider, R., A, Travers, and G. Muskhelishvili.** (2000) The expression of the *Escherichia coli fis* gene is strongly dependent on the superhelical density of DNA. *Mol Microbiol* **38** (1): 167-175.

**Schröder, I., S. Darie, and R. P. Gunsalus.** (1993) Activation of the *Escherichia coli* Nitrate Reductase (*narGHIJ*) Operon by NarL and Fnr Requires Integration Host Factor. *J Biol Chem* **268** (2): 771-774.

**Schroder, O., and R. Wagner.** (2000) The bacterial DNA-binding protein H-NS represses ribosomal RNA transcription by trapping RNA polymerase in the initiation complex. *J Mol Biol* **298** (5): 737-748.

**Shih, Y.-L., T. Le, and L. Rothfield.** (2003) Division site selection in *Escherichia coli* involves dynamic redistribution of Min proteins within coiled structures that extend between the two cell poles. *Proc Natl Acad Sci USA* **100** (13): 7865-7870.

**Simons, R. W., F. Houman, and N. Kleckner** (1987) Improved single and multicopy *lac*-based cloning vectors for protein and operon fusions. *Gene* **53** (1): 85-96.

**Snyder, L., and W. Champness.** (1997) Chapter 12: Global Regulatory Mechanisms, Molecular Genetics of Bacteria. ASM Press

**Soultanas, P., M. S. Dillingham, and D. B. Wigley.** (1998) *Escherichia coli* ribosomal protein L3 stimulates the helicase activity of the *Bacillus stearothermophilus* PcrA helicase. *Nuc Ac Res* **26** (10): 2374-2379.

**Steiner, W., G. Liu, W. D. Donachie, and P Kuempel.** (1999) The cytoplasmic domain of FtsK protein is required for resolution of chromosome dimers. *Mol Microbiol* **31** (2): 579-583.

**Stewart, G. C.** (2005) Taking shape: control of bacterial cell wall biosynthesis. *Mol Microbiol* **57** (5): 1177-1181.

**Stricker, J., P. Maddox, E. D. Salmon, and H. P. Erickson.** (2002) Rapid assembly dynamics of the *Escherichia coli* FtsZ-ring demonstrated by fluorescence recovery after photobleaching. *Proc Natl Acad Sci USA* **99** (5): 3171-3175.

**Sun, Q., and W. Margolin,** (1998) FtsZ Dynamics during the Division Cycle of Live *Escherichia coli* Cells. *J Bacteriol* **180** (8): 2050-2056.

**Sun, Q., X.-C. Yu, and W. Margolin.** (1998) Assembly of the FtsZ ring at the central division site in the absence of the chromosome. *Mol Microbiol* **29** (2): 491-503.

**Tagami, H., and H. Aiba.** (1995) Role of CRP in transcription activation at *Escherichia coli lac* promoter: CRP is dispensable after the formation of open complex. *Nuc Ac Res* **23**(4): 599-605.

**Takada, A., M. Wachi, and K. Nagai.** (1999) Negative Regulatory Role of the *Escherichia coli hfq* Gene in Cell Division. *Biochem Biophys Res Comms* **266**: 579-583.

**Takada, A., K. Nagai, and M. Wachi.** (2005) A decreased level of FtsZ is responsible for inviability of RNaseE-deficient cells. *Genes to Cells* **10**: 733-741.

**Taschner, P. E. M., P. G. Huls, E. Pas, and C. L. Woldringh.** (1988) Division Behavior and Shape Changes in Isogenic *fts*Z, *fts*Q, *fts*A, *pbp*B, and *fts*E Cell Division Mutants of *Escherichia coli* during Temperature Shift Experiments. *J Bacteriol* **170** (4): 1553-1540.

**Tétart, F., and J. –P. Bouché.** (1992) Regulation of the expression of the cell-cycle gene *fts*Z by DicF antisense RNA. Division does not require a fixed number of FtsZ molecules. *Mol Microbiol* **6** (5): 615-620.

**Travers, A., R. Schneider, and G. Muskhelishvili.** (2001) DNA supercoiling and transcription in *Escherichia coli*: The FIS connection. *Biochimie* **83**: 213-217.

**Travers, A., and G. Muskhelishvili.** (2005) DNA Supercoiling – A Global Transcriptional Regulator for Enterobacterial Growth. *Nat Revs Microbiol* **3**: 157-169.

**Traxler, M. F., D. E. Chang, and T. Conway.** (2006) Guanosine 3′, 5′-bispyrophosphate coordinates global gene expression during glucose-lactose diauxie in *Escherichia coli*. *PNAS* **103** (7): 2374-2379.

**Topping, T. B., D. A. Hoch, and L. M. Gloss.** (2004) Folding Mechanism of FIS, the Intertwined, Dimeric Factor for Inversion Stimulation. *J Mol Biol* **335**: 1065-1081.

**Ursinus, A., F. van den Ent, S. Brechtel, M. de Pedro, J.-V. Höltje, J. Löwe, and W. Vollmer.** (2004) Murein (Peptidoglycan) Binding Property of the Essential Cell Division Protein FtsN from *Escherichia coli*. *J Bacteriol* **186** (20): 6728-6737.

**Varma, A., and K. D. Young.** (2004) FtsZ Collaborates with Penicillin Binding Proteins To Generate Bacterial Cell Shape in *Escherichia coli*. *J Bacteriol* **186** (20): 6768-6774.

**Vicente, M., S. R. Kushner, T. Garrido, M. Aldea.** (1991) The role of the 'gearbox' in the transcription of essential genes. *Mol Microbiol* **5** (9): 2085-2091.

**Vicente, M., M. J. Gomez, and J. A. Ayala.** (1998) Regulation of transcription of cell division genes in the *Escherichia coli dcw* cluster. *Cell Mol Life Sci* **54**: 317-324.

**Vinella, D., C. Albrecht, M. Cashel, and R. D'Ari.** (2005) Iron limitation induces SpoT-dependent accumulation of ppGpp in *Escherichia coli*. *Mol Microbiol* **56** (4): 958-970.

**Vrentas, C. E., T. Gaal, W. Ross, R. Ebright, and R. L. Gourse.** (2005) Response of RNA polymerase to ppGpp: requirement for the ω subunit and relief of this requirement by DksA. *Genes & Dev* **19**: 2378-2387.

**Wang, L., M. M. Khattar, W. D. Donachie, and J. Lutkenhaus.** (1998) FtsI and FtsW Are Localised to the Septum in *Escherichia coli*. *J Bacteriol* **180** (11): 2810-2816.

**Wang, J., A. Galgoci, S. Kodali, K. B. Herath, H. Jayasuriya, K. Dorso, F. Vicente, A. Gonzalez, D. Cully, D. Bramhill, and S. Singh.** (2003) Discovery of a small molecule that inhibits cell division by blocking FtsZ, a novel therapeutic target of antibiotics. *J Biol Chem* **278** (45): 44424-44428.

**Wang, S., S. J. Ryan Arends, D. S. Weiss, and E. B. Newman.** (2005) A deficiency in S-adenosylmethionine synthetase interrupts assembly of the septal ring in *Escherichia coli* K-12. *Mol Microbiol* **58** (3): 791-799.

**Wang, X., and J. Lutkenhaus.** (1996) FtsZ ring: the eubacterial division apparatus conserved in archaebacteria. *Mol Microbiol* **21** (2): 313-319.

**Wang, X., J. Huang, A. Mukherjee, C. Cao, and J. Lutkenhaus.** (1997) Analysis of the Interaction of FtsZ with Itself, GTP, and FtsA. *J Bacteriol* **179** (17): 5551-5559.

**Ward, J. E. Jr. and J. Lutkenhaus.** (1985) Overproduction of FtsZ induces minicell formation in *E. coli*. *Cell* **42** (3): 941-949.

**Watson, J. D., T. A. Baker, S. P. Bell, A. Gann, M. Levine, and R. Losick.** (2004) Chapter 12: Mechanisms of Transcription. Molecular Biology of the Gene (5th Edition). CSHL Press.

**Weart, R. B., and P. A. Levin.** (2003) Growth Rate-Dependent Regulation of Medial FtsZ Ring Formation. *J Bacteriol* **185** (9): 2826-2834.

**Weiss, D. S., J. C. Chen, J.-M. Ghigo, D. Boyd, and J. Beckwith.** (1999) Localization of FtsI (PBP3) to the Septal Ring Requires Its Membrane Anchor, the Z Ring, FtsA, FtsQ, and FtsL. *J Bacteriol* **181** (2): 508-520.

**Weiss, D. S.** (2004) Bacterial cell division and the septal ring. *Mol Microbiol* **54** (3): 588-597.

**Wendrich, T. M., G. Blaha, D. N. Wilson, M. A. Marahiel, and K. H. Nierhaus.** (2002) Dissection of the Mechanism for the Stringent factor RelA. *Mol Cell* **10**: 779-788.

**Wissel, M. C., and D. S. Weiss.** (2004) Genetic Analysis of the Cell Division Protein FtsI (PBP3): Amino Acid Substitutions That Impair Septal Localization of FtsI and Recruitment of FtsN. *J Bacteriol* **186** (2): 490-502.

**Worbs, M., R. Huber, M. C. Wahl.** (2000) Crystal structure of ribosomal protein L4 shows RNA-binding sites for ribosome incorporation and feedback control of the S10 operon. *EMBO J* **19** (5): 807-818.

**Wu, L. J., and J. Errington.** (2004) Coordination of Cell Division and Chromosome Segregation by a Nucleoid Occlusion Protein in *Bacillus subtilis*. *Cell* **117**: 915-925.

**Xiao, H., M. Kalman, K. Ikehara, S. Zemel, G. Glaser, and M. Cashel.** (1991) Residual Guanosine 3′, 5′-Bispyrophosphate Synthetic Activity of *relA* Null Mutants Can Be Eliminated by *spoT* Null Mutations. *J BiolChem* **266** (9): 5980-5990.

**Yang, J.-C., F. van den Ent, D. Neuhaus, J. Brevier and J. Löwe.** (2004) Solution structure and domain architechture of the divisome protein FtsN. *Mol Microbiol* **52** (3): 651-660.

**Yang, X., and E. Ishiguro.** (2001) Involvement of the N Terminus of Ribosomal Protein L11 in Regulation of the RelA Protein of *Escherichia coli*. *J Bacteriol* **183** (22): 6532-6537.

**Yang, X., and E. Ishiguro.** (2003) Temperature-Sensitive Growth and Decreased Thermotolerance Associated with *rel*A Mutations in *Escherichia coli*. *J Bacteriol* **185** (19): 5765-5771.

**Yanisch-Perron, C., J. Vieira, and J. Messing.** (1985) Improved M13 phage cloning vectors and host strains: nucleotide sequences of the M13mp18 and pUC19 vectors. *Gene* **33**(1): 103-119.

**Yanofsky, C., K. V. Konan, and J. P. Sarsero.** (1996) Some novel transcription attenuation mechanisms used by bacteria. *Biochimie* **78** : 1017-1024.

**Yanofsky, C.** (2000) Transcription Attentuation: Once Viewed as a Novel Regulatory strategy. *J Bacteriol* **182** (1): 1-8.

**Yanofsky, C.** (2004) The different roles of tryptophan transfer RNA in regulating *trp* operon expression in *E. coli* versus *B. subtilis*. *Trends Genet* **20** (8): 367-374

**Yu, X.-C., and W. Margolin.** (1999) FtsZ ring clusters in *min* and partition mutants: role of both the Min system and the nucleoid in regulating FtsZ ring localization. *Mol Microbiol* **32** (2): 315-326.

**Zhi, H., X. Wang, J. E. Carbrera, R. C. Johnson, and D. J. Jin.** (2003) Fis Stabilizes the Interaction between RNA Polymerase and the Ribosomal Promoter *rrnB* P1, Leading to Transcriptional Activation. *J Biol Chem* **278** (47): 47340-47349.

**Zhou, P., and C. E. Helmstetter.** (1994) Relationship between *fts*Z Gene Expression and Chromosome Replication in *Escherichia coli*. *J Bacteriol* **176** (19): 6100-6106.

**Zurawski, G., and S. M. Zurawski.** (1985) Structure of the *Escherichia coli* S10 ribosomal protein operon. *Nuc Ac Res* **13** (12): 4521-4526.